TÉCNICO LISBOA

UNIVERSIDADE DE LISBOA
INSTITUTO SUPERIOR TÉCNICO

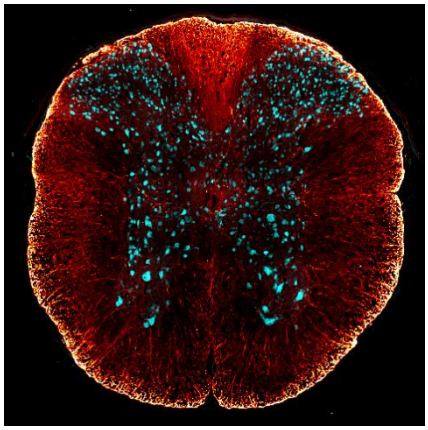

On the Role of Senescent Cells in Spinal Cord Injury

Diogo de Abreu Paramos de Carvalho

Supervisors: Doctor Maria Leonor Tavares Saúde
Doctor António Alfredo Coelho Jacinto
Co-supervisor: Doctor Cláudia Alexandra Martins Lobato da Silva

Thesis approved in public session to obtain the PhD Degree in

Bioengineering

Jury final classification: **Pass with Distinction**

2020

TÉCNICO LISBOA

UNIVERSIDADE DE LISBOA
INSTITUTO SUPERIOR TÉCNICO

On the Role of Senescent Cells in Spinal Cord Injury

Diogo de Abreu Paramos de Carvalho

Supervisors: Doctor Maria Leonor Tavares Saúde
Doctor António Alfredo Coelho Jacinto
Co-supervisor: Doctor Cláudia Alexandra Martins Lobato da Silva

Thesis approved in public session to obtain the PhD Degree in

Bioengineering

Jury final classification: **Pass with Distinction**

Chairperson: Doctor Joaquim Manuel Sampaio Cabral, Instituto Superior Técnico, Universidade de Lisboa

Members of the Committee:

Doctor Maria Leonor Tavares Saúde, Instituto de Histologia e Biologia do Desenvolvimento, Faculdade de Medicina, Universidade de Lisboa;

Doctor Ana Paula Gomes Moreira Pêgo, Instituto de Engenharia Biomédica - INEB;

Doctor Maria Margarida Fonseca Rodrigues Diogo, Instituto Superior Técnico, Universidade de Lisboa;

Doctor Domingos Manuel Pinto Henrique, Instituto de Histologia e Biologia do Desenvolvimento, Faculdade de Medicina, Universidade de Lisboa;

Doctor Elsa Clara Carvalho Logarinho Santos, Instituto de Biologia Molecular e Celular - IBMC;

Doctor César Miguel Pereira Soares Mendes, Faculdade de Ciências Médicas | NOVA Medical School, Universidade NOVA de Lisboa.

Funding Institution: Fundação para a Ciência e Tecnologia

2020

RESUMO

Uma lesão vertebro-medular (LVM) é uma doença devastadora e sem cura, que acarreta terríveis consequências físicas, psicológicas e socioeconómicas para o paciente. Trata-se de uma patologia complexa e tem vindo a tornar-se evidente que serão necessárias novas e combinadas estratégias terapêuticas para promover a recuperação motora e sensorial depois de uma lesão. Embora o conhecimento sobre os processos biológicos envolvidos numa LVM em mamíferos e espécies com capacidade regenerativa tenha aumentado consideravelmente nos últimos anos, pouco progresso tem havido quanto a opções terapêuticas. Isto sugere que outros tipos celulares ainda desconhecidos possam estar envolvidos numa lesão na medula espinhal.

A senescência foi classicamente concebida como um bloqueio do ciclo celular associado ao envelhecimento. No entanto, sabe-se agora que células senescentes (CSs) são metabolicamente activas e detêm um secretoma complexo através do qual conseguem modular o microambiente à sua volta. Consequentemente, as CSs surgiram como participantes activas em eventos de remodulação tecidual. Curiosamente, CSs transientes foram recentemente demonstradas como benéficas na reparação de tecidos, em contraste com CSs persistentes que estão subjacentes a doenças crónicas ligadas ao envelhecimento.

Neste estudo, identificámos as CSs como um novo e inesperado alvo no contexto de LVMs. Demonstrámos que perfis de senescência distintos são induzidos após uma LVM num modelo que regenera a sua medula espinhal, o peixe-zebra, e um modelo sem capacidade de regeneração, o ratinho. Surpreendentemente, enquanto no peixe-zebra existe uma acumulação transiente de CSs, no ratinho estas células acumulam-se e persistem ao longo do tempo. Deste modo, questionámos se a persistência de CSs poderá contribuir para o microambiente inibitório de reparação da medula espinhal em mamíferos. Testámos esta hipótese através do tratamento de ratinhos lesionados com ABT-263, um composto senolítico que induz apoptose em CSs *in*

vivo. Mostrámos que a eliminação de CSs induzidas após uma LVM por contusão em ratinho resulta em efeitos notáveis a nível celular, nomeadamente um aumento da preservação de mielina e fibras axonais, uma redução da cicatriz fibrótica e uma atenuação da inflamação. Estes resultados traduzem-se numa melhoria significativa da função locomotora, sensorial e da bexiga.

Tem vindo a tornar-se claro que a senescência é despoletada em resposta a dano tecidual, mas o nosso estudo indica que a capacidade de um organismo reparar ou regenerar um orgão lesionado está diretamente associada com a sua competência em controlar os níveis de CSs ao longo do tempo. Assim, este trabalho poderá não só ser relevante para LVMs mas também para estabelecer a senescência como um alvo noutros orgão sem capacidade de regeneração. Dado que diversos compostos senolíticos, como o ABT-263, estão neste momento em ensaios clínicos para o tratamento de cancro e doenças associadas so envelhecimento, este estudo poderá vir a contribuir para o redirecionamento do uso de senolíticos em reparação ou regeneração tecidual.

Palavras-chave: senescência, lesão vertebro-medular, células senescentes, compostos senolíticos, recuperação funcional

ABSTRACT

Spinal cord injury (SCI) is a devastating and non-resolving condition with dreadful physical, phycological and socioeconomical consequences for the affected individual. This is a complex pathology and it is becoming clear that novel and combined therapeutic strategies will be needed to overcome the limited motor and sensory function recovery after SCI. While considerable knowledge was achieved on the biological processes that occur after a SCI in mammals and regenerative species, small progress was obtained on medical options, suggesting that other cellular players might be relevant following an injury.

Cellular senescence was classically understood as a cell-cycle arrest response related to aging. However, it is now known that senescent cells (SCs) are metabolically active with a complex secretory phenotype through which they modulate the microenvironment around them. Consequently, SCs have now been put at the center of tissue remodeling events. Interestingly, transient SCs were recently shown to benefit tissue repair contrasting with persistent SCs known to underlie aging-related chronic disorders.

Here, we identify SCs as a new and unexpected player in the context of SCI. We show that distinct senescent profiles are induced upon SCI in a regenerating model, the zebrafish, and a non-regenerating mammalian model, the mouse. Strikingly, while in the zebrafish there is a transient burst of SCs which are then cleared out, in the mouse these cells persist and accumulate over time. We hypothesized that this persistence of SCs could contribute to the inhibitory microenvironment in mammalian spinal cord repair. We tested this hypothesis by treating injured mice with ABT-263, a senolytic drug that causes apoptosis of SCs *in vivo*. We show that elimination of induced-SCs after a murine contusion SCI leads to remarkable cellular outcomes, namely an increase in spared myelin and axonal fibers, a reduced fibrotic scar and attenuated inflammation. These effects are translated into locomotor (assessed with Open Field

and Horizontal Ladder), sensory (evaluated with Incremental Thermal Plate) and bladder function improvements.

It is becoming clear that senescence is triggered upon tissue damage, but our study indicates that the ability of an organism to repair or regenerate an injured organ is directly associated with its competence to control the levels of induced senescent cells over time. Therefore, we think our work is not only relevant for SCI but may also pave the way to establish senescence as a target in other mammalian non-regenerating damaged organs. Given that several senolytic drugs, namely ABT-263, are currently under clinical trials for the treatment of cancer and age-related diseases, our research can contribute to repurpose the use of senolytics to promote mammalian tissue repair or regeneration.

Keywords: senescence, spinal cord injury, senescent cells, senolytic drugs, functional recover

ACKNOWLEDGMENTS/AGRADECIMENTOS

Esta tese é dedicada à minha Família. Nomeadamente aos meus Pais. Por ser o fruto de toda a educação e suporte que me deram ao longo da vida.

A sua concretização é especialmente dedicada à Joana, pois foi ela que ao longo destes cinco anos de distância a tornou concretizável. Onde quer que eu chegue, ela será sempre a minha maior e melhor conquista.

Ao meu irmão, porque a sua existência é, por si só, um motivo de orgulho. Esta concretização não teria o mesmo valor se não pudesse ser com ele partilhada.

Finalmente, dedico esta tese aos meus Avós, por terem sido e continuarem a ser fonte de luz, força e inspiração.

Quero, primeiro que tudo, agradecer à Leonor e ao António. Não só por me terem acolhido nas suas equipas e por terem sido mentores extraordinários, mas sobretudo por me terem deixado perseguir um projecto novo e arriscado. Obrigado pela oportunidade, pelos ensinamentos e (já agora) por todo o suporte emocional e culinário aos fins-de-semana de marcação de tubos. A medalha de ouro do pódio dos eppendorfs será sempre vossa!! Finalmente, um obrigado especial à Leonor, por me ter concedido as condições necessárias para que pudesse consolidar este trabalho durante mais um ano.

Agradeço à Professora Cláudia Lobato da Silva, por ter aceite ser minha co-orientadora, por tudo o que me ensinou neste programa doutoral e, sobretudo, por ter demonstrado sempre uma disponibilidade absoluta para o que fosse preciso.

Aos meus companheiros e companheiras de equipa(s). Foram quatro anos dividido entre dois institutos e duas equipas compostas por pessoas absolutamente extraordinárias. Sem elas, seria impossível chegar a este ponto. Nem sempre foi fácil de conjugar o meu papel em ambas as equipas e tenho plena consciência de que, por vezes, não terei estado presente da forma como deveria. No entanto, não me esqueço de tudo o que vivi e aprendi com cada pessoa que delas fazem parte. Foi, sinceramente, um privilégio trabalhar com vocês.

À Caríssima Isaura, por ter sido uma companheira que muito me ouviu, ajudou e orientou ao longo deste percurso. Este trabalho não seria o mesmo sem ela.

À Ana Margarida e à Filipa, duas pessoas fantásticas que tiveram um contributo fundamental para este projecto.

À Dalila, por toda a ajuda nesta fase final e pela coragem que teve em assumir os nossos modelos.

Ao Telmo, por toda a ajuda e por ser aquele colega que sabe resolver tudo. O jeito que daria haver um Telmo de bolso... Toda a gente precisa de um Pocket-Telmo!

Um agradecimento especial à Fish Facility do IMM, cuja prestabilidade e companheirismo são inqualificáveis. Se alguma vez quiserem conhcer um sítio que reune consenso entre profissionalismo e fofura, vão à Fish Facility do IMM.

Ao meu grande amigo Ivo (e à sua Suki), um grande companheiro nesta viagem (e não só) que foi exímio na sua tolerância para comigo.

Ao Jorge, porque acima de tudo é um rapaz especial e um bom amigo, com uma cabeça e imaginação que vão além da idade que tem.

À Carolina, cuja amizade e doce personalidade foram imprescindíveis durante este caminho.

À Mafalda, pelo extraordinário coração e pela amizade omnipresente.

Aos meus caros Gamerz Apachers Alcoholics Anonymouz (Teammate, Bully e Mister). Que serões bem passados meus amigos. Que serões bem passados. Aconteça o que acontecer, esses serões já ninguém nos tira. Este Rookie fartou-se de aprender e divertir com vocês!

Ao Neto, por toda a amizade e confiança, não esquecendo a forma como sempre me recebeu quando necessitei.

Há sempre muito para agradecer, muitas pessoas especiais a mencionar, mas para mim não são as palavras num pedaço de papel que vão fazer jus ao reconhecimento que cada um merece. Desejo, do fundo do coração, que quem na sua vida lute pelas suas concretizações, tenha a sorte de ter uma Família e Amigos como eu tenho. Posso não ter memória fotográfica, mas dificilmente esqueço aquilo que cada pessoa faz por mim. Na falta de palavras, ficam guardados esses momentos e recordações que tornaram esta experiência muito mais rica.

“A Vida é Bela,

Nós é que damos cabo Dela.”

F.

INDEX

ABBREVIATIONS

ABT-263 – Navitoclax

AKT – protein kinase B

ATM – ataxia-telangiectasia mutated

ATR – ataxia-telangiectasia and Rad3 related

B2M – β2 microglobulin

BCKO – B-cell knockout mice

BCL – B-cell lymphoma

bFGF – basic fibroblast growth factor

BMS – Basso Mouse Scale

c/EBPβ – CCAAT/enhancer binding protein β

CCL – chemokine (C-C motif) ligand

CDK – cyclin-dependent kinase

CGs – cardiac glycosides

ChABC – chondroitinase ABC

CNS – central nervous system

CPGs – Central Pattern Generators

CSA – cross-sectional area

CSF1 – colony stimulating factor 1

CSPGs – chondroitin sulfate proteoglycans

CXCL – C-X-C motif ligand

D + Q – Dasatinib and Quercetin

DAMPs – damage-associated molecular patterns

DDR – DNA damage response

DMSO – dimethyl sulfoxide

DNA-SCARSs – DNA segments with chromatin alterations reinforcing senescence

dox – doxorubicin

dpf – days post-fertilization

dpi – days post-injury

ECM – extracellular matrix

FGF – fibroblast growth factor

GAP43 – growth-associated protein 43

GCV – Ganciclovir

GFAP – glial fibrillary acidic protein

GFP – green fluorescent protein

GO – graphene oxide

Gro – growth-regulated oncogene

HL – Horizontal ladder

HMGB1 – high mobility group box 1

hpf – hours post-fertilization

hpi – hours post-injury

HSCs – hepatic stellate cells

HSV-TK – herpes simplex virus thymidine kinase

i4F - OSKM factors in an inducible fashion

IFN-γ – interferon-gamma

IGFBP – insulin-like growth factor-binding protein

IL – interleukin

IPF – idiopathic pulmonary fibrosis

IPi – intraperitoneal injection

iPS – induced pluripotent stem

ITP – Incremental Thermal Plate

LAR – leukocyte common antigen-related phosphatase receptor

MAG – myelin-associated glycoprotein

MCP – monocyte chemoattractant protein

MDM2 – mouse double minute 2 homolog

MDSCs – myeloid-derived suppressor cells

MMP – matrix metalloproteinase

mpi – months post-injury

mTOR – mammalian target of rapamycin

MuSCs – muscle stem cells

nanoMIPs – molecularly imprinted NPs

NF-κB – nuclear factor kappa B

NgR – Nogo receptor

NK – natural killer

NPs – Nanoparticles

OIS – oncogene-induced senescence

OMgp – oligodendrocyte myelin glycoprotein

ON – overnight

OPCs – oligodendrocyte precursor cells

OSKM - OCT3/4, SOX2, KLF4 and c-MYC

p38MAPK – p38 mitogen-activated protein kinase

PAI – plasminogen activator inhibitor

PB – phosphate buffer

PBS – phosphate buffered saline 1x

PCR – polymerase chain reaction

PDGF-AA – platelet-growth factor AA

PDGFRβ – platelet-derived growth factor receptor beta

PFA – paraformaldehyde

PI3K – phosphoinositide 3-kinase

PTBP1 – polypyrimidine tract binding protein 1

PTPσ – protein tyrosine phosphatase sigma receptor

RB – Retinoblastoma

RFP – red fluorescent protein

RGM – repulsive guidance molecule

rho – rhodamine

RIPK – receptor-interacting protein kinase

rLUC – Renilla luciferase

RNS – reactive nitrogen species

ROS – reactive oxygen species

RT – room temperature

SA-β-gal – Senescence-associated β-galactosidase

SAHF – Senescence-associated heterochromatin foci

SASP – Senescence-associated secretory phenotype

SC – Senescent cell

SCI – spinal cord injury

sq – subcutaneously

STAT-3 – signal transducer and activator of transcription 3

T_{eff} – effector T

TGF-β – transforming growth factor beta

TIS – therapy-induced senescence

TNF-α – tumor necrosis factor alpha

VEGF – vascular endothelial growth factor

wpi – weeks post-injury

***wt* –** wild-type

X-gal – 5-bromo-4-chloro-3-indolyl β-D-galactoside

GENERAL INTRODUCTION

SENESCENCE: A CHAOS WAITING TO BE DECIPHERED

A great Portuguese writer once said *"Chaos is an order yet undeciphered"*. Cellular senescence is a highly complex, dynamic and programmed cellular state with diverse physiological and pathological roles across the lifespan of an organism. However, the more we know about this cellular phenomenon, the more there is to understand. Initially considered a culture artifact by some, senescence has evolved from an age-related circumstance to an intricate cellular defense mechanism in response to stress that is implicated in a wide spectrum of biological processes such as tissue remodeling, injury and cancer. This section reviews the currently known cellular and molecular features of senescence, describing its functional impact on different organismal contexts as well as the existing tools and clinical research landscape to target senescent cells (SCs).

Cellular Senescence: a Story between Life and Death

Cellular senescence was formerly described by Hayflick and colleagues, after witnessing that normal diploid cells in culture had a limit number of cell divisions and entered a permanent cell cycle arrest (Hayflick & Moorhead, 1961). He observed that the non-dividing cells remained viable for many weeks and suggested that this proliferative halt and finite lifetime *in vitro* represented aging at the cellular level (Hayflick, 1965). For that, he was called an idiot and his observations stood ignored for decades. Later, Hayflick's proposal was finally corroborated by attributing this proliferation limit to a progressive telomere shortening after propagation of cells in culture, which has become known as replicative senescence (Harley et al., 1990). The link between senescence and aging was further reinforced when it was shown that there was an age-dependent accumulation of cells exhibiting senescence markers *in vivo* (Dimri et al., 1995).

Two years later, a landmark study demonstrated that the expression of active mitogenic oncogenes (such as Ras) induced senescence in primary cells regardless of age (Serrano et al., 1997). This process became known as oncogene-induced senescence (OIS) and introduced the concept of senescence working as a tumor-suppressive mechanism to prevent aberrant proliferation after an oncogenic stimulus. Since then, it has been established that cellular senescence can be induced by a wide range of different stress signals, such as oxidative stress (Chen et al., 1995), chemotherapy (Schmitt et al., 2002), induced-pluripotent stem cell reprogramming (Krizhanovsky & Lowe, 2009), irradiation (Le et al., 2010) or cytokine treatment (Braumüller et al., 2013) (**Figure 1**).

It became then clear that senescence and aging are not synonymous and that SCs can be triggered by several stressful insults independently of organismal age (Rodier & Campisi, 2011). Importantly, SCs stopped being regarded as just undead or zombie cells that refuse to die. Though one might say they walk a fine line between life and death, it is now known that SCs are much more than what was initially thought. In fact, they suffer numerous phenotypic changes and remain highly metabolically active cells with a complex secretory phenotype, through which they can modify the surrounding microenvironment (Muñoz-Espín & Serrano, 2014) (**Figure 1**). Strikingly, SCs have recently emerged as beneficial players in various physiological processes, from embryonic development to cellular reprogramming and tissue injury responses such as wound healing and tissue repair (Rhinn et al., 2019).

The Hallmarks of Senescence

The most important rule about the hallmarks of senescence is that there is no specific hallmark of senescence, yet. Considerable knowledge about the causes and phenotypic consequences of SCs has been achieved over the last decade through the development of reporter ablation

models and the improvement of experimental tools. However, the lack of an exclusively specific marker still constitutes a major obstacle in the field of senescence, as will be discussed in this section. The real question is: what truly defines a SC?

Cell cycle arrest

The permanent exit from the cell cycle is arguably the central feature of a SC. Though this proliferative withdrawal was long thought to be strictly irreversible, recent studies have proved that, under particular circumstances, escape scenarios do exist and cell cycle re-entry may occur, especially in tumor cells (Milanovic et al., 2018; Patel et al., 2016; Saleh et al., 2019). The senescence-associated cell cycle arrest typically stalls cells in G1 or G2 phase and is primarily mediated by the upregulation of key tumor-suppressor proteins, namely p53, $p21^{CIP1}$ (encoded by the cdkn1a locus), $p16^{INK4a}$ and $p14^{ARF}$ ($p19^{ARF}$ in mouse) (both encoded by the cdkn2a locus) (Martínez-Zamudio et al., 2017; Narita et al., 2003) (**Figure 1**). While $p14^{ARF}$ is an important p53 stabilizer, $p21^{CIP1}$ and $p16^{INK4a}$ are inhibitors of cyclin-dependent kinases (CDKs) 2 and 4/6, respectively, which normally phosphorylate Retinoblastoma (RB) family proteins. Therefore, in SCs, inhibition of CDK2/4/6 leads to a persistent activation of RB proteins, which repress E2F transcription factor activity, required for cell cycle progression (Sharpless & Sherr, 2015). The ensuing cell cycle arrest differs from that of quiescent cells, which can be reversed, and of terminally differentiated cells, in which a stable replicative arrest is mediated by different pathways from those of senescence (He & Sharpless, 2017).

Resistance to apoptosis

SCs activate pro-survival pathways in order to endure, such as the upregulation of the anti-apoptotic phosphoinositide 3-kinase/protein kinase B (PI3K/AKT) pathway, overexpression of

anti-apoptotic B-cell lymphoma (BCL)-2 family proteins (including BCL-2, BCL-W and BCL-XL) and downregulation of apoptotic effectors like caspase-3 (Marcotte et al., 2004; Wang, 1995; Zhu et al., 2015). Consequently, SCs manifest a marked resistance to apoptosis, a factor that likely contributes to their accumulation *in vivo* if their clearance by the immune system becomes somehow compromised. In fact, studies have pinpointed DCR2, a decoy death receptor regulated by p53, as a common marker of SCs that protects them from immunity-mediated apoptosis (Collado et al., 2005; Sagiv et al., 2013). Both apoptosis and senescence are responses to a damage trigger, but their outcome is nothing alike. Senescence constitutes an alternative cell fate to programmed cellular death which has an active role to play in the context of tissue environment. So, the main question remains of what factors determine whether a cell undergoes senescence or apoptosis. Does it depend on the cell/tissue setting? Or the type/extent of damage? Whatever the cues, these anti-apoptotic regulators are crucial for the survival of SCs and their inhibition/downregulation leads to death by apoptosis, which has revealed to be a vital notion for the development of molecular tools targeting the elimination of SCs (Chang et al., 2016; Yosef et al., 2016).

Macromolecular damage

Telomeric DNA loop destabilization and uncapping after proliferative erosion activates the DNA damage response (DDR) and leads to replicative senescence (d'Adda di Fagagna, 2008). However, oncogenic stimuli and several genotoxic agents, such as ionizing radiation, oxidative stress and chemotherapy drugs, can also induce a DDR-mediated cell-cycle arrest (Gorgoulis et al., 2018; Halazonetis et al., 2008; Richter & Zglinicki, 2007; Robles & Adami, 1998). When activated, the DDR pathway triggers ataxia-telangiectasia mutated (ATM) or ATM- and Rad3-related (ATR)-mediated blocking of cell cycle progression through stabilization of p53 and

transcriptional activation of $p21^{CIP1}$ (Cazzalini et al., 2010; d'Adda di Fagagna et al., 2003; Fujita et al., 2009). In result, SCs often show a positive immunostaining for DNA damage markers, such as γH2AX, 53BP1, NBS1 and MDC1 (Calcinotto et al., 2019). SCs also generate nuclear DNA segments with chromatin alterations reinforcing senescence (DNA-SCARSs) (**Figure 1**), dynamic structures that sustain the activity of p53 and the secretory phenotype (Rodier et al., 2011).

Protein damage is another hallmark of cellular senescence that derives mainly from the increased levels of reactive oxygen species (ROS) due to metabolic dysfunction (*see Metabolic and morphological changes*) (Kaushik & Cuervo, 2015). ROS can oxidize and carbonylate a number of amino acid residues, leading to protein unfolding and aggregation (Höhn et al., 2017; Nyström, 2005). Crosslinking of protein aggregates with sugars and lipids forms insoluble lipofuscin aggresomes, which has emerged as another indicator of senescence (Evangelou et al., 2017; Gorgoulis et al., 2018). Interestingly, lipofuscin has been reported to stimulate the expression of the anti-apoptotic factor BCL-2 (McHugh & Gil, 2018).

Metabolic and morphological changes

SCs exhibit major mitochondrial dysfunction, showing increased mitochondrial abundance and mass but decreased membrane potential, fusion and fission rates (Kaplon et al., 2013; Passos et al., 2010). While mitochondria produce less ATP, they generate more ROS, which leads to telomere shortening and DDR activation as well as to protein damage (Korolchuk et al., 2017; Passos et al., 2007). Altered mitochondrial energetic outputs activates AMP-activated protein kinase sensor, contributing to cell cycle exit (Birch & Passos, 2017). In turn, ROS creates a feedback loop with PKCδ to stabilize p53 and $p16^{INK4a}$-RB, maintaining the proliferative arrest (Takahashi et al., 2006). Notably, mitochondrial dysfunction seems to play a key role in the

regulation and maintenance of the senescence secretome (*see Secretion*), which is suppressed after mitochondrial clearance (Korolchuk et al., 2017). Accordingly, progeroid mouse models accumulate SCs with increased levels of mitochondrial dysfunction and oxidative stress (Wiley et al., 2016).

Lysosomes also increase in number and size in SCs and their role is closely intertwined to that of mitochondria (Park et al., 2018). Though their number is elevated, they become dysfunctional leading to a decline in mitochondrial turnover. Consequently, ROS levels increase inducing damage in cellular structures, including lysosomes, forming a nefarious feedback loop (Park et al., 2018). It is possible that lysosomes continue to rise as a form of compensation for the dysfunctionality of existing lysosomes, but, in the end, lysosomal activity remains compromised. Remarkably, the increased lysosomal mass has been associated with arguably the most commonly-used biomarker of senescence – senescence-associated β-galactosidase (SA-β-gal) activity (Dimri et al., 1995) (**Figure 1**). Lysosomal activity of β-D-galactosidase, which is encoded by the GLB1 gene, is detectable at pH 6.0 in SCs, contrarily to the optimal pH 4.0 in normal cells (hence, SA-β-gal) (Lee et al., 2006).

Interestingly, SCs rely on autophagy to cope with the all the genetic remodeling and protein turnover that is required to make the efficient transition from a proliferative to a senescent state (Young et al., 2009). Therefore, autophagy seems to play a key metabolic role in the early establishment of senescence, from the cell cycle arrest to the production of secretory factors. However, after the establishment of the senescence program, autophagy slows down, which seems to be fundamental to maintain the levels of protein damage and mitochondrial dysfunction that characterize the senescence state (Kwon et al., 2017). Thus, autophagy plays a time-gated dual role in cellular senescence.

In addition, SCs are often marked by alterations in lipid metabolism and ROS-driven lipid damage and deposits in tissues (Correia-Melo et al., 2016; Ogrodnik et al., 2017). However, it still unclear how this contributes to the senescent phenotype.

Strikingly, SCs frequently increase in size and sometimes enlarge more than twofold comparing to the size of their non-senescent counterparts (Hayflick, 1965). Depending on the stress trigger, SCs may display a flattened morphology, multiple nuclei and extensive vacuolization (Denoyelle et al., 2006).

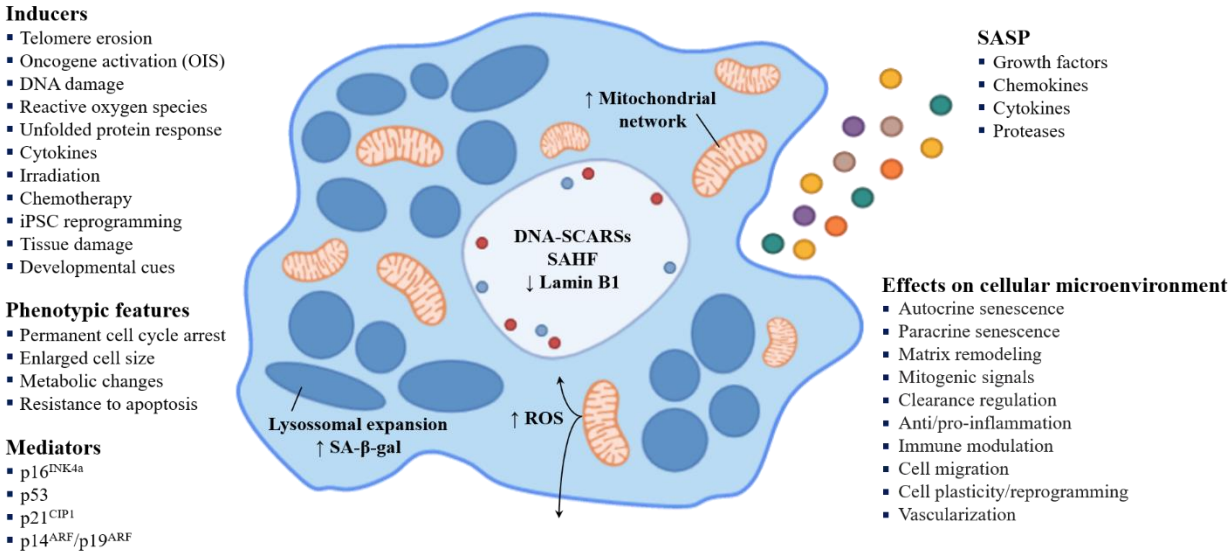

Figure 1. Hallmarks of cellular senescence. Senescence can be induced by different stimuli including telomere erosion, oncogene activation, DNA damage, metabolic stress, exposure to extracellular signals such as cytokines and mitogens, irradiation, chemotherapy, tissue damage or developmental cues. These stimuli result in the activation of key cell cycle regulators such as p53, p21, p16 and $p14^{ARF}/p19^{ARF}$, leading to a permanent cell cycle arrest and the acquisition of phenotypic changes such as resistance to apoptosis, expansion of mitochondrial and lysosomal networks, increased lysosomal senescence-associated β-galactosidase (SA-β-gal) activity, production of reactive oxygen species (ROS) and enlarged cell size. Senescent cells (SCs) suffer heterochromatin changes resulting in the presence of DNA damage foci, appearance of senescence-associated heterochromatin foci (SAHF) and a decrease in nuclear Lamin B1. Through a senescence-associated secretory phenotype (SASP), which comprises different growth factors, chemokines, cytokines and proteases, SCs can modulate the surrounding microenvironment, impacting on several biological processes (adapted from Yun, 2018).

Chromatin alterations

SCs also suffer morphological and epigenetic modifications in their chromatin landscape in order to reinforce the senescent state (Cheng et al., 2017). Yet, they are mostly context-dependent. First, their chromatin is reorganized into senescence-associated heterochromatin foci (SAHF) (**Figure 1**), which is translated in profound changes in gene expression, specifically in detriment of proliferation-associated genes and in favor of cell cycle arrest- and secretory-related genes (Chandra & Narita, 2013; Rai & Adams, 2012). Crucial for the maintenance of this chromatin structure is DNA methylation at specific CpG sites as well as histone modifications and variants, such as H3K9me3, H3K27ac, H4K16ac and H4K20me3 (Cheng et al., 2017; Di Micco et al., 2011; Hernandez-Segura et al., 2018; Salama et al., 2014). Accompanying the formation of SAHF is the downregulation of Lamin B1, a major component of the nuclear lamina that is spatially relocated within the nucleus to release H3K9me3 and alter chromatin structure (Salama et al., 2014). Therefore, loss of nuclear Lamin B1 is considered another feature of senescence (Shah et al., 2013; Shimi et al., 2011) (**Figure 1**).

Secretion

Among the hallmarks of senescence, perhaps the most relevant one is the development of a complex secretory program denominated by senescence-associated secretory phenotype (SASP), which comprises a plethora of different growth factors, chemokines, cytokines and proteases (Coppé et al., 2010) (**Figure 1; Table 1**). Primary transcriptional activators of the SASP include nuclear factor kappa B (NF-κB), CCAAT/enhancer binding protein β (c/EBPβ), GATA4, p53, mammalian target of rapamycin (mTOR), p38 mitogen-activated protein kinase (p38MAPK - regulates a DNA damage-independent SASP) and Notch1 (Acosta et al., 2008; Freund et al., 2011; Ito et al., 2017; Kang et al., 2015; Kuilman & Peeper, 2009). Some SASP

factors, like interleukin (IL)-1α (an activator of NF-κB and c/EBPβ pathways), are important for SASP initiation while others, like IL-6, are required for SASP maintenance (Acosta et al., 2013; Kuilman et al., 2008). In fact, IL-6, IL-8, growth-regulated oncogene (Gro)-α, insulin-like growth factor-binding protein (IGFBP)-7 and plasminogen activator inhibitor (PAI)-1 reinforce both the SASP and growth arrest in an autocrine manner (Acosta et al., 2008; Kuilman et al., 2008), whereas ROS, interferon-gamma (IFN-γ) and transforming growth factor beta (TGF-β) family ligands vascular endothelial growth factor (VEGF), chemokine (C-C motif) ligand 2 (CCL2) and CCL20 induce senescence in a paracrine fashion (Acosta et al., 2013; Calcinotto et al., 2019; Hubackova et al., 2012). Curiously, some SASP factors, such as colony stimulating factor 1 (CSF1), CCL2 and IL-8 recruit the immune system to promote self-clearance of SCs (Muñoz-Espín & Serrano, 2014). Through the SASP, SCs communicate with neighboring cells and modulate the microenvironment around them, exercising most of their pathophysiological effects. Thus, cellular senescence has been implicated in quite a few distinct biological activities, from aging and tumor progression or suppression to development, wound healing and even regeneration (Rhinn et al., 2019; Rodier & Campisi, 2011).

Type	**Factors**
Growth factors and regulators	Amphiregulin; epiregulin; heregulin; EGF; bFGF; HGF; KGF (FGF7); VEGF; angiogenin; CSF1; SDF-1; PIGF; NGF; IGFBP-2, -3, -4, -6, -7
Chemokines	IL-8; GRO-α, -β, -γ; CCL2, 3, 5, 8, 13, 20; HCC-4; eotaxin; eotaxin-3; TECK; ENA-78; I-309; I-TAC
Interleukins	IL-6; IL-7; IL-1α; IL-1β; IL-13; IL-15
Other inflammatory factors	TGF-β; TNF-α, GM-CSE; G-CSE; IFN-γ; BLC; MIF
Proteases and regulators	MMP-1, -3, -10, -12, -13, -14; TIMP-1; TIMP-2; PAI-1, -2; tPA; uPA; cathepsin B
Receptors and ligands	ICAM-1, -3; OPG; sTNFRI; sTNFRII; TRAIL-R3; Fas; uPAR; SGP130; EGF-R
Non-protein molecules	PGE2; nitric oxide; ROS
Insoluble factors	Fibronectin; collagens; laminin

Table 1. Senescence-associated secretory phenotype (SASP) factors (based on Coppé et al., 2010).

Identifying senescent cells

As we can see, cellular senescence has several biomarkers. However, none has absolute specificity. The cell cycle arrest is not exclusive of senescence and RB and p53 are also involved in other forms of proliferative withdrawal (Rodier & Campisi, 2011). Even $p16^{INK4a}$ might not be expressed in all SCs and is expressed in certain non-SCs (Hernandez-Segura et al., 2017; Sharpless & Sherr, 2015). The p53/$p21^{CIP1}$ pathway does not always drive senescence and, in some tissues, cells that stain positively for SA-β-gal lack the expression of $p21^{CIP1}$ (Huang & Rivera-Pérez, 2014; Xu et al., 2019). In fact, despite its prominence, SA-β-gal is not a requirement of the senescent phenotype and it is possible to have SA-β-gal^{-} SCs (e.g. those lacking GLB1) (Lee et al., 2006). Besides, it is important to take in account that false-positive SA-β-gal staining has been previously detected in macrophages (Hall et al., 2017). DNA-SCARSs and SAHF are stimulus-dependent and therefore cannot be regarded as a global feature of SCs (Di Micco et al., 2011; Kennedy et al., 2010; Rodier et al., 2011). The senescence-associated lipid profile seems to be variable depending on the trigger and mitochondrial dysfunction also portrays other cellular processes, so none of these are consistent biomarkers of senescence (Eisner et al., 2018; Quijano et al., 2012). Finally, the SASP, though a common feature of SCs, is highly heterogeneous and SASP factors are not exclusive of SCs (Rhinn et al., 2019).

It is clear that the manifestation of each senescence hallmark is context-dependent and varies according to factors such as the stress trigger, the cell or tissue type and, last but not least, time from induction of the senescent program (Calcinotto et al., 2019). In order to define a senescence signature, a multi-parametric approach is required. Data from transcriptome analysis and single-cell studies is proving to be an invaluable tool to provide senescence-gene-expression signatures in several different conditions, but a lot of information is still lacking,

especially *in vivo*. Meanwhile, a three-step multi-marker system has been proposed to identify SCs with more accuracy (Gorgoulis et al., 2019) (**Figure 2**).

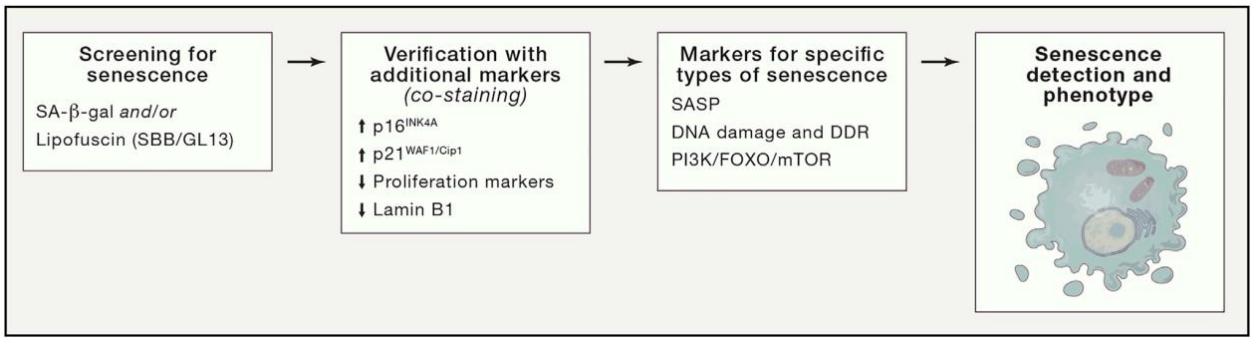

Figure 2. A multi-marker, three-step workflow for detecting senescent cells. The first step of the suggested workflow includes assessing senescence-associated beta-galactosidase (SA-β-gal) activity and/or lipofuscin accumulation (SBB or GL13 staining). Second, co-staining with other markers frequently observed in ($p16^{INK4A}$, $p21^{CIP1}$) or absent from (proliferation markers, lamin B1) senescent cells. Third, identification of factors anticipated to be altered in specific senescence contexts should be identified. This multi-marker workflow can lead to the recognition of senescent cells with the highest accuracy (from Gorgoulis et al., 2019).

In vivo Models to study Senescence

Much of what we know about the roles of senescence *in vivo* comes from progeroid and transgenic mouse models that allow the mimicking of human age-associated syndromes and genetic manipulation of SCs in different frameworks (Gorgoulis et al., 2019). These models have proven fundamental to not only assessing the *in vivo* function of SCs in different contexts but also testing senotherapeutics (*see Targeting Strategies for Cellular Senescence*).

Most transgenic models available make use of the $p16^{INK4a}$ promoter to drive the expression of specific fusion proteins that allow the measurement of $p16^{INK4a}$ expression, sorting of $p16^{+}$ cells and their targeted elimination (Gorgoulis et al., 2019). One of those models is the p16-INK-ATTAC, which expresses an enhanced green fluorescent protein (eGFP) and a FK506-binding-protein–caspase 8 that, upon administration of a drug (AP20187), induces apoptosis in $p16^{+}$ cells (Baker et al., 2011). The p16-3MR is another well-known transgenic model

(Demaria et al., 2014). This one uses a trimodal fusion protein (3MR) integrated in the mouse genome, which contains functional domains of a Renilla luciferase (rLUC), monomeric red fluorescent protein (mRFP) and herpes simplex virus thymidine kinase (HSV-TK). HSV-TK converts an administrable drug (Ganciclovir) into a toxic DNA chain terminator, causing death by apoptosis (R-M Laberge et al., 2013). Transgenic mice expressing LUC and eGFP under the control of the $p21^{CIP1}$ promoter also exist but are less used (Ohtani et al., 2007).

Crossbreeding of $p16^{INK4a}$ reporter transgenes with models of accelerated aging, such as $BubR1^{H/H}$ and $Ercc1^{-/\Delta}$, allows the monitoring of SCs through aging of live animals (Baker et al., 2011; Robinson et al., 2018; Yousefzadeh et al., 2018). BubR1 is an important mitotic spindle checkpoint gene, whereas Ercc1 is a vital DNA excision repair protein (Guo et al., 2012; Folgueras et al., 2018). Both models display numerous age-related features, increased expression of senescence markers in several tissues and markedly short lifespan. In $BubR1^{H/H}$ mice, elimination of $p16^{INK4a+}$ cells delayed the onset of age-related pathologies and attenuated the progression of already established age-related disorders (Baker et al., 2011). On the other hand, treatment of $Ercc1^{-/\Delta}$ mice with fisetin, a flavonoid with senolytic (induces apoptosis in SCs) activity, reduced the expression of senescence markers in multiple tissues, restoring homeostasis and extending lifespan (Yousefzadeh et al., 2018).

Senescence: The Good, the Bad and the Ugly

The discovery of additional cellular senescence features and biological roles provided a shifting view from a simple cell autonomous stress response to a dynamically active mobilization of environmental signaling cues with local or systemic repercussions for tissue function and, ultimately, organismal life. Some of these repercussions are beneficial while others are

detrimental. In some contexts, these seemingly paradoxical roles are challenging to reconcile. But, then, this is probably what makes senescence so interesting.

Aging

In rodents, primates and humans, SCs are found in many tissues throughout life (Campisi, 2005; Dimri et al., 1995; Jeyapalan et al., 2007). Though relatively rare in young organisms, they accumulate with age in several organs and tissues, such as the skin, heart, lung, spleen, kidney and liver (Wang et al., 2009; Yang & Fogo, 2010). As we know, aging entails a progressive loss of tissue functions that eventually leads to several chronic and age-related diseases (Campisi, 2013), so a causal link between cellular senescence and aging seems quite logical. In fact, senescence has been shown to contribute to a wide range of human age-associated pathologies, including cancer, fibrosis, cardiovascular diseases, type 2 diabetes, obesity, sarcopenia, osteoarthritis, osteoporosis and neurological disorders (Calcinotto et al., 2019; van Deursen, 2014) (**Figure 3**). Remarkably, the use of progeroid mouse models has provided evidence that ablation of $p16^{INK4a+}$ cells improves many of these disease symptoms, reinforcing a detrimental role of SCs in aged tissues (Rhinn et al., 2019).

Some studies have also suggested that, with aging, senescence plays a role in the decline of regenerative capacity, namely by functionally depleting stem cell progenitor pools (Braun et al., 2012; Janzen et al., 2006). This was recently proved during muscle regeneration in aged mice (Sousa-Victor et al., 2014). Through aging, geriatric muscle stem cells (MuSCs) suffer a quiescence-senescence switch triggered by an age-associated increase in p38MAPK activation and $p16^{INK4a}$ expression, becoming unable to activate and expand upon injury. Importantly, inhibition of p38MAPK or $p16^{INK4a}$ restored quiescence and regenerative functions in MuSCs (Cosgrove et al., 2014; Sousa-Victor et al., 2014).

Similar to a “chicken or the egg” paradox, one might wonder whether it is the accumulation of SCs that leads to aging or the opposite. The truth is that no one knows why SCs accumulate with age nor exactly how they influence disease progression. Some hypothesize that SCs develop ways to escape from immunosurveillance while others theorize that, with age, the immune system becomes progressively compromised and cannot efficiently clear SCs as it should or that the generation rate of SCs is just too big to cope with. Can they become increasingly resistant to apoptotic cues? In any case, there is a very important notion to take from the relationship between senescence and aging: the persistence of SCs is detrimental for tissue function.

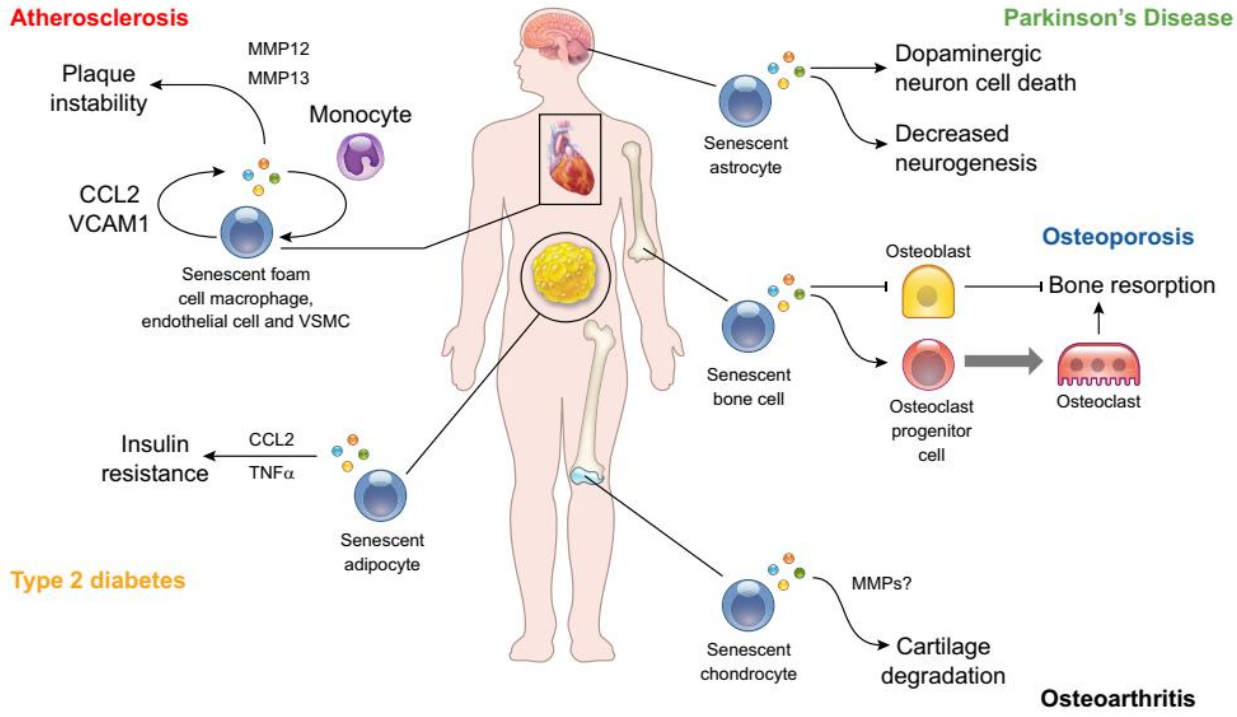

Figure 3. Senescent cells in age-related disease. In atherosclerosis, senescent foam cell macrophages secrete CCL2 and VCAM1 to recruit monocytes and trigger their conversion into senescent foam cells. Senescent endothelial and vascular smooth muscle cells secrete matrix metalloproteinase (MMP)-12 and MMP-13 to promote plaque instability. In osteoarthritis, senescent chondrocytes contribute to cartilage degradation possibly via MMP activity. In osteoporosis, the senescence-associated secretory phenotype (SASP) from senescent bone cells promote osteoclast progenitor survival and inhibit osteoblast activity. Together, these activities contribute to bone resorption. The SASP secreted from senescent astrocytes triggers dopaminergic neuronal cell death and

decreased neurogenesis in Parkinson's disease. Senescent adipocytes secrete factors including CCL2 and TNF-α, which promote insulin resistance in type 2 diabetes (from Calcinotto et al., 2019).

Cancer

Cellular senescence is a powerful barrier to tumorigenesis (Collado & Serrano, 2010). The first experimental evidence of OIS came from the overexpression of oncogenic RAS in human fibroblasts, resulting in upregulation of p53, $p16^{INK4a}$, RB and permanent cell cycle arrest (Serrano et al., 1997). This can be bypassed by inactivation of p53 and $p16^{INK4a}$ or co-expression of other oncogenes like c-MYC, E1A, or DRIL1 (Serrano et al., 1997). BRAF is another oncogene that promotes OIS by inducing $p16^{INK4a}$ expression, in a process that requires the co-expression of IGFBP7 (Wajapeyee et al., 2008). The loss or inactivation of tumor suppressor genes, such as PTEN, also induces a senescence response (Chen et al., 2005). Loss of PTEN drives p53 activation through activation of mTOR and ARF-mediated inhibition of MDM2, but also $p16^{INK4a}$ through upregulation of the transcription factor Ets2 (Ohtani et al., 2001). Contrarily to OIS, PTEN loss-induced senescence occurs in the absence of DDR but can also be bypassed by p53 inactivation (Ohtani et al., 2001).

The SASP of senescent tumor cells modulates the tumor microenvironment, which is also composed of non-senescent proliferating tumor cells, stromal cells and infiltrating immune cells (Calcinotto et al., 2019). Thus, the SASP can act as another blocker of tumor growth by reinforcing autocrine senescence or inducing paracrine senescence in neighboring tumor cells. For example, release of IL-1α by senescent cells spreads senescence to normal and tumor cells (Di Mitri & Alimonti, 2016). On the other hand, inhibition of IL-1α and IL-6 promotes OIS evasion (Di Mitri & Alimonti, 2016; Kuilman et al., 2008). Importantly, some SASP factors of tumor cells, such as TGF-β, VEGF, CCL2, and CCL20, also induce senescence in normal cells (Acosta et al., 2013). Highly relevant for tumor regression is the efficient removal of senescent

tumor cells by immune cells that are recruited by the SASP itself (Vicente et al., 2016). Likewise, the immune response can then limit tumorigenesis by releasing factors, such as IFN-γ, TNF-α (tumor necrosis factor alpha) and TGF-β, in the tumor microenvironment and inducing senescence in tumor cells, generating a positive feedback loop (**Figure 4**) (Braumüller et al., 2013; Calcinotto et al., 2019; Reimann et al., 2010). Yet, the SASP can also have immunosuppressive properties, attracting a high number of infiltrating myeloid-derived suppressor cells (MDSCs) that block the effect of other immune effector populations and inhibit the senescence response by releasing IL-1 receptor antagonist in the tumor microenvironment (Di Mitri et al., 2014).

Strikingly, the SASP of senescent tumor cells can also promote tumor progression, driving tumor vascularization and invasiveness through secretion of VEGF and a number of different matrix metalloproteinases (MMPs) (Coppé et al., 2010, 2006). Several other SASP factors, such as Gro-α, basic fibroblast growth factor (bFGF) and PAI-1, have been shown to stimulate malignant cell growth and cancer invasion. Secretion of IL-6 and IL-8 has been shown to promote both tumorigenesis and tumor suppression in different contexts (Rodier & Campisi, 2011). SASP effects on cancer progression/suppression seem to rely not only on the context but also the persistence of SCs through time. The SASP stands, therefore, as a double-edged sword, eliciting both antitumorigenic and tumor-promoting effects.

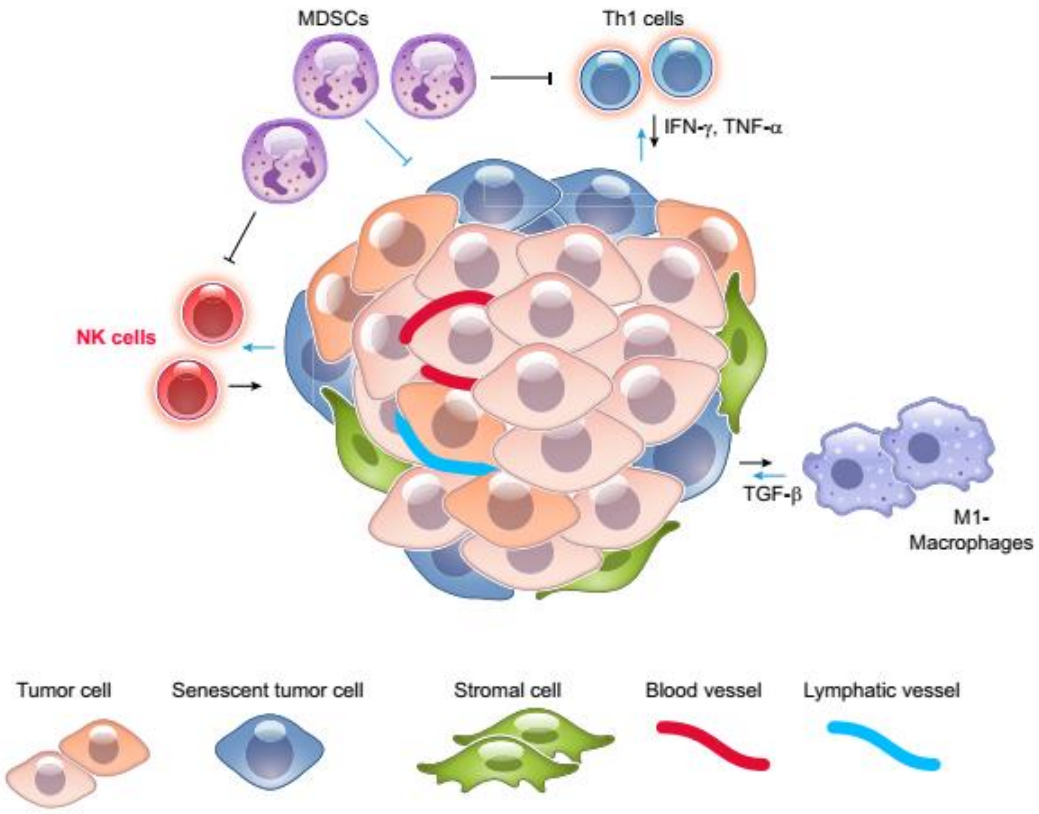

Figure 4. Paracrine modulation of senescence in cancer. Within the tumor microenvironment, the SASP of senescent tumor cells can recruit and activate several immune populations including M1 macrophages, natural killer (NK) cells and Th1 cells. Such tumor-infiltrating immune subsets can restrain tumor progression by mediating the clearance of senescent tumor cells and by promoting senescence in the neighboring cells. Conversely, myeloid-derived suppressor cells (MDSCs) are able to block the senescence induction and/or the antitumor immunity (from Calcinotto et al., 2019).

Senescence can also be induced in cancer cells by chemotherapy drugs or ionizing radiation, in what is called therapy-induced senescence (TIS) (Calcinotto et al., 2019). The mechanisms underlying TIS are usually connected to the DDR. Currently, several TIS drugs are used for human cancer treatment, including palbociclib, doxorubicin, bleomycin, docetaxel, cyclophosphamide, etoposide, vincristine and cisplatin (Ewald et al., 2010). Among all of them, the CDK4/6 inhibitor palbociclib is currently considered the most relevant prosenescent compound in the clinic. Although efficient in blocking tumor cell proliferation, TIS must be used and monitored with attentive care. By also affecting normal cells, the senescence response

might be so great that the immune system fails to efficiently clear SCs from the tumor microenvironment. Indeed, the accumulation of SCs after TIS has been shown to promote tumor relapse with increased malignancy and premature aging features in human adults and children after chemotherapy (Marcoux et al., 2013; Ness et al., 2015). Furthermore, a recent study has demonstrated that, after TIS, some senescent tumor cells are able to escape from cell cycle blockade and acquire stemness properties with highly aggressive growth potential, which has profound implications for the treatment outcome (Milanovic et al., 2018). This has been suggested as a form of tumor cell evasion from therapy, allowing their survival in a transient dormant state with potential to recover self-renewal capacity and lead to disease recurrence, normally with increased malignancy (Saleh et al., 2019). This led to a reassessment of treatment strategies, in view of taking advantage of the beneficial effects of senescence in blocking cancer cell proliferation but controlling subsequent detrimental outcomes due to its accumulation. As a result, current therapeutic strategies generally encompass a double approach, involving an initial pro-senescent step followed by an anti-senescent phase (**Figure 5**) (Calcinotto et al., 2019). In summary, chemo/radiotherapy or senescence-inducing drugs can be combined with senolytic drugs that eliminate excess senescent tumor cells that are not efficiently cleared by the immune system. Additionally, modulation of the SASP or MDSC function (e.g. with antagonists of CXCR2, a receptor for several SASP cytokines) may be used to enhance the efficacy of pro-senescence therapies and promote senescence immune surveillance (Calcinotto et al., 2019; Toso et al., 2014).

The role of senescence in cancer rightfully epitomizes the good, the bad and the ugly sides of this cellular phenomenon, by suppressing tumor growth in early stages, contributing to tumor development in later stage and eliciting tumor relapse and increased malignancy after arrest escape or chemotherapy.

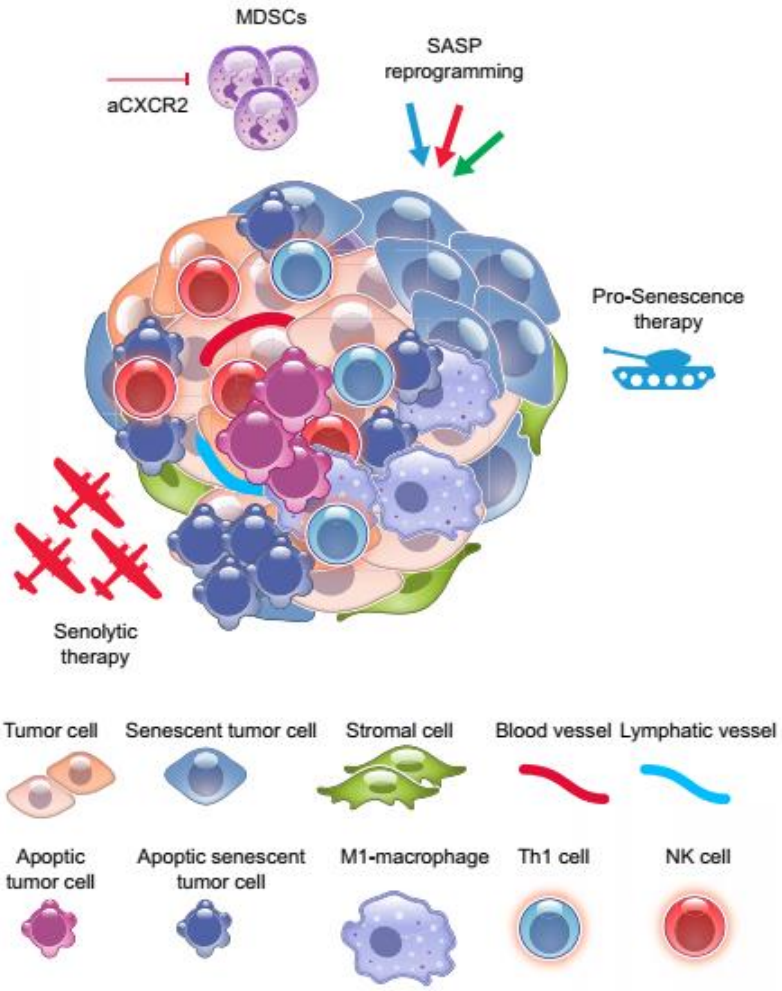

Figure 5. The double approach strategy. After treatment with pro-senescence therapies, pharmacological reprogramming of the SASP may increase the antitumor immune response. Senolytic therapies may remove senescent tumor cells in tumors where senescence surveillance is impaired to avoid negative effects induced by the SASP. Anti-CXCR2 strategies limit MDSC recruitment to the tumor and may favor senescence induction and/or the antitumor immunity (from Calcinotto et al., 2019).

Development

The discovery of SCs throughout embryonic development was very exciting and brought relevant insights to better understand the physiological roles of senescence. So far, SCs have been found during development of mouse and human embryos (Chuprin et al., 2013; Muñoz-Espín et al., 2013; Storer et al., 2013), but also in naked mole rat (Zhao et al., 2018), bird (Gibaja et al., 2019; Nacher et al., 2006; Storer et al., 2013), amphibian (Davaapil et al., 2017;

Villiard et al., 2017) and fish (Villiard et al., 2017) embryos (**Table 2**). SCs in developing structures exhibit SA-β-gal activity and up-regulation of $p21^{CIP1}$ while expression of other senescence markers, like p53, $p16^{INK4a}$ and DDR, is absent (Muñoz-Espín et al., 2013). This suggests a different senescence phenotype from that observed later in life and pinpoints the relevance of $p21^{CIP1}$ in developmental senescence. Indeed, genetic disruption of $p21^{CIP1}$ or senolytic treatment results in loss of senescence and patterning abnormalities in various structures (Davaapil et al., 2017; Gibaja et al., 2019; Muñoz-Espín et al., 2013; Storer et al., 2013). Interestingly, patterning defects are only observed transiently and are eventually compensated by other mechanisms, namely apoptosis (Muñoz-Espín et al., 2013; Storer et al., 2013). This suggests that SCs are intrinsic to development but not essential.

Overall, existing studies suggest that developmental senescence is not a damage-triggered event but rather a highly organized and programmed process with precise patterns in time and space. During development, SCs seem to contribute to tissue remodeling by controlling the balance of cell populations, fine-tuning of cell fate specification, morphogenetic signaling and structural degeneration (the latter mediated by macrophage-dependent elimination).

Species		Tissues where senescent cells were found	Reference(s)
Mammals	Human	Mesonephros, endolymphatic sac, placental syncytiotrophoblast	(Chuprin et al., 2013; Muñoz-Espín et al., 2013)
	Mouse	Apical ectodermal ridge (AER), hindbrain roofplate, mesonephros, endolymphatic sac, pharyngeal arches, gut endoderm, neural tube, tip of tail, vibrissae, interdigital webs, placental syncytiotrophoblasts	(Chuprin et al., 2013; Muñoz-Espín et al., 2013; Storer et al., 2013)
	Naked mole rat	Nail bed, skin (dermis, hair follicle), bone marrow	(Zhao et al., 2018)
Birds	Quail	Mesonephros	(Nacher et al., 2006)
	Chicken	Pharyngeal arches, neural tube, AER, eye, endolymphatic duct	(Gibaja et al., 2019; Storer et al., 2013)
Amphibians	Axolotl	Pronephros, olfactory epithelium nerve fascicles, lateral organs, gums	(Davaapil et al., 2017; Villiard et al., 2017)
	Xenopus	Cement gland, midbrain, hindbrain, pronephros, anterior cartilage	(Davaapil et al., 2017)
Fishes	Zebrafish	Yolk sac, gut	(Villiard et al., 2017)

Table 2. List of tissues where senescent cells have been detected during embryonic development of different species.

Wound healing and tissue repair

A role of senescence in wound healing and tissue repair has been described in several organs, such as the liver (Krizhanovsky et al., 2008), the skin (Demaria et al., 2014; Jun & Lau, 2010), the heart (Meyer et al., 2016; Zhu et al., 2013) and the lung (Schafer et al., 2017). In all cases, SCs seem to be closely associated with the levels of fibrotic tissue generated upon wound resolution, which in turn affect the outcome of the repair process (Yun, 2018). The deposition of extracellular matrix (ECM) is critical for the maintenance of tissue integrity during would healing but, if left unchecked, may lead to fibrosis and scarring. In the skin, CCN1, a matricellular protein expressed upon wound healing, elicits a senescence response in fibroblasts by triggering p53 and $p16^{INK4a}$ via ERK and p38MAPK pathways (Jun & Lau, 2010). This response controls the proliferation of fibroblasts and ECM deposition, limiting the fibrotic scar and contributing to the healing process. Importantly, defects in CCN1 lead to fibrosis exacerbation (Jun & Lau, 2010). Also in the skin, in a more recent study using the p16-3MR transgenic model, Demaria and colleagues demonstrated that a transient accumulation of senescent fibroblasts and endothelial cells at the wound site induces myofibroblast differentiation through secretion of platelet-growth factor AA (PDGF-AA) (**Figure 6**) (Demaria et al., 2014). Elimination of $p16^{+}$ cells resulted in delayed wound healing and increased fibrosis. Notably, topical administration of PDGF-AA reverted the delay in wound closure while maintaining the levels of fibrotic tissue, suggesting more SASP factors (likely MMPs) are involved in the healing process. In a mouse model of chronic liver damage, the administration of CCl_4 induces fibrotic scarring and senescence in hepatic stellate cells (HSCs) also via a CCN1/p53/$p16^{INK4a}$ pathway (Krizhanovsky et al., 2008). Senescent HSCs facilitate fibrotic resolution through secretion of MMPs (**Figure 6**). Finally, the cycle is completed by recruitment of natural killer (NK) cells to promote their own elimination. Moreover, CCl_4 treatment in p53;INK4A/ARF null mice caused decreased numbers of senescent HSCs and

extensive cirrhosis (Krizhanovsky et al., 2008). Similarly, in another mouse model of heart infarction, cardiac myofibroblasts enter senescence through a CCN1-dependent manner, reducing fibrosis and improving heart function (Meyer et al., 2016; Zhu et al., 2013).

However, in idiopathic pulmonary fibrosis (IPF), a chronic lung disease characterized by decreased lung function due to persistent scarring, SCs play an opposite role to that of other fibrotic lesions. In a mouse model of IPF induced by bleomycin treatment, senescent epithelial cells and fibroblasts accumulate persistently, inducing myofibroblast differentiation and exacerbating the fibrotic response (Schafer et al., 2017). In this case, the elimination of SCs improves the disease condition. Together, these results suggest that timely and coordinated activation of SCs controls the early fibrotic response and is beneficial for wound repair. Yet, in the absence of proper clearance, persistent SCs accumulate and have a negative impact in tissue repair.

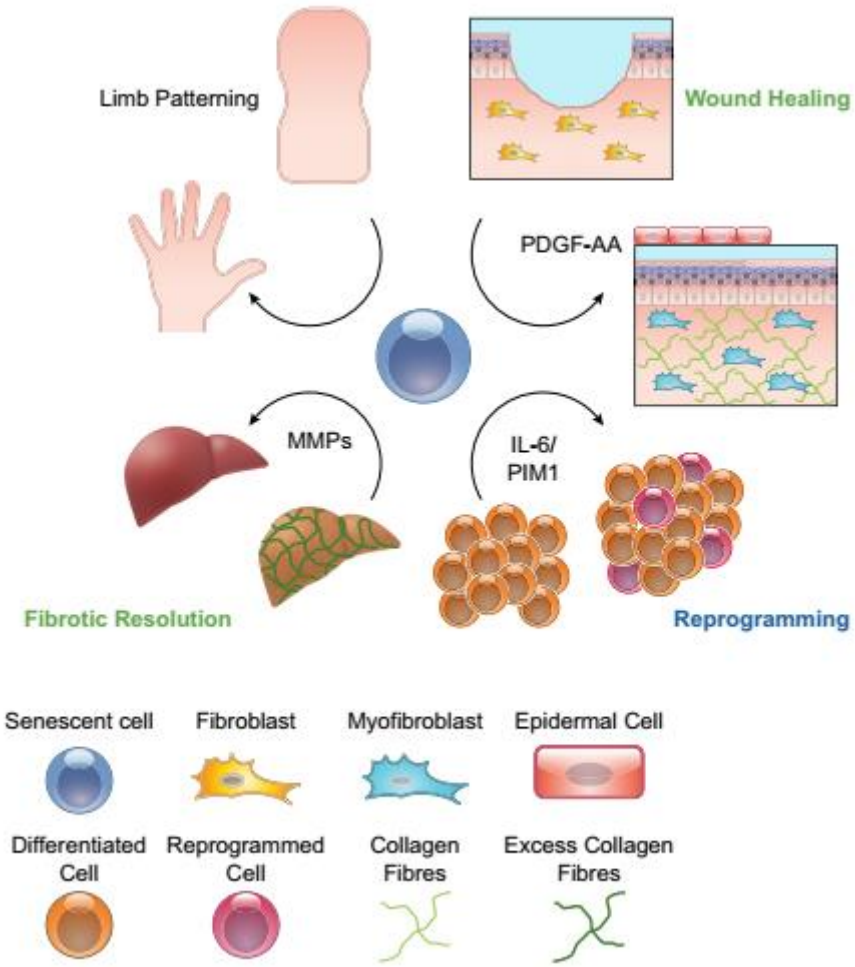

Figure 6. Role of senescence in tissue remodeling. Senescent cells secrete PDGF-AA in cutaneous wounds to induce myofibroblast differentiation and wound closure. They facilitate fibrotic resolution through matrix metalloproteinase (MMP) secretion and induce reprogramming in neighboring cells via an IL-6/PIM1 axis. Senescent cells also ensure limb patterning is correct during embryogenesis (Calcinotto et al., 2019).

Reprogramming

Recent studies have uncovered another unexpected facet of senescence: a role on cellular reprogramming. This facet became even more interesting when it was discovered that senescence has opposite effects on *in vitro* or *in vivo* reprogramming. *In vitro*, the expression of the four Yamanaka factors (OCT3/4, SOX2, KLF4 and c-MYC, OSKM) activates senescence markers in targeting cells, such as SA-β-gal, $p16^{INK4a}$, $p21^{CIP1}$ and SAHF (Banito et al., 2009). This seemingly intrinsic barrier to reprogramming probably explains why the

induced pluripotent stem (iPS) cell generation efficiency is so low (≈0.02 %) (Takahashi et al., 2007; Takahashi & Yamanaka, 2006). In fact, silencing of senescence-associated genes like p53, CIP1 and INK4a has been shown to increase iPS cell generation rate from mouse and human fibroblasts (Banito et al., 2009; Hong et al., 2009; Li et al., 2009). Strikingly, cellular senescence exerts a contrary effect on *in vivo* reprogramming. Such has been demonstrated in mice engineered to transiently express the four OSKM factors in an inducible fashion (i4F). i4F wild-type mice exhibited co-expression of SA-β-gal and NANOG, a pluripotency marker (Mosteiro et al., 2016). Without INK4a/ARF, this co-expression was lost. Remarkably, in mouse models of lung and muscle damage in which senescence is induced at the lesion sites, the efficiency of reprogramming of i4F mice was increased (Chiche et al., 2017; Mosteiro et al., 2016). This efficiency was also enhanced in conditions that elicit senescence activation, including palbociclib treatment, irradiation and even aging. On the other hand, reprogramming was decreased after $p16^{INK4a}$ deletion or treatment with the senolytic drug ABT-263 (Chiche et al., 2017; Mosteiro et al., 2016). This senescence-induced favorable environment for reprogramming was found to be mediated by secretion of the SASP factor IL-6 that activates the JAK/STAT target PIM1 to promote cellular plasticity (**Figure 6**), which can be reverted by treatment with anti-IL-6 antibodies (Chiche et al., 2017; Mosteiro et al., 2016). In another study, Ras-mediated OIS in the skin and liver was shown to induce the expression of stemness markers, such as CD34, Lgr6 and Nestin, in senescent keratinocytes (Ritschka et al., 2017). This was also demonstrated to be SASP-dependent, as it was abolished with NF-κB inhibition. However, the expression of stemness markers was overcome by senescence features upon a longer (six days) exposure to the OIS-driven SASP, which was proposed as a cell-intrinsic anti-tumorigenic response to counteract stemness. It is interesting to speculate that there is a risk that a short exposure to an oncogenic trigger can initiate a premature senescent response entailing a stemness profile with aberrant plasticity and high tumor-initiating capability. In any

case, the relationship between senescence and reprogramming seems to be defined by the time of exposure to the SASP (**Figure 7**).

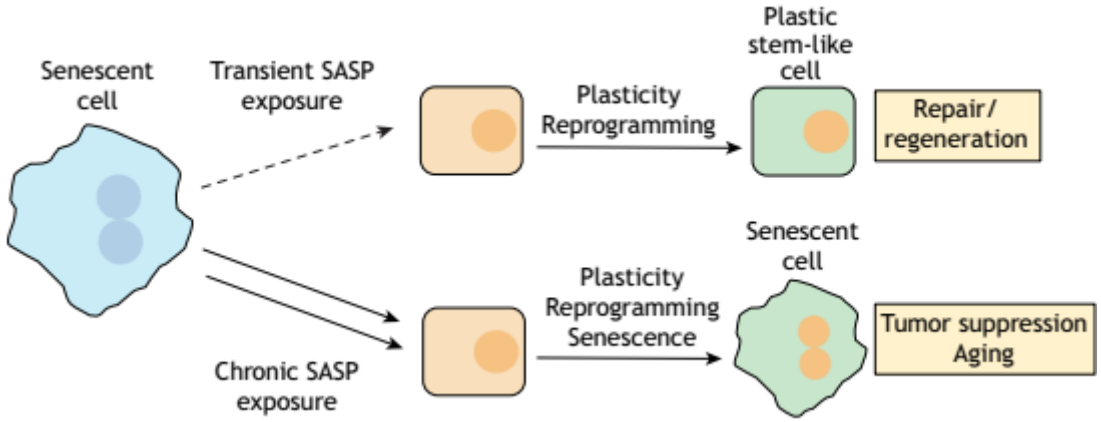

Figure 7. Senescence and reprogramming. Recent findings suggest that transient exposure to the SASP promotes plasticity and increases iPSC reprogramming capacity, ultimately favoring tissue repair and regeneration. However, chronic exposure to the SASP, although also sufficient to induce markers of plasticity and reprogramming, activates a cell-intrinsic senescence block to aberrant stemness and, ultimately, can contribute to tumor suppression and/or aging (from Rhinn et al., 2019).

Regeneration

If cellular senescence participates in wound healing and tissue repair, then why not also regeneration? Though still a very understudied topic, recent findings suggest that SCs have indeed a part to play in regenerative processes. In 2015, the team of Jeremy Brockes (UCL, London) reported a recurrent turnover of senescence during limb regeneration in the salamander (Yun et al., 2015). SCs were transiently induced near the amputation plane throughout regeneration and subsequently cleared by a macrophage-dependent immunosurveillance mechanism (**Figure 8**). This finding led to the obvious question of whether these transient SCs could be contributing to the regenerative response. Considering that salamanders regenerate through dedifferentiation (Tanaka et al., 2016), this model constitutes a good system to study the impact of senescence on this particular process of cellular plasticity. However, due to the scarcity of tools to manipulate SCs in this model system and

assess their function, it is still unclear how senescence contributes to limb regeneration. One hypothesis is that SCs might stimulate dedifferentiation and/or create a more pro-regenerative microenvironment through the SASP (e.g. ECM remodeling, vascularization). Recruited immune cells, namely macrophages and (NK) cells, can also execute pro-regenerative functions (Godwin et al., 2013; Lucas et al., 2010; Rajagopalan & Long, 2012). Another possibility is that SCs work as a population balancing mechanism, controlling the proliferation of certain cell types during tissue re-growth and patterning, much like during development. Yet, it is possible that SCs are just a consequence of the local tissue damage cues from the injury and need to be removed, which then still raises the question of why not follow the apoptosis route instead. Whatever the case, current understanding of the functions of cell senescence tells us that these cells are likely activating some kind of signaling to the surrounding microenvironment.

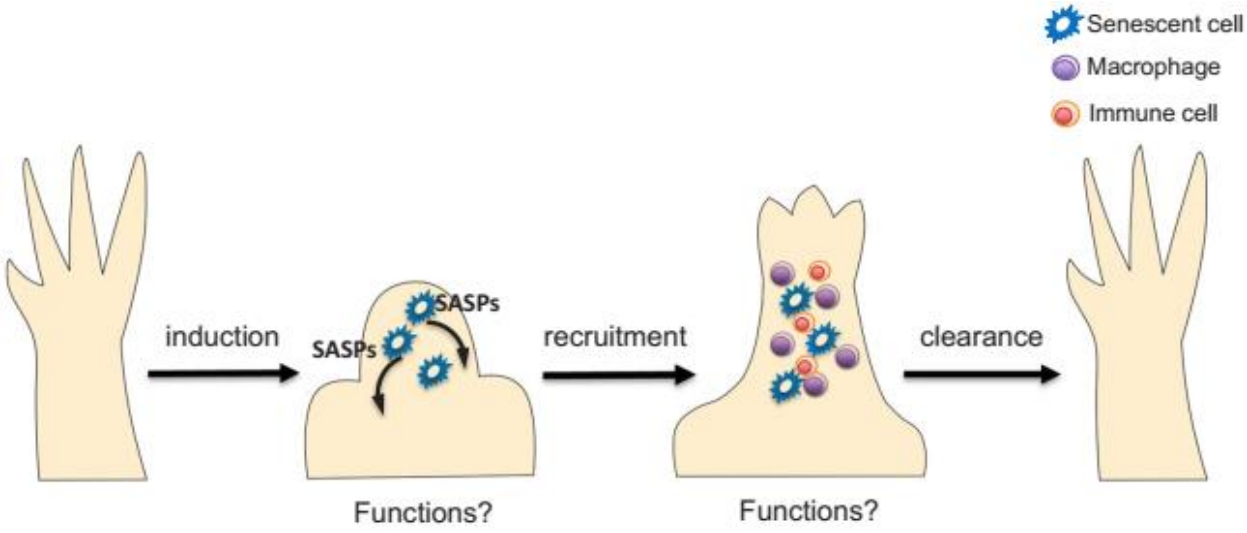

Figure 8. Cellular senescence in regeneration of a complex structure. After limb amputation in the salamander, senescent cells are induced and accumulate within the blastema. They produce a range of secreted molecules (SASP) which affect their microenvironment and could contribute, directly or indirectly, to different aspects of the regeneration process including matrix remodeling, vascularization, cell plasticity, growth and patterning. Senescent cells are subsequently cleared by an efficient mechanism of macrophage-dependent immunosurveillance (from M. Yun, 2018).

Since 2015, only two more studies have associated cellular senescence to regeneration. The first one reported a transient burst of SA-β-gal^{+} cardiac fibroblasts in zebrafish and neonatal mouse hearts after an injury (Sarig et al., 2019). However, how senescence affects cardiac regeneration is yet to be determined. The second one also showed evidence of a transient accumulation of SCs after zebrafish caudal fin amputation (Da Silva-Álvarez et al., 2019). In this case, removal of SCs with a senolytic drug impaired tissue regeneration.

Transversal to all these reports is the timely elimination of SCs, which suggests that their persistence could eventually turn detrimental for the regenerative response. Current knowledge seems to support this hypothesis, given the outcome of transient vs persistent SASP exposure in pathological conditions or aging.

Targeting Strategies for Cellular Senescence

The role of senescence in diverse pathological settings has elevated SCs to a hot target in a wide range of therapeutic approaches for injured or aged tissues (Paez-Ribes et al., 2019). In age-related scenarios, targeting senescence has become considered targeting aging itself. Thus, the last few years have witnessed a boom in the development of senescence-targeted strategic tools with translational impact. Given the lack of a specific biomarker that could be used for specific targeting, current senescence-directed therapeutic approaches rely on three main strategies: a) interference with important senescence pathways (e.g. pro-survival); b) manipulation of the SASP; and c) immune system activation (Paez-Ribes et al., 2019).

Targeting pro-survival pathways (senolytics)

In 2015, a RNA sequencing analysis revealed the upregulation of pro-survival genes in SCs, namely those involving the anti-apoptotic PI3K/AKT pathway and BCL-2 family proteins, as compared to normal cells (Zhu et al., 2015). This resulted in the identification of a new drug class: senolytics – drugs that induce apoptosis in SCs by interfering with pathways that are crucial for the maintenance of the senescence phenotype. In fact, senolytic approaches are currently the leading strategy to promote SC elimination *in vivo* (**Figure 9**) (Paez-Ribes et al., 2019).

Dasatinib, a tyrosine kinase inhibitor, and the flavonoid Quercetin, an inhibitor of the PI3K/AKT pathway, efficiently induce apoptosis of certain types of SCs *in vitro* and *in vivo* (**Figure 9**) (Roos et al., 2016; Zhu et al., 2015). Importantly, combinatorial administration of Dasatinib and Quercetin (D + Q) reduced the expression of $p16^{INK4a}$ and improved tissue function and healthspan of naturally aged and progeroid mice (Zhu et al., 2015). In another study, D + Q eliminated SCs and improved vasomotor function in aged and hypercholesterolemic mice (Roos et al., 2016). In a mouse model of IPF, D + Q reduced senescence and fibrosis markers in treated animals (Schafer et al., 2017). The promising effects of D + Q in preclinical studies led to a number of clinical trials that are currently undergoing to treat some senescence/age-associated disorders (**Table 3**). Recently, a screening study was performed to search for more flavonoid compounds with senolytic activity (Yousefzadeh et al., 2018). Consequently, a new potent senolytic arose – Fisetin. Fisetin administration significantly decreased the expression of senescence markers in multiple organs, restoring tissue homeostasis, reducing age-related pathology, and extending lifespan.

Navitoclax (ABT-263), a specific inhibitor of BCL-2, BCL-W and BCL-XL, is another powerful senolytic (**Figure 9**) (Zhu et al., 2016). *In vitro*, ABT-263 promoted apoptosis in several senescent cell types induced by different stress triggers. *In vivo*, ABT-263 treatment

was demonstrated to rejuvenate the hematopoietic system of normally aged mice, reducing the expression of $p16^{INK4a}$ and SASP factors TNF-α and CCL5 (Chang et al., 2016). In a mouse model of articular joint injury, ABT-263 decreased expression of senescent and inflammatory markers while also increasing expression of cartilage tissue extracellular matrix proteins, therefore attenuating the development of post-traumatic osteoarthritis (Jeon et al., 2017). The use of ABT-263 in combination with senescence-induced chemotherapies is currently undergoing several phase 1 and 1/2 clinical trials for cancer treatment (**Table 3**).

ABT-737, an analogue of ABT-263, is also an inhibitor of the BCL-2 family proteins with confirmed senolytic activity (**Figure 9**) (Yosef et al., 2016). In skin irradiated mice, elimination of SCs in the epidermis led to an increase in hair-follicle stem cell proliferation. However, both ABT-737 and ABT-263 are known to cause unwanted side effects, namely neutropenia and thrombocytopenia, which may prove limiting factors for clinical development (Cang et al., 2015; Rudin et al., 2012). For this reason, ABT-263 and ABT-737 are unsuitable for long-term use and, thus, are not currently trialed for anti-aging therapies. In view of overcoming these side effects, new BCL-2 inhibitor senolytics have been developed, such as A1331852 and A1155463 (**Figure 9**) (Zhu et al., 2017). A1331852 and A1155463 are BCL-XL specific inhibitors that were shown to avoid treatment-derived neutropenia and were suggested as better candidates for eventual translation into clinical interventions (Leverson et al., 2015; Zhu et al., 2017). However, they are still greatly underused as compared with ABT-263.

Piperlongumine is a natural senolytic isolated from *Piper* trees with anti-tumor activity that was proved to kill SCs induced by OIS, ionizing radiation or telomere shortening (**Figure 9**) (Wang et al., 2016). Interestingly, Piperlongumine exhibited a strong synergistic senolytic effect with ABT-263, even though its mechanism of action remains unclear. Another FDA-approved drug, Panobinostat, has been validated as a post-chemotherapy senolytic in non-small cell lung cancer and head and neck squamous cell carcinoma (Samaraweera et al., 2017).

Cardiac glycosides (CGs), such as Ouabain, Proscillaridin A and Digoxin, have also been recently identified as potent senolytics (**Figure 9**) (Guerrero et al., 2019; Triana-Martínez et al., 2019). Though they preferentially kill SCs, CGs target membrane Na^+/K^+-ATPase pumps disrupting cell electrochemical balance and, therefore, should be considered with caution in clinical applications and screened for possible non-senescent side effects.

Screening studies have pinpointed other promising targets for senolytic strategies. Compounds like FOXO4-DRI (a D-retro inverso isoform of FOXO4 which causes p53 nuclear exclusion), Alvespimycin/17-DMAG (a HSP90 inhibitor that downregulates the anti-apoptotic PI3K/AKT pathway), and KU60019 (an ATM inhibitor), have been classified as anti-senescence drugs and proposed as candidates for treatment of age-related diseases (**Figure 9**) (Baar et al., 2017; Fuhrmann-Stroissnigg et al., 2017; Kang et al., 2017).

SCs have also been determined to be sensitive to metabolism-interfering drugs, like 2-DG (a decoy substrate for glycolytic metabolism) and lysosomal V-ATPases inhibitors, revealing that the high energy demands of the senescence program and the hypercatabolic nature of SCs can be therapeutically exploitable (Dörr et al., 2013).

When designing senolytics, it is decisive to take into account that their efficiency will be correlated with the expression levels of their targets. Given the heterogeneity of SCs, targeting one survival pathway is insufficient to eliminate all different senescent populations. Also important is the fact that some SCs with beneficial physiological roles may also be targeted by senolytics systemically administered. In this regard, developing tools to specifically deliver senolytics in a designed and controlled manner (*see Emerging Tools: a New Hope*) might be fundamental to guarantee a proper treatment strategy.

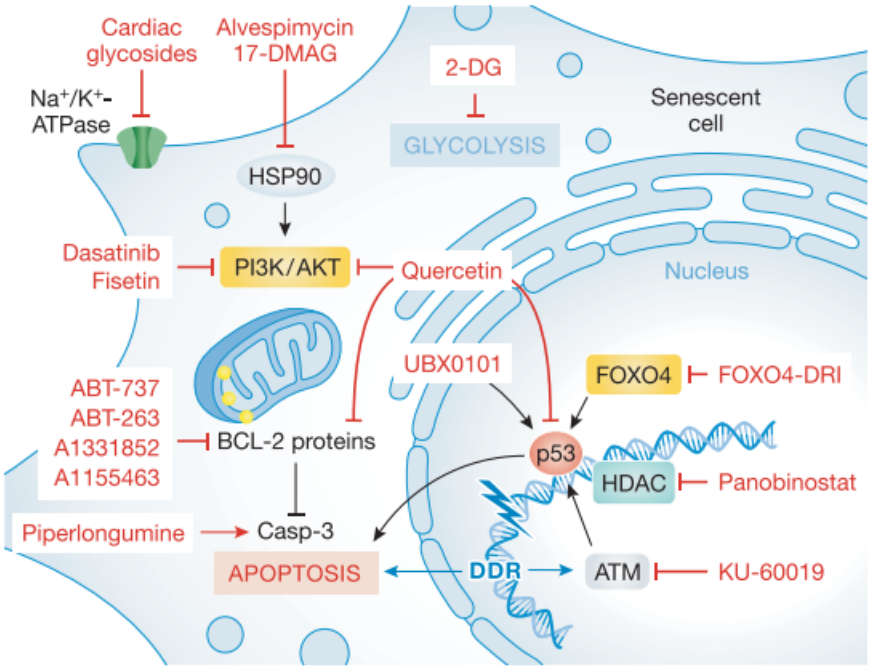

Figure 9. Senolysis through induction of apoptosis. The inhibition of pro-survival pathways by the use of apoptosis-inducing drugs is a leading approach. First and second generation of inhibitors of the BCL-2 cell death regulator family of proteins can induce selective apoptosis of senescent cells. Targeting senescence metabolism through glycolysis blockade and attenuation of ATM, HDAC, FOXO4 activities, as well as the PI3K cascade, have also been reported as effective approaches. BCL-2, B-cell lymphoma 2; HDAC, histone deacetylase; HSP90, heat shock protein 90 (from Paez-Ribes et al., 2019).

Manipulation of the SASP

A specific modulation of the detrimental effects of the SASP without compromising the cell cycle arrest can be therapeutically advantageous. Of course, this requires a deep characterization of the SASP nature in each particular setting. In view of this, a number of molecules and antibodies aiming at interfering with the transcriptional activation of the SASP or neutralizing specific factors have already been developed (**Figure 10**) (Paez-Ribes et al., 2019). Such compounds are called senostatics.

In SCs, mTOR controls NF-κB activation and IL-1α expression, making it a master SASP regulator (Herranz et al., 2015; Remi-Martin Laberge et al., 2015). mTOR inhibition with Rapamycin was shown to downregulate transcription of several SASP factors, including IL-6,

IL-8, IL-1α, and IL-1β, suppressing their pro-inflammatory effects (Herranz et al., 2015; Remi-Martin Laberge et al., 2015; Wang et al., 2017). Currently, two clinical trials (phase 1 and phase 2) are undergoing to evaluate the effects of Rapamycin on immune health, physical performance and senescence levels of patients over 70 years old (**Table 3**). Analogs of Rapamycin (Rapalogs) have also been developed to provide pharmacologically safer mTOR inhibitors for anti-aging therapies (**Figure 10**) (Lamming et al., 2013; Leontieva et al., 2015).

Most ways of modulating the SASP, directly or indirectly target NF-κB transcription (**Figure 10**). For example, NF-κB transcriptional activity is regulated by p38MAPK (Saha et al., 2007). Thus, various p38MAPK inhibitors, such as SB203580, UR-13756, BIRB 796, PF-3644022 and MK2.III, have been revealed as SASP attenuators decreasing the paracrine effects of SCs (Alimbetov et al., 2016; Freund et al., 2011). Mouse double minute 2 homolog (MDM2) inhibitors Nutlin-3a and MI-63 suppress NF-κB activity while stabilizing p53 and have been therefore considered attractive anti-cancer strategies (Dey et al., 2008; Wiley et al., 2018). Importantly, these inhibitors were found to reduce the expression of SASP factors IL-6 and IL-1α, attenuating the pro-inflammatory environment created by SCs and suppressing breast cancer cell aggressiveness. Metformin inhibits mTOR signaling and directly prevents the activation of NF-κB pathway by suppressing its nuclear translocation and was proved to repress the secretion of multiple SASP factors, including IL-6, IL-8, IL-1β and ENA-78 (Moiseeva et al., 2013; Sinnett-Smith et al., 2013). Consequently, pre-clinical studies have shown reduced levels of oxidative stress and inflammation in Metformin-treated mice (Barzilai et al., 2016). At present, five clinical trials are testing the effect of Metformin as an anti-aging drug and one of them is already in phase 4 (**Table 3**). Glucocorticoids, such as cortisol and corticosterone, and natural phenol compounds, such as Resveratrol, Kaempferol, Wogonin, and Apigenin, have also been demonstrated to interfere with NF-κB signaling and weaken the SASP, mitigating the inflammatory phenotype of SCs (Remi-Martin Laberge et al., 2012; Lim et al.,

2015; Perrott et al., 2017; Pitozzi et al., 2012). However, these results lack an *in vivo* proof of concept.

Activity of c/EBPβ, another primary SASP activator, is linked to the JAK/STAT signaling pathway, which mediates the pro-inflammatory effects of the SASP (Faget et al., 2019). Ruxolitinib and Tofacitinib are two FDA-approved drugs that inhibit JAK/STAT signaling and were shown to attenuate the SASP and symptoms of frailty in aged mice (**Figure 10**) (Xu et al., 2015, 2016).

A recent genome-wide transcriptome profiling identified a novel SASP modulating target – the polypyrimidine tract binding protein 1 (PTBP1), a regulator of alternative splicing (Georgilis et al., 2018). In a mouse model of hepatocellular carcinoma, knock-down of PTBP1 inhibited the secretion of pro-inflammatory SASP factors IL-6, IL-8, and IL-1α (Georgilis et al., 2018).

Interestingly, the use of antibodies to neutralize specific SASP factors has been speculated as another therapeutic option (Paez-Ribes et al., 2019). Though this proposition still lacks validation, Canakinumab, an IL-1β monoclonal antibody, is presently being tested in treatment of senescence-associated inflammatory disorders. Moreover, results from an ongoing clinical trial (NCT01327846) show that Canakinumab reduces the risk of lung cancer incidence (Ridker et al., 2017), which has been previously associated with the accumulation of SCs (Collado et al., 2005).

Similarly to senolytics, there are essential aspects to consider when designing senostatics. First, all SASP transcriptional regulators also have non-senescence-associated functions and, thus, their targeting might generate undesirable side effects (Kang, 2019). Secondly, the SASP is highly heterogeneous and the beneficial vs detrimental role of certain SASP factors is context-dependent. Therefore, a generalized inhibition of the SASP may prove disadvantageous.

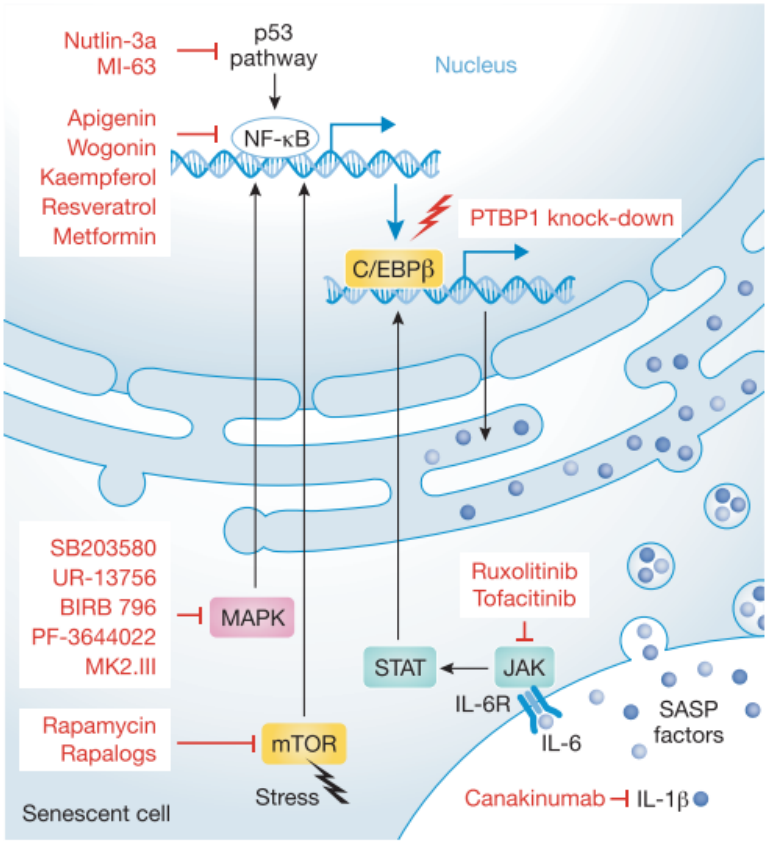

Figure 10. Manipulation of the SASP. A large number of molecules can interfere with NF-κB and C/EBPβ transcriptional activities or their upstream regulators, dampening the expression of SASP factors, such as IL-1, IL-6 and IL-8, and thus reducing the senescence-derived inflammatory milieu (from Paez-Ribes et al., 2019).

Immune system activation

The third strategy to target SCs consists on sensitizing immune cells to promote their clearance (**Figure 11**), a concept that may acquire particular relevance considering that the accumulation of SCs in aged tissues is thought to partially result from a declining immune system. In a mouse model of liver fibrosis, treatment with polyinosinic–polycytidylic acid (polyI:C), a NK cell Toll-like receptor 3 ligand, and IFN-γ, boosted the cytotoxic activity of NK cells against senescent hepatic stellate cells (Radaeva et al., 2006). *In vitro* studies also reported evidence for NK and $CD4^+$ T cell sensitization towards certain types of SCs upon administration of anti-DPP4 (a surface peptidase) and anti-vimentin (membrane-bound protein) antibodies, respectively (Frescas et al., 2017; Kim et al., 2017).

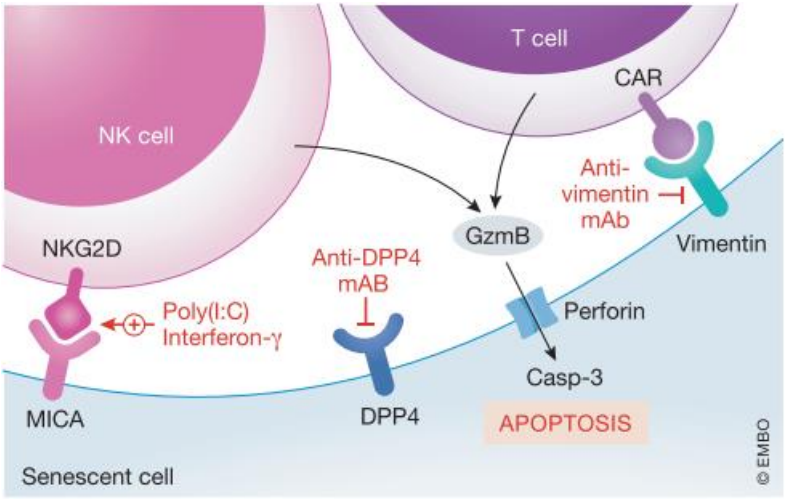

Figure 11. Activation of the immune system against senescent cells to stimulate their clearance. Enhancing the cytotoxic activity of NK cells against senescent cells and manipulating the humoral innate immunity with the use of antibodies against receptors, such as DPP4 and vimentin, are proposed attractive strategies. CAR, chimeric antigen receptor; GzmB, granzyme B; MICA, MHC class I polypeptide-related sequence A; NK, natural killer (from Paez-Ribes et al., 2019).

Senolytic agent	Disease	Trial phase	Trial ID
D + Q	Chronic kidney disease	Phase 2	NCT02848131
	IPF	Phase 1	NCT02874989
	Hematopoietic stem cell transplant	N/A	NCT02652052
ABT-263 + cancer therapies	Solid tumors	Phase 1	NCT00891605
			NCT02143401
			NCT00887757
			NCT00888108
		Phase 1/2	NCT00878449
			NCT01009073
			NCT02079740
			NCT01989585
			NCT02520778
			NCT02143401
	Advanced non-small-cell lung cancer		NCT00887757
		Phase 1b	NCT00888108
Metformin	Old adults with increased frailty	Phase 2	NCT02325245
		Phase 3	NCT02570672
			NCT03309007
			NCT03451006
		Phase 4	NCT02432287
Rapamycin	Old patients (>70 years old)	Phase 1	NCT01649960
		Phase 2	NCT02874924

Table 3. Senolytic drugs undergoing anti-senescent clinical trials (from Paez-Ribes et al., 2019).

Emerging Tools: a New Hope

From a therapeutic point of view, there is an urgent need of reliable tools for detection and targeting of SCs *in vivo*. Nowadays, the development of novel fluorescent probes and the recent advances in nanotechnology are providing promising tools with serious translational potential for diagnosis and targeted treatment of senescence-associated disorders.

Fluorescent probes

In recent years, a few fluorescent probes, such as AHGa and NIR-BG, have been developed in order to detect SCs *in vivo* (Lozano-Torres et al., 2017; Wang et al., 2019). Both activated by lysosomal SA-β-gal activity, these probes have been validated in *in vivo* mouse models bearing xenografted tumors undergoing TIS. Though this type of probes represents an innovative method to monitor SCs *in vivo*, their use is still limited by a poor tissue penetration depth (≈1 cm) and, therefore, they are currently only suitable for superficial tissues, like the skin (**Figure 12**) (Paez-Ribes et al., 2019).

Theranostic Nanoparticles

Nanoparticles (NPs) are a groundbreaking strategy for drug encapsulation and targeted delivery to specific cell/tissue types. Thus, they seem ideally suited for targeted administration of senolytics and senostatics. Over the last few years, several senescence-directed NPs have been designed (**Figure 12**) (Paez-Ribes et al., 2019). Amazingly, some of them are able to simultaneously detect and eliminate SCs (theranostic NPs).

The first SC-targeted NPs were capped mesoporous silica NPs coated with galacto-oligosaccharides (GosNPs) that were shown to be uptaken via endocytosis and successfully

release rhodamine (rho) inside lysosomes of SA-β-gal^{+} senescent human fibroblasts (Agostini et al., 2012). More recently, other silica matrix-based NPs efficiently delivered gal-encapsulated rho [GalNP(rho)] in tumor xenografts after TIS and fibrotic lungs in a mouse model of IPF (Muñoz-Espín et al., 2018). These GalNPs were then tested with encapsulated senescence-killing drugs, such as doxorubicin and ABT-263. While GalNP(dox) treatment selectively induced apoptosis in SCs, reduced the fibrotic scar and restored lung function in IPF mice, GalNP(ABT-263) was demonstrated to decrease tumor xenograft growth (Muñoz-Espín et al., 2018). Remarkably, encapsulated delivery of ABT-263 diminished its toxic side effects, namely thrombocytopenia, reinforcing the therapeutic potential of targeted drug delivery into SCs for clinical applications.

Another study has reported the targeted Rapamycin delivery into SCs using CD9 monoclonal antibody-conjugated lactose/polyethylene glycol-wrapped calcium carbonate NPs [CD9/Lac-PEG/$CaCO_3$ (Rapa) NPs] (Thapa et al., 2017). This formulation allows an enhanced drug release in the presence of SA-β-gal activity and uses CD9 receptors (overexpressed in proliferative-arrested cells) to promote specific targeting of SCs.

Pre-treatment with molybdenum disulphide nanoparticles (MoS_2 NPs) were also shown to inhibit H_2O_2-induced senescence by suppressing autophagy, which is essential for the early establishment of the senescence state (Ke et al., 2018).

Lastly, a new study reported innovative molecularly imprinted NPs (nanoMIPs) with theranostic potential (Ekpenyong-Akiba et al., 2019). NanoMIPs were designed to target extracellular epitopes of novel markers of SCs. This study identified β2 microglobulin (B2M) as one of those markers. Consequently, Dasatinib-loaded NanoMIPs were internalized by senescent bladder carcinoma cells after B2M binding, inducing significant cytotoxicity in culture. While internalization of fluorescein-tagged NanoMIPs in SCs was also validated *in*

vivo, no cytotoxic effects were found after a single dose and the clinical application of this technology needs further exploration.

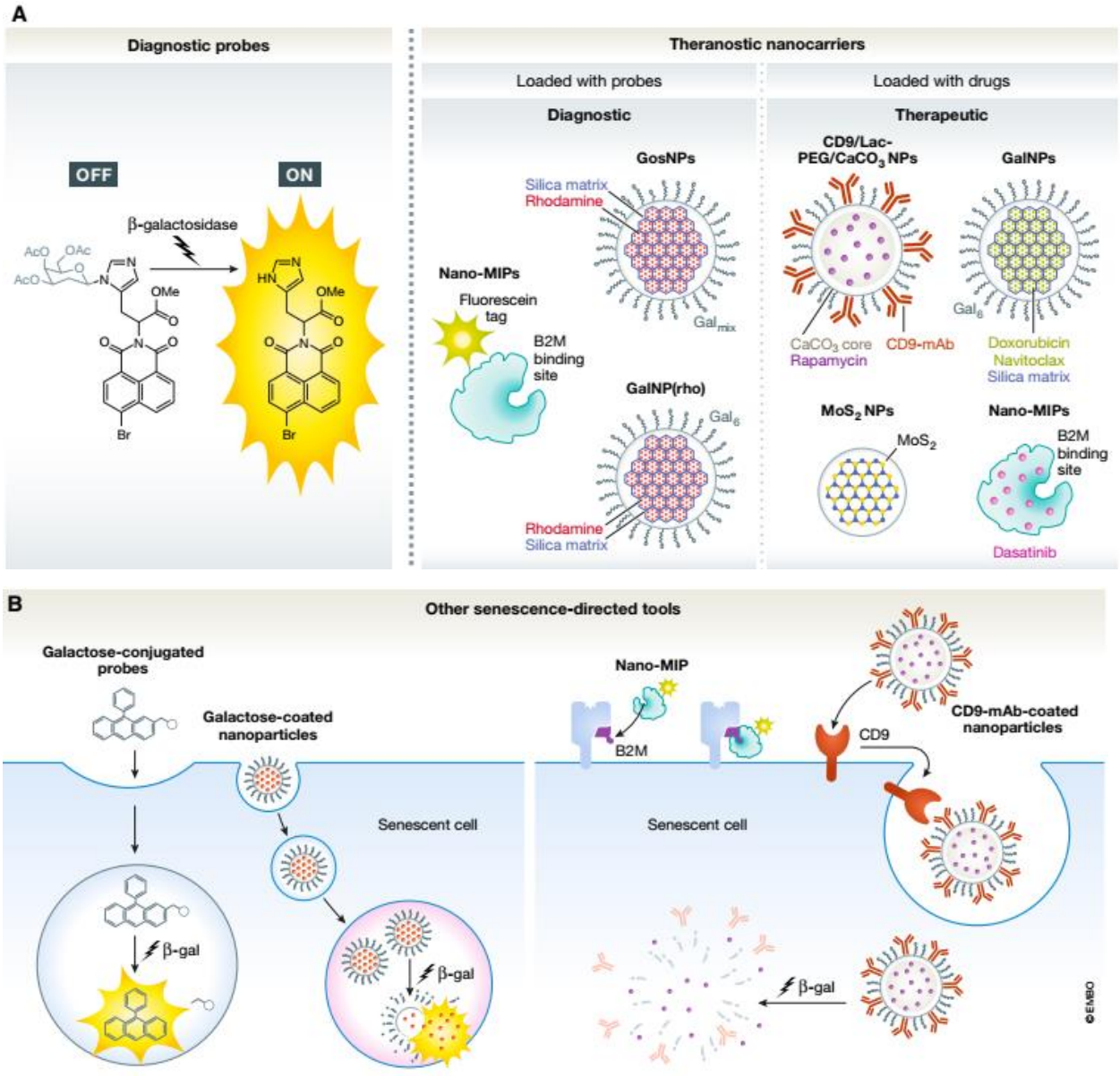

Figure 12. Emerging tools for detection and targeting of senescent cells. (A) Diagnostic probes are either fluorescent or chromogenic and can be detected upon β-galactosidase catalytic reaction. Nanocarriers are loaded or tagged with either fluorescent particles (such as rhodamine) or drugs/senolytics (doxorubicin, navitoclax, rapamycin) for different clinical interventions. Most of the senescence-directed nanoparticles (NPs) are coated or conjugated to galactose-derived residues or have been designed to bind to specific receptors. (B) Tracking the β-galactosidase activity of senescent cells is one of the commonest strategies for the development of probes and NPs. The enzymatic activity cleaves galactose residues conjugated to endocytosed probes or NPs and allows the release of carriers or the emission of color/fluorescence within the lysosomal compartment. Other developed tools can bind to receptors present on the membrane to either allow the detection of senescent cells (Nano-MIPs) or

subsequently become endocytosed and processed by β-galactosidase activity (CD9-mAb-coated nanoparticles) (from Paez-Ribes et al., 2019).

Wrapping Up: Final Considerations

The road ahead for senescence research is long. The more answers we seek, the more questions we find. While much progress has been achieved in understanding the biological roles of senescence, the apparently chaotic nature of this cellular phenomenon may yet reveal deeper complexities.

How can we reconcile such a heterogeneous and puzzling personality? Are there common denominators? In this regard, single-cell transcriptional analysis will yield invaluable information on context-specific senescent signatures and, in time, the development of sophisticated high-throughput methods and machine learning tools that can handle multi-omics data will hopefully provide answers to these questions.

Cellular senescence seems, fundamentally, a response to stress. It is becoming increasingly evident that SCs can be found in virtually every tissue. And, even though considerable knowledge was acquired on the possible different triggers of the senescence program, it is still unclear how SCs are induced *in vivo*. What cues drive cells into senescence instead of, for example, apoptosis? And why? How deep does this program modify the cellular phenotype in time? Is a senescent fibroblast still a fibroblast? The same question applies to every other kind of cell.

From an evolutionary perspective, studies indicate that senescence has a role to play in organismal life since very early on and may have originally arisen as a developmental mechanism. So, what happens to senescence later in life that makes it so different from its developmental counterpart and why, in some cases, can it not be tight-regulated like during

embryogenesis? Is it just an incredible old tool that can hardly cope with the increasing complexity of a developed organism? In some ways, senescence reminds of that amazing 20-year old computer we have in the basement that still works but barely processes, generates a short circuit every time we turn it on and, no matter what, we just won't get rid of it.

The recent findings on the role of SCs in tissue injury and regenerative responses are very exciting. Though, mechanistically, their functions remain mostly undeciphered, SCs have been shown to facilitate fibrotic resolution and also suggested to modulate cell plasticity during injury responses. These beneficial roles are primarily attributed to the SASP and are considered therapeutically relevant for pro-regenerative interventions. However, it is particularly pertinent to consider that many SASP factors are also known tissue damage signals secreted by non-SCs. Without a transcriptional analysis at the single-cell level, it will be hard to distinguish between them.

After all, are SCs good Samaritans or camouflaged villains? In this perspective, the reconciling factor seems to be "time". The notion that the functions of SCs are orchestrated by temporally regulated mechanisms is probably the most coherent senescence concept so far. While the beneficial roles of senescence all share a transient profile, the deleterious functions of SCs are associated to their lingering persistence (namely the chronic exposure to their SASP) (**Figure 13**) (Rhinn et al., 2019).

Targeting SCs is, for all the aforementioned reasons, currently a hot topic, so much so that several different biotechnology companies are investing in the development of SC-targeted therapies with translational relevance. Yet, the lack of a specific senescence biomarker remains a limiting factor for efficient translation. Moreover, there are a few important concerns regarding the clinical application of existing approaches. First, SCs play important physiological roles in some specific contexts (e.g. wound healing) and, therefore, their general targeting may compromise organismal health and must be carefully evaluated. The selectivity

of existing senolytics/senostatics must be improved and their delivery must be planned according to space and time. NPs represent a promising tool to specifically target pathological SCs in certain tissues, while diminishing drug-associated toxicity side effects, but this technology still needs further characterization and development. Ideally, targeting the SASP should aim at suppressing its deleterious effects while keeping or harnessing its beneficial roles. However, this will only be possible after an in-depth functional characterization of each SASP component in each different context. Another concern is that, given the multifaceted nature of SCs and the differences between humans and mice, existing pre-clinical studies might not reflect the complex microenvironment of diseased tissues from human age-related disorders. Therefore, when possible, SC characterization and senotherapy validation should be performed in human samples *ex vivo* obtained from different contexts. In the future, this will likely be fundamental to generate personalized anti-senescent strategies.

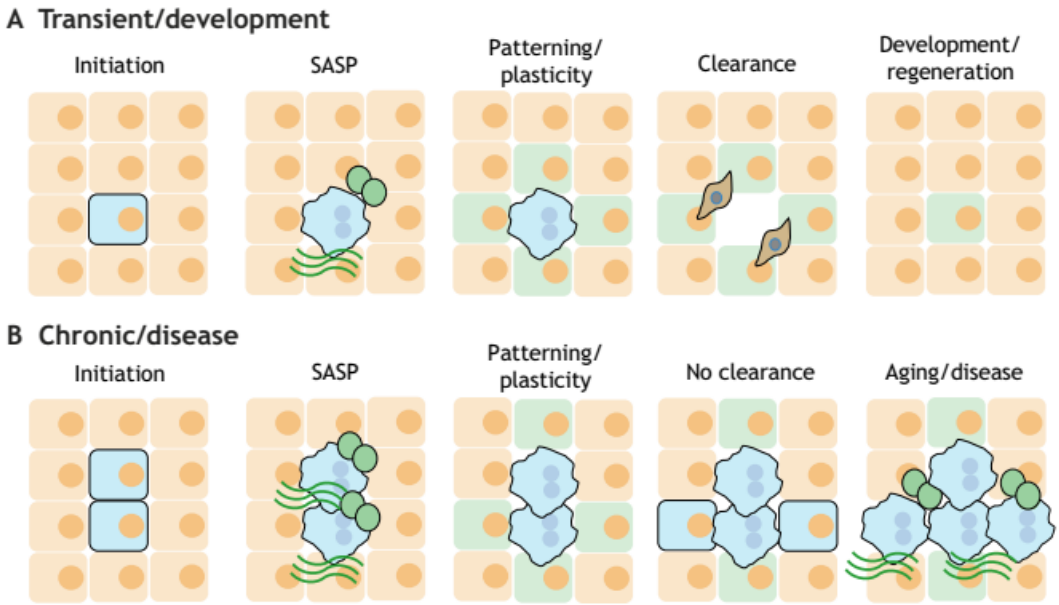

Figure 13. The time-gated senescence paradigm. Comparison of transient (A) with chronic (B) senescence. In response to an inducer, a cell initiates the senescence program (blue). This cell activates the secretion of SASP factors such as cytokines (green circles) and ECM factors (green lines). One effect of the SASP is to favor plasticity in neighboring cells, while also recruiting immune cells, such as macrophages (brown cells), to clear

senescent cells. This restores the pre-damaged state, or favors tissue development. In situations of chronic or disease states, the increased incidence of senescence and impaired clearance result in exaggerated features of the program, including prolonged SASP, enhanced plasticity and accumulation of senescent cells, thus further enhancing tissue dysfunction and damage, and resulting in aging/ disease (from Rhinn et al., 2019).

SPINAL CORD INJURY: RESTORING THE TREE OF LIFE

Spinal cord injury (SCI) is a dreadful non-resolving neurological condition with devastating consequences for the affected individual. Beyond the loss of essential motor and physiological functions, a traumatic SCI entails terrible socioeconomical burdens with estimated life-time costs ranging from one to five million dollars per person (Courtine & Sofroniew, 2019). Each year, 250000 to 500000 people suffer a traumatic spinal lesion (Quadri et al., 2018). Most of them result from traffic accidents, but some result from falls, sports injuries or even incidences of violence. Advancements in medical management have increased patient survival and life expectancy, but the pathophysiological mechanisms underlying SCI are so complex that, so far, small progress has been achieved in improving the recovery of injured patients (Alizadeh et al., 2019; Middleton et al., 2012). However, several studies using preclinical animal and injury models to recapitulate human SCI have provided important insights on the cellular and molecular mechanisms involved in the pathophysiology of this life-changing condition (Alizadeh et al., 2019). Remarkably, other vertebrate models, like zebrafish and newts, are able to regenerate their spinal cords, showing robust axonal regrowth and functional recovery (Becker & Becker, 2007). The use of such models has contributed to identify contrasting cellular responses and environmental differences between non-regenerating mammals and regenerating vertebrates. Understanding the mechanisms of endogenous regeneration may reveal important targets for future therapeutic approaches to promote mammalian spinal cord repair. Hope is also being deposited in the advances in engineering sciences that will eventually improve neurologic functions and increase recovery through neurotechnology and rehabilitation (Courtine & Sofroniew, 2019). Importantly, though most experimental research is focused on motor function recovery, tackling the restoration of autonomic (e.g. bladder) and sexual functions is often as essential, if not even more meaningful, to SCI patients (Anderson, 2004).

This section provides an overview on the currently known cellular and molecular features of SCI, existing animal models and translational regenerative therapies with clinical impact.

Primary Mechanisms of Spinal Cord Injury

A SCI is characterized by multiple symptoms and the clinical outcomes will depend on the severity and the location of the lesion. Typically, SCI patients have a partial or complete loss of motor and/or sensory function below the injury level (Wilson et al., 2012). Cervical lesions are the most common injuries, often leading to tetraplegia, followed by thoracic lesions that can cause paraplegia.

Primary injury

Primary injury is defined by mechanical damage that occurs at initial impact, when bone fragments, disc components and/or ligaments wound the spinal cord tissue (Dumont et al., 2001). The most common type of primary injury is a contusion, followed by a persistent compression due to vertebral fracture or dislocation (Choo et al., 2009; Suwanwela et al., 1962). Though less common, compression can also be transient. Other types of primary injury include vertebral stretching and spinal laceration/transection (Choo et al., 2009; Dumont et al., 2001). Transections can translate into anatomically complete lesions, which eliminate all neuronal communication across the injury, whereas contusions or stretching are smaller or discontinuous, allowing spared neuronal tissue to communicate across the lesion (**Figure 14**) (Courtine & Sofroniew, 2019). Upon impact, local blood vessels and cellular membranes are disrupted, increasing hemorrhage-driven local pressure, releasing cytotoxic factors and compromising oxygen supply, ultimately causing ischemia and edema (Popa et al., 2010; Tator

& Fehlings, 1991; Wolman, 1965). These initial features will progress and initiate the secondary injury response (Wilson et al., 2011). Therefore, the extent of the primary injury is considered the strongest prognostic indicator of the neurological outcome of SCI.

Neurological outcomes of SCI

Determining if a SCI is complete or incomplete is one of the most important predictors of the neurological outcome (Kehr & Kaech, 2014). SCI patients may spontaneously recover motor and sensory functions, but complete paraplegic or tetraplegic patients have a much poorer recovery prognosis than patients with incomplete paraplegia or tetraplegia. Patients with an incomplete injury exhibit functional recovery during the first three months post-injury (mpi) and generally reach a plateau after nine to twelve mpi (Kehr & Kaech, 2014). Strikingly, the spinal cord displays enough axonal plasticity to allow spontaneous circuit re-organization after an incomplete injury (Ballermann & Fouad, 2006; Bareyre et al., 2004; Courtine et al., 2008; Rosenzweig et al., 2010). In fact, intraspinal projection neurons are able to form detour circuits below or around the lesion, establish new connections and relay supraspinal information across the injury, promoting meaningful recovery (**Figure 14**).

Other important players in spontaneous recovery after SCI are the so called Central Pattern Generator networks (CPGs) (Grillner, 2006). Throughout life, CPG circuits dynamically control proprioceptive motor behaviors by translating sensory information and supraspinal inputs into adaptive muscle activation patterns. Amazingly, lumbar CPGs are still responsive to proprioceptive sensory information and able to generate motor behavior after complete loss of supraspinal inputs (Courtine et al., 2009; Edgerton et al., 2004). Below the injury, the spinal cord keeps receiving and interpreting sensory inputs and stimulation of CPGs even with the smallest amount of supraspinal information from spared circuits may significantly improve

motor function after SCI (Courtine & Sofroniew, 2019). Thus, incomplete SCI can often benefit from therapeutic strategies that aim at stimulating circuit re-organization and/or function of spared networks.

SCI Biology

Independently from the severity, a SCI can be divided into three distinct compartments: 1) a non-neural lesion core comprised of proliferating fibrotic cells (namely fibroblasts and pericytes), infiltrating immune cells and cystic cavities; 2) a glial scar border made of reactive astrocytes that surrounds the non-neural lesion core; and 3) a zone surrounding the astrocytic scar that contains reactive spared neural tissue (**Figure 14**) (Burda & Sofroniew, 2014; Göritz et al., 2011; O'Shea, Burda, et al., 2017; Sofroniew, 2015). The concept of this compartmentalized division is particularly relevant to understand the mechanisms of secondary injury and assessing the biological response is fundamental to define a proper treatment strategy.

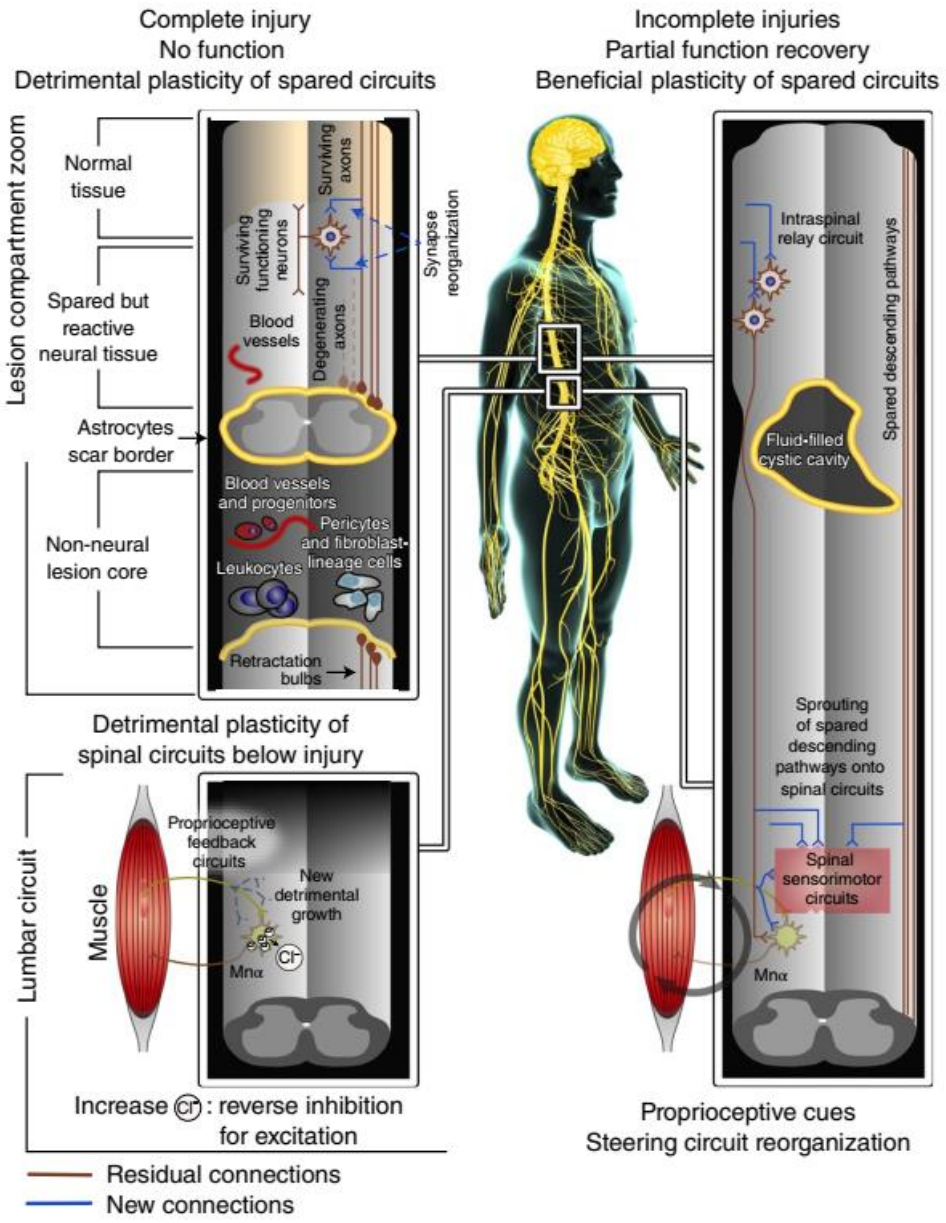

Figure 14. SCI biology and spontaneous recovery mechanisms. Spinal cord damage can be broadly divided into two categories: complete and incomplete SCI. Anatomically complete SCI is less common in humans. A clinically complete SCI is essentially defined functionally, when no motor and sensory functions can be detected below the injury. After such lesions, detrimental changes continue taking place for decades below the SCI. An incomplete SCI spares tissue bridges containing a variety of ascending and descending pathways, depending on the location of the injury. The anatomical and functional reorganization of these pathways and circuits below the injury support various degrees of functional recovery. Both complete and incomplete SCIs exhibit three distinct lesion compartments: (1) a central non-neural lesion core often referred to as a fibrotic, mesenchymal or connective tissue scar that often contains cystic cavities; (2) a narrow border of reactive astroglia and other cells that intimately surrounds the lesion core; and (3) a surrounding zone of viable neural tissue that is spared and functional but is also reactive and reorganizing. Some of the mechanisms highlighted in this figure have been

uncovered in animal models, and it is not yet certain whether human SCI involves similar mechanisms (from Courtine & Sofroniew, 2019).

Secondary Mechanisms of Spinal Cord Injury

The secondary injury encompasses a cascade of cellular, molecular and biochemical events that cause progressive tissue dysfunction and thwart neurological recovery, contributing to overall morbidity and mortality (Kehr & Kaech, 2014). It is triggered within minutes after the primary injury and often lasts for months, continuously propagating damage, not only around the lesion but also throughout the body. Temporally, it is divided in three distinct phases: acute, sub-acute and chronic (Quadri et al., 2018). The acute phase (0-72 hours post-injury, hpi) comprises the physical and biochemical alterations resulting from the initial trauma, including neurogenic shock, vascular damage, ischemia, edema, ionic imbalance, excitotoxicity, oxidative damage and necrotic cell death (Oyinbo, 2011). The sub-acute phase (3-14 days post-injury, dpi) involves lipid peroxidation, apoptosis, demyelination of surviving axons, Wallerian degeneration, matrix remodeling, the formation of a glial scar and immune-mediated neurotoxicity. Finally, the chronic phase includes progressive axonal death, maturation of the glial scar, formation of a cystic cavity and chronic inflammation (**Figure 15**) (Bradbury & Burnside, 2019; Oyinbo, 2011).

Vascular damage, Ischemia, Edema and Neurogenic Shock,

Following the initial injury, vascular disruption causes excessive bleeding and hypovolemia (Couillard-Despres et al., 2017). Leukocytes and blood extravasate to the injury site, promoting edema, and the blood flow to the rest of the spinal cord becomes compromised, leading to hypoxia and ischemia. In turn, this leads to ionic imbalance and release of highly reactive

oxygen species that exacerbate endothelial damage, vascular permeability and edema, causing cellular metabolic dysfunction and hemorrhagic necrosis (**Figure 15**). Consequently, SCI patients suffer neurogenic shock, which is characterized by severe arterial hypotension, bradycardia, hypothermia and autonomic dysfunction (Guha et al., 1989; Lee et al., 2016).

Ionic Imbalance and Excitotoxicity

Upon disruption of cellular membranes, cells become highly permeable to ions, especially calcium (Ca^{2+}) influx (Quadri et al., 2018). The excessive intracellular Ca^{2+} accumulation leads to mitochondrial dysfunction, oxidative stress and glutamate-driven excitotoxicity (**Figure 15**). Intracellular Ca^{2+} promotes glutamate release (Couillard-Despres et al., 2017). In turn, glutamate receptor activation results in more Ca^{2+} influx, generating a negative loop of intracellular Ca^{2+} and extracellular glutamate accumulation. In neurons, astrocytes and oligodendrocytes, glutamate receptor overactivity has been shown to induce mitochondrial Ca^{2+} overload, triggering apoptosis and/or necrosis (Li & Stys, 2000; Pivovarova & Andrews, 2010; Xu et al., 2008). Accordingly, administration of a NMDA glutamate receptor antagonist was demonstrated to improve functional recovery after SCI (Wada et al., 1999).

Mitochondrial dysfunction and Lipid Peroxidation

Mitochondrial Ca^{2+} overload further exacerbates ionic imbalance by suppressing respiration and depleting ATP, which disables NA^{+}/K^{+} ATPase pump and increases intracellular Na^{+} (Li & Stys, 2001; Starkov et al., 2004). In turn, intracellular Na^{+} induces the release of more glutamate and reverses the activity of Na^{+}/Ca^{2+} exchanger, supporting more Ca^{2+} influx (Li & Stys, 2001; Stys et al., 1992). Accumulation of Na^{+} also over-activates Na^{+}/H^{+} exchanger, increasing acidosis through intracellular H^{+} and, consequently, reinforcing Ca^{2+} permeability

in the membrane (Agrawal & Fehlings, 1996). Given that nodes of Ranvier are enriched in voltage-gated Na^+ channels that are crucial for neuronal signal conduction, axons are particularly vulnerable to damage caused by ionic imbalance (Oyinbo, 2011).

Mitochondrial Ca^{2+} overload also induces the massive production of noxious free radicals, namely ROS and RNS (reactive nitrogen species) (Quadri et al., 2018). Subsequently, oxidative stress potentiates mitochondrial dysfunction and generates a wide range of macromolecular damage, especially in membrane lipids. Lipid peroxidation is a major mechanism of secondary injury that occurs when ROS interacts with membrane polyunsaturated fatty acids, generating reactive lipid peroxyl radicals (Couillard-Despres et al., 2017; Oyinbo, 2011). Lipid peroxyl radicals react with fatty acids of neighboring cells, inducing more lipid peroxidation, destabilizing cell membranes and further deteriorating ionic imbalance. In addition, RNS also cause oxidative protein damage by nitrating tyrosine residues of amino acids (Alizadeh et al., 2019).

Altogether, mitochondrial dysfunction and lipid peroxidation establish an unending feedback loop with ionic imbalance that causes severe damage after SCI and triggers cellular death (**Figure 15**).

Cellular death

During the acute and sub-acute phases of injury, neurons and glial cells undergo major cell death (Beattie et al., 2002). Most of the aforementioned factors of secondary injury (ionic imbalance, excitotoxicity, ATP depletion, oxidative stress) induce instantaneous energy-independent non-programmed cell death, also known as necrosis. A recent study has reported evidence for the existence of lysosomal damage-mediated necroptosis (caspase-independent programmed necrosis) via accumulation of receptor-interacting protein kinases 1 and 3 (RIPK1

and RIPK3), after SCI (Liu et al., 2018). On the other hand, programmed energy-dependent apoptosis occurs in cells that survive the primary injury but ultimately activate apoptotic pathways due to the progress of secondary injury (Beattie et al., 2002). Apoptosis also occurs in areas distant to the injury site and affects mostly oligodendrocytes, microglia and astrocytes (Beattie et al., 2000). It can be triggered by activation of death receptors, such as Fas (activates caspase 8), or mitochondrial dysfunction-mediated release of cytochrome C (activates caspase 9) (Zhang et al., 2012).

After SCI, cellular death induces a widespread deposition of cellular debris that trigger gliosis and neuroinflammation (Bradbury & Burnside, 2019). Importantly, axons undergoing Wallerian degeneration continuously deposit myelin debris, such as myelin-associated glycoprotein (MAG), Nogo A and oligodendrocyte myelin glycoprotein (OMgp), that inhibit axonal regrowth and are not efficiently cleared by the immune system (**Figure 15**) (Bradbury & Burnside, 2019).

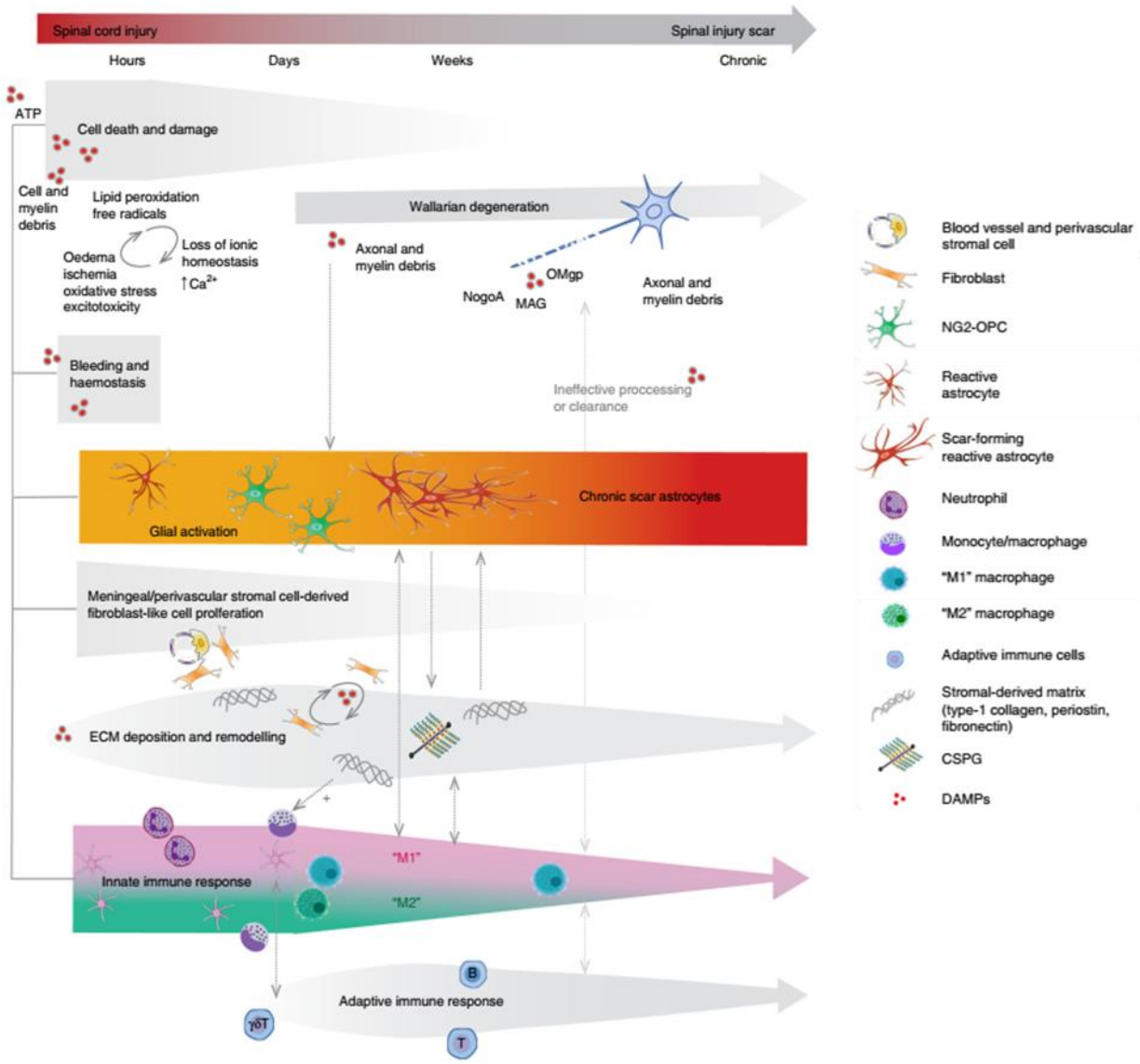

Figure 15. Time course of progressive secondary damage. Following traumatic spinal cord injury, acute cell death and damage triggers release of cell-derived and blood-derived damage-associated molecular patterns (DAMPs), ATP release, dysregulated ionic homeostasis, oxidative stress and excitotoxicity, which represent potent stimuli for triggering glial cell activation, stromal cell proliferation, deposition of ECM, and recruitment of circulating innate immune cells. Within a few days following injury, monocyte-derived macrophage/microglia adopt a predominantly M1 phenotype which does not favor resolution promotes fibrosis. Proinflammatory innate responders also present DAMP-derived antigens to T and B-cells. B cells, in turn, may present antigens to T-cells, triggering their expansion. During this time, reactive astrocytes proliferate, hypertrophy and overlap in order to isolate this zone of non-resolving pathology from spared tissue. They also secrete matrix chondroitin sulfate proteoglycans (CSPGs), which are known to downregulate neuronal plasticity. Wallerian degeneration of degenerating axonal tracts contributes to continued deposition of axonal and myelin debris, which is ineffectively processed by immune cells and leads to the deposition of myelin-associated molecules (MAG, Nogo, OMgp) which are known inhibitors of neuronal regrowth. Ongoing Wallerian degeneration at later post-injury stages further triggers gliosis and neuroinflammation. Dashed grey arrows show cross talk between different components

of the spinal injury scar, which is usually bidirectional. For example, CSPGs released by reactive astrocytes are thought to activate receptors on macrophages/microglia to induce a proinflammatory phenotype and in turn increasing inflammation induces further astrocytic reactivity and CSPG deposition. Cross talk between the innate and adaptive immune response also propagates inflammatory pathology and further influences glial activation and CSPG production. The dynamic interactions between inflammation, damaged tissue and ECM remodeling, reactive cells and extracellular cues drive the progressive, propagating pathology that culminates in the spinal injury scar (adapted from Bradbury & Burnside, 2019).

Inflammatory response

The neuroinflammatory response plays a key role in secondary injury contributing to local and systemic pathology (Brennan & Popovich, 2018). Beyond initial extravasation of immune cells due to vascular disruption, cellular debris represent damage-associated molecular patterns (DAMPs) that activate prototypical pathogen recognition receptors and act as potent inflammatory stimuli to surrounding cells (including neurons and glia) (**Figure 15**) (Bradbury & Burnside, 2019). In result, these cells will be stimulated to secrete proinflammatory cytokines and chemokines to recruit the immune system.

The inflammatory response begins almost immediately after the initial mechanical damage with blood-derived neutrophils being the first to arrive at the lesion site (Neirinckx et al., 2014). Neutrophils are thought to perform a dual role during the acute phase of the injury. While contributing to phagocytosis and debris clearance, they also release inflammatory cytokines, free radicals and proteases that propagate damage to the adjacent tissue (Taoka et al., 1997). Interestingly, ablation of neutrophils in injured mice at 24 and 48 hpi was shown to worsen the neurological and structural outcomes of SCI, confirming that neutrophils are fundamental players in the early acute stage of the injury (Stirling et al., 2009).

Succeeding neutrophil infiltration, microglia and macrophages (resident and blood-borne monocyte-derived) migrate to the injury site dominating the immune population (Perry & Teeling, 2013). Once there, they promote the expression of chemoattractant and adhesion

molecules in endothelial cells, increasing the extravasation of circulating myeloid cells and lymphocytes to the lesion. Depending on the microenvironmental cues, macrophages may polarized into two different subsets: a pro-inflammatory M1 phenotype and an anti-inflammatory/pro-regenerative M2 phenotype (Kigerl et al., 2009). Although both subtypes co-reside at the lesion epicenter during the first week after SCI, M1 macrophages seem to be preferentially polarized by the injury microenvironment and end up predominating the immune cell population (**Figure 15**) (Kroner et al., 2014). Some studies suggest that this polarization is induced by the T_h1 cytokine IFN-γ, while others indicate that it is driven by TNF-α and intracellular accumulation of iron (David & Kroner, 2011; Kroner et al., 2014). M1 macrophages express high levels of major histocompatibility complex class 2 (MHCII) and continuously activate T cells, contributing to autoimmunity (David et al., 2015). Moreover, they secrete pro-inflammatory cytokines, such as IL-12, IL-23, IL-1β and TNF-α, as well as ROS and RNS (David & Kroner, 2011). M1 macrophages are also associated with higher expression of chondroitin sulfate proteoglycans (CSPGs), which are major inhibitors of neuronal plasticity and axonal regeneration (*see Scarring and Extracellular matrix*) (Bradbury & Burnside, 2019; Martinez et al., 2006). Importantly, though most of this information was obtained from SCI in rodents, there is also evidence for a sustained M1-like polarization after human SCI (Huang et al., 2014). Furthermore, M1 macrophages produce repulsive guidance molecule (RGM) which elicits axonal retraction and inhibits neurite outgrowth (Schwab et al., 2005). In contrast, M2 pro-repair macrophages are polarized by T_h2 cytokines IL-4 and IL-13 and express high levels of immunoregulatory IL-10, TGF-β and arginase-1, while exhibiting reduced expression of NF-κB and pro-inflammatory cytokines (David & Kroner, 2011). Recent studies have shown that IL-10 polarized microglia display enhanced phagocytosis activity, which is important for repair (Dyck et al., 2018). Accordingly, IL-10 knock-out mice displayed

worse recovery of limb function after SCI, as compared with wild-type controls (Genovese et al., 2009).

In response to environmental cues after SCI, reactive astrocytes promote the recruitment of immune cells through secretion of numerous cytokines and chemokines (Pineau et al., 2010). By producing factors such as IL-1β, monocyte chemoattractant protein (MCP)-1, CCL2, C-X-C motif ligand 1 (CXCL1, also known as Gro-α), CXCL2 (Gro-β), TNF-α, IL-12 and IFN-γ, astrocytes recruit neutrophils and endorse the polarization of pro-inflammatory M1 macrophages in a NF-κB-dependent fashion (Cekanaviciute & Buckwalter, 2016; Pineau et al., 2010; Sun et al., 1995). Astrocytes can also induce polarization of pro-regenerative M2 macrophages through secretion of anti-inflammatory IL-10 and TGF-β (Brambilla et al., 2005; Cekanaviciute & Buckwalter, 2016). However, in SCI, stimulation of the M1 phenotype seems to be privileged. Importantly, continued Wallerian degeneration of axonal projections sustains the deposition of DAMPs near but also away from the lesion, activating reactive astrocytes and pro-inflammatory cells throughout the whole spinal cord (Bradbury & Burnside, 2019).

Adaptive T and B lymphocytes are known to infiltrate the injured spinal cord during the first week after mouse and rat SCI (**Figure 15**) (Ankeny et al., 2006; Jones, 2014). Highly stimulated by DAMPs, who work as self-antigens, they remain chronically active eliciting a detrimental autoimmune response that is toxic for neuronal and glial cells. T cells secrete several pro-inflammatory cytokines and chemokines, such as IL-1β, TNF-α, IL-12, CCL2, CCL5, and CXCL10 that promote M1-like macrophage polarization and induce Fas-mediated apoptosis in neurons and oligodendrocytes (Jones, 2014; Yu & Fehlings, 2011). Autoreactive $CD4^+$ effector T (T_{eff}) cells stimulate the activation of antibody-producing B cells that contribute to tissue damage and progressive neuronal loss/demyelination (Ankeny et al., 2009). B lymphocytes further contribute to injury by sustaining the activation of T_{eff} cells through production of pro-inflammatory cytokines (Jones, 2014). In agreement, B-cell knockout mice

(BCKO) showed improved locomotor recovery after contusion SCI, associated with a decreased lesion volume and lower levels of antibodies (IgM and IgG) in the cerebrospinal fluid (Ankeny et al., 2009). In human chronic SCI patients, serological assessment of reactive IgM and IgG levels also confirmed autoimmune activity of T and B cells (Hayes et al., 2002). Importantly, due to eventual leakage of DAMPs into circulation, a chronic activation of T and B lymphocytes can be systemically induced, which significantly deteriorates the pathological outcome of SCI (Ankeny et al., 2006).

Another critical consequence of SCI is the disruption of the neuroimmune communication between the spinal cord and peripheral organs (Brennan & Popovich, 2018). Neurons that control autonomic functions are severely damaged, compromising homeostasis in all organ systems and causing systemic disease (**Figure 16**). This is specially aggravated by the fact that SCI patients show a disruption in the gut microbiome homeostasis, which has a tremendous systemic impact in immune function (Gungor et al., 2016; Kigerl et al., 2016). While some organs, like the liver, display over-inflammation after SCI, others like the lungs or the spleen suffer from immune suppression, leaving SCI patients more prone to infection (Brennan & Popovich, 2018). Therefore, the behavior of the immune system towards a nervous system injury is one of the main causes of morbidity and mortality in SCI patients.

In conclusion, understanding the mechanisms underlying the neuroimmune crosstalk within and outside the spinal cord is paramount to design effective therapeutic strategies to reduce immune-associated tissue damage and stimulate the pro-repair properties of the immune system in order to promote recovery after SCI and restore peripheral organ functions.

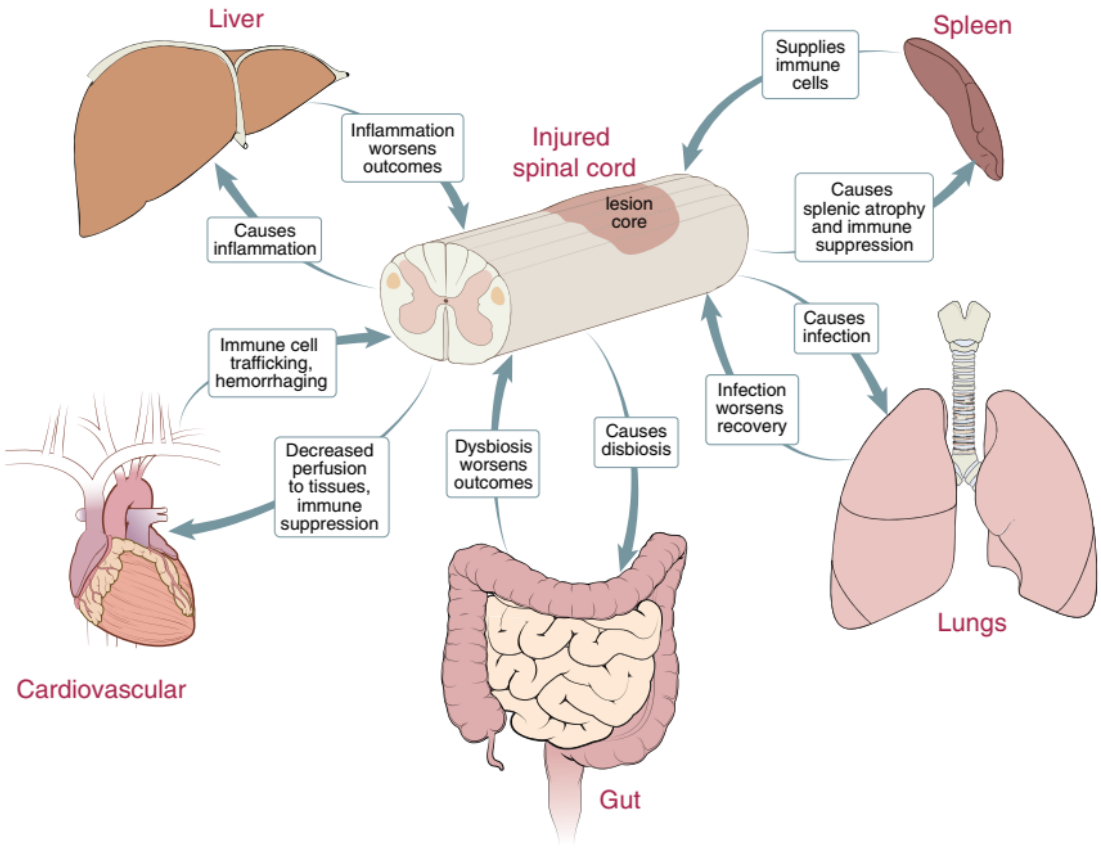

Figure 16. Spinal cord injury disrupts systemic neural–immune communication. Disrupted neuroimmune control in liver, cardiovascular/circulatory system, gut, lungs and spleen can exacerbate intraspinal pathology, impair neurological outcomes and contribute to increased morbidity and mortality after spinal cord injury (from Brennan & Popovich, 2018).

Scarring and Extracellular matrix

Reactive gliosis is one of the main pathological features of SCI and gives rise to a mature astrocytic scar, within which resides a fibrotic scar (Burda & Sofroniew, 2014). Astrocytic reactivity is triggered and enhanced by DAMPs, as well as pro-inflammatory cytokines, such as IFN-γ, IL-6, IL-1β and TNF-α (Sofroniew, 2014). SCI induces the proliferation and migration of parenchymal and ependymal stem/progenitor cells that give rise to scar forming astrocytes and $NG2^{+}$ oligodendrocyte precursor cells (OPCs) (Barnabé-Heider et al., 2010; Meletis et al., 2008). During astrogliosis, astrocytes become hypertrophic and over-

proliferative (Sofroniew, 2014). They also go through a spatial rearrangement and migrate to the lesion border where they surround the lesion core and form elongated processes between each other (**Figure 17**) (Bradbury & Burnside, 2019; Wanner et al., 2013). The formation of this barrier was shown to be mediated by signal transducer and activator of transcription 3 (STAT-3) signaling (Herrmann et al., 2008; Wanner et al., 2013). Importantly, the glial scar has been proved to constitute a vital neuroprotective barrier that avoids the spread of infiltrating immune cells to the adjacent spared tissue (Cregg et al., 2014). In fact, preventing astrocytic scar formation is detrimental for the functional outcome of SCI (Anderson et al., 2016; Okada et al., 2006). Despite this protective role, the chronic persistence of the glial scar is viewed as a potent inhibitor of spinal cord repair/regeneration (Cregg et al., 2014). Notably, in humans, the glial scar has been found to persist up to forty two years after SCI (Cregg et al., 2014; Huang et al., 2014).

The negative role of the glial scar is mainly mediated by secretion of factors and matrix components, such as proteoglycans, that are extremely inhibitory for axonal regrowth (Wiese et al., 2012). ECM composition is extremely important in the central nervous system (CNS), facilitating cellular migration, guidance and synaptogenesis and overall conferring neural stability (Bradbury & Burnside, 2019). However, after SCI, many ECM molecules become deregulated.

Inside the scar, a fibrotic core composed of proliferating PDGFRβ (platelet-derived growth factor receptor beta)$^{+}$ perivascular pericytes and fibroblasts becomes mature within two weeks following SCI (Soderblom et al., 2013). Fibroblasts produce matrix components such as fibronectin, collagen, nidogen and laminin, which are normally permissive to neuronal growth (Gaudet & Popovich, 2014). Yet, these components are highly upregulated in the injured spinal cord and contribute to pathological tissue remodeling, generating a non-permissive environment (**Figure 17**). Furthermore, ECM fragments act as DAMPs and promote

inflammation. Fibroblasts are also a source of chemorepellent semaphoring III, that inhibits axonal regeneration (Pasterkamp et al., 1999). A recent study reported that fibrotic scarring is equally sustained by PDGFRβ$^+$ pericyte-derived deposition of fibronectin and type-I collagen (Okada et al., 2007; Soderblom et al., 2013; Yokota et al., 2017). The latter was shown to be mediated by upregulation of another ECM molecule, periostin, that promotes the overexpression of TNF-α in infiltrating monocytes/macrophages, which in turn boosts the proliferation of PDGFRβ$^+$ pericytes (Yokota et al., 2017).

In turn, the glial scar, as well as reactive astrocytes distal from the lesion site, are responsible for upregulating and producing a number of ECM molecules repress axonal growth and prevent repair (Quadri et al., 2018). These include tenascin, semaphoring III, MAGs, OMgps, Nogo A and CSPGs. Myelin-associated debris (MAGs, OMgps, Nogo A) play the role of DAMPs during SCI, but are, by themselves, neuronal inhibitors (Bradbury & Burnside, 2019). Nogo A binds to membrane Nogo receptors 1 and 3 (NgR1 and NgR3) and activates RhoA/Rho kinase signaling pathway, destabilizing actin cytoskeleton, collapsing growth cones and repressing neurite elongation (Schwab & Strittmatter, 2014). Similarly, CSPGs (such as neurocan, brevican, versican, aggrecan, phosphacan and NG2) are strong inhibitors of neuronal plasticity and axonal regeneration (Ohtake & Li, 2015). They reach a peak of upregulation at two weeks post-injury but remain chronically upregulated (Asher et al., 2002; Buss et al., 2009). CSPGs can bind to other ECM molecules, like hyaluronic acid and tenascin, forming non-permissive perineuronal networks, which hamper growth-promoting adhesion molecules (such as laminin and integrins) and suppress neurite growth (Ohtake & Li, 2015). Interestingly, in astrocytes, CSPG production has been shown to be induced by TGF-β in a Smad-2- or PI3K/AKT- and mTOR-dependent manner (Jahan & Hannila, 2015; Schachtrup et al., 2010). Curiously, CSPGs can also bind to NgR1 and NgR3 (Dickendesher et al., 2012). However, CSPG inhibitory effects seem to be mainly mediated by signaling via receptor protein tyrosine phosphatase

sigma (PTPσ) and leukocyte common antigen-related phosphatase receptor (LAR) (Lang et al., 2015). Accordingly, blockade of PTPσ and LAR receptors has resulted in improved axonal regeneration after SCI. In another study, PTPσ and LAR inhibition promoted a shift from pro-inflammatory M1 to pro-regenerative M2 macrophage environment, accompanied by an upregulation of anti-inflammatory IL-10 and arginase-1 (Dyck et al., 2018). Given their potent inhibitory nature, CSPGs have been demarcated as an important therapeutic target to improve axonal regeneration after SCI. Indeed, enzymatic degradation of CSPGs using chondroitinase ABC (ChABC) in rodent models of SCI has been shown to promote axonal growth, reduce scarring, prevent axonal degeneration and improve locomotor function (Bradbury et al., 2002; Karimi-Abdolrezaee et al., 2010). Strikingly, this effect has been verified in multiple other species, including cats, dogs and even primates (Bradbury & Carter, 2011; Hu et al., 2018; Rosenzweig et al., 2019). However, translation of ChABC treatment to human patients is still lacking.

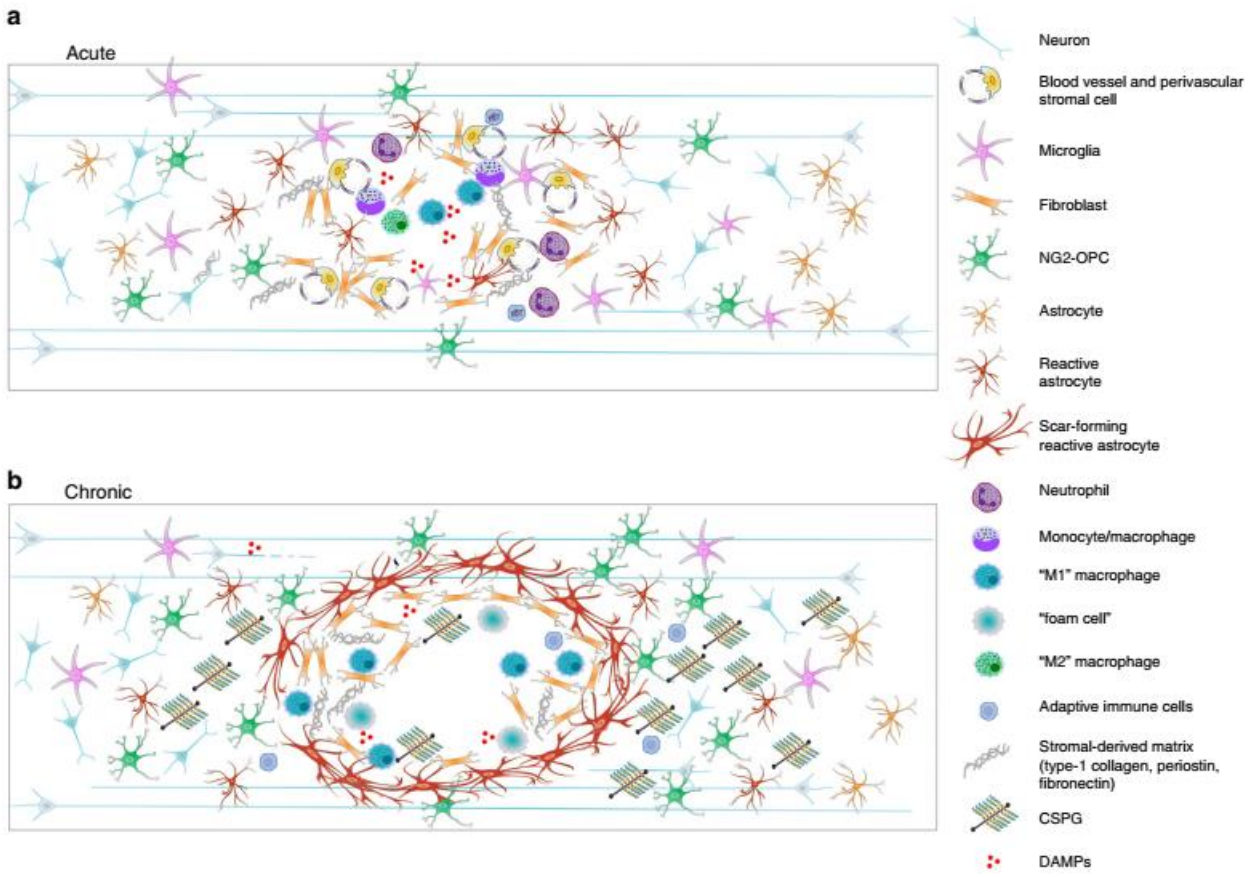

Figure 17. Cellular and extracellular composition of the spinal injury scar. Traumatic spinal cord injury triggers a complex cascade of events that culminate in the spinal injury scar which consists of multiple cell types as well as extracellular and non-neural components. **(a)** In the acute post-injury phase (0–72 h), cell death and damage lead to release of a number of cellular and blood-derived DAMPs (damage associated molecular patterns). These are powerful activating and inflammatory stimuli for stromal cells, astrocytes, $NG2^+$ OPCs and microglia. Fibroblast-like cells proliferate from perivascular origin. Activated cells increase deposition of extracellular matrix molecules such as chondroitin sulfate proteoglycans (CSPGs) and stromal-derived matrix. Circulating immune-responders (neutrophils, monocytes) are recruited, their relative expression of cytokines, chemokines and matrix metalloproteinases becomes shaped by the early injury environment, and a mixed immune cell phenotype (M1, pro-inflammatory; M2, pro-resolving) is initially adopted. This becomes increasingly pro-inflammatory. **(b)** In the chronic spinal injury scar, monocyte-derived macrophages/microglia adopt a predominant M1 phenotype. Rather than entering a phase of resolution, responding innate immune cells present DAMPs to circulating adaptive immune cells and pathology spreads. Reactive astrocytes hypertrophy, upregulate expression of intermediate-filament associated proteins and secrete matrix CSPGs. Fibroblast-like cells contribute to fibrotic tissue remodeling and deposition of stromal-derived matrix. Innate immune cells become unable to process cellular and matrix debris effectively and become synonymous with lipid-rich foam cells. Scar-forming reactive astrocytes organize into a barrier-like structure which separates spared tissue from a central region of inflammation and fibrosis where wound-healing fails to undergo resolution. In most mammalian species a chronic cystic cavity develops. Wallerian degeneration of injured axonal projections contributes to continued extracellular deposition

of axonal and myelin debris, which is ineffectively processed by immune cells, and along with CSPGs, acts to inhibit neuronal regeneration and neuroplasticity long-term (from Bradbury & Burnside, 2019).

Non-regenerating models of SCI

Currently, there are several available non-regenerating mammalian models to study SCI, ranging from rodents to large animals (cats, dogs, pigs) and non-human primates (Nardone et al., 2017). Though all of them have been extremely useful in providing valuable insights on primary and secondary mechanisms of SCI, it is important to take into account potential anatomical, molecular and functional differences towards humans. This is especially true for rodents (Nardone et al., 2017). Ideally, an animal model should recapitulate several pathophysiological features of human SCI in a reproduceable manner.

Animal models

Rodents are the most frequently used models of SCI, given their availability, convenience and cost-effectiveness (Nardone et al., 2017). Strikingly, rodent models exhibit high levels of spontaneous recovery from SCI. Compared to mice, rats are more similar to humans in terms of pathophysiological and neuroanatomical of SCI (Kjell & Olson, 2016; Metz et al., 2000). However, mice have the undeniable advantage of the amount of different available transgenic and mutant models that have been fundamental to study the molecular and cellular mechanisms of SCI. In rats, just like in humans, a fluid-filled cystic cavity is formed at the injury site, while in mice the lesion core is filled with dense fibrotic tissue (Sroga et al., 2003). Rats and mice also exhibit different temporal windows of inflammatory reactions. For example, rats have their neutrophil infiltration peak at 24-48 hpi whereas in mice neutrophil infiltration continues to

rise up until 14 dpi (Kigerl et al., 2006; Taoka et al., 1997). Such evidences reinforce the existence of distinct environmental cues between different models.

Large animals, like dogs and pigs, are considered an intermediate model between rodents and humans and have been used in a wide range of pre-clinical studies (Nardone et al., 2017). Curiously, the first model study of experimental SCI was performed on dogs in 1911 (Allen, 1911). Nowadays, though, the use of these models raises strong ethical issues. Yet, though rodents have been the standard SCI model over the past decades, large animals are becoming increasingly utilized for translational pre-clinical purposes (Kwon et al., 2015).

Primates resemble human-like features like no other model and have emerged as a unique model to expand our knowledge on SCI features and test candidate therapies before they are applied to human patients (Nout et al., 2012). Importantly, their size constitutes a great platform for electrophysiological and rehabilitation studies. Still, the need for specialized facilities, their maintenance-associated costs and ethical constraints, have so far limited their use in SCI research (Kwon et al., 2015).

Experimental injury models

In order to mimic various aspects of human SCI mechanics, three different experimental injury models are available: transection, contusion and compression models (Cheriyan et al., 2014).

Transection injuries very rarely happen in humans and, when they do, are usually the result of severe sharp bone fragment dislocations or missile injuries in the military (Dumont et al., 2001). Therefore, transection animal models do not authenticate normal human SCI and are less suitable for the development of new therapies. Nonetheless, they are useful to test the application of biomaterial scaffolds, study the role of propriospinal and sensory circuits (CPGs)

in locomotor recovery or even neuronal plasticity after a partial transection (Barbeau et al., 1999; Cheriyan et al., 2014).

Contusion models better resemble the transient mechanical impact that is characteristic of human SCI (Cheriyan et al., 2014). A contusion injury can be generated using a weight drop, an electromagnetic impactor or an air gun device. The first method is the most commonly used and involves a metal impactor of specific weight dropping in the exposed dorsal side of the spinal cord (Cheriyan et al., 2014). This type of devices has been improved through the years and impactors are now much more reliable and automated in view of better controlling injury parameters, such as the force, time and velocity of impact, as well as recording the tissue biomechanical response. Another advantage of the contusion impactors is the possibility of setting the impact force to produce different severities of SCI (Cheriyan et al., 2014). However, it is important to consider that the positioning of the impactor clamps in the spinal column is subject to some variability, which may cause some inconsistency in injury parameters. Nevertheless, impactor devices are extensively used in small and large animal models of SCI and have provided invaluable knowledge to understand secondary injury mechanisms (Cheriyan et al., 2014; Petteys et al., 2017).

Compression models are typically contusive-compressive models, as they consist of an initial contusion impact followed by a prolonged compression through force application (Cheriyan et al., 2014). Compression is achieved both dorsally and ventrally by applying a modified aneurysm clip to the injured spinal cord. In larger animals (cats, dogs and primates), compression is usually applied inserting a catheter with an inflatable balloon filled with air or saline in the epidural or subdural space (Fukuda et al., 2005; Nesathurai et al., 2006). These models has the advantage of better correlate to human SCI, though in humans compression may last indefinitely (Poon et al., 2007). However, they have the limitation of not being able

to measure the velocity and force of compression, which may create variabilities (Cheriyan et al., 2014).

Regenerating models of SCI

Regenerating models, such as the zebrafish and the salamander, are powerful tools to identify key differences in cellular and environmental responses to injury comparatively to non-regenerating mammals (Ghosh & Hui, 2018; Tazaki et al., 2017). Zebrafish offers a promising model to study SCI due to the availability of genome-editing and high-throughput DNA/RNA sequencing tools that allow human disease modeling. On the other hand, salamanders have benefited from recently developed CRISPR editing tools to study cellular responses to SCI. Strikingly, an intriguing mammalian model with regenerating properties, the spiny mouse (*Acomys cahirinus*), was recently discovered to have improved functional outcomes to SCI comparing to C57BL/6 (*Mus*) mice (Streeter et al., 2019). Thus, *Acomys* is currently suggested to be a useful model to study differences in the adaptive response to SCI towards other mammalian models.

The Zebrafish

Adult zebrafish (*Danio rerio*) have an outstanding ability to regenerate their spinal cord and achieve complete functional recovery after SCI (Becker & Becker, 2006; Ghosh & Hui, 2018). In contrast to mammals, zebrafish are capable of regrowing damaged axons and replace damaged cells, including neurons (Ghosh & Hui, 2018). Zebrafish axonal regeneration has been extensively evaluated in models of transection and crush injury, which have provided

evidence for key differences in cellular and molecular pathways involved in injury response relatively to mammals. However, some of these mechanisms are not yet fully understood.

After zebrafish SCI, ependymo-radial glial progenitors proliferate and migrate to the injury site, giving rise to new neurons (Reimer et al., 2008). Reported data suggest that neurogenesis occurs at the lesion epicenter and the adjacent area, which are both occupied by proliferating neuronal precursors ($Hu^+/BrdU^+$) and neuronally determined cells ($Hu^+/NeuroD^+$) (Hui et al., 2010). Interestingly, foxj1a was recently described as a pan-ependymal progenitor marker in zebrafish development, homeostasis and regeneration (Ribeiro et al., 2017). Previous evidence also suggests the existence of a quiescent population of neural progenitors in the adult mammalian CNS (Alvarez-Buylla et al., 2002; Gage, 2000; Morshead et al., 1994). In mammalian SCI, ependymal progenitors give rise to scar-forming astrocytes and OPCs, but not neurons (Barnabé-Heider et al., 2010; Meletis et al., 2008). Curiously, these cells were shown to differentiate into neurons *in vitro*, suggesting that their inability to do so *in vivo* results from inhibitory environmental signals (Meletis et al., 2008). This perspective has been recently contested by a transcriptomic study stating that ependymal progenitors lack neurogenic potential (Shah et al., 2018) and remains, therefore, controversial. In zebrafish, radial glial neurogenesis has been demonstrated to be dependent on Wnt/β-catenin signaling, stimulated by high mobility group box 1 (HMGB1) and inhibited by Notch signaling (Briona et al., 2015; Dias et al., 2012; Fang et al., 2014). Moreover, motor neuron polarization was shown to be mediated by sonic hedgehog signaling (Reimer et al., 2009). Importantly, proliferation and differentiation of motor neurons was observed until 6 weeks post-injury (wpi) (Reimer et al., 2008).

Following SCI, fishes become paralyzed caudal to the lesion site but, remarkably, they display a gradual functional recovery and regain their normal swimming behavior within 4−6 weeks (Becker et al., 2004; Becker & Becker, 2014; Becker et al., 1997; Hui et al., 2010). Severed

axons are able to regrow and, by 14 dpi, they have crossed to the distal part of the lesion (Becker et al., 1997; Goldshmit et al., 2012). By 42 dpi, regrowing axons project at least 3.5 mm beyond the injury site. Strikingly, during the first six dpi, axotomized upper motor neurons of the brainstem upregulate anti-apoptotic factors, such as BCL-2 (Ogai et al., 2012). These motor neurons do not only survive also regrow their severed axons, which descend and cross the injury site. Intriguingly, most regenerating axons preferentially re-route through the gray matter and not the white matter, which is thought to be mediated by macrophages and microglia (Becker & Becker, 2001). This indicates that, though zebrafish accomplish a full functional recovery, their spinal cord may present structural differences after recovery from SCI. Previous studies have shown that axonal regrowth in zebrafish is correlated with upregulation of L1-related recognition proteins, namely L1.1 and L1.2, contactins and major vault protein (Becker et al., 2004; Pan et al., 2013; Schweitzer et al., 2007). Additionally, syntenin-a, a protein involved in synapse formation, is upregulated caudal to the lesion site at 6 and 11 dpi (Yu & Schachner, 2013).

In zebrafish, there is no evidence of astrogliosis or a CSPG-expressing glial scar (Becker & Becker, 2014). Instead, there is the formation of a growth-permissive glial bridge that guides migrating axons across the lesion site (Goldshmit et al., 2012; Hui et al., 2010). The formation of this glial bridge has proven to be necessary for proper axonal regeneration and is dependent on fibroblast growth factor (FGF) and Wnt/β-catenin signaling (Goldshmit et al., 2012; Strand et al., 2016). Myelin-associated inhibitory molecules, such as Nogo A, also exist in the zebrafish CNS and there is even evidence for NgRs in regenerating axons (Abdesselem et al., 2009). However, Nogo A-specific N-terminal inhibitory domain is missing and Nogo A fails to induce growth cone collapse. Importantly, in zebrafish SCI, myelin debris are efficiently removed by macrophages (Hui et al., 2010). In addition, Schwann cells are broadly present at the lesion site and play a key role in remyelination of regrowing axons.

There is also a transient apoptosis-mediated mechanism of debris clearance that peaks at 1 dpi and is practically absent at 7 dpi (Hui et al., 2010). This seems to be fundamental to avoid the progression of secondary injury. Similarly to mammals, neutrophils and macrophages infiltrate the lesion site immediately after zebrafish SCI. Yet, in contrast, their inflammatory response is transient during the first 10 dpi and their role seems to be primarily associated with phagocyting debris and promoting remyelination, contributing to an efficient repair process (Hui et al., 2010).

Due to the availability of a wide range of genetic tools, zebrafish reporter and transgenic lines have been extensively used to study the cellular and molecular dynamics after SCI. Though a powerful tool, zebrafish SCI models have the limitation of being totally manually performed by experimenters, which generates variability between injuries. Still, it represents a very convenient model given the low cost of maintenance, as well as the ease and swiftness of generating significant numbers for experimentation. In fact, zebrafish larvae can regenerate their spinal cords and recover their locomotor function in a matter of 5 days (Briona & Dorsky, 2014). Thus, zebrafish larvae have been proposed as a drug screening platform to test new therapeutic strategies for SCI (Chapela et al., 2019).

Therapeutic strategies for SCI

Several therapies have provided promising pre-clinical data but, so far, translation into human clinical trials has failed to demonstrate the efficacy of a repair strategy in meaningful improved recovery after SCI (Courtine & Sofroniew, 2019). Current therapeutic approaches for chronic SCI are based on cell therapies (repopulation of lost cells), molecular therapies (specific targeting), biomaterials (modulation of ECM) and bioengineering strategies (enable motor

control, bypass lesion or promote neurorehabilitation) (Courtine & Sofroniew, 2019; Dalamagkas et al., 2018).

Stem cell transplantation takes advantage of cellular plasticity to repopulate lost cells and can be applied alone or in combination with growth factors and/or biocompatible scaffolds to restore neuronal circuitry (Dalamagkas et al., 2018). Several types of stem cells have reached up to clinical trials phase I/II, including adult neural stem cells (*"Pathway Study" by Stemcell Inc.*), human spinal cord stem cells (*"NSI-566" by NeuralStem Inc.*), olfactory ensheathing cells (*"Walk Again Project"*), autologous Schwann cells (*"Miami Project"*), umbilical cord blood-derived mononuclear cells (*"ChinaSCINet"*), adult mesenchymal cells (*"Puerta de Hierro"*), and autologous bone-marrow-derived stem cells (*"Neurocell" by Neuroplast*) (Dalamagkas et al., 2018). While some of these clinical trials have provided some evidence of functional recovery and are still ongoing, others have been stalled, halted or even shut down due to cost-efficiency issues, patient recruitment setbacks or inconclusive results. *"Neurocell"* is estimated to start phase I in February 2020 (NCT04205019).

An interesting molecular therapy (*"Nogo Trap" by ReNetX Bio*) using a decoy receptor for myelin-associated axonal growth inhibitors, such as Nogo A, has demonstrated functional improvements in multiple animal models and is now recruiting chronic SCI patients for phase I/II clinical trial (NCT03989440). The CHASE initiative was born in 2014 when Bradbury's team reported that administration of the bacterial enzyme ChABC degrades inhibitory CSPGs, reducing the glial scar, modulating macrophages to a M2 phenotype, promoting axonal growth and improving motor function (Bartus et al., 2014; Bradbury et al., 2002). Since then, ChABC has been molecularly engineered to be delivered via gene therapy and can now be expressed in human cells in a controlled inducible manner, using doxycycline (Muir et al., 2017). Currently, the gene therapy approach is being optimized to make it clinically acceptable for clinical trials. Though ChABC treatment showed unprecedented improvements in locomotor function in

rodents, it is yet unclear if the same effects will be translated into humans. Another pre-clinical study is using ChABC in combination with intracellular sigma peptide, a modulator of PTPσ activity (Tran et al., 2018). This combined treatment was shown to enhance axonal outgrowth and is being prepared to enter clinical trialing.

The use of biomaterials primarily aims at providing the environmental properties (mechanical and chemical) of the native ECM in order to stimulate tissue regeneration (Dalamagkas et al., 2018). Notwithstanding, they also play a fundamental role in controlled delivery of transplanted cells, as well as growth and chemoattractant factors (Anderson et al., 2018; Dalamagkas et al., 2018). Furthermore, they can be engineered with specifically aligned guidance channels to direct axonal growth and prevent unfavorable trajectories. Promising biomaterials with solid pre-clinical data include scaffolds based on graphene oxide (GO), fibrin, collagen/heparin and chitosan/laminin (Dalamagkas et al., 2018). GO bioscaffolds are showing considerable potential in several pre-clinical studies and is currently regarded as an emerging technology for future treatment of SCI (Dalamagkas et al., 2018; Domínguez-Bajo et al., 2017; López-Dolado et al., 2016). FDA-approved fibrin glue has been used in combination with FGF to improve motor and sensory functions is SCI patients (Wu et al., 2011). Pre-clinical studies have also shown motor and sensory improvements by using peripheral nerve grafts combined with a chitosan/laminin scaffold co-transplanted with bone marrow-derived mesenchymal stem cells (Amr et al., 2014). Though slowly advancing, biomaterial and tissue engineering technologies hold great promise in SCI repair (O'Shea et al., 2017).

The main purpose of engineering strategies is harnessing the intrinsic capacity of spared circuits to generate movement (Courtine & Sofroniew, 2019). Chemical/electrical neuromodulation/stimulation, delivered directly to spared sensorimotor circuits below the lesion, has enabled unexpected levels of motor control both in animal models and human SCI

patients. Strikingly, patients with chronic complete paralysis regained relatively fine voluntary control of paralyzed muscles after epidural electrical stimulation (Angeli et al., 2014; Grahn et al., 2017). Interestingly, electrical stimulation was also demonstrated to improve autonomic respiratory and cardiovascular functions (Hachmann et al., 2017; Phillips et al., 2018). Another strategy is targeting proprioceptive fibers associated to specific lumbar-sacral posterior roots in order to stimulate motor neurons located in the spinal segment that is enervated by these roots (Courtine & Sofroniew, 2019). This method has also triggered control over movements of paralyzed legs in animal models and human SCI. In these studies, a controlled spatiotemporal electrical stimulation improved the amplitude and robustness of leg movements, as compared to continuous stimulation.

Neurorehabilitation remains a common medical practice in treating SCI. It is well accepted that the repeated activation of the sensorimotor system promotes plasticity of spared circuits and brings meaningful recovery benefits (Côté et al., 2017; Courtine & Sofroniew, 2019). Thus, activity-based neurorehabilitation is frequently used in combination with neuromodulation and cortex stimulation strategies to improve neural plasticity. Though the mechanisms underlying activity-mediated neuroplasticity are still unclear, accumulating evidence suggests an important role of the interplay between supraspinal signals and proprioceptive information (Courtine & Sofroniew, 2019).

The use of brain-computer interfaces is an innovative therapeutic strategy that aims at re-establishing bidirectional communication between the brain and denervated body parts (Courtine & Sofroniew, 2019). In recent years, intracortical stimulation of the human somatosensory cortex has achieved astonishing results, such as restoration of reaching and grasping movements in paraplegic and tetraplegic patients (Ajiboye et al., 2017; Bouton et al., 2016; Capogrosso et al., 2016; Ethier et al., 2012; Flesher et al., 2016). However, this technology currently faces a number of practical and financial roadblocks that overshadow

their modest functional benefits, a challenge that likely only time will resolve (Borton et al., 2013).

Wrapping Up: The Road Ahead

It is clear that SCI is a very complex and multifaceted pathology. For reasons that are not yet understood, our CNS is uncapable of regenerating and, even though much has been learned about cellular and molecular responses to CNS injury, we are still far away from a groundbreaking therapy. SCI involves an intricate interplay between numerous different cell types (neurons, glial cells, perivascular cells, immune cells), their intracellular changes and signaling pathways, as well as the extracellular microenvironment. Perhaps even more relevantly, these players modulate and feedback on each other in variable ways during different temporal windows. Therefore, it is believed that only a combined therapeutic approach can achieve significant recovery improvements. Ideally, a therapy should be able to simultaneously tackle multiple SCI features, such as replacing lost neuronal cell populations, promoting neural plasticity, activating intrinsic neuronal growth programs, preventing axonal degeneration, controlling/resolving inflammation, establishing a growth-permissive microenvironment and stimulating/guiding axonal regeneration through and beyond that environment. However, combinatorial therapies should take in consideration the way these mechanisms interact with one another over the course of recovery from SCI and, thus, should be tailored accordingly. Importantly, while most therapies envisage restoring motor functions, we should not forget that, for many SCI patients, recovering some of their autonomic functions, such as control of bladder movement and sexual function, is among their top priorities. Therefore, such functions should be equally tackled during pre-clinical studies.

The small progress that is being obtained on therapeutic options raises relevant questions: do we know all cellular players involved in SCI? With so many different environmental cues happening in space and time, are there any cell intrinsic mechanisms we are missing?

The use of pre-clinical animal models has been fundamental to increase our understanding of SCI mechanisms. However, the majority of these models cannot fully reproduce the hallmarks of human SCI. In result, several therapies that obtain promising pre-clinical results fail to generate functional improvements with meaningful clinical impact in humans. This could be particularly countered by the use of non-human primates but translational research using this model still faces technical, logistic and cost-related difficulties, as well as daunting ethical constraints.

The field of neuroprosthetics is steadily advancing but current technologies still lack further refinement. The truth is that SCI patients still prefer a wheelchair over an exoskeleton (Gorgey, 2018).

The appearance of regenerating models of SCI, like the zebrafish, has provided a fantastic tool to investigate what differences lie in the injury response that allow these animals to fully recover their locomotor functions. In fact, accumulating evidence points at clear environmental differences in the zebrafish spinal cord towards the mammalian counterpart. In the zebrafish, cellular death and inflammation are temporally controlled and, instead of an inhibitory glial scar, a glial bridge is formed at the injury site to help axons regrow and reconnect beyond the lesion. So, why are mammals unable to effectively resolve their reactive cellular responses to SCI like the zebrafish? Why are these responses maintained chronically? Though much of the cellular and molecular mechanisms underlying zebrafish SCI are yet to be clarified, the answer to these questions seems to indeed lie in distinct *in vivo* microenvironments. Thus, understanding these differences may shed a light on novel therapeutic avenues for SCI.

While many challenges still await us ahead, efforts are being joined in the field of biology and engineering to decipher the complex nature of traumatic SCI and provide a better quality of life to patients. Will we ever be able to regenerate the spinal cord?

RESEARCH AIMS AND PROJECT OUTLINE

The main objective of this thesis project was to study the role of Senescent Cells (SCs) in Spinal Cord Injury (SCI) using two animal models with distinct regeneration outcomes – the Zebrafish and the Mouse.

The first part of the project (**Chapter I**) comprised the following aims:

- **Investigate if SCs exist in the spinal cord.** To do that, we performed the widely used senescence-associated β-galactosidase (SA-β-gal) assay. Then, we looked for co-expression of SA-β-gal with other senescence biomarkers, namely $p16^{INK4a}$, $p21^{CIP21}$ and γ-H2AX.
- **Characterize the senescence profile induced after SCI,** quantifying the number of SA-β-gal^{+} cells at several time-points following injury.
- **Identify which cell types compose the SC population,** searching for co-expression of SA-β-gal with different cellular markers.
- **Compare differences between a regenerating model (the zebrafish) and a non-regenerating model (the mouse).**

The second part of the project (**Chapter II**) consisted on investigating the functional contribution of SCs to the injury process, encompassing the following aims:

- **Optimize a pharmacological protocol to successfully eliminate SCs inside the zebrafish spinal cord.** Considering the lack of a senescence-targeted zebrafish transgenic line or of a described protocol to pharmacologically target SCs in the zebrafish, we tried to optimize the administration of drugs with known senolytic activity.
- **Deplete SCs in the injured mouse spinal cord adapting a previously described senolytic protocol.** We depleted SCs in vivo by oral administration of a senolytic drug, ABT-263. The impact of eliminating SCs was assessed on locomotor and sensory recovery. We also evaluated the effect of ABT-263 on myelin preservation, scarring, inflammation and axonal growth.

- **Characterize the transcriptome and secretome of induced-SCs through time,** taking advantage of an existing $p16^{INK4a}$-tagged transgenic mouse model to sort these cells. Additionally, we used this model to genetically ablate SCs and see the effect on functional recovery in a completely independent manner.

METHODS

1. Ethics statement

All handling, surgical and post-operative care procedures were approved by Instituto de Medicina Molecular Internal Committee (ORBEA) and the Portuguese Animal Ethics Committee (DGAV), in accordance with the European Community guidelines (Directive 2010/63/EU) and the Portuguese national legislation on animal care (DL 113/2013). All efforts were made to minimize the number of animals used and to decrease suffering of the animals used in the study.

2. Senescence-associated β-galactosidase (SA-β-gal) staining

The SA-β-gal assay is the gold standard method to identify senescent cells *in vitro* or *in vivo* (Dimri et al., 1995) and it was performed in all samples during this project. SA-β-gal activity was determined in isolated spinal cords using the SA-β-gal kit (Cell Signalling, #9860) according to manufacturer's instructions, with minor adaptations. Spinal cords were fixed overnight (ON) in 4% paraformaldehyde (PFA, pH 7.4), washed three times during the day in phosphate buffered saline 1x (PBS, 17 mM KH_2PO_4, 5 mM Na_2HPO_4, 150 mM NaCl, pH 7.4) and stained overnight (ON) at 37°C (in a dry incubator with no CO_2) with fresh SA-β-gal staining solution: 1 mg of 5-bromo-4-chloro-3-indolyl β-D-galactoside (X-Gal) per ml (stock = 20 mg/mL in dimethylformamide)/40 mM citric acid/sodium phosphate, pH 6.0/5 mM potassium ferrocyanide/5 mM potassium ferricyanide/150 mM NaCl/2 mM $MgCl_2$. Final pH was set to 5.9-6.1 with 1N HCl. All components of the formulation were provided in the kit. The following morning, samples were washed three times (3 x 5 min) in PBS, fixed in 4% PFA for 4 hours at room temperature (RT), washed three more times (3 x 5 min) in PBS and processed as described in the methodological sections below.

3. Zebrafish (*Danio rerio*)

3.1. Maintenance, handling and transgenic lines

All adult wild-type (*wt*) AB strain and transgenic zebrafish lines were maintained in a re-circulating system with a 14-hour light and 10-hour dark cycle periods at 28°C, following the standard guidelines for fish care and maintenance protocols. Male and female fish were used in the experiments. Zebrafish transgenic reporter lines used in this project were kindly provided by other laboratories and established at our fish facility. Their source and purpose within this study are described in **Table 1**.

Transgenic Reporter Line	Source	Description
Tg(gfap:GFP)	Bernardos & Raymond, 2006	GFP expression in all glial cells
Tg(foxj1a:GFP)	Caron et al., 2012	GFP expression in ependymal progenitors

Table 1. List of transgenic lines used in this project.

3.2. Spinal cord injury (SCI) model

Adult zebrafish spinal cord injury procedures were performed according to a previously described method (Fang et al., 2012). Zebrafish (6 months old) were anaesthetized in 0.016% tricaine (Sigma, MS222). Upon cessation of opercular respiratory movements, the fish were transferred into a fixed thin filter paper (3 cm x 2 cm) placed on crushed ice and positioned on their side with their head pointing left, under a stereoscope. With a dissecting knife (Fine Science Tools, 10055-12), 4-5 squamae were removed and an incision was made at a distance 4 mm caudal to the brainstem/spinal cord junction. The skin and muscle were cut with a spring scissor (Fine Science Tools, 15024-10) until the spinal cord was exposed. The spinal cord was

then crushed using Dumont #55 forceps (Fine Science Tools, 11255-20). Special attention was given not to damage the ventral vertebrae under the spinal cord, which may compromise the recovery process. Finally, the wound was sealed with tissue adhesive surgical glue (3M Vetbond™, 1469SB). Animals were allowed to recover at 28°C in individual tanks until different experimental time-points (3, 7, 15, 30 and 60 days post-injury, dpi), upon which they were sacrificed and the spinal cords (5-6 mm width) dissected. In control fish, a sham injury was performed by making an incision at the side of the animal, exposing the spinal cord but leaving it intact before sealing the wound. All surgical instruments were autoclaved and disinfected with 70% ethanol before the surgery.

3.3. Tissue Processing

The vertebral column of adult zebrafish was dissected and fixed in 4% PFA at 4°C ON. After fixation, the spinal cord was isolated from the vertebral column. Samples were washed three times in PBS during the day and incubated ON with SA-β-gal staining solution (*see details in **2.***). Following the SA-β-gal staining protocol, samples were cryoprotected in 30% sucrose/0.12 M phosphate buffer (PB) for a minimum of 72h at 4°C or until the tissue sinks to the bottom of the vial, followed by another embedding in 7.5% gelatin (Sigma, G6144)/15% sucrose/0.12 M PB and subsequently frozen. The samples were cryosectioned in 12 µm-thick longitudinal slices using a Cryostat LEICA CM 3050S and either processed for immunohistochemistry or counterstained with eosin for SA-β-gal quantifications.

3.4. Quantification of SA-β-gal$^+$ cells after SCI (Senescence profile characterization)

To characterize the senescence profile in zebrafish after SCI, SA-β-gal$^+$ cells were quantified and averaged across 4 longitudinal sections imaged at the lesion periphery (from 0.5 to 2.5 mm

laterally to the injury, rostral and caudal) around the center canal. A 0.5 mm interval was established between the lesion border and the beginning of the quantification regions. SA-β-gal$^+$ cells were quantified in the gray matter but not in the white matter. Quantifications were performed at 3, 7, 15, 30 and 60 dpi and, in each section, the number of SA-β-gal$^+$ cells counted was normalized to the total area of grey matter analyzed. Rostral and caudal quantifications were grouped together and presented as SA-β-gal$^+$ cells/mm^2 at the lateral side of the injury. In control uninjured (sham) zebrafish, SA-β-gal$^+$ cells were quantified in the same regions.

3.5. Senescence profiling during zebrafish embryonic development

Following the arrangement of mating pairs, zebrafish *wt* AB strain embryos were collected and kept at 28°C in a Petri dish containing E3 embryo medium (5 mM NaCl, 0.17 mM KCl, 0.33 mM $CaCl_2$, 0.33 mM $MgSO_4$, 0.01% Methylene Blue, pH 7.4) until the desired developmental stage (3, 8, 24, 48 and 72 hours post-fertilization, hpf). Selected embryos or larvae were fixed with 4% PFA overnight ON at 4°C, washed in PBS and incubated with SA-β-Gal staining solution (*see details in **2.***) at 37°C ON in a dry incubator. Next day, samples were washed in PBS and fixated with 4% PFA for another 4h at RT. 3, 8 and 24 hpf embryos were mounted in glycerol for imaging while 48 and 72 hpf larvae were embedded in a 5-30% sucrose (in PBS, 0.1% sodium azide) gradient, followed by another embedding in 7.5% gelatin/15% sucrose (in PBS), prior to cryosectioning. The sections were counterstained with eosine. Images were obtained using a Zeiss AxioImager Z2 microscope equipped with an Axiocam 105 color camera and a Zeiss Lumar V-12 stereoscope equipped with a Zeiss digital color camera using a 0,8X air objective and the Zen 2 PRO software.

3.6. Senescence profiling upon larvae SCI

Zebrafish *wt* AB strain larvae with 5 days post-fertilization (dpf) were anesthetized in 0.016% tricaine (Sigma, MS222), placed in a lateral position under a stereoscope and a transection injury was performed at the level of the anal pore using a sharp 28-gauge injection needle. Injured larvae were then transferred to a petri dish with E3 embryo medium (5 mM NaCl, 0.17 mM KCl, 0.33 mM $CaCl_2$, 0.33 mM $MgSO_4$, 0.01% Methylene Blue, pH 7.4). Animals were sacrificed at 1, 2, 3 and 4 dpi, fixed with 4% PFA at 4°C ON, washed in PBS and incubated with SA-β-Gal staining solution (*see details in **2.***) at 37°C ON in a dry incubator. Following another wash, samples were fixated with 4% PFA for another 4h at RT. Whole-mount images were obtained with a Zeiss Lumar V-12 stereoscope equipped with a Zeiss digital color camera using a 0,8X air objective and the Zen 2 PRO software, before samples were embedded in a 5-30% sucrose (in PBS, 0.1% sodium azide) gradient, followed by another embedding in 7.5% gelatin/15% sucrose (in PBS), prior to cryosectioning. The sections were counterstained with eosine and images were assessed using a Zeiss AxioImager Z2 microscope equipped with an Axiocam 105 color camera.

3.7. Drug treatment

In order to eliminate SCs in the zebrafish, optimizations were performed concerning ABT-263 (Navitoclax), a drug with previously described senolytic activity (Chang et al., 2016).

First, the effect of ABT-263 was tested after larval spinal cord injury. For that, injuries were performed at 5 dpf in several zebrafish larvae (*see **3.6.***), who were then transferred to six-well plates containing either 0.1-100 µM ABT-263 or vehicle (Dimethyl sulfoxide, DMSO). Both substances were diluted in E3 embryo medium (5 mM NaCl, 0.17 mM KCl, 0.33 mM $CaCl_2$, 0.33 mM $MgSO_4$, 0.01% Methylene Blue, pH 7.4), which was replaced at 1 dpi. Zebrafish

larvae were sacrificed at 2 dpi, fixed whole-mount with 4% PFA at 4°C ON, washed in PBS and incubated with SA-β-Gal staining solution (*see details in **2.***) at 37°C ON in a dry incubator. ABT-263 was also tested in different incubation temperatures (28-33°C) and a diluted embryo medium composition (E1, 1,67 mM NaCl, 0.06 mM KCl, 0.11 mM $CaCl_2$, 0.11 mM $MgSO_4$, 0.003% Methylene Blue, pH 7.4, 10 mM HEPES buffer).

In adult zebrafish, three different administration protocols were tested. In the first, 100-500 µM ABT-263 or Vehicle (polyethylene glycol 400:Phosal 50PG:Ethanol, 30:60:10 v/v) were administrated by intraperitoneal injection (IPi) every 48h starting at 5 dpi until 9 dpi; spinal cords were dissected at 10 dpi. In the second, 100-500 µM ABT-263 or Vehicle were administrated via oral gavage following a previously described protocol (Dang et al., 2016). Gavages were performed every 48h starting at 5 dpi until 9 dpi and spinal cords were dissected at 10 dpi. In the third, 100 µM ABT-263 was applied using an absorbable GELFOAM® Sterile Sponge (Pfizer) placed adjacent to the lesion site right after the injury (before wound closure). Spinal cords were isolated the following day.

4. Mouse (*Mus Musculus*)

4.1. Maintenance, handling and transgenic lines

Adult (8-9 weeks old) female C57BL/6J mice were purchased from Charles River Laboratory. The p16-3MR transgenic line (Demaria et al., 2014) was kindly provided by Marco Demaria (European Research Institute for the Biology of Aging, Groningen, Netherlands). Both male and female p16-3MR mice were used in the experiments. Animals were housed in the Instituto de Medicina Molecular animal facility under conventional conditions on a 12-hour light-dark cycle with *ad libitum* access to food and water.

4.2. p16-3MR genotyping

p16-3MR experimental mice were bred from the p16-3MR progenitors provided by Marco Demaria. Breeding pairs were set up between p16-3MR-expressing progenitors and *wt* C57BL/6J mice in order to generate p16-3MR-expressing offspring and control *wt* littermates. Tissue for genotyping was obtained by ear punching upon weaning. Each ear sample was incubated in 200 µL of 25 mM NaOH/0.2 mM EDTA at 98°C for 1 hour. After vortexing, 30 µL of 100 mM Tris-HCl pH 8.0 were added and samples were centrifuged at full speed rpm for 10 minutes at RT. gDNA was obtained from the resulting supernatant, quantified in NanoDrop and stored at 4°C. For DNA fragment amplification, a standard polymerase chain reaction (PCR) protocol was performed using DreamTaq DNA polymerase (5 U/µL, Thermo Fisher Scientific, EP0701) and primers specifically designed to hybridize the 3MR target sequence (*see details in* ***Table 2***). Thermal cycling conditions were as follows: initial denaturation step at 95°C for 3 minutes, followed by 35 cycles of a three step temperature cycle (denaturation: 95°C for 30 sec; primer annealing: 58°C for 30 sec; polymerase extension: 72°C) and a final extension step at 72°C for 5 min. DNase/RNase free water and gDNA from p16-3MR progenitors were used as negative and positive controls, respectively. PCR products were analyzed in a 2% agarose gel (TAE buffer 1x) adding 1:20000 RedSafe™ Nucleic Acid Staining Solution (iNtRON, 21141) for DNA visualization.

Amplified sequence	Forward primer (5'>3')	Reverse primer (5'>3')	Annealing temperature (°C)	Product length (BP)
3-MR	GACGTGCCTC CACAGGTAG	CGAGAACGC CGTGATTTT	58	61

Table 2. Primer sequence and details for p16-3MR genotyping.

4.3. Spinal cord injury (SCI) model and post-operative care

Before being assigned to SCI, mice went through a two weeks-period of handling and acclimatization, during which animals got used to the experimenters and body weight was assessed to ensure ideal surgery weight (18-20 g). Animals (10-11 weeks old) were anesthetized using a cocktail of ketamine (120 mg/kg) and xylazine (16 mg/kg) administered by IPi. For spinal contusion injuries, a laminectomy of the ninth thoracic vertebra (T9), identified based on anatomical landmarks (Harrison et al., 2013), was first performed followed by a moderate (75 kdyne) contusion using the Infinite Horizon Impactor (Precision Systems and Instrumentation, LLC.) (Scheff et al., 2003). Briefly, a midline incision was made in a rostral-caudal direction starting above the inferior angle of the scapulae and the fat and muscle were cut until the spinous processes were revealed and the dorsal surface of the lamina could be felt. With the help of spring scissors (Fine Science Tools, 15024-10) and Extra Fine Graefe Forceps (Fine Science Tools, 11153-10), the muscles over the laminae at T8-T10 were cleared to expose the foramen, where the modified clamps of the Impactor stabilization platform are to be placed. While holding the T8 vertebral body, the T9 lamina was cut and taken off with the spring scissors, exposing the spinal cord. Finally, using fine tipped forceps (Fine Science Tools, 11255-20), the dura was removed and the animal was mounted in the stabilization platform, preceding the contusion injury.

Inclusion criteria considered injury displacements between 550 and 750 μm (moderate to severe lesion). The mean applied force and tissue displacement for each experimental group are shown in **Figure 16** and **Figure 28** in **Chapter II**. There were no differences in injury parameters between experimental groups.

After SCI, the muscle and skin were closed with 4.0 polyglycolic absorbable sutures (Safil, G1048213). In control uninjured mice (sham), the wound was closed and sutured after the T9 laminectomy and the spinal cord was not touched. Animals were injected with saline (0.5 ml)

subcutaneously (sq) and then placed into warmed cages (35°C) until they recovered from anaesthesia and for the following recovery period (three days). To prevent dehydration mice were supplemented daily with saline (0.5 ml, sq) for the first 5 dpi. Bladders were manually voided twice daily for the duration of experiments. Body weight was monitored weekly.

4.4. Drug treatment

The senolytic drug ABT-263 (Navitoclax), a specific inhibitor of anti-apoptotic proteins BCL-2 and BCL-xL, was used to pharmacologically deplete senescent cells. ABT-263 (Selleckchem, S1001, 50 mg/kg/day) or vehicle (Corn oil, Sigma, C8267) were administered by oral gavage, as described previously (Chang et al., 2016), for 10 consecutive days starting at 5 dpi until 14 dpi. After spinal cord injuries, mice were randomly assigned to each group for each experimental endpoint, 15 dpi (n = 10), 30 dpi (n = 14) and 60 dpi (n = 13). Within the same cage, animals received different treatments to exclude specific environmental cage input. Experimenters were blinded for the whole duration of the study by coding the treatment.

Ganciclovir (GCV) was used to genetically ablate $p16^{INK4a+}$ senescent cells in the p16-3MR model. GCV (Sigma, G2536, 25 mg/kg/day) was administered by IPi for 25 consecutive days starting at 5 dpi and finishing at 29 dpi. Control mice received PBS for the same period of time. In total, the experiment comprised four different experimental groups: GCV-treated p16-3MR mice, PBS-treated p16-3MR mice, GCV-treated *wt* mice and PBS-treated *wt* mice. After spinal cord injuries, mice were randomly assigned to each group (n = 23) for the experimental endpoint (30 dpi). Within the same cage, animals have received different treatments to exclude specific environmental cage input. Experimenters were blinded for the whole duration of the study by coding the treatment.

4.5. Behaviour assessment

Basso Mouse Scale (BMS). Two weeks before the beginning of the study, mice were habituated to the open-field arena to decrease anxiety and distress. Locomotor behaviour (BMS scores and subscores) was assessed at 0 (baseline), 1, 3, 5, 7, 10, 12, 15, 21, 30, 45 and 60 dpi. On the day of the behavioural test, two investigators, blind to treatment, assessed mouse hind limb function and locomotion using the BMS scoring system (Basso et al., 2006). This test relies on two independent observers to identify, during four minutes, visually perceptible attributes of locomotor recovery, namely plantar stepping, weight support, limb coordination, paw positioning and trunk stability. These observations are then translated into a ranked scale based on the frequency of such attributes. Definitions of scoring, subscoring parameters and featuring criteria are described in **Table 3, 4** and **5**, respectively.

Score	Definition
0	No ankle movement
1	Slight ankle movement
2	Extensive ankle movement
3	Plantar placing of the paw with or without weight support -OR- Occasional, frequent or consistent dorsal stepping but no plantar stepping
4	Occasional plantar stepping
5	Frequent or consistent plantar stepping, no coordination -OR- Frequent or consistent plantar stepping, *some* coordination, paws *rotated* at initial contact and lift off (R/R)
6	Frequent or consistent plantar stepping, *some* coordination, paws *parallel* at initial contact (P/R, P/P) -OR- Frequent or consistent plantar stepping, *mostly* coordinated, paws *rotated* at initial contact and lift off (R/R)
7	Frequent or consistent plantar stepping, *mostly* coordinated, paws *parallel* at initial contact and *rotated* at lift off (P/R) -OR- Frequent or consistent plantar stepping, *mostly* coordinated, paws *parallel* at initial contact and lift off (P/P), and *severe* trunk instability
8	Frequent or consistent plantar stepping, *mostly* coordinated, paws *parallel* at initial contact and lift off (P/P), and *mild* trunk instability -OR- Frequent or consistent plantar stepping, *mostly* coordinated, paws *parallel* at initial contact and lift off (P/P), and *normal* trunk stability and tail *down or up* & *down*
9	Frequent or consistent plantar stepping, *mostly* coordinated, paws *parallel* at initial contact and lift off (P/P), and *normal* trunk stability and tail *always* up

Table 3. BMS scoring definitions (from Basso et al., 2006).

Feature	Scoring
Plantar stepping	Frequent = 0; Consistent =1 (scored for each paw)
Coordination	None = 0; Some = 1; Most = 2
Paw Position	Rotated thru out = 0; Parallel and rotated = 1; Parallel thru out = 2 (scored for each paw)
Trunk stability	Severe = 0; Mild = 1; Normal = 2
Tail position	Down = 0; Up & Down = 0; Up = 1

Table 4. BMS subscoring parameters (adapted from Basso et al., 2006).

Criteria	Definition
Slight	Moves less than half of the ankle joint excursion
Extensive	Moves more than half of the ankle joint excursion
Plantar placing	Paw is actively placed with both the thumb and the last toe of the paw touching the ground
Weight support	(dorsal or plantar): The hindquarters must be elevated enough that the hind end near the base of the tail is raised off of the surface and the knees do not touch the ground during the step cycle
Stepping	(dorsal or plantar): Weight support at lift off, forward limb advancement and re-establishment of weight support at initial contact
Occasional	Stepping less than or equal to half of the time moving forward
Frequent	Stepping more than half the time moving forward
Consistent	Plantar stepping all of the time moving forward with less than 5 missed steps (due to medial placement at initial contact, butt down, knee down, skiing, scoliosis, spasms or dragging) or dorsal steps
Coordination	For every forelimb step a hindlimb step is taken and the hindlimbs alternate during an assessable pass. For a pass to be assessable, a mouse must move at a consistent speed and a distance of at least 3 body lengths. Short or halting bouts are not assessable for coordination. At least 3 assessable passes must occur in order to evaluate coordination. If less than 3 passes occur then the mouse is scored as having no coordination
Some coordination	Of all assessable passes (a minimum of 3), most of them are *not* coordinated
Most coordination	Of all assessable passes (a minimum of 3), most of them *are* coordinated
Paw position	*Digits* of the paw are parallel to the body (P), turned out away from the body (external rotation: E) or turned inward toward midline (internal rotation; I)
Severe trunk instability	Severe trunk instability occurs in two ways: (1) The hindquarters show severe postural deficits such as extreme lean, pronounced waddle and/or near collapse of the hindquarters predominantly during the test. -OR- (2) Five or more of any of the following *events* stop stepping of one or both hindlimbs: • Haunch hit: the side of hindquarters rapidly contacts the ground • Spasms: sustained muscle contraction of the hindlimb which appears to immobilize the limb in a flexed or extended position • Scoliosis: lateral deviation of the spinal column to appear "C" shaped instead of straight
Mild trunk instability	Less than 5 events listed above and some sway in the hindquarters. Mild trunk instability is scored when the pelvis and haunches predominantly dip, rock, or tilt from side-to-side (tilt). If the tail is up, the swaying of the pelvis and/or haunches produces side-to-side movements of the distal third of the tail which also indicates mild trunk instability (side tail)
Normal trunk stability	No lean or sway of the trunk, and the distal third of the tail is steady and unwavering during locomotion. No severe postural deficits or events and less than 5 instances of mild instability

Table 5. BMS scoring criteria (from Basso et al., 2006).

Horizontal Ladder (HL). On the previous week before SCI, mice were trained to walk along a HL as previously described (Cummings et al., 2007). This task requires mice to walk across a

HL that consists of a 60 cm length x 8 cm width transparent corridor with rungs spaced 1 cm apart. A mirror was placed underneath the ladder and mice were video-recorded from the side view to be able to see paw placement on the rung in the mirror. Each rung was posteriorly analysed, frame-by-frame. Home cage bedding and/or treat-pellets were placed at the end to stimulate motivation. Ideally, each mouse was able to perform at least three successful trials along the ladder. The three best attempts were scored. For a trial to be illegible, the mouse must exhibit active step cycling over 50% of total distance. Baseline data were assessed 1 day before SCI. Mice were tested on the HL at 15, 30 and 60 dpi. A paw falling below the rungs of the ladder during a step in the forward direction was counted as one mistake. The total number of mistakes was averaged across the three trials per mouse and quantified as mistakes per centimetre. The total number of positive and negative events for each paw in each rung were also quantified and are divided as singular positive events (plantar step, toe step and skip) or singular negative events (slip, miss and drag). If the mouse stops while crossing, the previous and following events (1 event = 1 rung) are not scored. The definitions of each type of event are described in **Table 5**.

Event	Definition
Plantar step	The plantar surface of the hind paw makes initial contact with the rung. Toes are visible. The paw does not need to fully grasp the rung but is kept above the horizontal plane of the rung in the direction of forward movement throughout an active step cycle
Toe step	Toes make contact with the rung and are not visible. The hind paw is kept above the horizontal plane of the rung in the direction of forward movement throughout an active step cycle
Skip	The hind paw skips (no contact) over the rung during a normal active step cycle
Slip	Initial contact (plantar or toe) with the rung is visualized but the hind paw then drops below the horizontal plane of the rung due to loss of balance.
Miss	The hind paw falls below the horizontal plane between two rungs without touching them. A step cycle was attempted but no contact with the rungs was made. The rung scored as a Miss is the first of the two rungs.
Drag	The dorsal surface of the hind paw contacts the rung. Usually follows a slip or a miss. Also, when the limb is in spasm while moving.

Table 5. Operational definitions of positive (green) and negative (red) events observed during HL crossing (adapted from Cummings et al., 2007).

Hot/Cold Incremental Plate. Each mouse was placed into the observation chamber of the IITC's Incremental Hot Cold Plate (IITC Inc. Life Science) with a starting temperature of 37°C, as previously described (Yalcin et al., 2009). The plate was then either heated up to 49°C or cooled down to 0°C at a rate of 6°C per minute until the animal showed nocifensive behaviour involving either hindpaw. The typical response was hindpaw licking, shaking and lifting of the paw, jumping and extensor spasm. The plate temperature evoking any of these nocifensive reactions confined to any paw was regarded as the noxious heat/cold threshold of the animal. Following the recording of the threshold temperature, the animal was immediately removed from the plate. The threshold measurement was repeated after 30 min and the mean of the two thresholds was considered as the control noxious heat/cold threshold of the animal. Animals were tested in the Hot/Cold Incremental Plate at 30 and 60 dpi.

Bladder function. Bladder function was assessed everyday by attributing a gross score to the amount of urine retained. Bladders were voided twice a day and the time of day of each collection was maintained constant throughout the experiment to avoid interference in the results from environmental factors. Bladder function scoring system is described is **Table 6**.

Score	Designation	Amount of urine collected (drops)
0	empty	0
1	small	< 3
2	medium	3-6
3	large	>6

Table 6. Scoring system criteria to assess bladder function.

4.6. Tissue Processing

Mice were anesthetized with ketamine/xylazine mix (120 mg/kg + 16 mg/kg, ip) and then transcardially perfused with 0.9% NaCl followed by 4% PFA. Post-mortem anatomical

assessment of the T9 was confirmed to ensure correct thoracic contusion. Spinal cords were removed, post-fixed in 4% PFA for 2h and then incubated ON with SA-β-gal staining solution (*see **2.***). Like in zebrafish, mouse spinal cords were cryoprotected in 30% sucrose/0.12 M PB for a minimum of 72h at 4°C or until the tissue sinks to the bottom of the vial, followed by another embedding in 7.5% gelatin (Sigma, G6144)/15% sucrose/0.12 M PB and subsequently frozen. However, mouse spinal cords were divided in two segments: a thoracic segment centred on the impact site and a lumbar-sacral segment immediately following the thirteenth thoracic vertebra (T13). Both segments measured 1 cm in length. Tissue sections were cut in series either transversally (10 µm thick, 10 slides per series) or longitudinally (10 µm thick, 6 slides per series) using a Cryostat LEICA CM 3050S. For each time-point, samples were distributed as equally as possible in cuts along the coronal (rostral-caudal) axis and horizontal (dorsal-ventral) axis. Slides were stored at -20°C until needed. One series was counterstained with eosin for SA-β-gal quantifications. Every block, as well as every slide, was coded until the end of each analysis.

Liver and spleen were also dissected, weighted and post-fixed in formaldehyde until processed for histology (*for details see **4.13.***).

4.7. Quantification of SA-β-gal$^+$ cells after SCI (Senescence profile characterization)

To characterize the senescence profile in mouse after SCI, SA-β-gal$^+$ cells were quantified and averaged across 8 longitudinal sections imaged at the lesion periphery (from 0.5 to 2.5 mm laterally to the injury, rostral and caudal) around the center canal. A 0.5 mm interval was established between the lesion border and the beginning of the quantification regions. SA-β-gal$^+$ cells were quantified in the gray matter but not in the white matter. Quantifications were performed at 3, 7, 15, 30 and 60 dpi and, in each section, the number of SA-β-gal$^+$ cells counted

was normalized to the total area of grey matter analyzed. Rostral and caudal quantifications were grouped together and presented as SA-β-gal$^+$ cells/mm^2 at the lateral side of the injury. In control laminectomized (sham) mice, SA-β-gal$^+$ cells were quantified in the same regions.

4.8. Quantification of SA-β-gal$^+$ cells after ABT-263 administration

The ABT-263 senolytic effect after SCI was evaluated by quantifying and averaging the number of SA-β-gal$^+$ cells in 5 transversal sections imaged at the lesion periphery (from 0.5 to 2.5 mm rostrally or caudally to the lesion) at 15, 30 and 60 dpi. A 0.5 mm interval was established between the lesion border and the beginning of the quantification regions. In this assessment, a distinction was made between rostral and caudal quantifications. Additionally, 10 transversal sections (spaced 1 mm apart) were quantified and averaged at the lumbar-sacral region. SA-β-gal$^+$ cells were quantified in the gray matter but not in the white matter. In these quantifications, as in each section we were looking at the whole dorsal-ventral spinal area, SA-β-gal$^+$ cells were counted per section and not normalized to the total area like in the senescence profile characterization (*see **3.4.** and **4.7.***).

4.9. White Matter Sparing

One set of sections spaced 0.1 mm apart and spanning the entire block was thawed, washed in PBS at 37°C and stained with FluoroMyelin^{TM} Green (1:300, ThermoFisher Scientific, F34651) in PBS/0.1% Triton X-100 for 1 hour. The slides were washed in PBS and mounted in Mowiol medium. The percentage of cross-sectional area (% CSA) with spared myelin was calculated by measuring the area of stained myelin in FIJI and normalizing it to the total cross-sectional area in each section. % CSA was quantified along 4 mm (2 mm rostral and 2 mm

caudal) around the lesion epicenter, which was identified as the section with the smallest % CSA.

4.10. Fibrotic Scar

A distinct set of sections was stained with anti-PDGFRβ and anti-GFAP (glial fibrillary acidic protein) in order to identify the fibrotic scar area and border (*see protocol details in **5.***). The percentage of fibrotic scar area at lesion epicenter was calculated by outlining the PDGFRβ$^+$ area and normalizing it to the total cross-sectional area. Measurements were performed using FIJI tools. Using the set of sections stained for PDGFRβ and GFAP, the rostral and caudal extents of PDGFRβ$^+$ fibrosis were determined for each lesion, and total lesion length was calculated by multiplying the number of sections containing fibrotic tissue by the distance between each section (0.1 mm).

4.11. Inflammation

Spinal sections 0.1 mm apart extending from 1 mm rostral to 1 mm caudal to the lesion epicenter were stained for the pan macrophage marker F4/80 and the M2-phenotype specific marker CD206. Due to the fact that macrophages are difficult to be individually distinguished within the central lesion core, the measurements of F4/80$^+$ and CD206$^+$ cells were expressed as a percentage of the total cross-sectional area. The areas of F4/80$^+$ and CD206$^+$ staining were measured using a custom-made macro in FIJI that, after manually setting a threshold value, calculated the F4/80$^+$ and CD206$^+$ areas and normalized them to the total cross-sectional area.

4.12. Axonal Preservation

$GAP43^+$ axons were counted based on previously described methods (Almutiri et al., 2018; Hata et al., 2006). Quantifications of $GAP43^+$ fibers were performed in 3 longitudinal spinal sections of the dorsal horn region using a custom-made macro in FIJI that, after manually establishing a threshold value and defining the lesion epicenter, determined the number of positive fibers from 4 mm rostral to 4 mm caudal to the lesion site and normalized it to the tissue length covered in each measurement. Axon number was calculated as a percentage towards the ratio (fibers/mm) obtained 4 mm above the lesion, where the spinal tracts were intact.

4.13. Peripheral drug effects (Liver and Spleen)

To check for peripheral drug effects, the liver and the spleen were also collected from every mouse. Each organ was weighed upon dissection and post-fixed in formaldehyde until processed for histology. Organ weight was normalized to total body weight before sacrifice. Livers and spleens were embedded in paraffin and 10 µm-thick sections were obtained using a microtome (Leica RM2245). A histopathological analysis was blindly performed by an anatomopathologist that searched for markers of cellular damage in the liver (inflammation, necrosis and lipidosis) and the spleen (lymphoid hyperplasia, hemosiderosis). A score from 0 to 5 (0 = no damage; 5 = maximum damage) was attributed to each sample depending on the amount of cellular damage markers visualized.

5. Immunohistochemistry

To perform immunostaining in sections, the gelatin was removed from the cryosections using PBS heated to 37°C (4 x 5 min washes). After incubation with blocking solution for 2h at RT,

the sections were incubated ON with primary antibody solution at 4°C. Sections were then washed in PBS/0.1% Triton X-100 and incubated with the secondary antibody (1:500) and 1 mg ml^{-1} DAPI (Sigma, D9564) for 2h at RT. Due to the fact that the immunostainings were all performed on top of previously SA-β-gal-stained sections, each protocol had to be fine-tuned in order to obtain a proper antibody incorporation. In most cases, this required a stronger permeabilization with higher Triton X-100 concentrations. Details on blocking solutions, primary and secondary antibodies used are described in **Table 7** and **8**. After incubation with the secondary antibodies, the sections were washed in PBS and mounted in Mowiol mounting medium.

Antigen	Host	Dilution	Retrieval	Blocking Solution	Source/Reference
HuC/D	Mouse	1:500	-	1% bovine albumin serum/0.1% Tx in PBS	Life Technologies/A21271
p21	Rabbit	1:100	-	1% bovine albumin serum/1% DMSO/0.3% Tx in PBS	Santa Cruz/C-397
γ-H2AX	Rabbit	1:500	-	1% bovine albumin serum/1% DMSO/0.3% Tx in PBS	Novus Biologicals/NB100-384
p16	Rabbit	1:50	-	1% bovine albumin serum/1% DMSO/0.3% Tx in PBS	ProteIntech/10883-1-AP
NeuN	Rabbit	1:100	-	5% bovine albumin serum/0.3% Tx in PBS	ProteIntech/26975-1-AP
GFAP	Rat	1:400	-	5% goat serum/0.5% Tx in PBS	ThermoFisher Scientific/13-0300
PDGFRβ	Rabbit	1:200	-	5% goat serum/0.5% Tx in PBS	Abcam/ab32570
F4/80	Rat	1:100	-	5% bovine albumin serum/0.3% Tx in PBS	Abcam/ab6640
CD206	Goat	1:50	-	5% bovine albumin serum/0.3% Tx in PBS	R&D Systems/AF2535
GAP43	Rabbit	1:500	Sodium Citrate Buffer pH 6.0	5% goat serum/0.3% Tx in PBS	Novus Biologicals/NB300-143

Table 7. List of primary antibodies.

Specificity	Host	Fluorophore	Source/Reference
Rabbit	Goat	Alexa Fluor 488	ThermoFisher Scientific/A11008
Rabbit	Goat	Alexa Fluor 568	ThermoFisher Scientific/A11011
Mouse	Goat	Alexa Fluor 594	ThermoFisher Scientific/A11005
Rat	Goat	Alexa Fluor 488	ThermoFisher Scientific/A11006
Goat	Donkey	Alexa Fluor 568	ThermoFisher Scientific/A11057

Table 8. List of secondary antibodies.

6. Imaging

The colorimetric images of SA-β-gal-stained sections were acquired using a NanoZoomer-SQ digital slide scanner (Hamamatsu) or a Leica DM2500 brightfield microscope with HC PL FLUOTAR 20x / 0.5 Dry objective. Immunostained sections were imaged using an Axio Observer motorized widefield fluorescence microscope or a Cell Observer SD confocal microscope with Plan-Apochromat 20x / 0.80 Dry objectives. F4/80- and GAP43-stained immunosections were imaged using a ZEISS Axio Scan.Z1. Each image is a maximum intensity projection of a z-stack acquired from the 10/12 µm cryosection. The processing of acquired images was performed using NDP.view2 or Zeiss ZEN 2 (blue edition) and the image analysis software FIJI (Schindelin et al., 2012). Adobe ILLUSTRATOR was used for assembly of figures.

7. Data Analysis

GraphPad Prism was used for data visualization and SigmaPlot 14 for statistical analysis. The senescence profile after SCI was analysed using a one-way ANOVA followed by a Bonferroni's post hoc test (zebrafish) or a non-parametric Kruskal-Wallis one-way ANOVA test (mouse). BMS and Bladder Score data were analysed using a two-way repeated-measures ANOVA, followed by a Bonferroni's post hoc test. HL, Incremental Plate, Fibrotic Area, White

Matter Sparing, Inflammation and Axonal Preservation data were analysed using a normal two-way ANOVA, followed by a Bonferroni's post hoc test. All data were expressed as mean ± SEM, with statistical significance determined at p-values<0.05.

CHAPTER I - DISTINCT SENESCENT PROFILES BETWEEN ZEBRAFISH AND MOUSE UPON SPINAL CORD INJURY

Part of the content of the following section is contained in the manuscript **"Depletion of senescent cells improves functional recovery after spinal cord injury"** (*submitted*).

ABSTRACT

Senescence is a multifaced cellular phenomenon that comprises an irreversible cell cycle arrest combined with highly metabolic and pronounced secretory activities. While classically associated with aging, senescent cells (SCs) have been recently demonstrated to play a functional role in embryonic development, reprogramming and tissue repair. Interestingly, whether senescence is beneficial or harmful in a given context, seems to be closely related to the time during which senescent cells are active.

Here, we describe for the first time the presence of SCs in the spinal cord of two models with opposite regenerative outcomes – the zebrafish and the mouse. These cells have been identified as neurons and exhibit senescence hallmarks such as enlarged morphology and co-expression of senescence-associated β-galactosidase (SA-β-gal), cell cycle inhibitors $p16^{INK4a}$ and $p21^{CIP1}$, and the DNA damage marker γH2AX. Strikingly, upon a spinal cord injury (SCI), SCs are induced at the lesion periphery where they accumulate over time. However, while in the zebrafish there is a transient burst of SCs which are then cleared out, in the mouse these cells persist over time and are never eliminated. Curiously, we have detected the presence of SA-β-gal^{+} cells in the spinal cord during zebrafish development and a similar transient profile was also observed after SCI in zebrafish larvae.

Our results reveal two clearly distinct senescence profiles in an injured spinal cord, a transient profile observed in regenerating zebrafish and a persistent one observed in non-regenerating mice.

Keywords: senescence, spinal cord injury, induced-senescent cells, zebrafish, mouse

INTRODUCTION

Senescence is a cellular concept traditionally seen as an irreversible cell-cycle arrest response related to aging (Gorgoulis et al., 2019; Herranz & Gil, 2018; van Deursen, 2014). Studies in recent years changed the way we perceive cellular senescence, placing it at the center of tissue remodeling in disease settings by limiting fibrosis, namely in wound healing (Demaria et al., 2014; Jun & Lau, 2010), damaged livers (Kong et al., 2012; Krizhanovsky et al., 2008) and infarcted hearts (Meyer et al., 2016). In regenerative models, such as salamander limbs, zebrafish hearts and fins and neonatal mouse hearts, a burst of transient senescent cells (SCs) was shown to be induced after an injury (Da Silva-Álvarez et al., 2019; Sarig et al., 2019; Yun et al., 2015). These cells were shown to be efficiently cleared from the tissues as regeneration progressed possibly by macrophages (Yun et al., 2015). Remarkably, if this initial senescence is eliminated, zebrafish fin regeneration is impaired (Da Silva-Álvarez et al., 2019), suggesting that a transient accumulation of SCs appears to have beneficial functions. Persistent senescence, on the other hand, is detrimental for tissue and organ function in ageing and aged-related diseases, such as atherosclerosis, osteoporosis, diabetes and neurodegeneration (Calcinotto et al., 2019). Key to their various roles is the fact that SCs secrete a plethora of factors known as senescence-associated secretory phenotype (SASP), which were shown to modulate the tissue microenvironment (Acosta et al., 2013; Calcinotto et al., 2019).

Spinal cord injury (SCI) is a complex pathological condition that results in permanent functional deficits that have devasting consequences for the lives of affected individuals (Courtine & Sofroniew, 2019). In mammals, the inability to regenerate spinal tissue and regrow axons after a SCI stems from multiple factors that altogether contribute to an inhibitory non-supporting environment for repair (Kehr & Kaech, 2014; Oyinbo, 2011). On the other hand,

regenerating models, such as the zebrafish, can regenerate their spinal cord after injury and fully recover their locomotor function (Ghosh & Hui, 2018). Both mammalian and zebrafish models have been extensively used to investigate the cellular and molecular mechanisms underlying SCI (Vajn et al., 2013). Accumulating evidence advocates for the existence of key environmental differences between mammals and zebrafish that, in the case of the latter, are extremely more favorable for axonal regeneration. Though our knowledge of SCI features and mechanisms has advanced significantly over the past decades, there is still a lack of therapeutic options with meaningful clinical impact (Courtine & Sofroniew, 2019). This suggests that there might be other intrinsic or extrinsic determinants of SCI which are still unknown to us.

Here, we investigated the presence of a new cellular player in SCI – SCs, which are known microenvironment modulators and have been shown to respond to injury in other systems (Yun, 2018). Our data has revealed the presence of SCs in both zebrafish and mammalian spinal cords. Upon injury, these cells are induced at the lesion periphery and accumulate over time. However, while in the zebrafish this accumulation is transient, in the mouse it chronically persists. These results implicate a novel and unexpected player in SCI which may have a major contribution to the functional outcome of this condition.

RESULTS

1. The Zebrafish

1.1. SA-β-gal^{+} cells are present in the zebrafish spinal cord

At the beginning of this project, the presence of senescent cells (SCs) in the spinal cord was still unknown. We were prompted to investigate the existence of SCs in the zebrafish spinal cord after the publication of a study reporting an unexpected turnover of these cells during the regeneration process of an amputated limb in the salamander (Yun et al., 2015).

First, we tested if we could detect SCs in the zebrafish spinal cord, and for that we used the gold standard method to identify SCs – the senescence-associated β-galactosidase (SA-β-gal) assay (Itahana et al., 2007). This technique takes advantage of the fact that SCs display a β-gal activity that is histochemically detectable at pH 6.0 by using the artificial substrate X-gal, which results in the formation of a blue precipitate (Dimri et al., 1995). Although SA-β-gal staining protocols are standardized, minor adaptations are usually required depending on factors such as tissue isolation, fixation or the type of tissue being stained. For staining in whole mount tissues, glutaraldehyde (0.5%) is typically the preferred fixating agent. In our hands, glutaraldehyde generated a very clean SA-β-gal staining, but tissue integrity became greatly compromised (**Figure 1A-A'**). In fact, the spinal cord is a soft and fragile tissue and usually requires a stronger fixation agent, like 4% paraformaldehyde (PFA), to ensure tissue cohesion after isolation (i.e. vertebrae removal). Indeed, with 4% PFA, we were able to maintain spinal cord integrity while guaranteeing a clear, albeit less clean (some staining is trapped in the white matter), SA-β-gal staining (**Figure 1B-B'**). Therefore, we decided that 4% PFA would offer the best compromise between staining quality and tissue integrity.

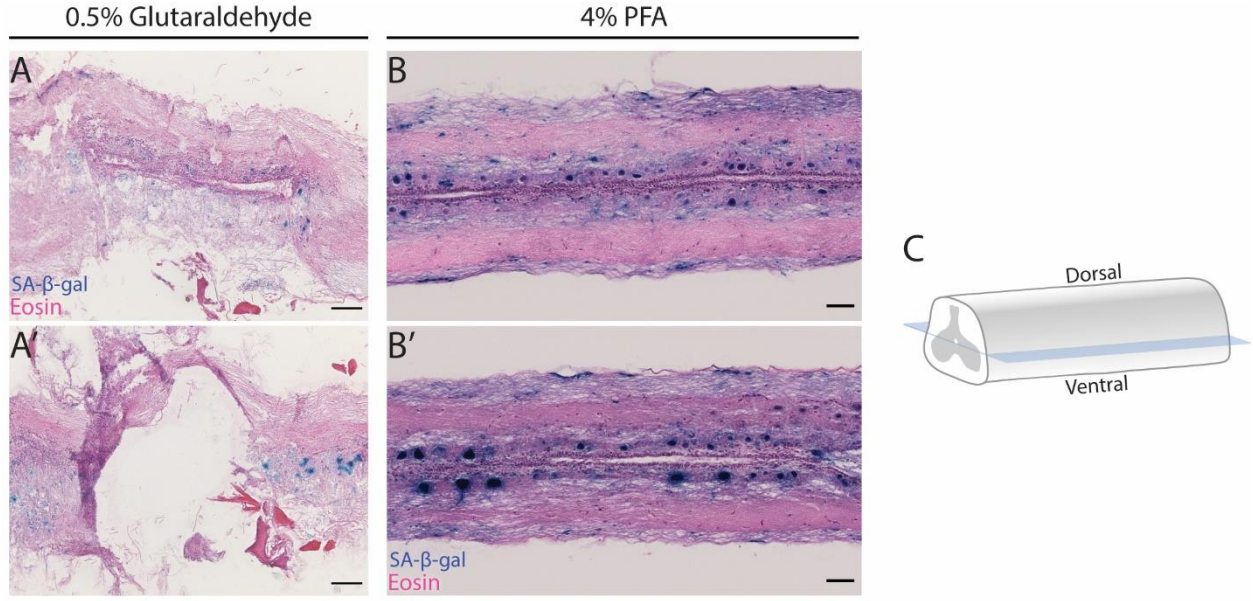

Figure 1. SA-β-gal staining optimizations. Longitudinal sections of SA-β-gal-stained (blue) zebrafish spinal cords that were submitted to two different fixation agents – (**A-A'**) 0.5% Glutaraldehyde and (**B-B'**) 4% PFA. An eosin (pink) counterstaining was performed after cryosectioning. (C) Schematic representation of the sectional plane (in blue). Spinal cords were sectioned longitudinally from dorsal to ventral. Scale bars: 50 µm.

1.2. There is a transient accumulation of SA-β-gal$^+$ cells after a zebrafish spinal cord injury

Besides the salamander limb, a transient senescent profile was recently described in the regenerating heart and caudal fin of the zebrafish (Da Silva-Álvarez et al., 2019; Sarig et al., 2019). In this project, we questioned if a similar profile could be induced after a spinal cord injury.

In the regenerative zebrafish, SA-β-gal$^+$ cells were found mainly in the spinal cord gray matter and accumulated laterally to the injury site (**Figure 2A**). Remarkably, when comparing to uninjured (Sham) animals, these cells were induced at the lesion periphery (**Figure 2B**), reaching a peak at 15 days post-injury (dpi) and then returning to basal levels at 60 dpi (**Figure 2C**).

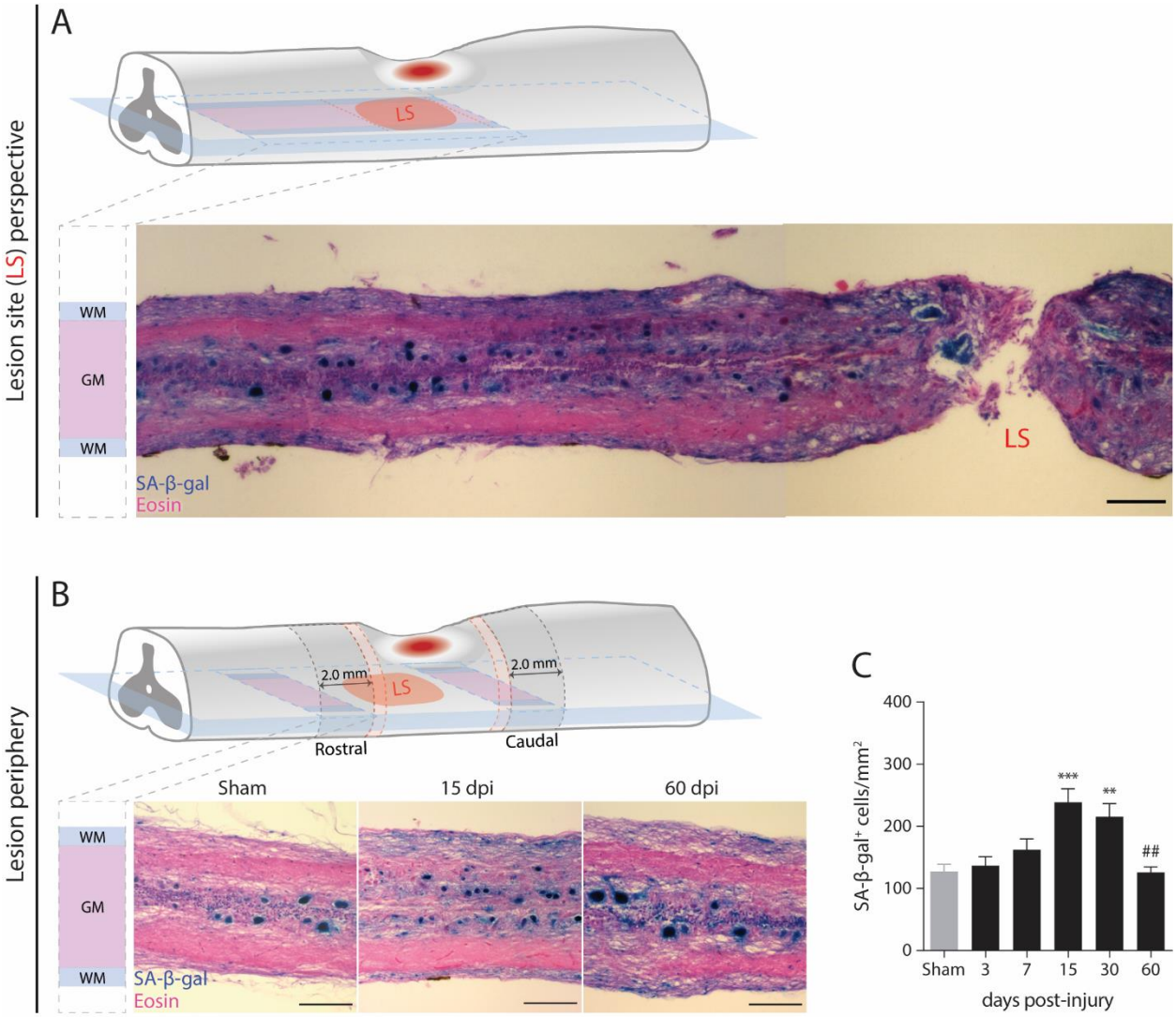

Figure 2. Turnover of SA-β-gal$^+$ cells after a spinal cord injury in zebrafish. (**A**) SA-β-gal$^+$ cells (blue) were detected around the lesion site (LS). An eosin counterstaining (pink) was performed after cryosectioning. SA-β-gal$^+$ cells were (**B**) detected and (**C**) quantified in mouse laminectomized (sham) and injured spinal cords at different time-points (3, 7, 15, 30 and 60 days-post-injury, dpi). *n* = 5-9. Cells were quantified at the lesion periphery along 2.0 mm in longitudinal sections. A 0.5 mm interval (red dashed zone) was established between the lesion border and the beginning of the quantification region. SA-β-gal$^+$ cells were quantified along the whole ventral horn region only in the gray matter (GM) and not in the white matter (WM). Data are presented as mean ± SEM. $^{**}p<0.01$, $^{***}p<0.001$, versus Sham. $^{\#\#}p<0.01$, versus 30 dpi. Scale bars: 100 µm.

1.3. In the zebrafish spinal cord, SA-β-gal$^+$ cells co-express other senescence biomarkers

One major bottleneck in the senescence field is the absence of exclusively specific senescent hallmarks (Calcinotto et al., 2019). Thus, it is necessary to identify more than one

characterizing feature in order to define a SC. SCs are typically characterized by increased size, absence of proliferation markers and expression of cell cycle inhibitors like $p16^{INK4a}$ and $p21^{CIP1}$ (Narita et al., 2003). In zebrafish, characterizing SCs stands a particularly difficult task as this model lacks a bona fide cdkn2a gene locus, which encodes for $p16^{INK4a}$, one of the most reliable senescent biomarkers currently known (Alcorta et al., 1996; Sharpless, 2005; Shim et al., 2017).

We verified that the majority of SA-β-gal^+ cells indeed exhibited an enlarged morphology compared to SA-β-gal^- cells (**Figure 3**). We confirmed by immunofluorescence that SA-β-gal^+ cells were devoid of the proliferation marker BrdU, which is expressed mainly in the ependymal progenitors surrounding the center canal (**Figure 3A**). Finally, SA-β-gal^+ cells also co-localized with the cell-cycle regulator $p21^{CIP1}$, thus validating their senescent nature (**Figure 3B**). Noteworthy, $p21^{CIP1}$ was not expressed in every SA-β-gal^+ cell, for which there two possible explanations: a) unlike $p16^{INK4a}$, $p21^{CIP1}$ upregulation during the senescence program is usually transient and therefore its expression may not always be detected (Shtutman et al., 2017; Stein et al., 1999); b) given the nature of the SA-β-gal staining, a stronger precipitate formation may sometimes prevent a good antibody incorporation during immunofluorescence protocols.

We also tested for co-localization with the DNA damage marker γ-H2AX, but were unable to verify its expression in SA-β-gal^+ cells. Whether this was due to SA-β-gal staining preventing γ-H2AX incorporation or the fact that this senescence response is not mediated by a DDR, we do not know.

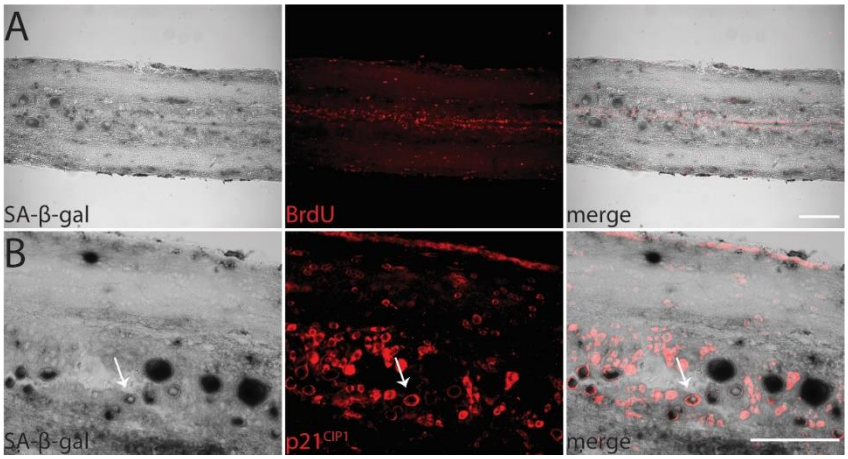

Figure 3. Co-localization of SA-β-gal with other senescence biomarkers in the zebrafish spinal cord. (**A**) In zebrafish, no co-localization was found between SA-β-gal (black) and the proliferation marker BrdU (red). (**B**) SA-β-gal^{+} cells co-localized with the senescence biomarker p21^{CIP1} (red). Images were taken at 15 days post-injury. White arrows point to representative examples of co-localization. Scale bars: 100 µm.

1.4. SA-β-gal^{+} cells in the zebrafish spinal cord are mostly neurons

The next step was to identify which cell types compose the SA-β-gal^{+} population. To do this, we tested for co-localization with some cell type-specific markers, namely the neuronal marker HuC/D (**Figure 4A**), the glial marker GFAP (**Figure 4B**) and the ependymal progenitor marker foxj1a (**Figure 4C**). Strikingly, in the injured spinal cord, 83.3% to 89.1% of SA-β-gal^{+} cells co-localized with HuC/D at all time-points analyzed during the regenerating period (**Figure 4D**). Interestingly, when we quantified the percentage of total HuC/D^{+} neurons that were also SA-β-gal^{+}, we verified a similar turnover profile to that of SA-β-gal^{+} cells observed previously (**Figure 4E**). Curiously, we found no colocalization of SA-β-gal with GFAP or foxj1a. Though our results indicate that the majority of SCs in the zebrafish injured spinal cord are neurons, the remaining percentage of SA-β-gal^{+} cells remains unidentified.

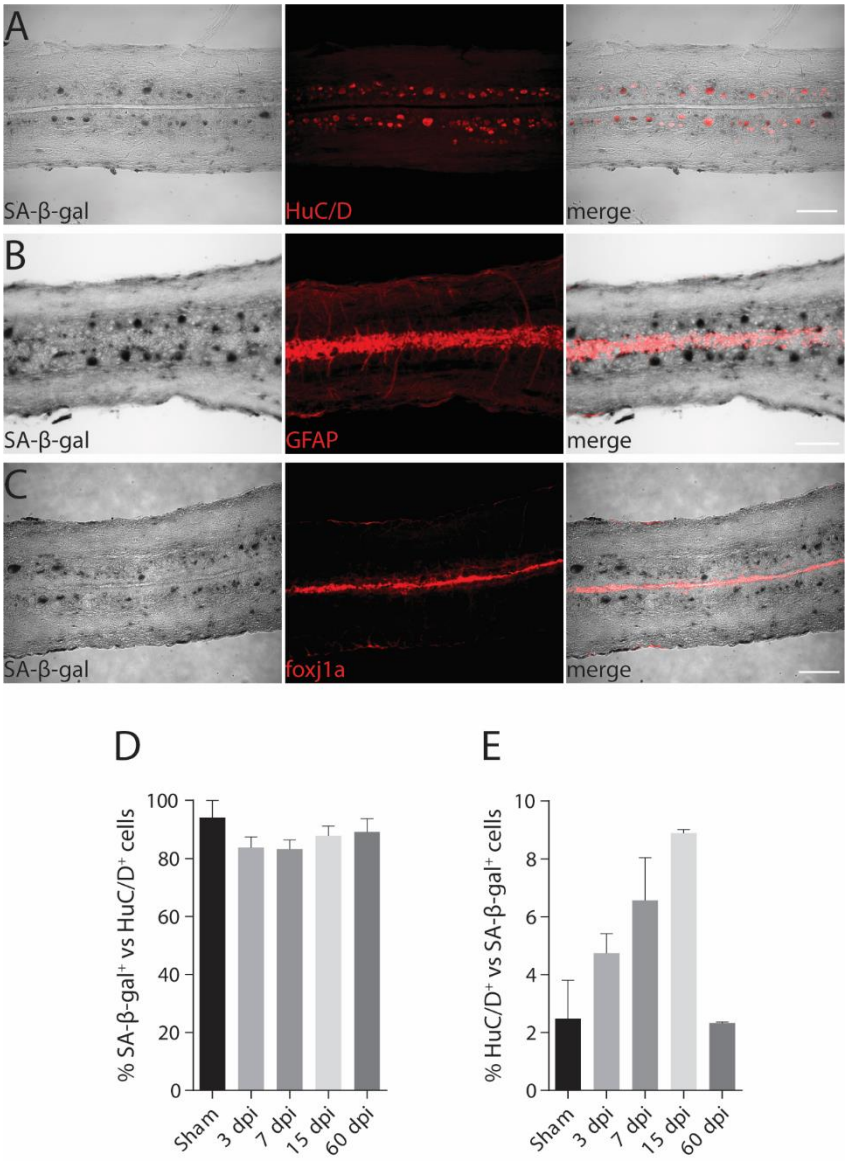

Figure 4. Identification of SA-β-gal$^+$ cells in the zebrafish spinal cord. In zebrafish, SA-β-gal$^+$ cells (black) co-localized with the (**A**) neuronal marker HuC/D (red). No co-localization was found with the (**B**) pan-glial marker GFAP or the (**C**) ependymal cell marker foxj1a. Representative images were taken at 15 days post-injury (dpi). The percentages of (**D**) total SA-β-gal$^+$ cells that are HuC/D$^+$ and of (**E**) total HuC/D$^+$ neurons that are SA-β-gal$^+$ were calculated in uninjured (Sham) zebrafish and at 3, 7, 15 and 60 dpi. *n* = 2. Scale bars: 100 µm.

1.5. A turnover of SA-β-gal activity is also detected after spinal cord injury in zebrafish larvae

Zebrafish larvae can fully regenerate their transected spinal cord and recover their locomotor function after 6 dpi (Chapela et al., 2019). To evaluate if senescence is also involved in larval

spinal cord regeneration, we performed a complete spinal cord transection at the level of the anal pore in 5 days post-fertilization (dpf) larvae. SA-β-gal staining was performed in uninjured (Sham), as well as 1, 2, 3 and 4 dpi animals. We found that, much like in the adult zebrafish, a transient SA-β-gal^{+} staining occurs at the lesion site in zebrafish larvae, which peaks at 1 dpi and disappears by 4 dpi (**Figure 5A-E**). This was further confirmed by staining analysis after cryosectioning (**Figure 5A'-D'**).

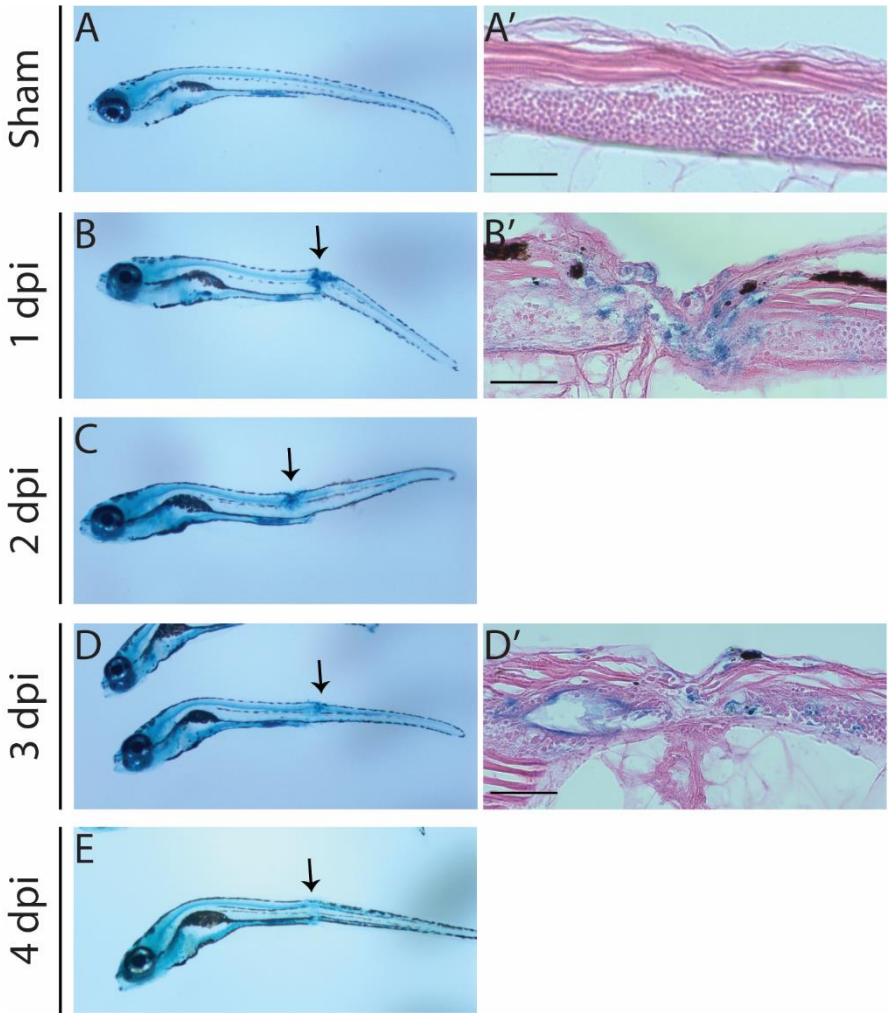

Figure 5. SA-β-gal staining profile after zebrafish larval spinal cord injury. SA-β-gal staining was performed and evaluated in (**A**) uninjured (Sham) and injured zebrafish larvae at (**B**) 1, (**C**) 2, (**D**) 3 and (**E**) 4 days post-injury (dpi). Black arrows point to the lesion site. (**A'**) Sham, (**B'**) 1 dpi and **(D')** 3 dpi larvae were cryosectioned and the presence of SA-β-gal^{+} staining was confirmed at the lesion area. An eosin (pink) counterstaining was performed after cryosectioning. Scale bars: 50 µm.

1.6. SA-β-gal^{+} cells are detected in several organs during zebrafish developmental larval stages

Developmental senescence has been described in several model organisms, in which SCs seem to play a role in the fine-tuning of cell fate specification and tissue patterning (Rhinn et al., 2019). In the zebrafish, SCs have been found in the yolk sac and the gut during embryonic development (Villiard et al., 2017). Given the interesting proposition that regeneration processes might be, to some extent, a recapitulation of conserved developmental mechanisms, we wondered if senescence could also be involved in the development of other zebrafish organs, namely the spinal cord. So, we performed SA-β-gal stainings at different embryonic and larval stages. At 3 (**Figure 6A**), 8 (**Figure 6B**), 24 (**Figure 6C**) and 48 (**Figure 6D**) hours post-fertilization (hpf), we detected no SA-β-gal activity under the stereoscope, except in the yolk sack. We do think, however, that this staining found in the yolk sac is non-specific. Notably, at the larval stage of 72 hpf, we found signs of SA-β-gal activity in the developing heart (**Figure 6E**).

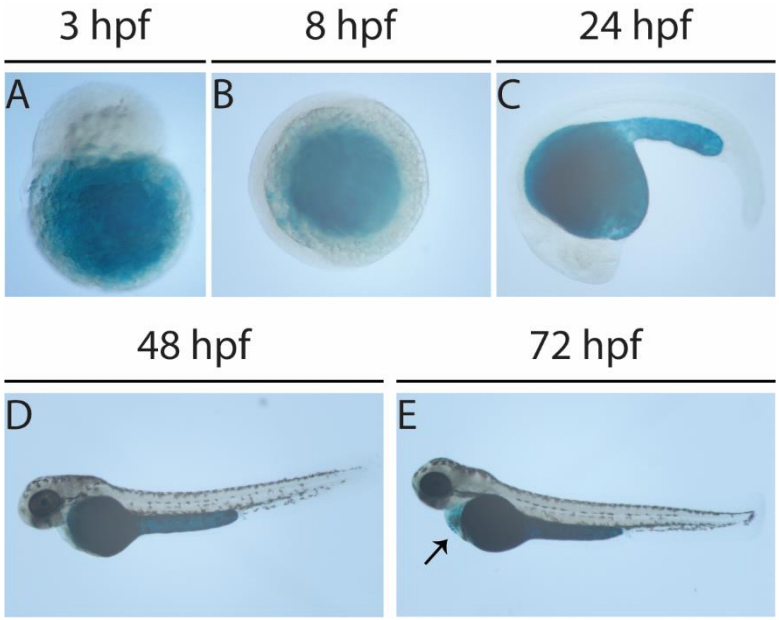

Figure 6. Senescence during zebrafish embryonic development. SA-β-gal staining was performed and evaluated in (**A**) 3, (**B**) 8 and (**C**) 24 hours post-fertilization (hpf) stage embryos, as well as (**D**) 48 and (**E**) 72 hpf

stage larvae. While the yolk sack trapped the SA-β-gal forming precipitate, no staining was visible until 48 hpf under the stereoscope. However, at 72 hpf, SA-β-gal^{+} staining was detected in the heart (black arrows).

We cryosectioned 72 hpf larvae in order to assess SA-β-gal activity in more detail, confirming the the presence of SA-β-gal^{+} staining in the pericardial region (**Figure 7A-A''**). Surprisingly, we also detected SA-β-gal activity in other locations, namely the brain (**Figure 7B-B'**), the spinal cord (**Figure 7C-C'**) and the ventral-posterior trunk region (**Figure 7D-D'**). In the brain, SA-β-gal staining was spotted in the ventricular zone and peripheral meninges (**Figure 7E-E''**), while in the spinal it was mainly found surrounding the center canal and blood vessels in the ventral region (**Figure 7F-F''**). Data suggests that senescence is present in several organs during early larval development.

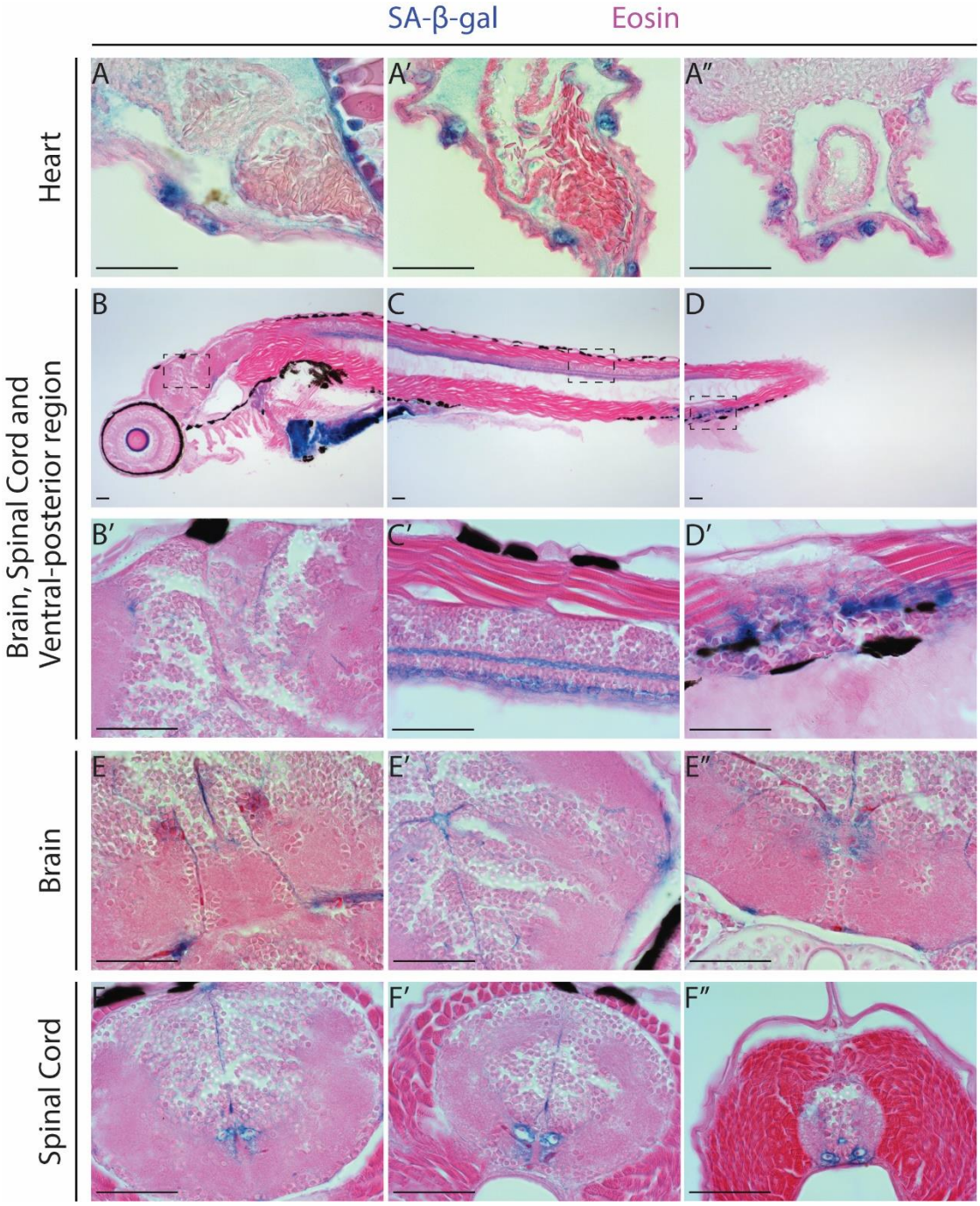

Figure 7. SA-β-gal staining is detected in different zebrafish organs at 72 hours post-fertilization. At 72 hours post-fertilization, SA-β-gal staining was detected in the zebrafish (**A-A''**) heart, (**B-B'**) brain, (**C-C'**) spinal cord and (**D-D'**) ventral-posterior region. (**E-E''**) In the brain, SA-β-gal staining was spotted along blood vessels and tissue periphery. (**F-F''**) In the spinal cord, SA-β-gal staining was present mainly in the floor plate. An eosin (pink) counterstaining was performed after cryosectioning. Scale bars: 50 µm.

2. The Mouse

2.1. SA-β-gal$^+$ cells accumulate and persist over time after a mouse spinal cord contusion injury

After defining a transient senescent profile in the regenerating zebrafish, we asked what happens in a mammalian model that is unable to regenerate the spinal cord after a lesion. Curiously, the senescence profile in injured non-regenerating organs was never characterized. Therefore, we investigated the dynamics of senescence in a mouse spinal cord contusion injury model. We found that, in the mouse, SA-β-gal$^+$ cells are also around the lesion site after an injury (**Figure 8A**). Of note, the same staining protocol generates much cleaner SA-β-gal$^+$ precipitates in mice than those of the zebrafish (**Figure 8B**). In the scarring non-regenerative mouse, SA-β-gal$^+$ cells were also detected mainly in the spinal cord grey matter of sham animals and induced at the lesion periphery upon injury (**Figure 8C**). However, in clear contrast to its regenerating counterpart, these SA-β-gal$^+$ cells did not return to basal levels and instead accumulated over time (**Figure 8D**).

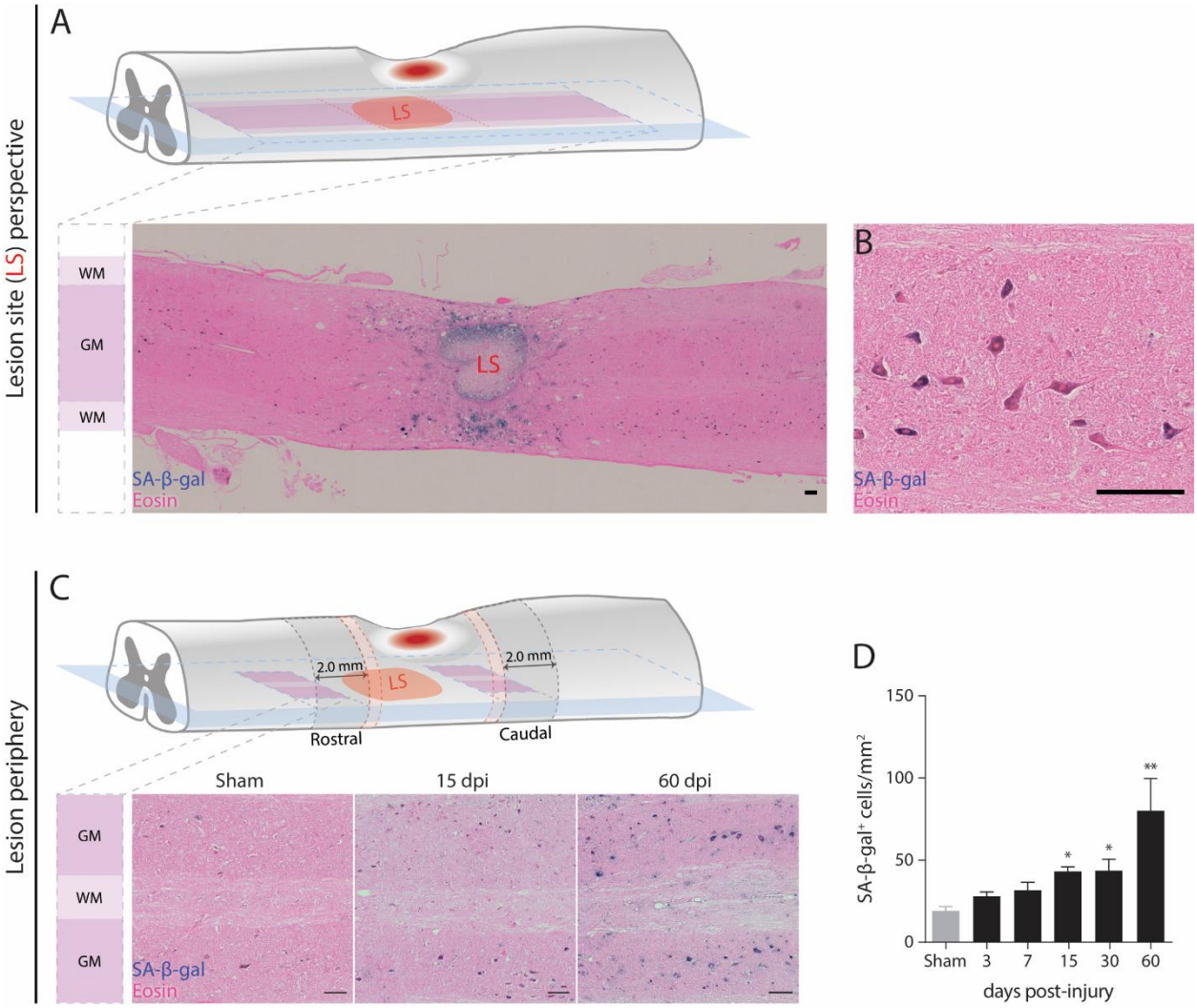

Figure 8. Persistent accumulation of SA-β-gal$^+$ cells after a spinal cord injury in mouse. (**A**) SA-β-gal$^+$ cells (blue) were detected around the lesion site (LS). An eosin counterstaining (pink) was performed after cryosectioning. (**B**) Representative section displaying a clean SA-β-gal staining forming a blue precipitate in the cytoplasm but not in the nucleus. SA-β-gal$^+$ cells were (**C**) detected and (**D**) quantified in mouse laminectomized (sham) and injured spinal cords at different time-points (3, 7, 15, 30 and 60 days-post-injury, dpi). *n* = 4-7. Cells were quantified at the lesion periphery along 2.0 mm in longitudinal sections. A 0.5 mm interval (red dashed zone) was established between the lesion border and the beginning of the quantification region. SA-β-gal$^+$ cells were quantified along the whole ventral horn region only in the gray matter (GM) and not in the white matter (WM). Data are presented as mean ± SEM. **p<0.05, **p<0.01,* versus Sham. Scale bars: 100 µm.

2.2. In the mouse spinal cord, SA-β-gal$^+$ cells co-express other senescence biomarkers

We confirmed by immunofluorescence that SA-β-gal$^+$ cells co-localized with other senescence biomarkers, namely the cell-cycle regulator p16^{INK4a} (**Figure 9A**) and the DNA damage marker γH2AX (**Figure 9B**), reinforcing the concept that these cells are indeed senescent.

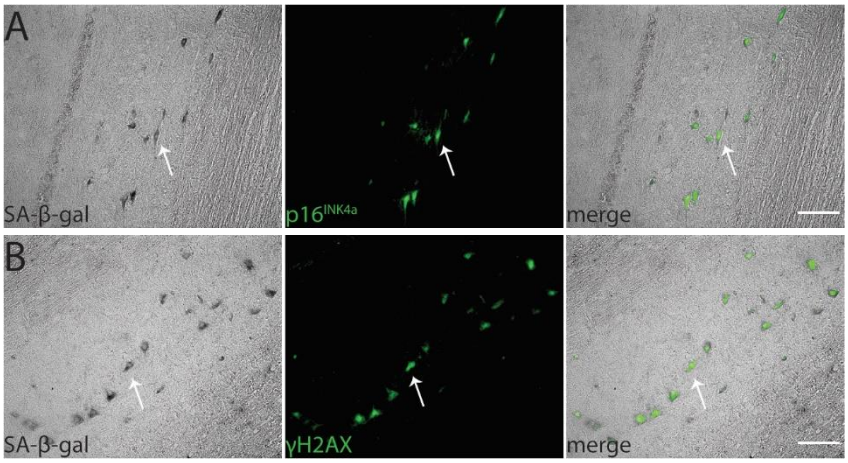

Figure 9. Co-localization of SA-β-gal with other senescence biomarkers in the mouse spinal cord. In mouse, SA-β-gal$^+$ cells (black) co-localized with the senescence biomarkers (**A**) p16 and (**B**) γH2AX (green). Images were taken at 15 days post-injury. White arrows point to representative examples of co-localization. Scale bars: 100 μm.

2.3. SA-β-gal$^+$ cells in the mouse spinal cord are mostly neurons

To identify which cell types comprise the SA-β-gal$^+$ population, we searched for co-localization with the pan-neuronal marker NeuN (**Figure 10A**) and the glial marker GFAP (**Figure 10B**). While GFAP never co-localized with SA-β-gal, we discovered that in laminectomized (Sham) animals, 94.6% of SA-β-gal$^+$ cells co-localized with NeuN (**Figure 10C**). Accordingly, at all time-points analyzed after injury, the percentage of total SCs that are neurons (90.6-96.0%) remained statistically unchanged. When we quantified the percentage of total NeuN$^+$ neurons that were also SA-β-gal$^+$, we observed an accumulating profile that reached a total of 35.3% senescent neurons by 60 dpi (**Figure 10D**).

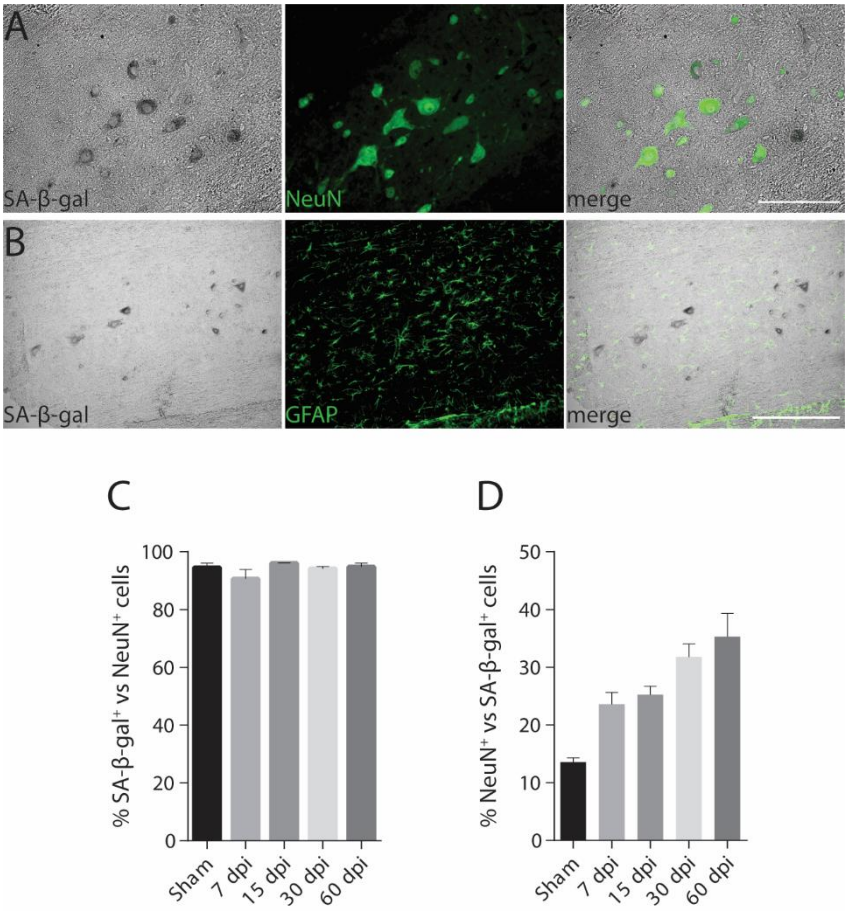

Figure 10. Identification of SA-β-gal$^+$ cells in the mouse spinal cord. In mouse, SA-β-gal$^+$ cells (black) co-localized with the (**A**) pan-neuronal marker NeuN (green). No co-localization was found with the (**B**) pan-glial marker GFAP. Representative images were taken at 15 dpi. The percentages of (**C**) total SA-β-gal$^+$ cells that are NeuN$^+$ and of (**D**) total NeuN$^+$ neurons that are SA-β-gal$^+$ were calculated in laminectomized (Sham) mice and at 7, 15, 30 and 60 days post-injury (dpi). *n* = 2-4. Scale bars: 100 µm.

2.4. Mice reach a locomotor recovery plateau after a spinal cord injury

To correlate the senescent profile after a mouse spinal cord contusion injury with functional recovery, we also assessed locomotor behavior in the open field using the Basso Mouse Scale (BMS) (Basso et al., 2006) score and subscore at several time-points throughout the experiment. In our hands, in a moderate-to-severe (550-750 µm displacement, 75 Kdyne force) contusion injury model, C57BL/6J mice exhibited near complete to complete paralysis of the hind-limbs at 1 dpi and gradually recovered their locomotor function until reaching a plateau at around 21 dpi (**Figure 11A-B**). At 21 dpi, most injured mice were able to perform occasional

(BMS score of 4) or frequent stepping (BMS score of 5) in the open field, but their recovery became stagnant from that point onwards. To reach higher scores, mice would need to display features like consistent stepping, limb coordination, normal trunk stability, parallel paw placement and tail up, which are all subscoring parameters (*for details, see Methods 4.5.*). Laminectomized (Sham) C57BL/6J mice displayed normal BMS scores of 9 throughout the experiment.

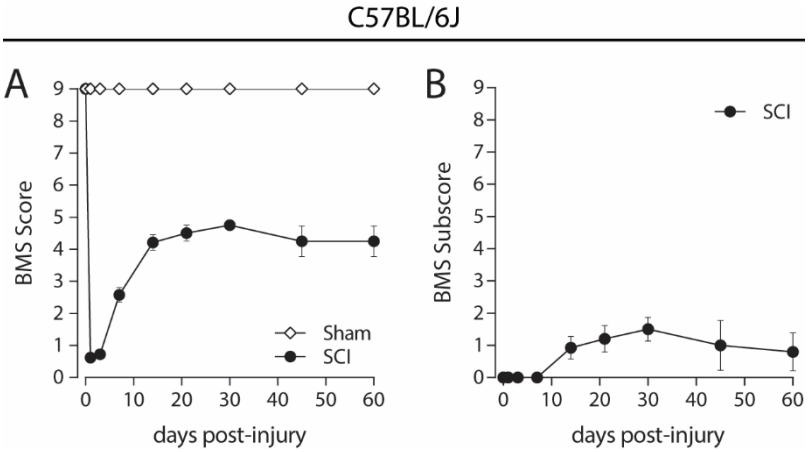

Figure 11. Locomotor recovery characterization of the C57BL/6J contusion injury model. Locomotor behavior of the C57BL/6J contusion injury model was characterized by assessing the (**A**) Basso Mouse Locomotor Scale (BMS) score and (**B**) subscore in an open field at different time-points (0, 1, 7, 15, 21, 30, 45 and 60 days post-injury). While laminectomized (Sham) control animals display a continuous maximum BMS score of 9, spinal cord injured (SCI) C57BL/6J mice exhibit expected BMS score values between 0 and 1 at 1 dpi and then gradually recover until reaching a plateau at around 21 dpi. *n* = 9-17.

3. Zebrafish vs Mouse

3.1. Different senescent cell dynamics are induced after spinal cord injury in zebrafish and in mouse

Comparing both models, the two share one common main fact – SCs are induced at the lesion periphery upon an injury. However, while in the zebrafish these cells reach a peak at 15 dpi

and return to basal (Sham) levels by 60 dpi (**Figure 12A**), in the mouse SA-β-gal$^+$ cells keep accumulating over time and are not cleared out (**Figure 12B**). These results reveal two clearly distinct senescence profiles in an injured spinal cord, a transient profile observed in regenerating zebrafish and a persistent one observed in non-regenerating mice.

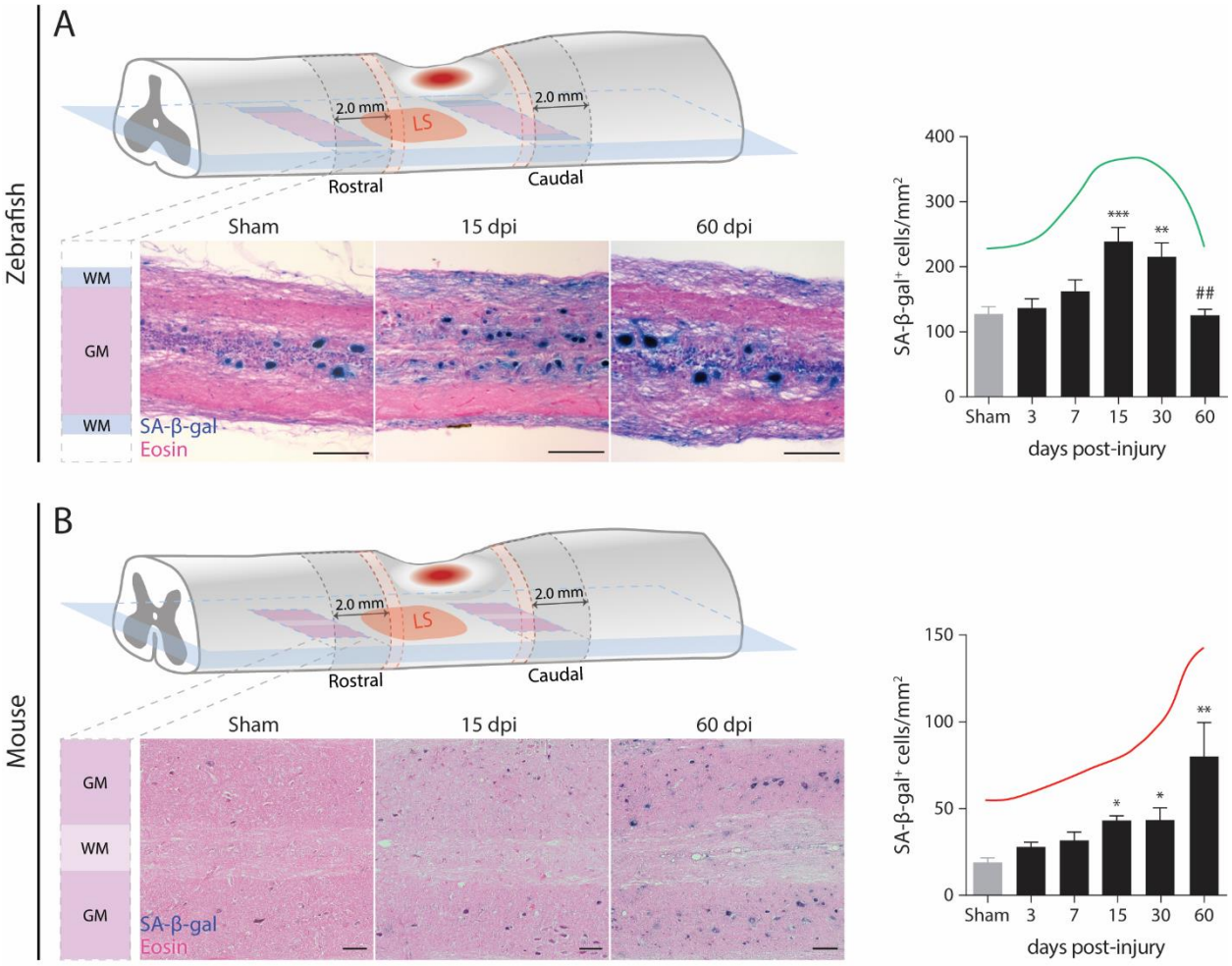

Figure 12. Distinct senescent profiles between zebrafish and mouse after a spinal cord injury. SA-β-gal$^+$ cells (blue) were (**A**) detected around the lesion site (LS) and (**B**) quantified in non-injured (sham) and injured zebrafish spinal cords at different time-points (3, 7, 15, 30 and 60 days-post-injury, dpi). *n* = 5-9. Similarly, SA-β-gal$^+$ cells were (**C**) detected and (**D**) quantified in mouse laminectomized (sham) and injured spinal cords at the same time-points. *n* = 4-7. An eosin counterstaining (pink) was performed after cryosectioning. Cells were quantified at the lesion periphery along 2.0 mm in longitudinal sections. A 0.5 mm interval (red dashed zone) was established between the lesion border and the beginning of the quantification region. SA-β-gal$^+$ cells were quantified along the whole ventral horn region only in the gray matter (GM) and not in the white matter (WM). Data are presented as mean ± SEM. *$p<0.05$, **$p<0.01$, ***$p<0.001$, versus Sham. $^{\#\#}p<0.01$, versus 30 dpi. Scale bars: 100 µm.

3.2. Induced SA-β-gal$^+$ neurons have distinct profiles between zebrafish and mouse

Surprisingly, neuronal cells seem to equally dominate the SA-β-gal$^+$ population in zebrafish and mouse injured spinal cords (**Figure 13A-B**). At 15 and 60 dpi, 87.8% to 96.0% of total SCs are neurons (HuC/D$^+$ or NeuN$^+$) (**Figure 13C**). Yet, both the percentages and dynamics of total neurons that are senescent over time are completely different (**Figure 13D**). While in the zebrafish the percentage of total neurons that are SA-β-gal$^+$ reach a peak of 8.9% at 15 dpi and then return to basal levels (2.3%) at 60 dpi, the mouse displays 25.3% of senescent neurons at 15 dpi. Strikingly, this number keeps increasing until 60 dpi, reaching 35.3% of total neurons.

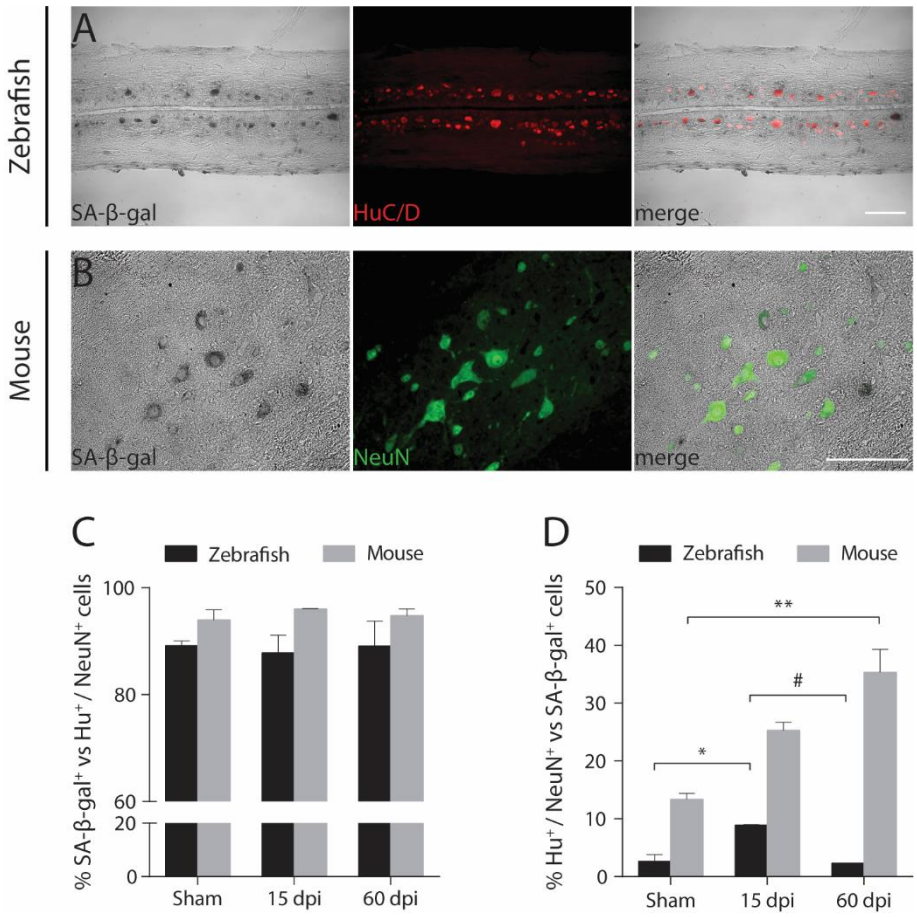

Figure 13. Different profiles of SA-β-gal$^+$ neuronal populations between zebrafish and mouse. In zebrafish and mouse, SA-β-gal$^+$ cells (black) co-localized with the neuronal markers (**A**) HuC/D (red) and (**B**) NeuN (green), respectively. Representative images were taken at 15 dpi. In (**C**) and (**D**), the percentages of total SA-β-gal$^+$ cells that are HuC/D$^+$ or NeuN$^+$ and of total HuC/D$^+$ or NeuN$^+$ neurons that are SA-β-gal$^+$ are compared

between both models. Calculations are presented for uninjured/laminectomized (Sham) zebrafish/mice and at 15 and 60 days post-injury (dpi). n = 2-4. Data are presented as mean ± SEM. $*p<0.05$, $**p<0.01$, versus Sham. $^{\#}p<0.05$, versus 15 dpi. Scale bars: 100 µm.

DISCUSSION

The concepts of cellular senescence and their SASP have evolved remarkably over the last years. Senescence is now recognized as a multifaceted cellular phenomenon that participates in a wide range of different biological contexts (Rodier and Campisi 2011). Yet, most of the mechanisms underlying the complexity of each senescent program remain unknown. While further studies are necessary to understand and reconcile the physiological and pathological roles of senescence, current knowledge favors the premise that transient and controlled induction of SCs is beneficial whereas accumulation and persistence of SCs is detrimental (Rhinn et al., 2019). Interestingly, the role of senescence in wound repair and organ regeneration contexts is still quite uncharted ground.

Here, we describe the induction of SCs as a new cellular response triggered by an injury in the spinal cord. In the regenerating zebrafish model, SCs start to accumulate essentially at the lesion periphery but are eventually cleared and returned to basal levels. This transient profile of SCs induction seems to be a conserved injury-response in organs with regenerative capacities, since it was also described in amputated appendages and damaged hearts of zebrafish, salamanders and neonatal mice (Da Silva-Álvarez et al., 2019; Sarig et al., 2019; Yun et al., 2015). In the non-regenerating mouse however, the induced SCs persist at the lesion periphery and do not show any signs of being efficiently reduced over time. How are these transient vs. persistent senescent profiles established is not known, but it is possible that these are associated with a specific SASP with different capacities to support a cell clearance mechanism. This seems to be the case in the salamander regenerative limb paradigm, where macrophages were proposed to be an essential part of the mechanism that eliminates SCs (Yun et al., 2015). The functional demonstration of the positive role of transient SCs in a regenerative

context comes from the observation that reducing SCs leads to a regeneration delay of amputated pectoral fins in zebrafish (Da Silva-Álvarez et al., 2019). These findings are in line with what was previously reported for skin wound healing, where transient SCs were found to be important for tissue remodeling and repair (Demaria et al., 2014). All these scenarios suggest that a timely removal of SCs is required for proper tissue repair and regeneration to occur.

It is interesting to correlate the senescence profile of zebrafish and mice with their cellular response and functional recovery dynamics after SCI. In the zebrafish, accumulation of SCs is barely noticeable until 7 dpi, peaks at 15 dpi and then starts decreasing. At 10 dpi, apoptosis, debris clearance and the initial inflammatory response have already been resolved (Hui et al., 2010). However, proliferation of ependymo-radial glial progenitors peaks at 14 dpi and is maintained up to 6 weeks post-injury (wpi) (Reimer et al., 2008). Curiously, normal swimming behavior is restored within 4-6 wpi (Becker et al., 2004; Becker & Becker, 2014; Becker et al., 1997; Hui et al., 2010). Though we cannot assume that SCs are actively contributing to the regenerative process, their peak of accumulation does coincide with that of progenitor proliferation. Therefore, it is reasonable to speculate that, following zebrafish SCI, senescence may somehow function as a proliferation-control mechanism. Such role has been previously described during embryonic development, when senescence contributes to tissue patterning by controlling the balance of cell populations and fine-tuning cell fate specification (Rhinn et al., 2019). In fact, we have detected the presence of SA-β-gal^{+} staining in the spinal cord of early developing zebrafish larvae. Thus, we might be looking at a conserved mechanism of morphogenetic signaling that is recapitulated in the adult fish. Indeed, injured larvae exhibited a similar turnover of SA-β-gal^{+} cells, supporting the idea that SCs may play a role in structural specification during spinal cord regeneration.

On the other hand, in mice, SCs start accumulating as soon as 3 dpi, though a significant accumulation is only detectable at 15 dpi. Their accumulation then persists over time. The 15

dpi time-point coincides with the transition from a sub-acute to a chronic stage of injury (Alizadeh et al., 2019). It is also between 15 and 21 dpi that mice hit their plateau of locomotor recovery. Inhibitory CSPGs reach their peak of expression exactly at 2 wpi, remaining chronically upregulated afterwards (Asher et al., 2002; Buss et al., 2009). Interestingly, upregulation of CSPGs has been found to be mediated by PI3K/AKT and mTOR signaling, which happen to be two major senescence-associated pathways (Herranz et al., 2015; Jahan & Hannila, 2015; Laberge et al., 2015; Zhu et al., 2015). In turn, microglia/macrophage population reaches its peak at 10 dpi, but their peak of phagocytic activity is only achieved at 15 dpi (Greenhalgh & David, 2014). Importantly, macrophages persist indefinitely in the injured spinal cord and contribute to chronic inflammation. Considering that a persistent SASP is known to be pro-inflammatory, it becomes plausible to conceive a correlation between the accumulation of SCs and the chronic propagation of the inflammation. Altogether, evidence suggest that persisting SCs might be contributing to an inhibitory microenvironment, which represses axonal regeneration and limits functional recovery following SCI.

In order to detect SCs in the spinal cord, we looked for expression of different senescence markers. In the zebrafish, this task proved to be significantly more challenging than in the mouse, due not only to the limited availability of antibodies but also to the absence of a bona fide $p16^{INK4a}$ (Shim et al., 2017). Nevertheless, we were able to detect co-localization between two senescence biomarkers, SA-β-gal and $p21^{CIP1}$. We noticed that $p21^{CIP1}$ was also expressed in many SA-β-gal^{-} cells. This is likely due to the fact that post-mitotic neurons can also upregulate the cell cycle regulator $p21^{CIP1}$ (Mallick & D'Mello, 2014; Pechnick et al., 2008). The absence of $p21^{CIP1}$ in SA-β-gal^{+} cells has been previously reported (Shtutman et al., 2017; Stein et al., 1999). Indeed, in our samples we found some SA-β-gal^{+}/$p21^{CIP1-}$ cells. However, we cannot exclude the possibility that the SA-β-gal staining-derived precipitate can interfere with antibody incorporation. SA-β-gal staining was performed in all our fixed samples after

isolation and prior to cryosectioning. In truth, when we compared the same immune-protocols between SA-β-gal-stained and unstained samples, we could observe that antibody incorporation was usually more efficient in unstained samples. Consequently, several immunostaining protocols had to be optimized, normally requiring stronger permeabilization steps and increased antibody concentrations, if not also antigen retrieval. In the zebrafish, we were unable to verify the co-expression of SA-β-gal and the DNA damage marker γ-H2AX, another common hallmark of SCs (Gorgoulis et al., 2019). Still, SA-β-gal^{+} cells exhibited an enlarged morphology and lacked expression of the proliferation marker BrdU, two other features of SCs (Gorgoulis et al., 2019). Together, the expression of SA-β-gal and p21^{CIP1}, the absence of BrdU and the display of increased size, validate the characterization of SCs in the zebrafish spinal cord.

On the other hand, SCs in the mouse spinal cord were shown to co-localize SA-β-gal with p16^{INK4a} and γ-H2AX, matching the proposed multi-marker three-step work flow to detect SCs (Gorgoulis et al., 2019). Though we cannot be sure if, contrarily to mouse, γ-H2AX is indeed absent in zebrafish SCs at 15 dpi, it is interesting to speculate that we might be in the presence of two different types of senescence responses to zebrafish and mouse SCI. In some cases, such as during development, senescence has been shown to not be mediated by DDR (Muñoz-Espín et al., 2013; Ohtani et al., 2001). Curiously, we know that zebrafish is able to resolve the cellular damage-associated response to SCI in the first 10 dpi (Hui et al., 2010). In contrast, at 15 dpi, mice still exhibit an exacerbated damage-associated response that involves axonal degeneration, cellular debris and CSPG deposition (Alizadeh et al., 2019). Therefore, we are likely observing two clearly distinct senescence programs that are mediated by different intrinsic mechanisms. Looking at both profiles, a DDR-absent senescence response goes in accordance with the speculation that, in zebrafish SCI, SCs carry out a programmed role of controlling cell populations, such as during development. In turn, in mouse SCI, senescence is

likely a consequence to all the unresolved tissue damage and is, therefore, an unprogrammed response that involves DDR and persists over time.

We were very surprised to find out that the majority of SA-β-gal$^+$ cells that are induced in the spinal cord are neurons. This seems to be the case even in uninjured animals. In the mouse, SA-β-gal$^+$ neurons appear to particularly accumulate in the ventral horn. Interestingly, a previous study has reported evidence for the accumulation of autophagosomes in ventral horn motor neurons following SCI (Liu et al., 2016). Not only is senescence characterized by autophagosome accumulation but autophagy dysfunction is also known to contribute to neuronal loss (Kwon et al., 2017; Liu & Levine, 2015). Curiously, reactive astrocytes are known to activate NF-κB expression and secretion of several chemokines which are well acknowledged SASP factors, such as CCL2, CXCL1, CXCL2, TNF-α and IFN-γ (Cekanaviciute & Buckwalter, 2016; Pineau et al., 2010). In fact, senescent astrocytes have already been put at the central stage of CNS dysfunction, contributing to age-related pathologies such as neurodegenerative diseases (Cohen & Torres, 2019). Yet, we failed to see any co-localization between SA-β-gal and the glial marker GFAP. Thus, the remnant population of non-neuronal SA-β-gal$^+$ cells remains to be identified.

Our observations might have significant implications for SCI pathology. First, while the zebrafish is able to clear senescent neurons and repopulate them through neurogenesis, the mouse has a progressive and irreversible loss of neurons after SCI (Beattie et al., 2002; Hui et al., 2010). Now, it seems a big percentage of surviving neurons activate a persisting senescence response. Moreover, though 35.3% of total neurons exhibit senescent features at 60 dpi, we do not know if this number keeps increasing after this time-point. Whether these are neurons that have been axotomized after injury and/or that are degenerating, remains to be elucidated. It is possible that a senescence program is activated in response to axonal damage, in view of recruiting the immune system to promote self-clearance. However, the immune system is

incapable to efficiently process the massive amount of damage cues present in and around the lesion site (Bradbury & Burnside, 2019). Thus, SCs might not be able to be efficiently cleared and instead keep accumulating. We do not know how deep the neuronal phenotype of SA-β-gal^{+} cells is affected by a prolonged senescent program but it is likely that they acquire a pro-inflammatory SASP that potentiates inflammation and contributes to secondary injury. In order to investigate this, a transcriptomic characterization at the single cell level will be necessary.

So, having uncovered distinct senescent profiles in two SCI models with different regeneration outcomes, the next big question is: what is the actual functional role of SCs in SCI?

CHAPTER II - DEPLETION OF SENESCENT CELLS IMPROVES FUNCTIONAL RECOVERY AFTER MAMMALIAN SPINAL CORD INJURY

Part of the content of the following section is contained in the manuscript **"Depletion of senescent cells improves functional recovery after spinal cord injury"** (*submitted*).

ABSTRACT

Transient senescent cells (SCs) were shown to benefit tissue repair contrasting with persistent SCs known to underlie ageing-related chronic disorders. Knowing that two distinct senescence profiles are induced after spinal cord injury (SCI) in zebrafish and in mouse, we aimed at investigating the role of induced-SCs in both models by pharmacologically or genetically depleting them.

In the zebrafish, we tried to optimize a protocol for the administration of senolytics, drugs that selectively kill SCs by apoptosis, in order to assess the functional role of transient SCs in spinal cord regeneration. In the mouse, we hypothesized that the persistence of SCs could contribute to the inhibitory microenvironment in mammalian spinal cord repair. We tested this hypothesis by treating injured mice with ABT-263, a powerful senolytic drug. We show that depletion of induced-SCs after a murine spinal cord contusion injury improves locomotor (assessed with Open Field and Horizontal Ladder), sensory (evaluated with Incremental Thermal Plate) and bladder functions. At the cellular level, ABT-263 treatment increased the amount of spared myelin and axons, reduced the fibrotic scar and attenuated inflammation. Furthermore, preliminary data suggest that ABT-263 may have a beneficial effect on SCI-induced liver pathology by limiting lipidosis. Finally, using p16-3MR transgenic mice, we demonstrate in a completely independent approach that the selective elimination of $p16^{INK4a}$-expressing cells improves locomotor recovery.

Our data shows that the accumulation of SCs after SCI in the mouse is detrimental for repair and that, by eliminating them, we can improve functional recovery.

Keywords: spinal cord injury, senescent cells, senolytics, ABT-263, functional recovery

INTRODUCTION

A spinal cord injury (SCI) is a major cause of disability in humans and other mammals, often leading to permanent loss of locomotor and sensory functions. This type of traumatic lesion is defined by three biological features: a lesion core or fibrotic scar with no viable neural tissue; an astrocytic scar around the lesion core; and a surrounding area of spared neural tissue with limited function, which may exhibit some functional plasticity (O'Shea et al., 2017). Although the lesion scar provides structural support, it also creates an inhibitory microenvironment for the regrowth of severed axons, thus preventing re-enervation of the original targets (Cregg et al., 2014). A SCI is further defined as an inflammatory condition mediated by activated astrocytes and infiltrating macrophages that remain in the spinal cord indefinitely (Donnelly & Popovich, 2008). Immediately after the injury, the blood-spinal cord barrier is disrupted and, although it gradually recovers, it remains compromised for a long period (Whetstone et al., 2003). This facilitates the extravasation of immune cells contributing to the establishment of a chronic inflammatory state (Beck et al., 2010).

In contrast to mammals, the zebrafish spinal cord has the remarkable capacity to recover motor and sensory functions after injury. This regenerative ability seems to stem from the supportive microenvironment where there is no formation of a glial or fibrotic scar and inflammation is dynamically controlled by macrophages (Tsarouchas et al., 2018), allowing neurogenesis and regrowth of severed axons (Becker et al., 1997; Vajn et al., 2013).

While considerable knowledge was achieved on the biological processes that occur after a SCI in mammals and regenerative species, small progress was obtained on therapeutic options, suggesting that other cellular players might be relevant following an injury. Cellular senescence rises as a plausible novel player in SCI, considering its secretory features and associated

potential to modulate the microenvironment (Acosta et al., 2013; Calcinotto et al., 2019). Previous results from our lab show that there are distinct senescence profiles between zebrafish and mice after SCI. While the regenerating zebrafish displays a transient burst of SCs that is later cleared out, the non-regenerating mouse exhibits a persistent accumulation of SCs through time.

Here we aim at unveiling the role of SCs induced after SCI. To investigate the functional contribution of SCs to the repair process in zebrafish and mouse SCI, we have targeted them pharmacologically using a senolytic approach. In the mouse, we also depleted SCs through genetic ablation using a p16-3MR transgenic line. Our data provide evidence for a detrimental role of persistent SCs in the mammalian spinal cord following injury and support the potential use of therapeutics targeting SCs to promote spinal cord repair.

RESULTS

1. Elimination of SCs in the Zebrafish – Senolytics

1.1. The senolytic drug ABT-263 fails to eliminate senescent cells in the zebrafish spinal cord

The lack of an exclusive biomarker of SCs makes their specific targeting extremely difficult and the scarcity of proper tools to manipulate them has been a major barrier to study the role of SCs *in vivo*. In recent years, a few transgenic mouse models were developed using the promoter of $p16^{INK4a}$ to induce the expression of a fluorescent protein by $p16^{+}$ cells and/or allow their elimination upon administration of a drug (Baker et al., 2011; Demaria et al., 2014). In the zebrafish, much effort has been done by several labs around the world in order to generate a reliable transgenic line but, due to the absence of a properly characterized cdkn2a/b locus, so far those efforts remain unsuccessful. Another method to target SCs *in vivo* is the use of senolytic drugs, compounds that kill SCs by interfering with crucial signaling pathways for the maintenance of the senescent phenotype (Zhu et al., 2015). Of those currently available, Navitoclax (ABT-263), an inhibitor of the anti-apoptotic proteins BCL-2 and BCL-xL, is one of the most promising senolytics in terms of efficiency and selectivity (Chang et al., 2016). Unfortunately, though, a successful administration protocol for senolytic drugs in the zebrafish model had not yet been described.

After uncovering a transient senescent profile of SCs upon zebrafish spinal cord injury, our main questions became: What are these cells doing there? Are they somehow helping regeneration? Are they just a consequence of all the damage caused by the lesion and play a passive role in the regenerative process until removed? So, to address these questions, we set

out to optimize an administration protocol for ABT-263 in the zebrafish in order to investigate the outcome of depleting SCs *in vivo* after spinal cord injury.

We decided to start testing the administration of ABT-263 in larvae, not only because of the swiftness of the regenerating period but also to ensure a greater accessibility of the drug to the injury which, in the case of larval spinal cord injury, is completely exposed. According to the manufacturer (Selleckchem), ABT-263 is insoluble in water, which is a major adversity to our model. Thus, we tried to counter this by testing different solvent compositions and incubation temperatures in view of facilitating drug miscibility. ABT-263 stock solution was reconstituted in DMSO and diluted in embryo medium (E3 or E1) to a range of different concentrations (0.1-100 µM) (**Figure 14**). With E3 medium, at 28°C, ABT-263 completely precipitated inside the incubation wells unless the final concentration was lower than 10 µM. We used a lower concentration of embryo medium (E1) and added HEPES buffer to better control salt concentration and pH effects on drug stability. In these conditions, we saw no precipitation up until 10 µM. We also increased the incubation temperature to 33°C to promote drug solubility. In the end, in all scenarios tested, we observed no decrease in SA-β-gal staining at the lesion site.

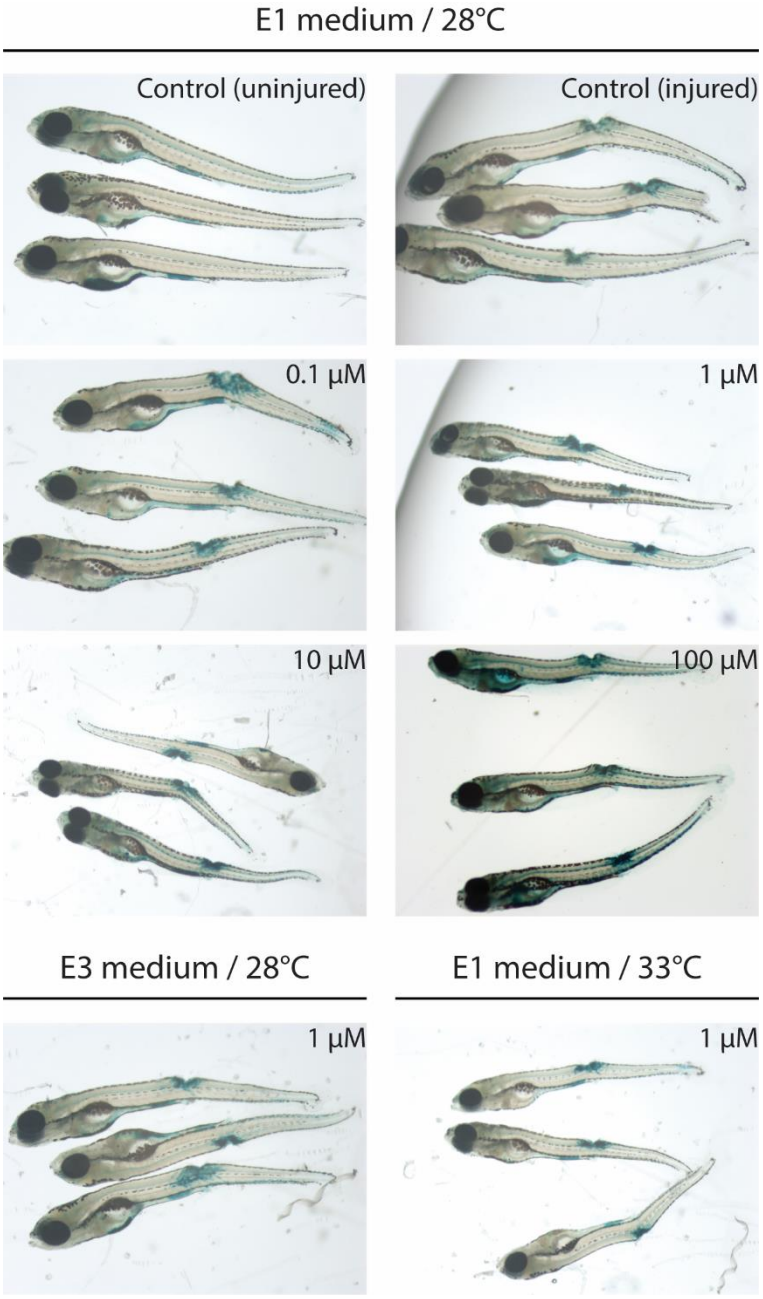

Figure 14. SA-β-gal staining is not decreased with ABT-263 after larval spinal cord injury. SA-β-gal staining was performed at 2 days post-injury in zebrafish larvae that were submitted to different ABT-263 concentrations (0.1-100 µM), incubation temperatures (28-33°C) and embryo medium composition (E1-E3). For E1 medium (1,67 mM NaCl, 0.06 mM KCl, 0.11 mM $CaCl_2$, 0.11 mM $MgSO_4$, 0.003% Methylene Blue, pH 7.4), 10 mM HEPES buffer was added.

Subsequently, we opted to administrate ABT-263 directly in the adult zebrafish. Here, we came across another difficulty – ABT-263 does not cross the blood-brain barrier (Vogler et al., 2011; Yamaguchi & Perkins, 2012). Counting on vessel leakiness at the injury site to ensure drug

accessibility, we started by administrating ABT-263 by intraperitoneal injection (IPi) at 5 dpi, to allow a period of recovery after the injury in which the zebrafish are still fragile to endure another anesthesia. We performed consecutive administrations every 48 hours of 100-500 µM ABT-263 or Vehicle (polyethylene glycol 400:Phosal 50PG:Ethanol, 30:60:10 v/v). While 500 µM ABT-263 was revealed to be toxic (>90% deaths after first IPi), 100 µM ABT-263 was better tolerated (≈30% deaths each IPi) until three consecutive IPi. However, we noticed that this great amount of deaths was mainly due to the toxicity of the Vehicle itself. The animals that survived were sacrificed and stained for SA-β-gal. After three IPi, ABT-263 (100 µM) failed to decrease the number of SA-β-gal$^+$ cells in the injured spinal cord (**Figure 15A**).

Given that, according to previous studies, ABT-263 formulation is optimized for oral administration (Chang et al., 2016; Demaria et al., 2014), we chose to administrate this drug by oral gavage, following a previously described protocol (Dang et al., 2016). 500 µM ABT-263 continue to result in major deaths, even though animals tolerated more consecutive administrations than by IPi. Zebrafish were much more tolerable to the oral administration of 100 µM ABT-263, but, after three consecutive gavages, we still saw no effect on SA-β-gal$^+$ cells (**Figure 15B**). Finally, we tested another formerly described administration protocol (Mokalled et al., 2016) by using an absorbable sponge soaked with ABT-263 that is placed at the lesion site right after the injury, before wound closure. While this only allows a single administration, it also guarantees that the drug reaches the target region. Still, ABT-263 was unable to reduce the number of SA-β-gal$^+$ cells at the lesion periphery (**Figure 15C**).

Throughout these optimizations, we also tried different Vehicle compositions (namely DMSO and polyethylene glycol 400:DMSO) but, in the end, we were never able to observe a decrease in the number of SCs in the zebrafish spinal cord with the senolytic drug ABT-263.

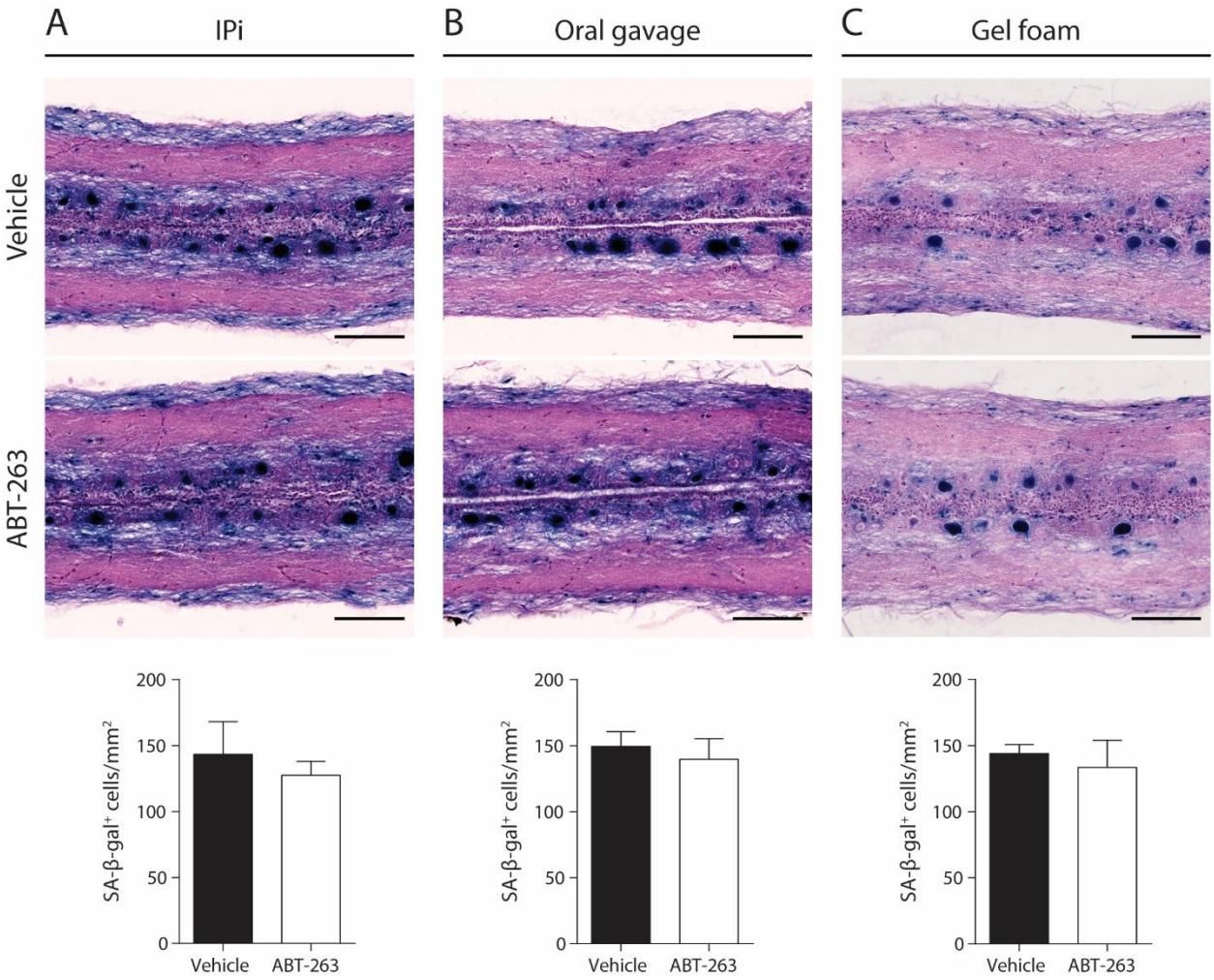

Figure 15. Different ABT-263 administration protocols fail to reduce the number of SA-β-gal$^+$ cells in the adult zebrafish injured spinal cord. SA-β-gal$^+$ cells (blue) were quantified at the lesion periphery after delivering Vehicle (polyethylene glycol 400:Phosal 50PG:Ethanol, 30:60:10 v/v) or ABT-263 (100 µM) by (**A**) intraperitoneal injection (IPi), (**B**) oral gavage or (**C**) gel foam application to spinal cord-injured zebrafish. Scale bars: 100 µm.

2. Elimination of SCs in the Mouse - Senolytics

2.1. The senolytic drug ABT-263 successfully eliminates senescent cells in the mouse spinal cord after a contusion injury

The accumulation or persistence of SCs and subsequent chronic exposure to their senescence-associated secretory phenotype (SASP) have been shown to contribute to loss of tissue function and diminish the repair capacity in aged tissues (Acosta et al., 2013; Calcinotto et al., 2019;

Campisi, 2013; Childs et al., 2015). Given the contrast of the senescent profile observed between two models with opposite regenerative outcomes, we hypothesized that the accumulation of SCs in the injured mouse spinal cord is an important detrimental factor contributing for the inhibitory microenvironment that undermines its regenerative potential. Therefore, we designed an experiment to evaluate the impact of eliminating SCs in a mouse contusion model of spinal cord injury.

Contrarily to the zebrafish, the administration of ABT-263 in mouse models has been previously demonstrated (Chang et al., 2016; Demaria et al., 2014). We administered ABT-263 by oral gavage within the first 14 dpi (sub-acute injury phase), during which the blood-spinal cord barrier remains leaky (Whetstone et al., 2003), thus ensuring maximum accessibility of this drug to the tissue (**Figure 16A**). We defined three main experimental end-points (15, 30 and 60 dpi) and, throughout the experiment, we assessed locomotor function using the Basso Mouse Scale (BMS) and Horizontal ladder (HL), as well as sensory function using the Incremental Thermal Plate (ITP). After the surgical procedures, animals were randomly distributed in two treatment groups – Vehicle (corn oil) and ABT-263 (50 mg/kg/day). No differences were observed in injury displacement (Vehicle: 647.6 ± 12.2 μm; ABT-263: 650.4 ± 11.6 μm, **Figure 16B**) or force (Vehicle: 77.2 ± 2.0 Kdyne; ABT-263: 77.3 ± 2.6 Kdyne, **Figure 16C**) between the two experimental cohorts.

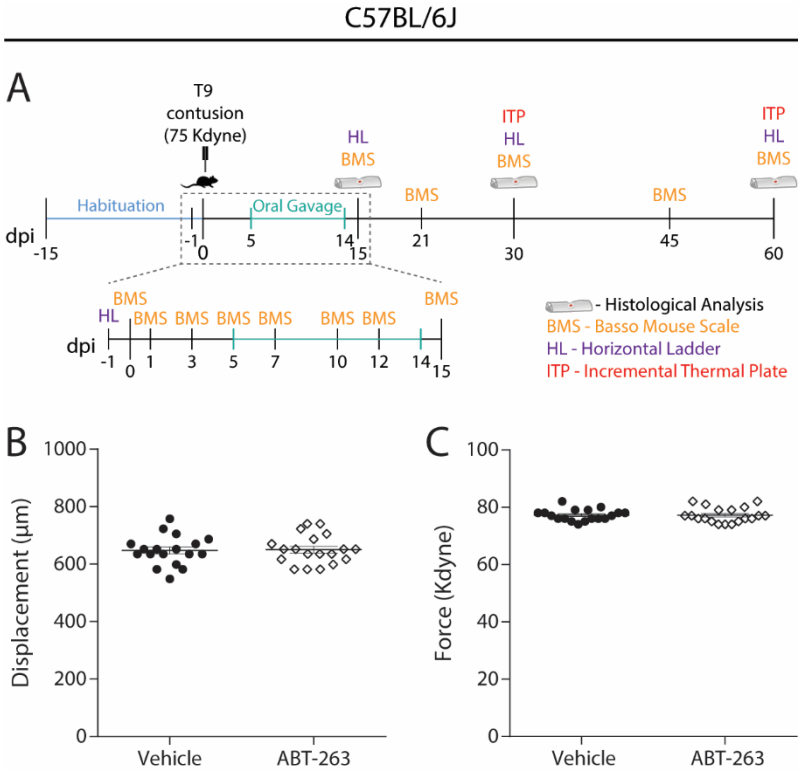

Figure 16. Experimental design and injury biomechanics for the different experimental cohorts of C57BL/6J mice. (**A**) Schematic of the experimental setup. C57BL/6J mice were habituated to the different behavioral setups for a 15-day period, before being submitted to a moderate-to-severe (force: 75 Kdyne; displacement: 550-750 µm) T9 contusion injury. Injured animals received daily Vehicle (corn oil) or ABT-263 (50 mg/kg/day) via oral gavage, from 5 to 14 days-post-injury (dpi). (**B**) Spinal cord tissue displacement (in micrometers, µm) and (**C**) impact force (in kilodynes, Kdyne) at the time of the contusion injury for the experimental groups. No differences were observed in displacement (Vehicle: 647.6 ± 12.2 µm; ABT-263: 650.4 ± 11.6 µm) or force (Vehicle: 77.2 ± 2.0 Kdyne; ABT-263: 77.3 ± 2.6 Kdyne). *n* = 18-19. Data are presented as mean ± SEM.

First, we confirmed that ABT-263 administration by oral gavage from 5 to 14 dpi reduced the number of SA-β-gal$^+$ cells in the mouse spinal cord at the lesion periphery, when compared to Vehicle (**Figure 17A-B**). At 15 dpi, ABT-263 treatment significantly decreased the number of SA-β-gal$^+$ cells/mm^2 in the total sectional gray matter by 68,4% (**Figure 17C**). After the end of treatment, by 30 and 60 dpi, SA-β-gal$^+$ cells seem to be re-emerging. When we quantified SA-β-gal$^+$ cells only in the ventral horn, we found a similar accumulation dynamic in the Vehicle-treated mice to that of the initial senescence profiling (**Figure 17D**).

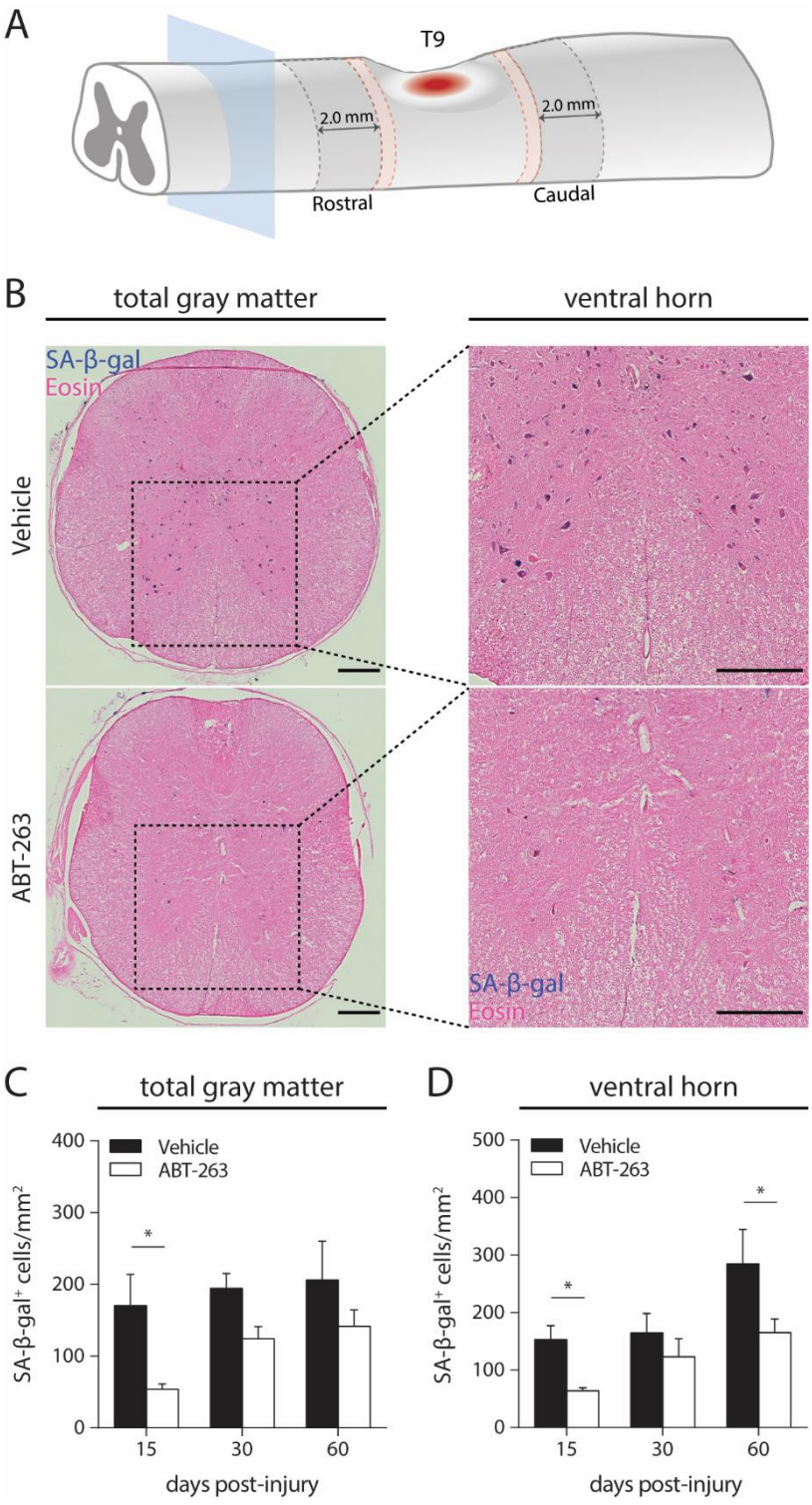

Figure 17. ABT-263 successfully eliminates senescent cells in the mouse spinal cord. (**A**) SA-β-gal^{+} cells were quantified in a total of ten different transversal sections (five rostral and five caudal) along 2.0 mm at the lesion periphery. A 0.5 mm interval (red dashed zone) was established between the lesion and the beginning of the quantification region. (**B**) An eosin (pink) counterstaining was performed after cryosectioning. SA-β-gal^{+} cells (blue) were quantified in the total sectional gray matter and only at the ventral horn. (**C**-**D**) Quantifications were performed at all experimental endpoints (15, 30 and 60 days post-injury). At 15 dpi, ABT-263 treatment

significantly decreased the number of SA-β-gal$^+$ cells/mm^2 in the total gray matter and in the ventral horn by 68,4% and 58,0%, respectively. At 60 dpi, a significant reduction (41,9%) of SA-β-gal$^+$ cells/mm^2 in ABT-263-treated animals was still observed in the ventral horn. *n* (15 dpi) = 3-4; *n* (30 dpi) = 3-4; *n* (60 dpi) = 2-3. Data are presented as mean ± SEM. **p*<0.05, ABT-263 versus Vehicle. Scale bars: 200 μm.

We further confirmed that ABT-263 has similar elimination efficiencies in the rostral (73.0%) and caudal (69.2%) sides of the injury at 15 dpi (**Figure 18A-D**). Interestingly, the effects of ABT-263 treatment are perceived even in the lumbar-sacral region, further away from the lesion site, where 61.9% of SA-β-gal$^+$ cells were still eliminated (**Figure 18E**). However, in all regions analyzed, there is a gradual re-emergence of SA-β-gal$^+$ cells after 15 dpi, which suggests that SCs can still be induced after ceasing ABT-263 treatment.

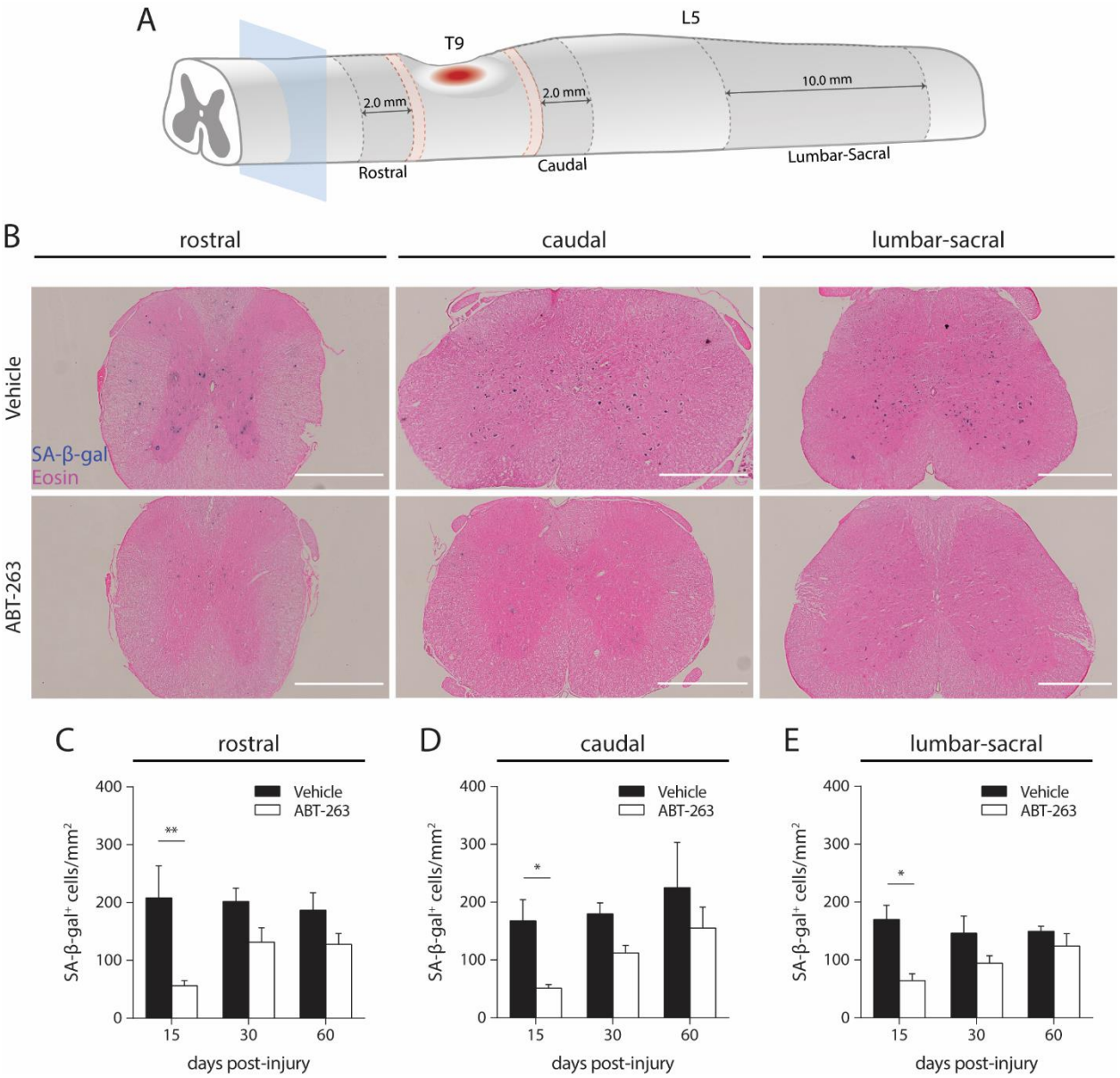

Figure 18. ABT-263 kills senescent cells in different spinal cord regions. (**A**) SA-β-gal$^+$ cells were quantified in three different spinal cord regions towards the lesion epicenter (rostral, caudal and lumbar-sacral). A 0.5 mm interval (red dashed zone) was established between the lesion and the beginning of the quantification regions. The lumbar-sacral quantification region started at the L5 segment. (**B**) An eosin (pink) counterstaining was performed after cryosectioning. SA-β-gal$^+$ cells (blue) were only quantified in the total gray matter (dark pink) and not in the white matter (light pink). (**C** and **D**) In the thoracic region, SA-β-gal$^+$ cells were manually counted in five different rostral or caudal sections along 2.0 mm at the lesion periphery. (**E**) In the lumbar-sacral region, SA-β-gal$^+$ cells were quantified in ten sections spaced 1 mm apart. Quantifications were performed at all experimental endpoints (15, 30 and 60 days post-injury). At 15 dpi, ABT-263 treatment significantly decreased the number of SA-β-gal$^+$ cells/mm^2 in the rostral, caudal and lumbar-sacral regions by 73,0%, 69,2% and 61,9%. *n* (15 dpi) = 3-4; *n* (30 dpi) = 3-4; *n* (60 dpi) = 2-3. Data are presented as mean ± SEM. *p<0.05, **p<0.01, ABT-263 versus Vehicle. Scale bars: 500 µm.

2.2. Depletion of senescent cells with ABT-263 improves motor, sensory and bladder function recovery following a spinal cord injury in mice

During the habituation period, we verified that mice presented normal locomotor behavior with maximum BMS scores of 9 in the open field test (Basso et al., 2006). After injury, most mice exhibited complete hindlimb paralysis at 1 dpi and gradually improved locomotor ability reaching a plateau at around 21 dpi (**Figure 19A**), as expected for a contusion injury model in C57BL/6J mice (Basso et al., 2006). In ABT-263-treated animals, BMS scores were significantly higher from 7 dpi (2 days after the beginning of administration) until 30 dpi, when compared with Vehicle-treated mice (**Figure 19A**). In turn, BMS subscores were significantly higher from 12 to 60 dpi in animals treated with ABT-263 (**Figure 19B)**. Strikingly, at 30 dpi, all ABT-263-treated mice achieved frequent plantar stepping with 93% (14 out of 15) of mice displaying parallel placement of both hindpaws at initial contact and 40% (6 out of 15) also at lift off. Remarkably, 33% (5 out of 15) of mice treated with ABT-263 exhibited consistent plantar stepping and mild trunk stability, one animal showed normal trunk stability with mostly coordinated fore-hindlimb walking, and a second animal displayed some fore-hindlimb coordination, improvements never achieved in Vehicle-treated mice.

Comparing to the BMS, the HL test allows a finer assessment of locomotion by monitoring the precise paw placement in each ladder rung in video-recorded attempts (Cummings et al., 2007). Before the injury, all mice completed the HL with no difficulty displaying few to no mistakes or negative events (**Figure 19C-D**). Notably, ABT-263-treated mice made significantly fewer stepping mistakes (**Figure 19C**) and displayed significantly more positive stepping events (**Figure 19D**) at 30 and 60 dpi, when compared with animals treated with Vehicle, thus largely corroborating the BMS results obtained in the open-field.

Thermal allodynia, i.e. hypersensitivity to normally non-noxious stimuli, is a common pain-related symptom associated with spinal cord injuries (Nakae et al., 2011; Watson et al., 2014).

Using an ITP, we were able to compare the temperature threshold necessary to elicit an avoidance behavior to a cold or a hot stimulus between the two experimental groups. Considering that uninjured C57BL/6J mice only exhibit nocifensive reaction to cold between 2 to 4°C (Yalcin et al., 2009), ABT-263 treatment significantly decreased cold hypersensitivity at 30 dpi, compared to Vehicle-treated animals who showed an average temperature reaction to cold of 10.6°C (**Figure 19E**). We found no effect of ABT-263 administration on the threshold temperature required to prompt a nocifensive reaction to a hot stimulus, when compared to Vehicle administration (**Figure 19F**).

Bladder dysfunction is another common consequence of spinal cord injury that severely compromises patients' daily lives (Yoshimura, 1999). In our model, mice lose the ability to contract the bladder muscle, resulting in urine retention and possibly urinary tract infections unless the organ is manually emptied by the caretakers. Consequently, we assessed bladder function by attributing a score to the amount of urine retained each day. In contrast to injured mice treated with Vehicle, ABT-263-treated animals exhibited smaller volumes of retained urine from 9 to 15 dpi (**Figure 19G**). This effect is lost after 15 dpi.

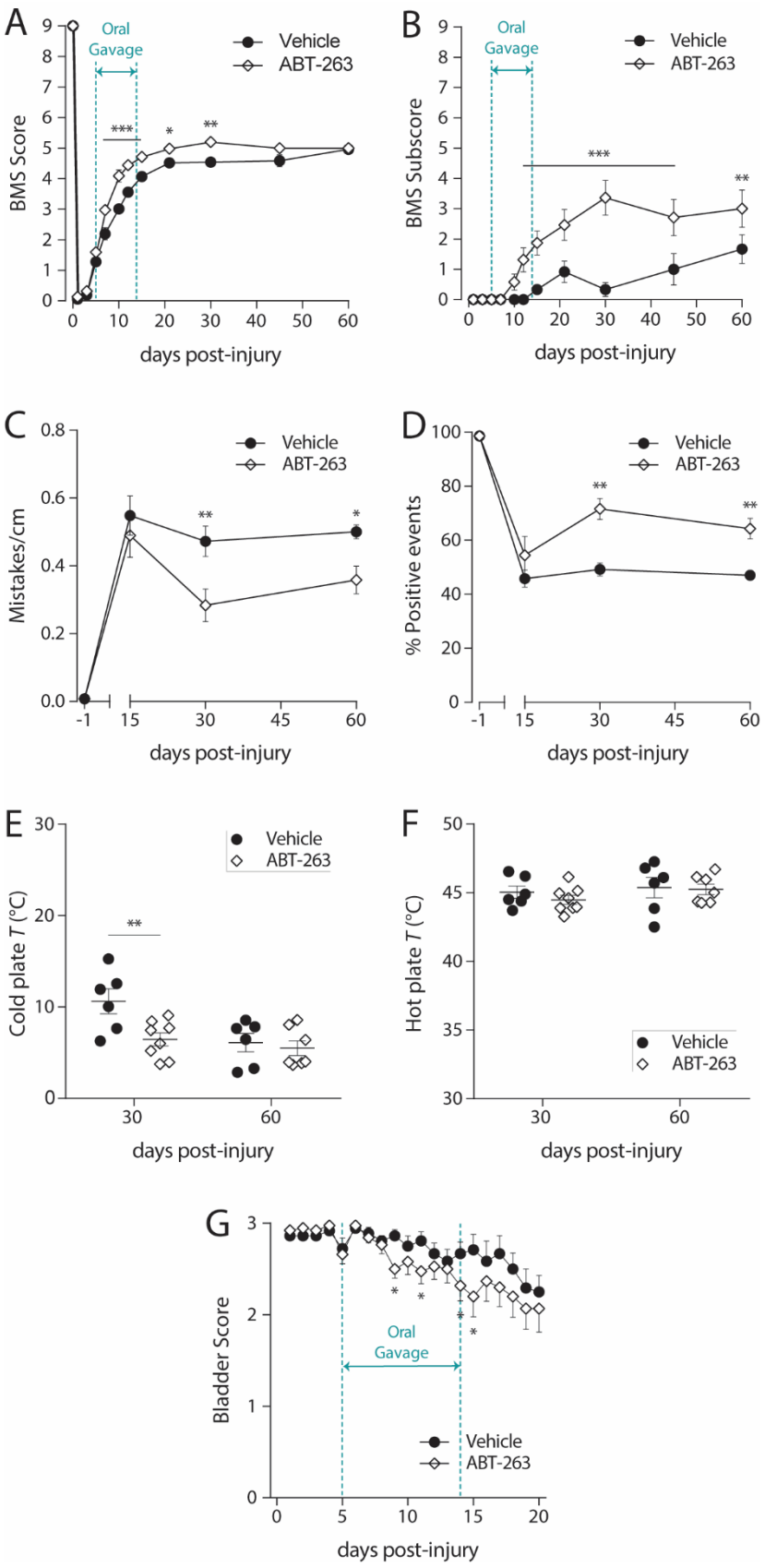

Figure 19. Effects of ABT-263 treatment in locomotor, sensory and bladder function after a spinal cord injury in mice. (**A-B**) Basso Mouse Locomotor Scale (BMS) score and subscore were evaluated in an open field

at different time-points (0, 1, 3, 5, 7, 10, 12, 15, 21, 30, 45 and 60 days post-injury, dpi). Vehicle (corn oil) or ABT-263 were delivered daily from 5 dpi to 14 dpi by oral gavage. *n* = 18-19. (**C-D**) The locomotor performance in the Horizontal Ladder was assessed at -1 (control), 15, 30 and 60 dpi by quantifying the total number of mistakes per centimeter and the percentage of singular positive events (plantar step, toe step and skip) measured and averaged across three successful trials. *n* = 3-6. (**E-F**) Thermal allodynia was tested at 30 and 60 dpi by determining the temperature at which injured mice reacted to a cold or hot stimulus. *n* = 6-8. (**H**) Bladder function was grossly evaluated by attributing a bladder score to the amount of urine collected each time a bladder was manually voided. *n* = 18-19. Data are presented as mean ± SEM. **p<0.05, **p<0.01, ***p<0.001*, ABT-263 versus Vehicle.

2.3. The senolytic ABT-263 promotes myelin preservation after spinal cord injury

After a spinal cord injury, oligodendrocytes undergo both necrotic and apoptotic cell death, which results in demyelination around the lesion and, consequently, impaired function of unprotected fibers and spared circuits (Emery et al., 1998; Totoiu & Keirstead, 2005).

To evaluate the effect of eliminating SCs on the demyelination status after injury, we used the FluoroMyelin^{TM} Green fluorescent myelin staining to compare the spared white matter area per total cross-sectional area (% CSA) between ABT-263-treated mice and vehicle-treated mice along 2 mm around the lesion epicenter. Remarkably, ABT-263 treatment consistently resulted in significantly greater white matter sparing levels across all experimental timepoints, an effect that is more prominent at the caudal side of the lesion (**Figure 20A-C**).

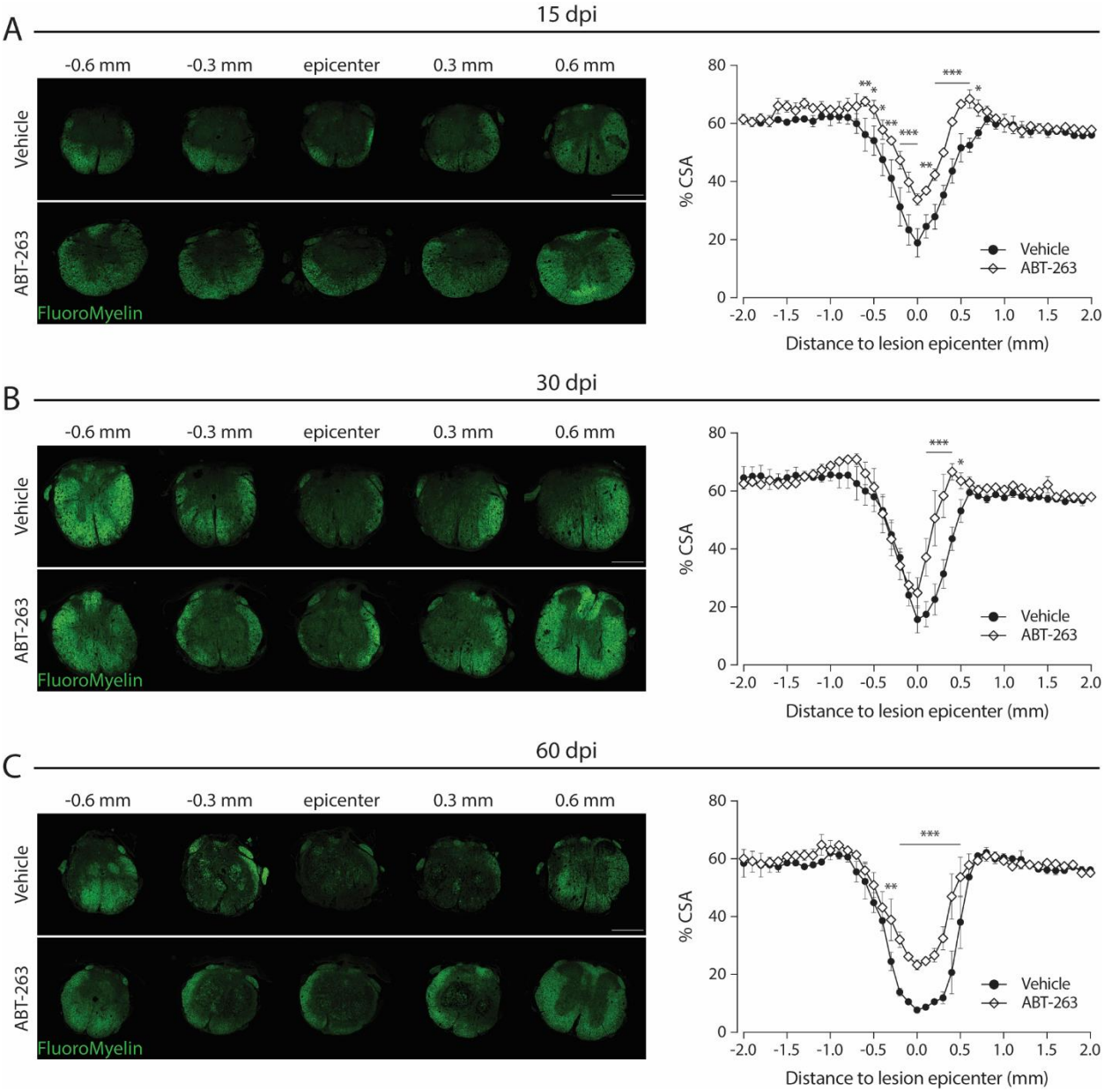

Figure 20. White matter sparing is increased after eliminating senescent cells with ABT-263. Transversal sections at different distances from the lesion epicenter of an injured spinal cord (**A**) at 15 days-post-injury (dpi), (**B**) at 30 dpi and (**C**) at 60 dpi, treated with Vehicle and ABT-263 and stained with FluoroMyelin (green) and the corresponding quantifications. In (**A-C**), white matter sparing was assessed by normalizing the area stained with FluoroMyelin (green) to the total cross-sectional area (CSA) of spinal cord sections every 100 µm ranging from 2 mm rostral and 2 mm caudal to the lesion epicenter. *n* (15 dpi) = 3-4; *n* (30 dpi) = 3-4; *n* (60 dpi) = 2-3. Data are expressed as % CSA and presented as mean ± SEM. **p<0.05, **p<0.01, ***p<0.001*, ABT-263 versus Vehicle. Scale bars: 500 µm.

2.4. ABT-263 supports axonal growth after spinal cord injury

The normal neural circuit organization is disrupted after a spinal cord injury. However, spared neural tissue can, to a certain extent (depending on the severity of the lesion), reorganize itself in order to establish new lines of communication across and beyond the injury (Courtine & Sofroniew, 2019). This plasticity potential explains why after an incomplete lesion (e.g. our contusion injury model) mice can partially restore their locomotor function. Still, the secondary injury cascade of events inevitably leads to progressive neuronal cell death and axonal degeneration, both rostrally and caudally to the lesion epicentre (Qian et al. 2010). Therefore, it is essential to comprehend the different cellular and molecular players that regulate axonal growth and formation of new functional synapses.

We hypothesized that eliminating SCs would provide a more favorable environment for axonal preservation and growth after a spinal cord injury. To assess this, we tested the expression of neuronal growth-associated protein 43 (GAP43), which is highly expressed in neuronal growth cones during development and axonal regeneration (Benowitz & Routtenberg, 1987). We performed immunostainings for GAP43 in dorsal-ventral longitudinal sections spanning the ventral horn (where the motor neurons are located) and quantified the number of $GAP43^{+}$ fibers at specific distances from the lesion epicenter (**Figure 21A**), as previously described (Almutiri et al., 2018; Hata et al., 2006). At 30 dpi, ABT-263-treated mice had a significant increased number of $GAP43^{+}$ axons across most inspected regions, including at the lesion epicenter, compared to Vehicle-treated mice (**Figure 21B, C**).

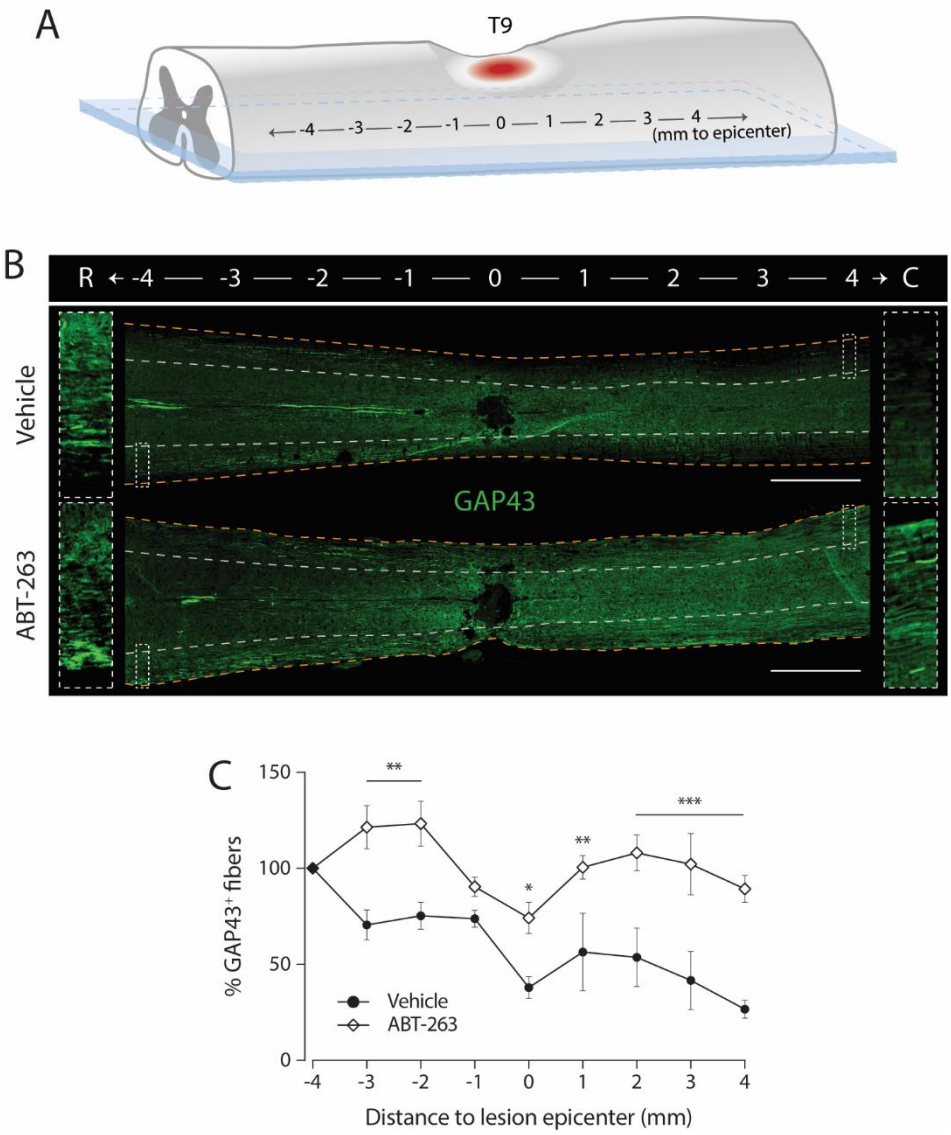

Figure 21. ABT-263 administration increases the number of GAP43$^+$ fibers. (**A**) Longitudinal coronal sections of the ventral region of the spinal cord (delineated in blue) were obtained. GAP43$^+$ axonal fibers were counted at specific distances (every 1 mm) from the lesion epicenter along the rostral (R)-caudal (C) axis of injured spinal cords. (**B**) Longitudinal coronal section of the ventral region of a spinal cord treated with Vehicle or ABT-263 and stained with GAP43. GAP43$^+$ axonal fibers were counted at specific distances (every 1 mm) from the lesion epicenter along the rostral (R)-caudal (C) axis. Fibers were quantified only in the white matter in the ventral region of the spinal cord (delineated in blue). Light grey dashed lines delimitate the white matter from the grey matter. Orange dashed lines outline the limit of the spinal cord section. (**C**) Axon number was calculated at 30 days post-injury (dpi) as a ratio of the total GAP43$^+$ fibers at 4 mm rostral (-4) from the lesion epicenter (0). n = 3. Data are presented as mean ± SEM. *p<0.05, **p<0.01, ***p<0.001, ABT-263 versus Vehicle. Scale bars: 1000 µm.

2.5. Administration of the senolytic ABT-263 reduces the fibrotic scar

Scar formation following spinal cord injury constitutes a major barrier for axonal regrowth (Cregg et al., 2014). Inside the lesion core, a subset of proliferating PDGFRβ^{+} perivascular cells give rise to a fibrotic scar with dense deposition of extracellular matrix components (Soderblom et al., 2013). In fact, it has been shown that reducing the pericyte-derived fibrotic scar facilitates functional recovery after spinal cord injury in mice (Dias et al., 2018). In this study, we examined the size and length of the fibrotic scar using a double immunostaining with PDGFRβ (a pericyte marker that labels the fibrotic component of the scar) and GFAP (a glial marker that helps delineate the fibrotic scar compartment). At the lesion epicenter, mice treated with the senolytic exhibited a significantly reduced PDGFRβ^{+} area at 15 and 60 dpi when compared to mice treated with Vehicle (**Figure 22A-D**).

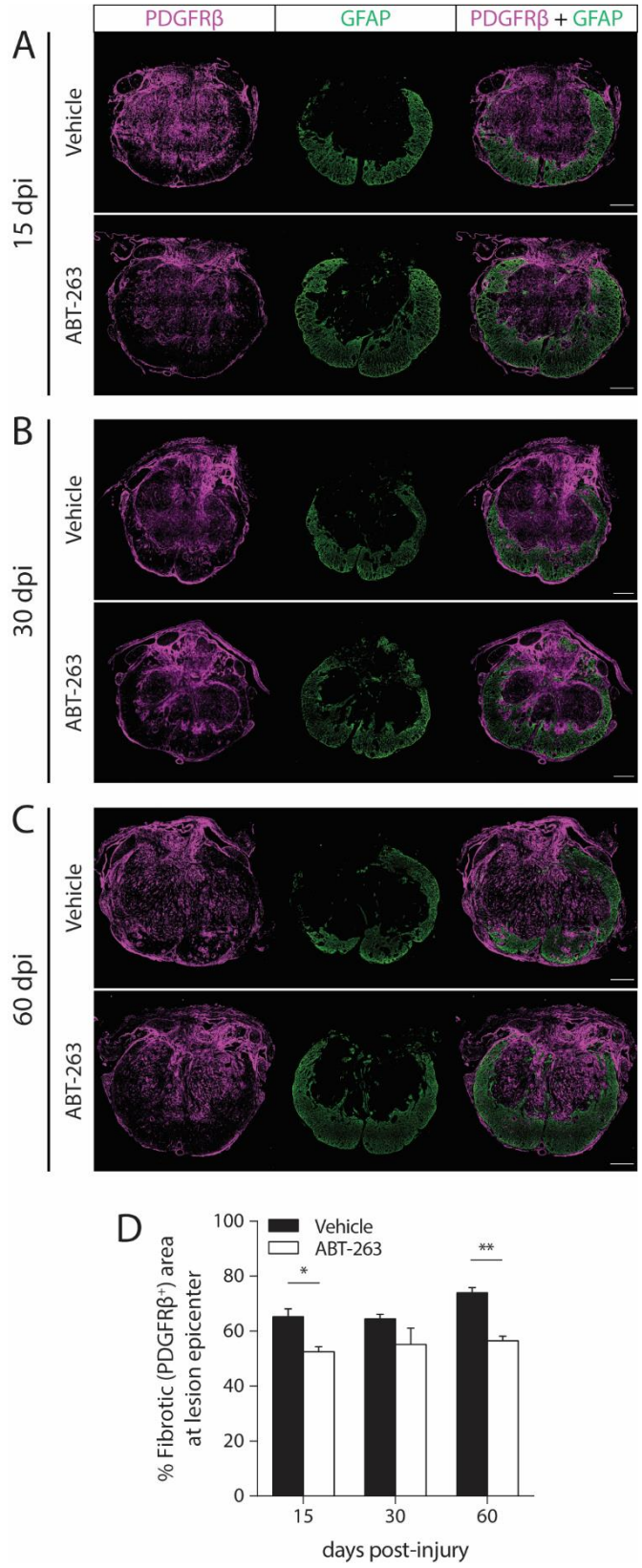

Figure 22. Eliminating senescent cells leads to a reduction of the fibrotic scar area. Transversal sections at the lesion epicenter of an injured spinal cord (**A**) at 15 days-post-injury (dpi), (**B**) at 30 dpi and (**C**) at 60 dpi treated with Vehicle and ABT-263 and stained with the fibrotic scar marker PDGFRβ^{+} area (magenta) and with the astrocytic scar marker GFAP (green). The fibrotic scar area was evaluated by normalizing the PDGFRβ^{+} area

(magenta) to the total cross-sectional area at the lesion epicenter. GFAP$^+$ tissue (green) surrounds the fibrotic core. *n* (15 dpi) = 3-4; *n* (30 dpi) = 3-4; *n* (60 dpi) = 2-3. (**D**) The percentage of fibrotic tissue in the injury core was quantified at 15, 30 and 60 dpi. Data are presented as mean ± SEM. **p*<0.05, ***p*<0.01, ABT-263 versus Vehicle. Scale bars: 200 µm.

Using the same double immunostaining, we were able to define the extension of the scar by tracing, rostrally and caudally to the epicenter, signs of fibrotic PDGFRβ$^+$ staining in the dorsal side of the spinal cord (**Figure 23A**). With this analysis, we observed that the total length of the fibrotic scar was shorter at 15 dpi in ABT-263-treated mice, an effect sustained until 30 dpi only at the caudal side (**Figure 23B**).

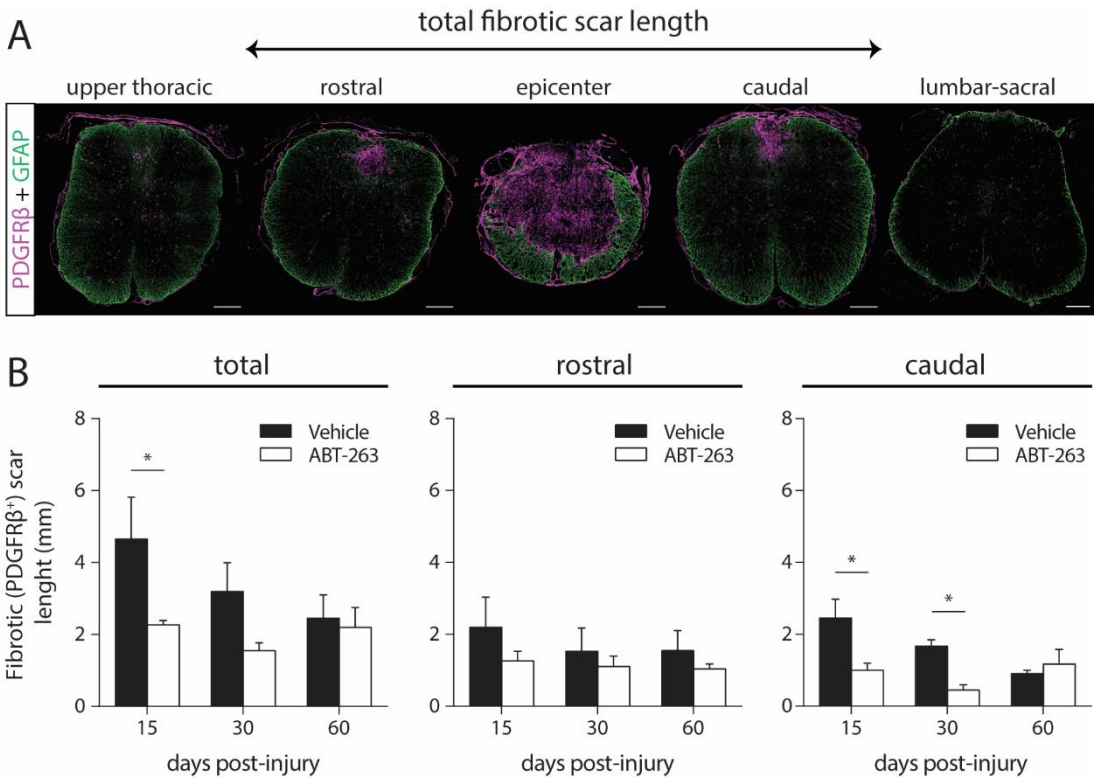

Figure 23. Depletion of senescent cells leads to a reduced fibrotic scar extension. (**A**) The total lenght of the fibrotic scar was measured by calculating the distance, rostral and caudal from the lesion epicenter, until which scarring PDGFRβ$^+$ (magenta) tissue was visualized, i.e the rostral-caudal distance spanned by sections containing fibrotic tissue. GFAP$^+$ tissue (green) surrounds the fibrotic tissue. (**B**) Total, rostral and caudal fibrotic extensions were calculated at 15, 30 and 60 days post-injury. *n* (15 dpi) = 3-4; *n* (30 dpi) = 3-4; *n* (60 dpi) = 2-3. Data are presented as mean ± SEM. **p*<0.05, ABT-263 versus Vehicle. Scale bars: 200 µm.

2.6. Macrophage numbers at the injury site are reduced following ABT-263 treatment

A spinal cord lesion in mice elicits a strong and long-lasting inflammatory response that potentiates secondary injury (Blight, 1985; Popovich et al., 1997). Macrophages are the most abundant inflammatory cells in a spinal lesion, infiltrating the injury core and releasing several molecules, namely nitrogen/oxygen metabolites, cytokines, proteases and chondroitin sulphate proteoglycans that can cause cellular damage and inhibit axonal growth (Fitch & Silver, 1997). Importantly, depletion of macrophages was demonstrated to promote repair and partial motor recovery after spinal cord injury in rats (Popovich et al., 1999). Additionally, senescence is closely linked to inflammation. SCs, through their SASP, can secrete a plethora of immune modulators and proinflammatory cytokines like TNF-α and CCL2 (two potent macrophage recruiters), IL-6, IL-8 and IL-1α (Coppé et al., 2010). Consequently, the accumulation/persistence of SCs in tissues is usually associated with chronic inflammation. To investigate the impact of the accumulation of SCs on inflammation in the mouse spinal cord after an injury, we performed immunostainings with the pan-macrophage marker F4/80. As anticipated, by eliminating SCs with ABT-263, we observed lower levels of inflammatory macrophages (% $F4/80^{+}$ area) in spinal cord sections spanning the lesion area, particularly at 30 dpi (**Figure 24A-C**).

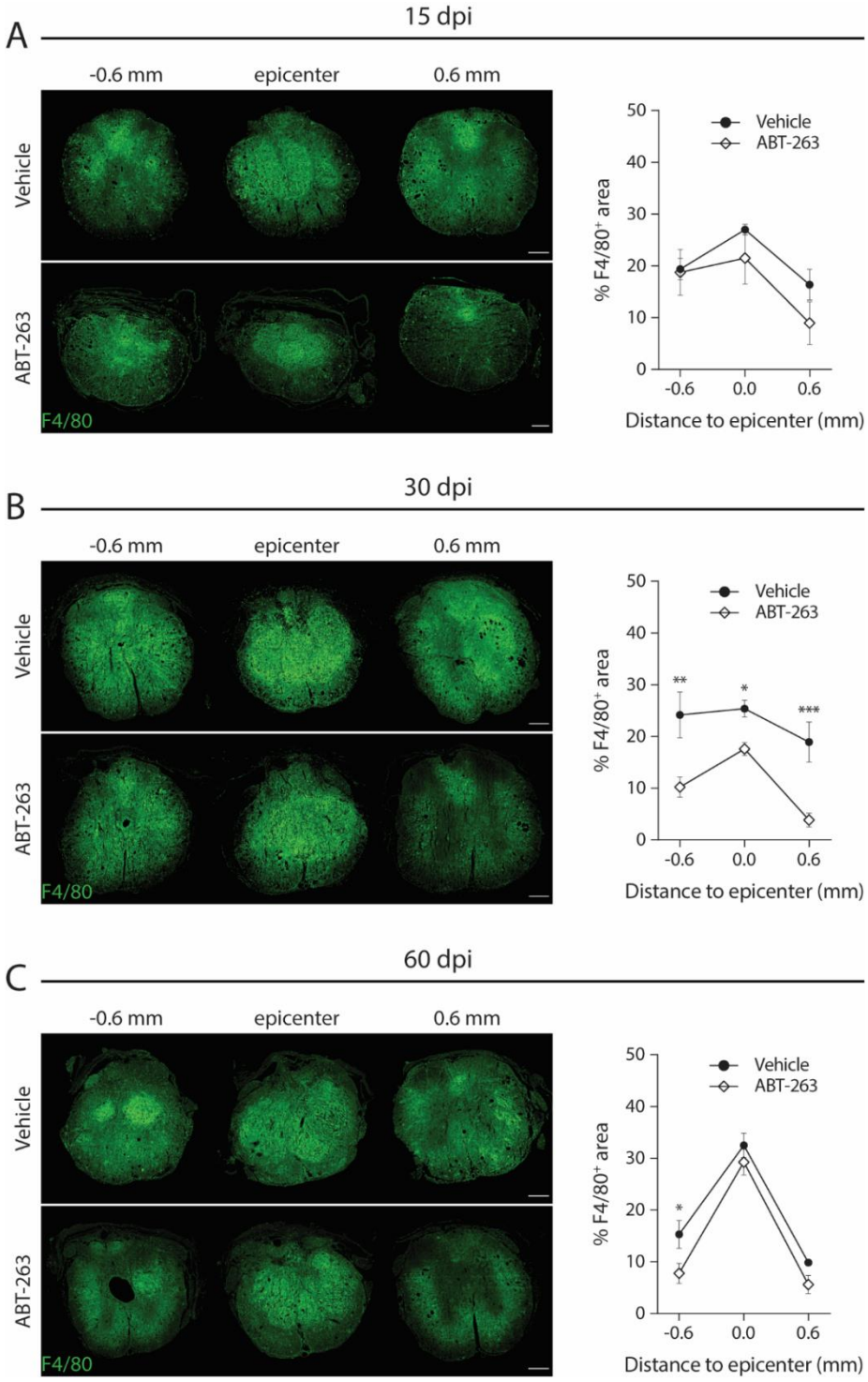

Figure 24. ABT-263 treatment decreases the number of macrophages at the injury site. Transversal sections at the lesion epicenter of an injured spinal cord (**A**) at 15 days-post-injury (dpi), (**B**) at 30 dpi and (**C**) at 60 dpi treated with Vehicle and ABT-263 and stained with the pan-macrophage marker F4/80 (green). In (**A-C**), the area of F4/80$^+$ tissue was measured at lesion epicenter and 600 µm rostral and caudal from the epicenter. Measurements are expressed as a percentage of the total cross-sectional area. *n* (15 dpi) = 3-4; *n* (30 dpi) = 3-4; *n* (60 dpi) = 2-3. Data are presented as mean ± SEM. **p*<0.05, ***p*<0.01, ****p*<0.001, ABT-263 versus Vehicle. Scale bars: 200 µm.

Like in other lesioned tissues, macrophages have been shown to have a dual role in spinal cord injury, promoting secondary damage but also repair (Barrette et al., 2008; Blight, 1994; Giulian & Robertson, 1990; Popovich et al., 1999). This duality is mainly attributed to the balance between two distinct macrophage subpopulations – a M1 pro-inflammatory subtype and a M2 pro-regenerative subtype (Kigerl et al., 2009). In a mouse contusion injury model, persistent pro-inflammatory signaling mechanisms induce an exacerbated and long-lasting M1 macrophage response at the lesion site which is neurotoxic for axonal growth. In turn, M2 macrophages promote long-distance axon growth but their response is smaller and rapidly overwhelmed by M1 macrophages (Kigerl et al., 2009). Therefore, it has been suggested that polarizing the differentiation of resident microglia and infiltrating monocytes towards a M2 phenotype can limit secondary injury and promote repair after a spinal cord lesion.

Here, we aimed at unveiling the proportion of M1 and M2 subtypes present at the lesion site after ABT-263 treatment, in order to check if the elimination of SCs promotes a shift to a more pro-regenerative microenvironment. To do that, we used two specific markers of M1 and M2 macrophages – CD16/32 and CD206, respectively (Kigerl et al., 2009). Regrettably, due to SA-β-gal staining-mediated restraints, we were unsuccessful in optimizing an immunoprotocol for CD16/32. However, we used CD206 to measure the percentage of M2 macrophages towards the total $F4/80^{+}$ macrophage population (**Figure 25A**). Surprisingly, at 15, 30 and 60 dpi, the number of M2 macrophages (by itself) at the lesion site, assessed by the percentage of $CD206^{+}$ area, remains unchanged between Vehicle- and ABT-263-treated animals (**Figure 25B-D**). Yet, given that the percentage of total macrophages is reduced upon ABT-263 treatment, the ratio M2/total macrophages ($CD206^{+}$ / $F4/80^{+}$) increases at the injury site (**Figure 25B-D**). Even though we cannot affirm that, by eliminating SCs, we are promoting a shift to a more pro-regenerative microenvironment, these results suggest that ABT-263 is in fact controlling the M1 response after a spinal cord injury.

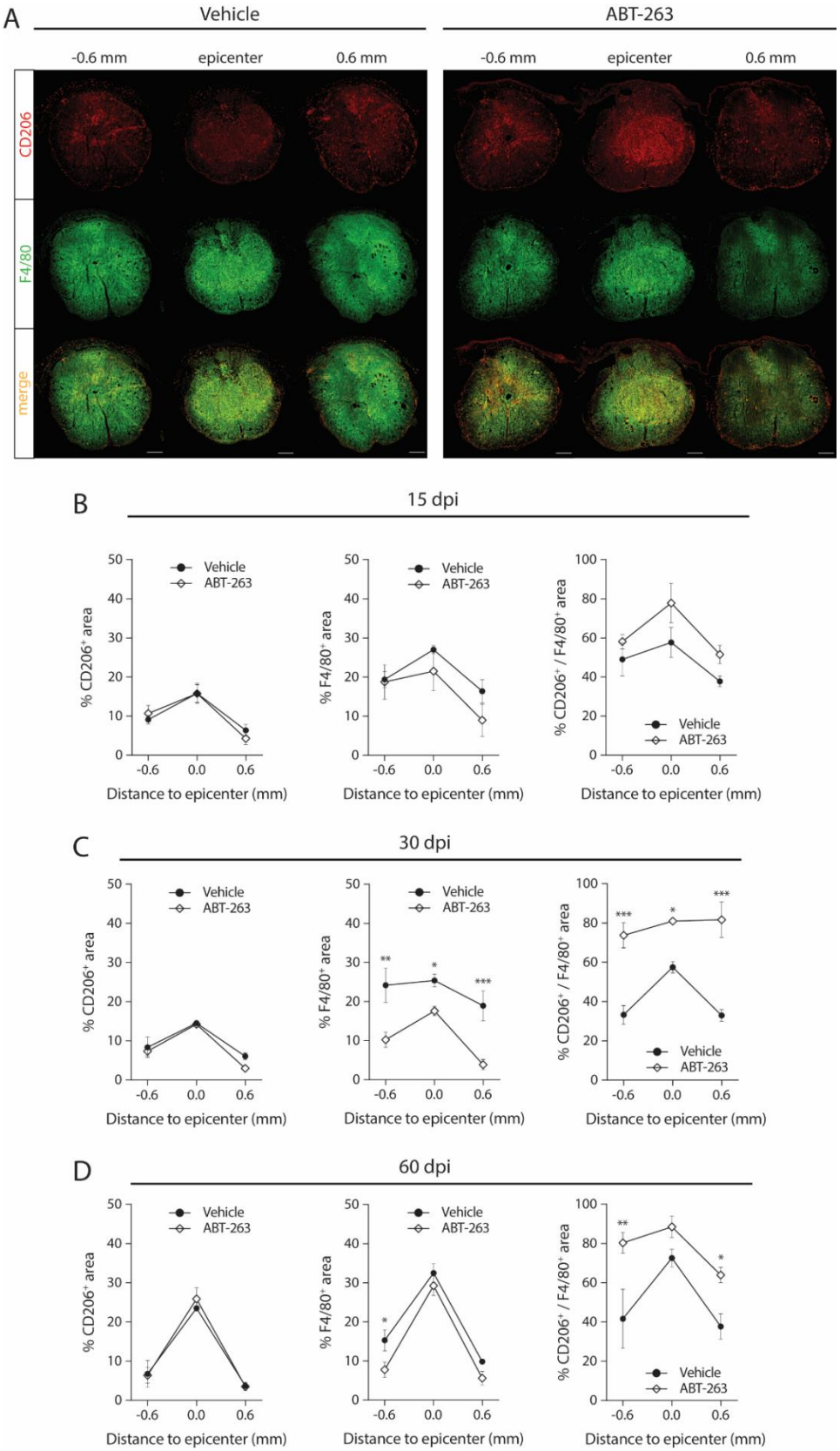

Figure 25. ABT-263 effects on the percentage of M2-type macrophages present at the injury site. (**A**) Representative transversal sections at the lesion epicenter of injured spinal cords at 30 days-post-injury (dpi), treated with Vehicle and ABT-263 and stained with both the pan-macrophage marker F4/80 (green) and the M2-

phenotype specific marker CD206 (red). The areas of $CD206^+$ and $F4/80^+$ tissue were measured at lesion epicenter and 600 µm rostral and caudal from the epicenter at (**B**) 15, (**C**) 30 and (**D**) 60 dpi. Measurements are expressed as a percentage of the total cross-sectional area. A ratio between $CD206^+$ and $F4/80^+$ areas was calculated to infer the % of M2-type macrophages towards the total $F4/80^+$ macrophage population. *n* (15 dpi) = 3-4; *n* (30 dpi) = 3-4; *n* (60 dpi) = 2-3. Data are presented as mean ± SEM. **p*<0.05, ***p*<0.01, ****p*<0.001, ABT-263 versus Vehicle. Scale bars: 200 µm.

2.7. ABT-263 limits liver damage after spinal cord injury

Beyond a chronic inflammatory response *in loco*, a traumatic spinal cord injury also disrupts the systemic neuroimmune crosstalk, severely affecting various organs and contributing to systemic organ dysfunction and increased morbidity/mortality (Brennan & Popovich, 2018).

In the spleen, the disruption of tonic supraspinal sympathetic control leads to splenic atrophy and dysfunction of several splenocyte populations, such as leukocytes (Noble et al., 2018). In the liver, a critical organ for metabolic homeostasis, spinal cord injury elicits a number of hepatic changes, namely cellular damage, excess lipid accumulation, metabolic dysfunction and uncontrolled inflammation, which altogether contribute to systemic inflammation, cardiovascular disease, and metabolic syndrome (Sauerbeck et al., 2015).

To investigate if ABT-263 has any effect (direct or indirect) on the spleen or the liver after spinal cord injury, we weighed these organs upon isolation and looked for signs of cellular damage. While ABT-263- and Vehicle-treated animals did not differ in spleen weight, ABT treatment significantly reduced liver weight to control levels, as compared to Vehicle (**Figure 26A-B**). A global histopathological analysis of liver sections did not reveal statistical differences in hepatocellular damage (inflammation, necrosis and lipidosis) scoring (**Figure 26C**). However, the size of lipid droplets (lipidosis) was smaller in ABT-263-treated mice (**Figure 26D**), suggesting an impact of drug treatment on metabolic function. To confirm if ABT-263 has a positive influence on lipid accumulation in the liver after spinal cord injury, we performed Oil Red O staining to quantify lipid deposition after both treatments, but no

differences were observed (**Figure 26E**). This might be explained by the fact that we did not account for this specific analysis upon organ collection and samples were not properly processed in order to perform this staining. Still, we think these results constitute some interesting preliminary data that will be taken in consideration for future studies.

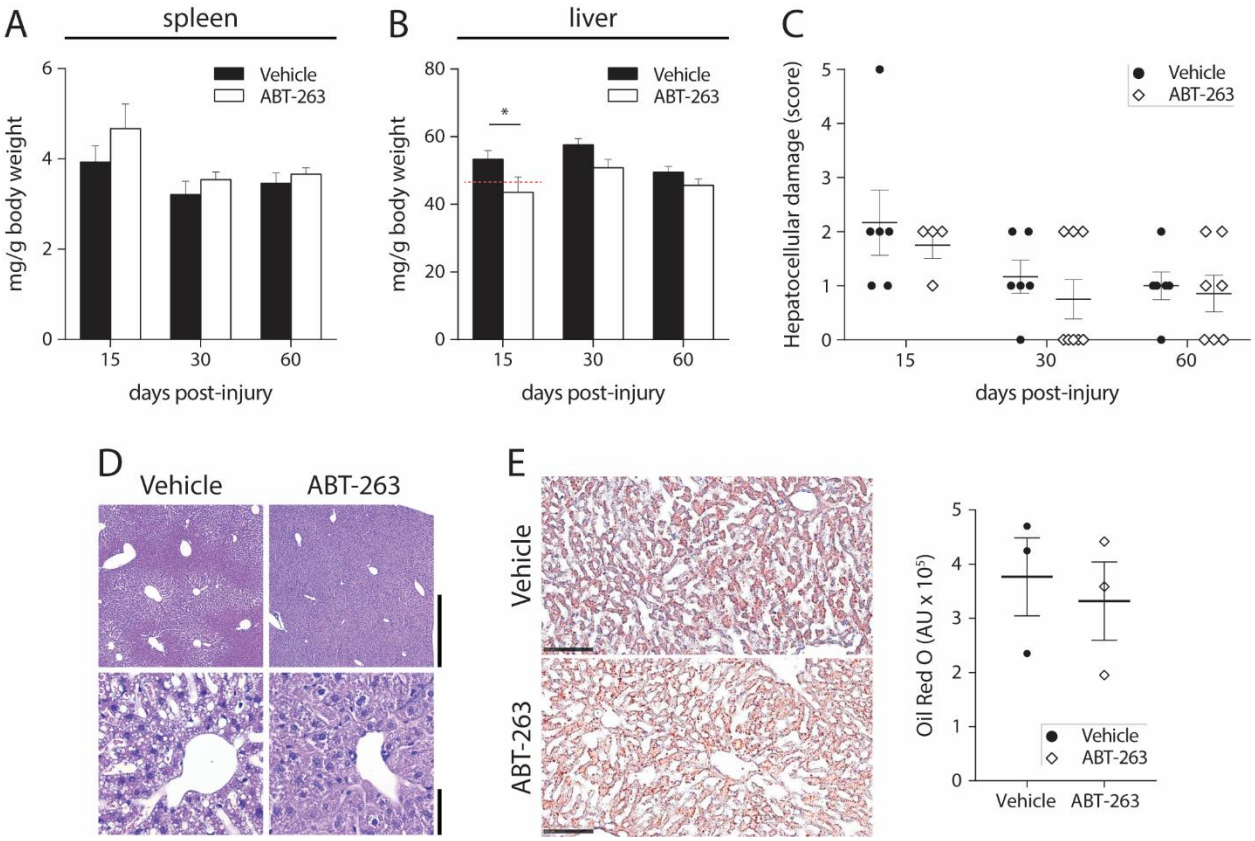

Figure 26. Peripheral effects of ABT-263 on spleen and liver. Perfused (**A**) spleen and (**B**) liver organs were collected and weighted at the experimental time-points (15, 30 and 60 days post-injury). Organ weight was normalized to the total animal body weight before sacrifice. The red dashed line indicates the normal liver weight of uninjured C57BL/6J mice of equal age. (**C**) Signs of hepatocellular damage (e.g. immune cell infiltration, necrosis, lipidosis) were analyzed by an histopathologist who attributed a damage score depending on the diagnosis. (**D**) Representative microphotographs of liver of Vehicle- and ABT-263-treated injured mice depict the hepatocellular vacuolation (lipidosis) characterized by the presence of one or more small to large well-defined rounded vacuoles in the cytoplasm of each cell. A hematoxylin and eosin staining was performed prior to histopathological analysis. Scale bars: 250 µm (upper panel), 25 µm (lower panel). (**E**) At 30 days post-injury, an Oil Red O staining was performed in order to quantify lipid levels. Scale bars: 100 µm. Data are presented as mean ± SEM. **p*<0.05, ABT-263 versus Vehicle.

3. Elimination of SCs in the Mouse – Transgenics

3.1. $p16^{+}$ cells are eliminated in spinal cord of p16-3MR transgenic mice

The creation of mouse transgenic models that allow the tagging of SCs *in vivo* constitutes a fundamental tool to investigate the role of senescence in several different biological contexts. During this thesis project, p16-3MR transgenic mice (Demaria et al., 2014) were kindly provided to us by Marco Demaria (European Research Institute for the Biology of Aging, Groningen, Netherlands). The particularity of this line relies on a tri-modality fusion protein (3MR) (Ray et al., 2004), which contains functional domains of a synthetic Renilla luciferase (LUC), monomeric red fluorescent protein (mRFP), and truncated herpes simplex virus 1 (HSV-1) thymidine kinase (HSV-TK), that is expressed under the control of the $p16^{INK4a}$ promoter. Thus, such versatile model allows not only the detection of $p16^{+}$ cells by luminescence and their sorting from tissues, but also their selective killing upon administration of a drug, Ganciclovir (GCV) (Demaria et al., 2014). GCV is converted by HSV-TK into a toxic DNA chain terminator causing death by apoptosis in the $p16^{INK4a+}$ cells (R-M Laberge et al., 2013). Contrarily to ABT-263, GCV is known to cross the blood-spinal cord barrier (Gynther et al., 2015; Natale et al., 2015) and can, therefore, induce the elimination of SCs for longer periods.

First, we performed a small trial experiment to confirm if $p16^{INK4a+}$ cells were eliminated in the spinal cord after GCV administration. Both in Sham (laminectomized) and spinal cord-injured p16-3MR mice the number of RFP-expressing cells was reduced upon five consecutive daily administrations (from 5 to 9 dpi) of GCV (**Figure 27A-B**). With this preliminary experiment, we confirmed the feasibility of the p16-3MR model and, more importantly, proved that SCs can be eliminated in the spinal cord, even in the absence of injury.

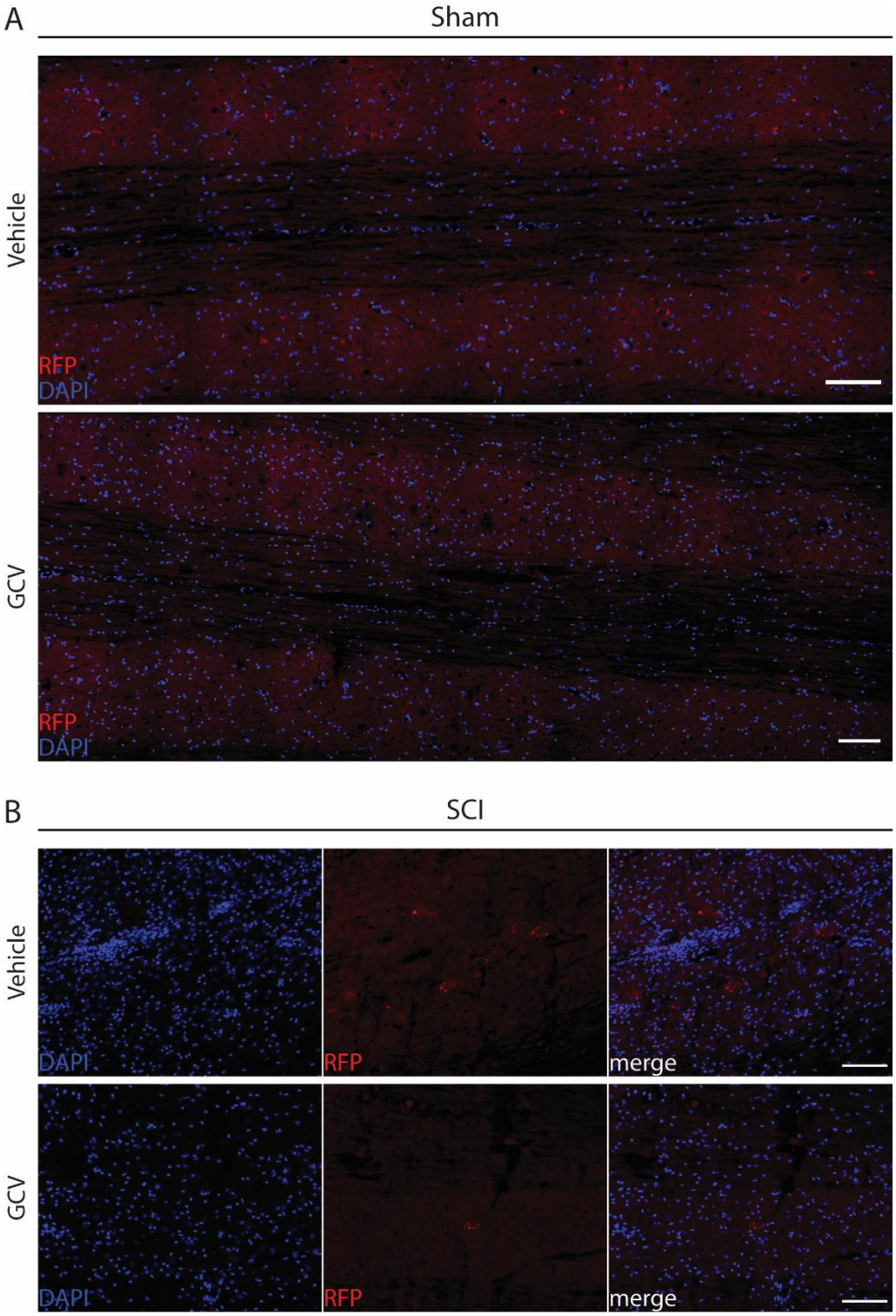

Figure 27. Ganciclovir eliminates p16^{INK4a+} cells in the spinal cord of p16-3MR transgenic mice. After five daily administrations, Ganciclovir (GCV) reduced the number of RFP-expressing (red) p16^{INK4a+} cells both in (**A**) laminectomized (Sham) and (**B**) spinal cord-injured (SCI) p16-3MR transgenic mice. Scale bars: 100 µm.

3.2. Elimination of p16^{+} cells with Ganciclovir improves locomotor recovery following a spinal cord injury in p16-3MR transgenic mice

To evaluate the impact of eliminating SCs in a p16-3MR mouse contusion model of spinal cord injury, we designed an experiment in which we administered Vehicle (PBS) or GCV (25 mg/kg/day) by IPi from 5 dpi until 29 dpi (**Figure 28A**). Due to breeding number constraints, we had only enough animals for one experimental end-point (30 dpi). Similarly to ABT-263, we assessed locomotor function using the BMS and HL. After the surgical procedures, animals were randomly distributed in four treatment groups (including wild types, *wt*). No differences were observed in injury displacement (Vehicle p16^{+}: 632.7 ± 12.9 µm; GCV p16^{+}: 608.1 ± 21.0 µm; Vehicle *wt*: 605.0 ± 31.2 µm; GCV *wt*: 675.7 ± 15.6 µm, **Figure 28B**) or force (Vehicle p16^{+}: 75.7 ± 0.5 Kdyne; GCV p16^{+}: 76.1 ± 0.5 Kdyne; Vehicle *wt*: 76.0 ± 1.0 Kdyne; GCV *wt*: 75.7 ± 1.7 Kdyne, **Figure 28C**) between the four experimental cohorts.

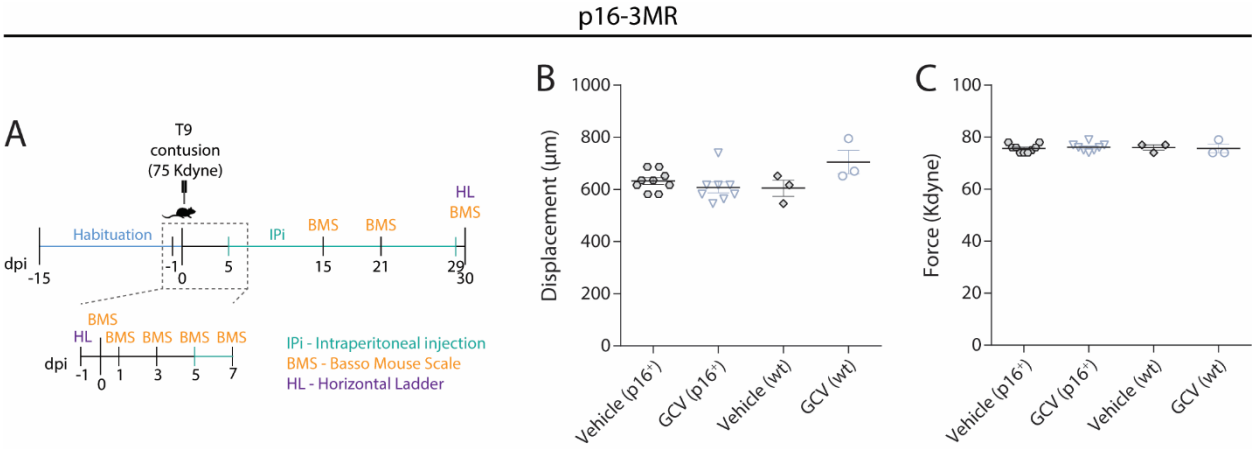

Figure 28. Experimental design and injury biomechanics for the different experimental cohorts of p16-3MR transgenic mice. (**A**) Schematic of the experimental setup. p16-3MR (p16^{+}) and wild-type (*wt*) mice were habituated to the different behavioral setups for a 15-day period, before being submitted to a moderate-to-severe (force: 75 Kdyne; displacement: 550-750 µm) T9 contusion injury. Injured animals received daily vehicle (PBS) or Ganciclovir (GCV) via intraperitoneal injection (IPi), from 5 to 29 days-post-injury (dpi). (**B**) Spinal cord tissue displacement (in micrometers, µm) and (**C**) impact force (in kilodynes, Kdyne) at the time of the contusion injury for the experimental groups of p16-3MR (p16^{+}) mice and wild type (*wt*) control littermates. No differences were observed in displacement (Vehicle p16^{+}: 632.7 ± 12.9 µm; GCV p16^{+}: 608.1 ± 21.0 µm; Vehicle *wt*: 605.0 ± 31.2

μm; GCV *wt*: 675.7 ± 15.6 μm) or force (Vehicle p16^{+}: 75.7 ± 0.5 Kdyne; GCV p16^{+}: 76.1 ± 0.5 Kdyne; Vehicle *wt*: 76.0 ± 1.0 Kdyne; GCV wt: 75.7 ± 1.7 Kdyne). *n* = 3-9. Data are presented as mean ± SEM.

In a completely independent and genetic approach, selective killing of p16^{INK4a}-expressing cells upon administration of GCV promoted locomotor recovery, which is translated in higher BMS scores and improved HL performances compared to Vehicle-treated mice (**Figure 29A-C**). These results corroborate with those of ABT-263, reinforcing the positive impact of eliminating SCs on locomotor function recovery after a spinal cord injury.

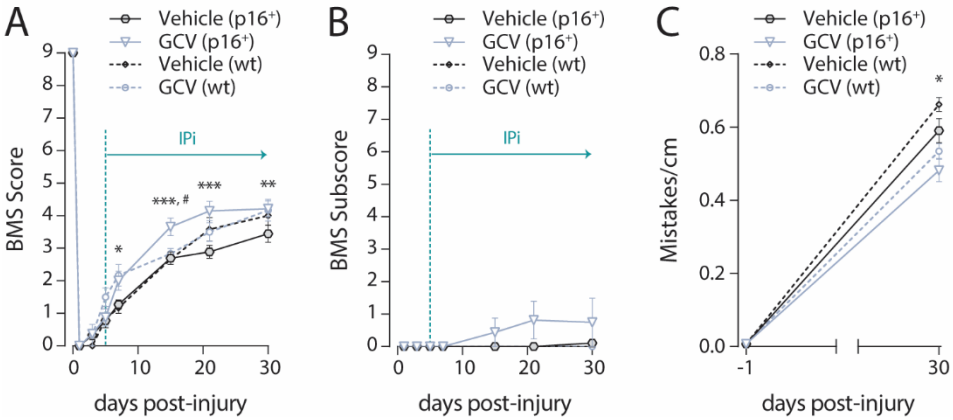

Figure 29. Effects of Ganciclovir treatment in locomotor function after a spinal cord injury in p16-3MR mice. (**A-B**) Basso Mouse Locomotor Scale (BMS) score and subscore were evaluated in an open field at different time-points (0, 1, 3, 5, 7, 15, 21 and 30 days post-injury, dpi). Vehicle (PBS) or Ganciclovir (GCV) were delivered daily since 5 dpi by intraperitoneal injection (IPi). *n* = 3-9. (**C**) The locomotor performance in the horizontal ladder was also assessed at -1 (control) and 30 dpi by quantifying the total number of mistakes per centimeter. *n* = 2-7. Data are presented as mean ± SEM. *p< 0.05, **p<0.01, and ***p<0.001, GCV vs Vehicle. #p<0.05, p16^{+} vs *wt*.

However, a few aspects and considerations of this experiment should be mentioned. First, breeding outcomes were too low to have a decent number of *wt* control littermates. With only three wt animals for each experimental group, it was impossible to guarantee an even behavioral scoring prior to drug administration (*wt* animals that were given GCV had a higher BMS score at 5 dpi). Second, several animals weighted 15-18 g before surgery, considerably below ideal surgery weight (18-20 g). This may have caused a substantial impact on injury

severity and, consequently, result in poorer locomotor performances than usual (BMS curve values were generally lower compared with previous studies). Finally, we observed that from between 15-20 dpi onwards, animals began exhibiting signs of stress and frustration upon drug administration or during behavior assessment. Furthermore, some animals displayed signs of inflammation near the IPi site and two animals died mid-experiment. We think that the constant daily manipulation and injections might have been detrimental for the well being and performances of the experimental animals and, therefore, a different administration strategy should be considered in future studies.

3.3. By 30 dpi, Ganciclovir successive daily administration failed to reduce the number of SA-β-gal$^+$ cells in the spinal cord of p16-3MR transgenic mice

Finally, we checked if GCV in fact depleted the number of SA-β-gal$^+$ cells after 30 dpi. Surprisingly, at 30 dpi, the number of SA-β-gal$^+$ cells at the lesion periphery in GCV- or Vehicle-treated animals was not statistically different in the total sectional gray matter nor in the ventral horn (**Figure 30A-D**). We suspect that the absence of a GCV-driven effect at 30 dpi might be related to the aforementioned observations during this experiment. Additionally, we performed immunostainings for RFP in order to quantify the number of p16-RFP$^+$ cells. However, unexpectedly, we failed to observe any endogenous RFP expression, suggesting that the epitope might have been lost to progeny along successive breedings.

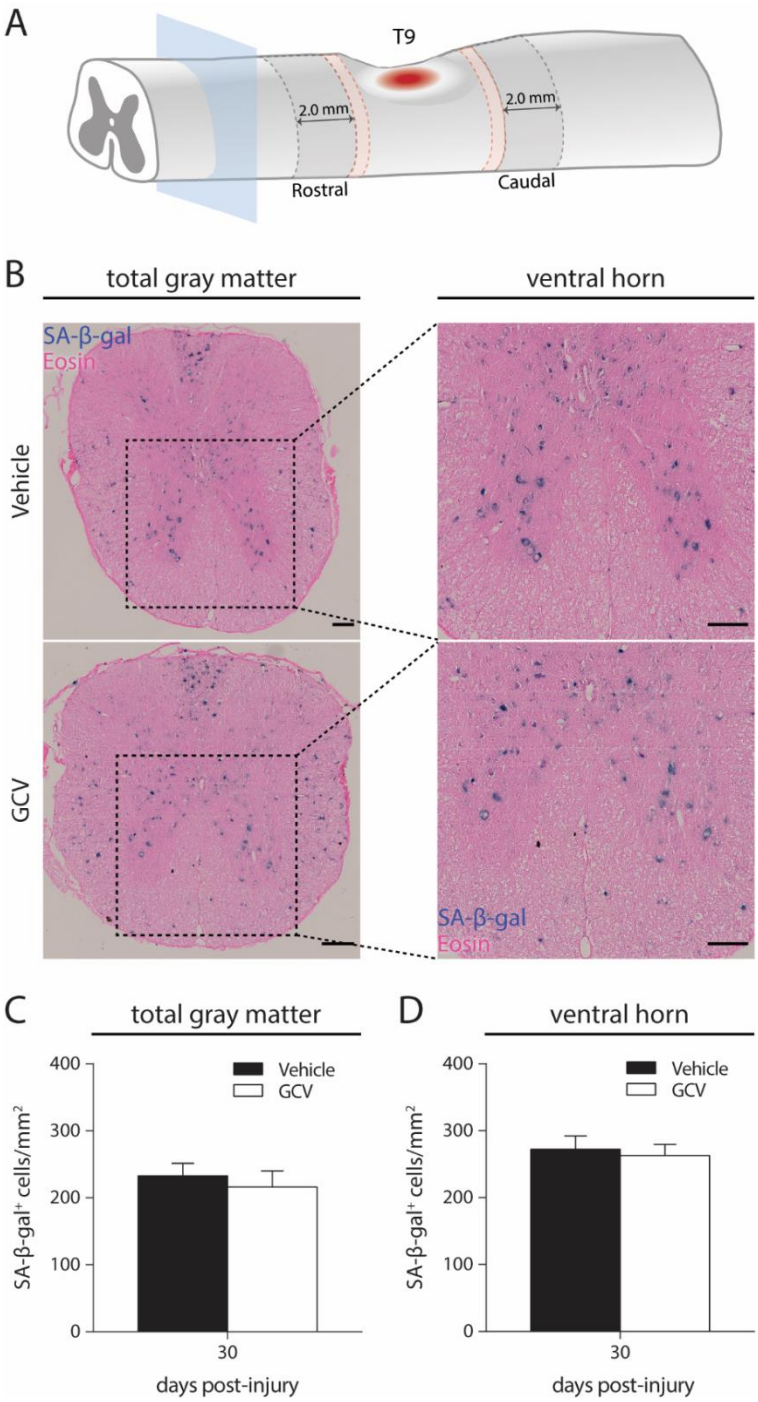

Figure 30. Ganciclovir failed to decrease the number of SA-β-gal$^+$ cells in the spinal cord of p16-3MR transgenic mice at 30 days post-injury. (**A**) SA-β-gal$^+$ cells were quantified in a total of ten different transversal sections (five rostral and five caudal) along 2.0 mm at the lesion periphery. A 0.5 mm interval (red dashed zone) was established between the lesion and the beginning of the quantification region. (**B**) An eosin (pink) counterstaining was performed after cryosectioning. SA-β-gal$^+$ cells (blue) were quantified in the total sectional gray matter and only at the ventral horn. (**C**-**D**) Quantifications were performed at the experimental endpoint (30 days post-injury). Ganciclovir (GCV) treatment significantly failed to decrease the number of SA-β-gal$^+$ cells/mm^2 in the total grey matter and in the ventral horn, comparted to vehicle (PBS). *n* = 4. Data are presented as mean ± SEM. Scale bars: 200 µm.

DISCUSSION

In this part of the project, we aimed at investigating the functional role of SCs in zebrafish and mouse SCI. On one hand, we sought to evaluate if transient SCs effectively play an active role after zebrafish SCI and contribute somehow to the regenerative process. On the other hand, we wanted to test our hypothesis that the persistent accumulation of SCs is detrimental for the outcome of mouse SCI.

If the availability of tools that allow the *in vivo* manipulation of SCs in the mouse are scarce, then in the zebrafish such tools are non-existent. This argument was recently contested by evidence of a role of SCs in zebrafish caudal fin regeneration (Da Silva-Álvarez et al., 2019). In this study, fin regeneration was reported to be impaired after eliminating SCs with the senolytic drug ABT-263. In our hands, ABT-263 failed to eliminate SCs in the zebrafish spinal cord using several different doses, vehicle solvents and administration routes. Though the superficiality of the caudal fin may be advantageous for drug accessibility, we cannot discard the possibility that senescence in the zebrafish spinal cord may not be mediated by upregulation of anti-apoptotic BCL-2 family proteins. However, we did test the administration of two other compounds with known senolytic activity. Ouabain (cardiac glycoside that inhibits Na^+/K^+-ATPase pumps) and PF-573228 (a focal adhesion kinase inhibitor) have been recently identified as senolytic agents (Gil et al., 2018; Guerrero et al., 2019; Triana-Martínez et al., 2019). Given their mechanism of action, these drugs can have strong off-target effects beyond SCs. Preliminary experiments revealed heavy toxicity of Ouabain and PF-573228 towards injured zebrafish following IPi at 5 dpi. Reducing drug concentration to tolerable doses allowed us to perform up to 5 consecutive (every 48 hours) injections of Ouabain or PF-573228. Still,

we found no effect on the number of SA-β-gal^{+} cells in the injured spinal cord when compared to Vehicle-treated animals.

A zebrafish transgenic line that would allow the elimination of SCs in a similar fashion to the p16-3MR mouse will certainly be a revolutionary tool to study senescence in this regenerating model. However, zebrafish lacks a bona fide *cdkn2a* locus that encodes for p16^{INK4a} (Shim et al., 2017). In mammals, *cdkn2a* and *cdkn2b* genes encode structurally similar proteins, p16^{INK4a} and p15^{INK4b}, respectively (Kim & Sharpless, 2006). Instead, in zebrafish there is only one *cdkn2* gene, named *cdkn2a/b* (Shim et al., 2017). This gene has not yet been fully characterized and is not clear whether it might mediate senescence. Throughout the world, several labs have been trying to develop a reliable transgenic line harnessing this locus, but so far without success. Our group is currently collaborating with other labs in order to develop a transgenic reporter by cloning constructs using the human *cdkn2a* or the zebrafish *cdkn2a/b* promoters driving the expression of GFP. To date, we were unable to obtain animals displaying a stable expression of GFP. Also in collaboration, we are trying to generate a *knock in* of a reporter into the *cdkn2a/b* locus.

In the mouse, we used a previously validated pharmacologic approach to selectively eliminate SCs *in vivo* (Chang et al., 2016; Demaria et al., 2014). The senolytic drug ABT-263 was used to eliminate SCs after a spinal cord T9 contusion injury and its effects on motor, sensory and bladder function recovery were evaluated. We targeted the elimination of SCs in the subacute injury phase to guarantee that we were acting when macrophage infiltration, reactive astrogliosis and scar formation are taking place (Siddiqui et al., 2015) and also when SCs start to accumulate at the lesion periphery. The end limit (14 dpi) of the administration time window was restricted by the fact that ABT-263 does not cross the blood-brain barrier, so we could only ensure drug accessibility in the period during which this barrier is leaky following SCI (Vogler et al., 2011; Whetstone et al., 2003; Yamaguchi & Perkins, 2012). We were able to

show that SCs were eliminated in injured mice treated with ABT-263, with elimination efficiencies similar to what was previously described (Demaria et al., 2014). Interestingly, ABT-263 was able to decrease the numbers of SA-β-gal^{+} cells even in the spinal segments spanning the end of lumbar and sacral regions, where SCs are also induced after SCI. Though the functional impact of eliminating SCs further away from the lesion, namely in the remote lumbar-sacral segments, lacks clarification, it is possible that such effect may have repercussions in the function of distal CPG circuits. Although the number of SCs are significantly reduced at 15 dpi, they start to slowly re-emerge after the end of ABT-263 administration. This might be a consequence of paracrine senescence, a SASP-mediated event where the remaining SCs can induce senescence in nearby cells (Herranz & Gil, 2018). Noteworthy, ABT-263 does not prevent SCs to be induced but instead kills by apoptosis SCs that are already present (Chang et al., 2016; Zhu et al., 2015). This becomes relevant when thinking in a translational approach where the administration window should be carefully established for high-efficacy with low-toxicity. Importantly, designing a senolytic therapy for SCI must take in account the temporal and spatial differences in the cellular response between species.

The treatment of spinal cord injured mice with the senolytic ABT-263 significantly improved locomotor performance in BMS and HL tests, an effect maintained until the end of the study (i.e. 60 dpi). Interestingly, at 30 dpi, ABT-263-treated animals showed a normal sensitivity to a non-noxious cold stimulus but no effects were observed upon a hot stimulus. This may indicate that ABT-263 is acting through specific neural substrates, namely through transient receptor potential member 8 (Trpm8) cation channels - primary molecular transducers of cold somatosensation (Ran et al., 2016). Together, these results suggest that eliminating SCs with ABT-263 improves motor and sensory functions following mammalian SCI.

Bladder function was also ameliorated during ABT-263 administration, though the effect was lost beyond that period. It would be interesting to see if bladder function would continue to improve should we be able to continue to deplete SCs after 15 dpi. De-enervation of the spleen following SCI leads to a gradual splenic atrophy (Brennan & Popovich, 2018; Noble et al., 2018). In our study, we found no differences in spleen weight after perfusion between ABT-263- and Vehicle-treated animals. This is corroborated by a previous study demonstrating that, in fact, splenic atrophy (and consequent loss of spleen weight) occurs in T3 SCI mice but not in T9 SCI mice (Zhang et al., 2013). On the other hand, after SCI, the liver suffers from excess lipid deposition, cellular damage and over-inflammation (Brennan & Popovich, 2018; Sauerbeck et al., 2015). Though we did not observe significant differences in hepatocellular damage scoring between experimental groups, ABT-263-treated animals had their liver weight reverted to control (uninjured) values. Furthermore, we found preliminary evidence that ABT-263 treatment reduces the levels of liver lipidosis following SCI. In future studies, an appropriate sample processing (i.e. fixation/preservation protocol) will be taken into account in view of properly elucidating these effects.

If the effects on bladder or liver functions are indirectly mediated by the effects of ABT-263 on the spinal cord or just a result of the systemic effect of the drug, remains to be elucidated. A spinal cord injury causes severe systemic consequences in autonomic functions, which result from the disruption of neural-immune communication between the spinal cord and peripheral organs (Brennan & Popovich, 2018; Noble et al., 2018). With severe consequences for the daily life, the recovery of autonomic functions has become a top priority of spinal cord injury patients (Anderson, 2004). In future studies, the emergence of SCs after a spinal cord lesion in organs such as the bladder, the spleen, the liver, the gut and the lungs, should also be evaluated. Independently of a possible direct or indirect effect of ABT-263 on these organs, we predict that the elimination of persistent SCs may result in improved outcomes for their autonomic

functions and, ultimately, contribute to decreased morbidity and mortality after spinal cord injury.

Persistent senescent fibroblasts and myogenic cells were shown to promote a pro-fibrotic response and to limit tissue repair in fibrotic lung disease (Schafer et al., 2017) and injured muscles (Le Roux et al., 2015), respectively. Accordingly, we showed that the effect of ABT-263 on SCs depletion was translated into a consistently reduced fibrotic scar area and length. In addition, SCs depletion with ABT-263 results in a higher myelin preservation over time. While decreasing demyelination helps preserve the function of spared axons, a smaller scar provides a better microenvironment for the reorganization of spared axons around the lesion (Courtine & Sofroniew, 2019). Consistent with this scenario, ABT-263 treatment promoted an increased expression of the growth-associated GAP43 protein at 30 dpi. Altogether, these effects are likely underlying the locomotor improvements observed. Noteworthy, the effects of ABT-263 seem to be more pronounced at the caudal side of the lesion. However, we failed to observe a difference in ABT-263 elimination efficiency between rostral and caudal effects. These differences in lesion responses to treatment suggest the existence of different SASP programs between the rostral and caudal sides, something that requires further investigation in the future.

The neuroinflammatory response after SCI worsens throughout the secondary damage phase, becomes chronic and is associated with neurotoxicity (Fleming et al., 2006). Preventing the accumulation of SCs during the subacute injury phase with the administration of ABT-263, led to a reduction in the number of inflammatory macrophages. Interestingly, persistent SCs are known to create a chronic inflammatory tissue microenvironment by secreting proinflammatory cytokines like IL-1α, IL-1β, IL-6, IL-8 or TNF-α, which are all well-established components of the SASP (Coppé et al., 2010, 2008). Therefore, this evidence

supports a close association between the accumulation of SCs and the non-resolving inflammatory response in a lesioned spinal cord.

In this study, we tried to go further and investigate if ABT-263 treatment could interfere with the balance between pro-inflammatory M1 and pro-regenerative M2 macrophage subpopulations. To do that, we performed immunostainings for the M1 and M2 markers CD16/32 and CD206, respectively (Guerrero et al., 2012). During this project, we realized that a few antibodies that worked perfectly in unstained samples were never successfully optimized after SA-β-gal staining. Such was the case with CD16/32. Thus, we were only able to successfully trace the expression of the M2 marker CD206. Our data indicates that ABT-263 did not modify, in any of the time-points analyzed, the levels of CD206 expression towards Vehicle treatment, suggesting the numbers of pro-regenerative M2 macrophages stay the same after SCs removal. Given that ABT-263 significantly reduces the number of total macrophages (assessed by F4/80 expression) at the lesion site, we predict that eliminating SCs has a direct impact on the number of pro-inflammatory M1 macrophages. Though we have been unable to confirm the expression levels of CD16/32, this hypothesis goes in accordance with the pro-inflammatory properties of a persistent SASP (Coppé et al., 2010, 2008). In fact, SASP factors IL-1β and TNF-α are known to promote polarizers of M1 macrophages and their neutralization has already been shown to improve functional recovery after SCI (Genovese et al., 2008; Kroner et al., 2014; Nesic et al., 2001). Curiously, though the SASP comprises several ILs, IL-4 and IL-10, polarizers of M2 macrophages, are not among them (Coppé et al., 2010, 2008; David & Kroner, 2011). Importantly, there is evidence that defends an ambiguity of M1 and M2 phenotypes in SCI, in which a macrophage can express markers of both subtypes (David & Kroner, 2011; Gensel & Zhang, 2015; Ren & Young, 2013). One possible explanation is that a macrophage cell is transitioning from one phenotype to the other. Nonetheless, data suggests that targeting SCs is a promising way to tackle the exacerbated inflammatory response

after a SCI that likely favors a less inhibitory *in vivo* microenvironment which is more prone for axonal preservation and injury repair.

Additionally, we used a completely independent genetic approach with the p16-3MR transgenic line (Demaria et al., 2014) to validate our results on locomotor recovery. With the p16-3MR model, we mainly aimed at: a) investigating the impact of eliminating SCs for longer periods of time on locomotor recovery; and b) sorting $p16^{INK4a+}$ cells at different time-points after injury for an in-depth cellular and transcriptomic characterization. Due to the time-window of this thesis project, we were only able to tackle the first point. Unfortunately, we ran into several unexpected problems with this model. In addition to low breeding rates, the daily injections and manipulation were revealed to be detrimental for animal welfare and experimental output. We had not enough numbers of *wt* control littermates to assuredly compare the effect of GCV between p16-3MR and *wt* mice. This is especially relevant given that GCV was previously suggested to have a neuroprotective role in the CNS (Ding et al., 2014). In the end, we were unable to prove that GCV administration successfully eliminates $p16^{Ink4a+}$ cells after 30 dpi. Considering that animals stopped recovering from 21 dpi onwards and actually started exhibiting signs of deterioration, we are unsure how the course of our experimental conditions affected the spinal cord itself and the senescence response. Furthermore, RFP expression seems to have been lost after successive breedings. In fact, we had been advised by Demaria beforehand that RFP expression could be unreliable in this model, though LUC and HSV-TK expression should work without concerns. Despite these setbacks, in our experimental conditions, GCV treatment significantly improved locomotor performances assessed in the open field and the HL. Although this model needs to be refined in future experiments, behavioral data suggest that the elimination of SCs, using an independent genetic method, promotes locomotor recovery after SCI, supporting the previous findings with the senolytic approach.

Our data provides evidence for the remarkable beneficial outcomes of eliminating SCs in the context of a SCI, namely by reducing inflammation, limiting scaring, preserving myelin and allowing axonal growth. Concomitantly, depletion of SCs promoted significant locomotor and sensory recovery, as well as improved bladder function. With this study, we identified SCs as a novel therapeutic target in spinal cord injury.

CONCLUSIONS AND FUTURE PERSPECTIVES

In this project, a multifaceted unmet medical condition meets a multifaceted undeciphered cellular phenomenon. As a result, a new and unexpected player in SCI has been identified – SCs.

Our data shows evidence that SCs play a key role in SCI and their elimination can bring remarkably beneficial outcomes during recovery. By targeting SCs, we have tackled several different aspects that comprise the outcome of a spinal lesion: locomotion, sensory and autonomic functions, as well as demyelination, fibrosis, inflammation and axonal preservation. The fact that we managed to affect each of these aspects is determinant to expose the vital part that SCs play in the functional impairment after SCI. By establishing SCs as druggable targets in the spinal cord, we propose that the use of senolytics should be considered as a therapeutic strategy for SCI. Consequently, we are currently seeking protection for such approach through the provisional patent GB1913338.8 – "Treatment of spinal cord injury" (*see Annexing Information*).

One of our main goals was to uncover the mechanism behind the detrimental role of SCs in mouse SCI. To do this, we intended to use the p16-3MR model to sort $p16^{INK4a+}$ cells and characterize their transcriptome. However, due to time restrictions and experimental setbacks concerning the p16-3MR model, we were unable to do this within the time frame of this thesis project. A precise characterization of the SASP components will be fundamental to a detailed understanding of the role of persistent SCs in the injured tissue microenvironment and might unveil new and more targeted therapeutic strategies to control senescence effector pathways after SCI. In the future, a single-cell RNA-seq will be essential to obtain an in-depth characterization of SCs in SCI, which is now the main priority of this project. This analysis should be done at different time-points in order to determine the temporal impact of the senescence program in each cellular phenotype.

Importantly, no matter how fascinating these results might be, they will mean nothing if they cannot be translated into human SCI patients. Most therapies that show promising pre-clinical results end up failing in humans due to the inherent differences between species. In view of this, it will be of paramount concern to, first of all, test if cellular senescence is also involved in human SCI. This will likely require access to *post-mortem* human spinal cord samples that can be scanned for senescence features. Then, if these cells do exist in the human spinal cord, it will be important to define an appropriate therapeutic window, considering the primary and secondary mechanisms of human SCI.

It is expected that, before an eventual translation into humans, a senescence-targeted therapy for SCI shall require more pre-clinical testing, namely in other larger animal models. Larger animals are being increasingly used for pre-clinical studies. However, their molecular and cellular characterization of SCI is massively understudied compared to rodents. Therefore, it might be difficult to outline a proper therapeutic window. In fact, if SCs carry out, as we anticipate, an immunomodulatory role in SCI, it will be important to take in account the differences in immune infiltration time windows among species. In line with this, it would be valuable to perform ABT-263 treatment at the time of injury to determine if acute accumulation of SCs is acting in a beneficial manner, before their persistence becomes detrimental.

It will be of particular interest to investigate if depleting SCs for longer periods of time will result in additional functional improvements. In order to do this, we need either efficient senolytic drugs which are capable of crossing the blood-spinal cord barrier or tools which allow the delivery of senolytics on site in a time-controlled manner. The transgenic p16-3MR model allows an extended elimination of $p16^{INK4a+}$ cells after a spinal cord injury. However, we have seen that this is not an easy nor reliable model to work with. The advantageous versatility of the p16-3MR model relies on the expression of RFP, which provides an easy means to sort these cells and characterize their transcriptome. If RFP expression is not trustworthy, this

model loses its main utility. Furthermore, in our experimental model, the amount of animal manipulation considering daily intraperitoneal injections of GCV for long periods may come to partially compromise behavioral assessments in later stages. Therefore, the experimental setup needs to be reassessed in future experiments and other more reliable transgenic lines should be considered.

Investigating the role of transient SCs in the regenerating zebrafish was another aim of this project. Thus far, we were unable to optimize a senolytic protocol to successfully deplete SCs in the zebrafish spinal cord. Additionally, there is currently no senescence-tagged zebrafish transgenic line available in the world. Therefore, the role of transiently induced SCs in zebrafish SCI remains to be elucidated. The development and optimization of senolytic or genetic methods to deplete SCs in zebrafish will provide an essential set of tools to reveal what distinguishes these cells in regenerating and non-regenerating scenarios.

Why do SCs accumulate and in certain circumstances cannot be properly eliminated? Exactly how and when does senescence become harmful in injury contexts? These are outstanding questions to which there is yet no answer. What we know so far is that there seems to be a tight association between the emergence of persistent SCs and unresolved tissue injuries. Considering this, we think that peripheral organs which are affected by SCI should also be scanned for senescence responses.

It is indeed an exciting time to work on senescence. As time goes by, this puzzling cellular phenomenon is getting slowly deciphered. Or so it seems. With each new answer often comes two novel questions. Perhaps we should wonder… are we making the right questions?

Targeted elimination of SCs emerges as a promising therapeutic approach to promote functional repair of an injured spinal cord, repurposing the use of senolytic therapies already under clinical trials for cancer and age-related disorders (Paez-Ribes et al., 2019). Given the

extreme complexity and multifaceted mechanisms underlying spinal cord repair, it is doubtful that, by itself, a senolytic drug can generate clinically meaningful functional improvements. We do believe though that this strategy shows great potential to be combined with other existing biological and engineering approaches in a combinatorial therapeutic logic.

REFERENCES

Abdesselem, H., Shypitsyna, A., Solis, G. P., Bodrikov, V., & Stuermer, C. A. O. (2009). No Nogo66- and NgR-mediated inhibition of regenerating axons in the zebrafish optic nerve. *The Journal of Neuroscience : The Official Journal of the Society for Neuroscience*, *29*(49), 15489–15498. https://doi.org/10.1523/JNEUROSCI.3561-09.2009

Acosta, Juan C, O'Loghlen, A., Banito, A., Guijarro, M. V, Augert, A., Raguz, S., Fumagalli, M., Da Costa, M., Brown, C., Popov, N., Takatsu, Y., Melamed, J., d'Adda di Fagagna, F., Bernard, D., Hernando, E., & Gil, J. (2008). Chemokine Signaling via the CXCR2 Receptor Reinforces Senescence. *Cell*, *133*(6), 1006–1018. https://doi.org/10.1016/j.cell.2008.03.038

Acosta, Juan Carlos, Banito, A., Wuestefeld, T., Georgilis, A., Janich, P., Morton, J. P., Athineos, D., Kang, T.-W., Lasitschka, F., Andrulis, M., Pascual, G., Morris, K. J., Khan, S., Jin, H., Dharmalingam, G., Snijders, A. P., Carroll, T., Capper, D., Pritchard, C., … Gil, J. (2013). A complex secretory program orchestrated by the inflammasome controls paracrine senescence. *Nature Cell Biology*, *15*(8), 978–990. https://doi.org/10.1038/ncb2784

Agostini, A., Mondragón, L., Bernardos, A., Martínez-Máñez, R., Marcos, M. D., Sancenón, F., Soto, J., Costero, A., Manguan-García, C., Perona, R., Moreno-Torres, M., Aparicio-Sanchis, R., & Murguía, J. R. (2012). Targeted Cargo Delivery in Senescent Cells Using Capped Mesoporous Silica Nanoparticles. *Angewandte Chemie International Edition*, *51*(42), 10556–10560. https://doi.org/10.1002/anie.201204663

Agrawal, S. K., & Fehlings, M. G. (1996). Mechanisms of secondary injury to spinal cord axons in vitro: role of Na+, Na(+)-K(+)-ATPase, the Na(+)-H+ exchanger, and the Na(+)-Ca2+ exchanger. *The Journal of Neuroscience : The Official Journal of the Society for Neuroscience*, *16*(2), 545–552. https://doi.org/10.1523/JNEUROSCI.16-02-00545.1996

Ajiboye, A. B., Willett, F. R., Young, D. R., Memberg, W. D., Murphy, B. A., Miller, J. P., Walter, B. L., Sweet, J. A., Hoyen, H. A., Keith, M. W., Peckham, P. H., Simeral, J. D., Donoghue, J. P., Hochberg, L. R., & Kirsch, R. F. (2017). Restoration of reaching and grasping movements through brain-controlled muscle stimulation in a person with tetraplegia: a proof-of-concept demonstration. *Lancet (London, England)*, *389*(10081), 1821–1830. https://doi.org/10.1016/S0140-6736(17)30601-3

Alcorta, D. A., Xiong, Y., Phelps, D., Hannon, G., Beach, D., & Barrett, J. C. (1996). Involvement of the cyclin-dependent kinase inhibitor p16 (INK4a) in replicative senescence of normal human fibroblasts. *Proceedings of the National Academy of Sciences of the United States of America*, *93*(24), 13742–13747. https://doi.org/10.1073/pnas.93.24.13742

Alimbetov, D., Davis, T., Brook, A. J. C., Cox, L. S., Faragher, R. G. A., Nurgozhin, T., Zhumadilov, Z., & Kipling, D. (2016). Suppression of the senescence-associated secretory phenotype (SASP) in human fibroblasts using small molecule inhibitors of p38 MAP kinase and MK2. *Biogerontology*, *17*(2), 305–315. https://doi.org/10.1007/s10522-015-9610-z

Alizadeh, A., Dyck, S. M., & Karimi-Abdolrezaee, S. (2019). Traumatic Spinal Cord Injury: An Overview of Pathophysiology, Models and Acute Injury Mechanisms. *Frontiers in Neurology*, *10*, 282. https://doi.org/10.3389/fneur.2019.00282

Allen, A. R. (1911). SURGERY OF EXPERIMENTAL LESION OF SPINAL CORD EQUIVALENT TO CRUSH INJURY OF FRACTURE DISLOCATION OF SPINAL COLUMN: A PRELIMINARY REPORT. *Journal of the American Medical Association*, *LVII*(11), 878–880. https://doi.org/10.1001/jama.1911.04260090100008

Almutiri, S., Berry, M., Logan, A., & Ahmed, Z. (2018). Non-viral-mediated suppression of AMIGO3 promotes disinhibited NT3-mediated regeneration of spinal cord dorsal column axons. *Scientific Reports*, *8*(1), 10707. https://doi.org/10.1038/s41598-018-29124-z

Alvarez-Buylla, A., Seri, B., & Doetsch, F. (2002). Identification of neural stem cells in the adult vertebrate brain. *Brain Research Bulletin*, *57*(6), 751–758.

https://doi.org/https://doi.org/10.1016/S0361-9230(01)00770-5

Amr, S. M., Gouda, A., Koptan, W. T., Galal, A. A., Abdel-Fattah, D. S., Rashed, L. A., Atta, H. M., & Abdel-Aziz, M. T. (2014). Bridging defects in chronic spinal cord injury using peripheral nerve grafts combined with a chitosan-laminin scaffold and enhancing regeneration through them by co-transplantation with bone-marrow-derived mesenchymal stem cells: case series of 14 patient. *The Journal of Spinal Cord Medicine*, *37*(1), 54–71. https://doi.org/10.1179/2045772312Y.0000000069

Anderson, K. D. (2004). Targeting Recovery: Priorities of the Spinal Cord-Injured Population. *Journal of Neurotrauma*, *21*(10), 1371–1383. https://doi.org/10.1089/neu.2004.21.1371

Anderson, M. A., Burda, J. E., Ren, Y., Ao, Y., O'Shea, T. M., Kawaguchi, R., Coppola, G., Khakh, B. S., Deming, T. J., & Sofroniew, M. V. (2016). Astrocyte scar formation aids central nervous system axon regeneration. *Nature*, *532*(7598), 195–200. https://doi.org/10.1038/nature17623

Anderson, M. A., O'Shea, T. M., Burda, J. E., Ao, Y., Barlatey, S. L., Bernstein, A. M., Kim, J. H., James, N. D., Rogers, A., Kato, B., Wollenberg, A. L., Kawaguchi, R., Coppola, G., Wang, C., Deming, T. J., He, Z., Courtine, G., & Sofroniew, M. V. (2018). Required growth facilitators propel axon regeneration across complete spinal cord injury. *Nature*, *561*(7723), 396–400. https://doi.org/10.1038/s41586-018-0467-6

Angeli, C. A., Edgerton, V. R., Gerasimenko, Y. P., & Harkema, S. J. (2014). Altering spinal cord excitability enables voluntary movements after chronic complete paralysis in humans. *Brain : A Journal of Neurology*, *137*(Pt 5), 1394–1409. https://doi.org/10.1093/brain/awu038

Ankeny, D. P., Guan, Z., & Popovich, P. G. (2009). B cells produce pathogenic antibodies and impair recovery after spinal cord injury in mice. *The Journal of Clinical Investigation*, *119*(10), 2990–2999. https://doi.org/10.1172/JCI39780

Ankeny, D. P., Lucin, K. M., Sanders, V. M., McGaughy, V. M., & Popovich, P. G. (2006). Spinal cord injury triggers systemic autoimmunity: evidence for chronic B lymphocyte activation and lupus-like autoantibody synthesis. *Journal of Neurochemistry*, *99*(4), 1073–1087. https://doi.org/10.1111/j.1471-4159.2006.04147.x

Asher, R. A., Morgenstern, D. A., Shearer, M. C., Adcock, K. H., Pesheva, P., & Fawcett, J. W. (2002). Versican is upregulated in CNS injury and is a product of oligodendrocyte lineage cells. *The Journal of Neuroscience : The Official Journal of the Society for Neuroscience*, *22*(6), 2225–2236. https://doi.org/10.1523/JNEUROSCI.22-06-02225.2002

Baar, M. P., Brandt, R. M. C., Putavet, D. A., Klein, J. D. D., Derks, K. W. J., Bourgeois, B. R. M., Stryeck, S., Rijksen, Y., van Willigenburg, H., Feijtel, D. A., van der Pluijm, I., Essers, J., van Cappellen, W. A., van IJcken, W. F., Houtsmuller, A. B., Pothof, J., de Bruin, R. W. F., Madl, T., Hoeijmakers, J. H. J., … de Keizer, P. L. J. (2017). Targeted Apoptosis of Senescent Cells Restores Tissue Homeostasis in Response to Chemotoxicity and Aging. *Cell*, *169*(1), 132-147.e16. https://doi.org/10.1016/j.cell.2017.02.031

Baker, D. J., Wijshake, T., Tchkonia, T., LeBrasseur, N. K., Childs, B. G., van de Sluis, B., Kirkland, J. L., & van Deursen, J. M. (2011). Clearance of p16Ink4a-positive senescent cells delays ageing-associated disorders. *Nature*, *479*(7372), 232–236. https://doi.org/10.1038/nature10600

Ballermann, M., & Fouad, K. (2006). Spontaneous locomotor recovery in spinal cord injured rats is accompanied by anatomical plasticity of reticulospinal fibers. *European Journal of Neuroscience*, *23*(8), 1988–1996. https://doi.org/10.1111/j.1460-9568.2006.04726.x

Banito, A., Rashid, S. T., Acosta, J. C., Li, S., Pereira, C. F., Geti, I., Pinho, S., Silva, J. C., Azuara, V., Walsh, M., Vallier, L., & Gil, J. (2009). Senescence impairs successful reprogramming to pluripotent stem cells. *Genes & Development*, *23*(18), 2134–2139. https://doi.org/10.1101/gad.1811609

Barbeau, H., McCrea, D. A., O'Donovan, M. J., Rossignol, S., Grill, W. M., & Lemay, M. A. (1999). Tapping into spinal circuits to restore motor function. *Brain Research Reviews*, *30*(1), 27–51. https://doi.org/https://doi.org/10.1016/S0165-0173(99)00008-9

Bareyre, F. M., Kerschensteiner, M., Raineteau, O., Mettenleiter, T. C., Weinmann, O., & Schwab, M. E. (2004). The injured spinal cord spontaneously forms a new intraspinal circuit in adult rats. *Nature Neuroscience*, *7*(3), 269–277. https://doi.org/10.1038/nn1195

Barnabé-Heider, F., Göritz, C., Sabelström, H., Takebayashi, H., Pfrieger, F. W., Meletis, K., & Frisén, J. (2010). Origin of New Glial Cells in Intact and Injured Adult Spinal Cord. *Cell Stem Cell*, *7*(4), 470–482. https://doi.org/10.1016/j.stem.2010.07.014

Barrette, B., Hébert, M.-A., Filali, M., Lafortune, K., Vallières, N., Gowing, G., Julien, J.-P., & Lacroix, S. (2008). Requirement of Myeloid Cells for Axon Regeneration. *The Journal of Neuroscience*, *28*(38), 9363 LP – 9376. https://doi.org/10.1523/JNEUROSCI.1447-08.2008

Bartus, K., James, N. D., Didangelos, A., Bosch, K. D., Verhaagen, J., Yáñez-Muñoz, R. J., Rogers, J. H., Schneider, B. L., Muir, E. M., & Bradbury, E. J. (2014). Large-scale chondroitin sulfate proteoglycan digestion with chondroitinase gene therapy leads to reduced pathology and modulates macrophage phenotype following spinal cord contusion injury. *The Journal of Neuroscience : The Official Journal of the Society for Neuroscience*, *34*(14), 4822–4836. https://doi.org/10.1523/JNEUROSCI.4369-13.2014

Barzilai, N., Crandall, J. P., Kritchevsky, S. B., & Espeland, M. A. (2016). Metformin as a Tool to Target Aging. *Cell Metabolism*, *23*(6), 1060–1065. https://doi.org/10.1016/j.cmet.2016.05.011

Basso, D. M., Fisher, L. C., Anderson, A. J., Jakeman, L. B., Mctigue, D. M., & Popovich, P. G. (2006). Basso Mouse Scale for Locomotion Detects Differences in Recovery after Spinal Cord Injury in Five Common Mouse Strains. *Journal of Neurotrauma*, *23*(5), 635–659. https://doi.org/10.1089/neu.2006.23.635

Beattie, M. S., Farooqui, A. A., & Bresnahan, J. C. (2000). Review of Current Evidence for Apoptosis After Spinal Cord Injury. *Journal of Neurotrauma*, *17*(10), 915–925. https://doi.org/10.1089/neu.2000.17.915

Beattie, M. S., Hermann, G. E., Rogers, R. C., & Bresnahan, J. C. (2002). Chapter 4 Cell death in models of spinal cord injury. In L. McKerracher, G. Doucet, & S. B. T.-P. in B. R. Rossignol (Eds.), *Spinal Cord Trauma: Regeneration, Neural Repair and Functional Recovery* (Vol. 137, pp. 37–47). Elsevier. https://doi.org/https://doi.org/10.1016/S0079-6123(02)37006-7

Beck, K. D., Nguyen, H. X., Galvan, M. D., Salazar, D. L., Woodruff, T. M., & Anderson, A. J. (2010). Quantitative analysis of cellular inflammation after traumatic spinal cord injury: evidence for a multiphasic inflammatory response in the acute to chronic environment. *Brain*, *133*(2), 433–447. https://doi.org/10.1093/brain/awp322

Becker, C G, & Becker, T. (2007). *Model Organisms in Spinal Cord Regeneration*. https://doi.org/10.1002/9783527610365

Becker, Catherina G, & Becker, T. (2006). Zebrafish as a Model System for Successful Spinal Cord Regeneration. In *Model Organisms in Spinal Cord Regeneration* (pp. 289–319). https://doi.org/doi:10.1002/9783527610365.ch10

Becker, Catherina G, Lieberoth, B. C., Morellini, F., Feldner, J., Becker, T., & Schachner, M. (2004). L1.1 is involved in spinal cord regeneration in adult zebrafish. *The Journal of Neuroscience : The Official Journal of the Society for Neuroscience*, *24*(36), 7837–7842. https://doi.org/10.1523/JNEUROSCI.2420-04.2004

Becker, T., & Becker, C. G. (2001). Regenerating descending axons preferentially reroute to the gray matter in the presence of a general macrophage/microglial reaction caudal to a spinal transection

in adult zebrafish. *Journal of Comparative Neurology*, *433*(1), 131–147. https://doi.org/10.1002/cne.1131

Becker, T., & Becker, C. G. (2014). Axonal regeneration in zebrafish. *Current Opinion in Neurobiology*, *27*, 186–191. https://doi.org/https://doi.org/10.1016/j.conb.2014.03.019

Becker, T., Wullimann, M. F., Becker, C. G., Bernhardt, R. R., & Schachner, M. (1997). Axonal regrowth after spinal cord transection in adult zebrafish. *Journal of Comparative Neurology*, *377*(4), 577–595. https://doi.org/10.1002/(SICI)1096-9861(19970127)377:4<577::AID-CNE8>3.0.CO;2-#

Benowitz, L. I., & Routtenberg, A. (1987). A membrane phosphoprotein associated with neural development, axonal regeneration, phospholipid metabolism, and synaptic plasticity. *Trends in Neurosciences*, *10*(12), 527–532. https://doi.org/10.1016/0166-2236(87)90135-4

Bernardos, R. L., & Raymond, P. A. (2006). GFAP transgenic zebrafish. *Gene Expression Patterns*, *6*(8), 1007–1013. https://doi.org/https://doi.org/10.1016/j.modgep.2006.04.006

Birch, J., & Passos, J. F. (2017). Targeting the SASP to combat ageing: Mitochondria as possible intracellular allies? *BioEssays*, *39*(5), 1600235. https://doi.org/10.1002/bies.201600235

Blight, A R. (1994). Effects of silica on the outcome from experimental spinal cord injury: Implication of macrophages in secondary tissue damage. *Neuroscience*, *60*(1), 263–273. https://doi.org/https://doi.org/10.1016/0306-4522(94)90220-8

Blight, Andrew R. (1985). No TitlDelayed demyelination and macrophage invasion: a candidate for secondary cell damage in spinal cord injury. *Central Nervous System Trauma : Journal of the American Paralysis Association*, 299–315.

Borton, D., Micera, S., Millán, J. del R., & Courtine, G. (2013). Personalized Neuroprosthetics. *Science Translational Medicine*, *5*(210), 210rv2 LP-210rv2. https://doi.org/10.1126/scitranslmed.3005968

Bouton, C. E., Shaikhouni, A., Annetta, N. V, Bockbrader, M. A., Friedenberg, D. A., Nielson, D. M., Sharma, G., Sederberg, P. B., Glenn, B. C., Mysiw, W. J., Morgan, A. G., Deogaonkar, M., & Rezai, A. R. (2016). Restoring cortical control of functional movement in a human with quadriplegia. *Nature*, *533*(7602), 247–250. https://doi.org/10.1038/nature17435

Bradbury, E. J., & Burnside, E. R. (2019). Moving beyond the glial scar for spinal cord repair. *Nature Communications*, *10*(1), 3879. https://doi.org/10.1038/s41467-019-11707-7

Bradbury, E. J., & Carter, L. M. (2011). Manipulating the glial scar: Chondroitinase ABC as a therapy for spinal cord injury. *Brain Research Bulletin*, *84*(4), 306–316. https://doi.org/https://doi.org/10.1016/j.brainresbull.2010.06.015

Bradbury, E. J., Moon, L. D. F., Popat, R. J., King, V. R., Bennett, G. S., Patel, P. N., Fawcett, J. W., & McMahon, S. B. (2002). Chondroitinase ABC promotes functional recovery after spinal cord injury. *Nature*, *416*(6881), 636–640. https://doi.org/10.1038/416636a

Brambilla, R., Bracchi-Ricard, V., Hu, W.-H., Frydel, B., Bramwell, A., Karmally, S., Green, E. J., & Bethea, J. R. (2005). Inhibition of astroglial nuclear factor kappaB reduces inflammation and improves functional recovery after spinal cord injury. *The Journal of Experimental Medicine*, *202*(1), 145–156. https://doi.org/10.1084/jem.20041918

Braumüller, H., Wieder, T., Brenner, E., Aßmann, S., Hahn, M., Alkhaled, M., Schilbach, K., Essmann, F., Kneilling, M., Griessinger, C., Ranta, F., Ullrich, S., Mocikat, R., Braungart, K., Mehra, T., Fehrenbacher, B., Berdel, J., Niessner, H., Meier, F., … Röcken, M. (2013). T-helper-1-cell cytokines drive cancer into senescence. *Nature*, *494*(7437), 361–365. https://doi.org/10.1038/nature11824

Braun, H., Schmidt, B. M. W., Raiss, M., Baisantry, A., Mircea-Constantin, D., Wang, S., Gross, M.-L., Serrano, M., Schmitt, R., & Melk, A. (2012). Cellular senescence limits regenerative capacity and allograft survival. *Journal of the American Society of Nephrology : JASN*, *23*(9), 1467–1473. https://doi.org/10.1681/ASN.2011100967

Brennan, F. H., & Popovich, P. G. (2018). Emerging targets for reprograming the immune response to promote repair and recovery of function after spinal cord injury. *Current Opinion in Neurology*, *31*(3). https://journals.lww.com/co-neurology/Fulltext/2018/06000/Emerging_targets_for_reprograming_the_immune.18.aspx

Briona, L. K., & Dorsky, R. I. (2014). Spinal cord transection in the larval zebrafish. *Journal of Visualized Experiments : JoVE*, *87*, 51479. https://doi.org/10.3791/51479

Briona, L. K., Poulain, F. E., Mosimann, C., & Dorsky, R. I. (2015). Wnt/ß-catenin signaling is required for radial glial neurogenesis following spinal cord injury. *Developmental Biology*, *403*(1), 15–21. https://doi.org/10.1016/j.ydbio.2015.03.025

Burda, J. E., & Sofroniew, M. V. (2014). Reactive gliosis and the multicellular response to CNS damage and disease. *Neuron*, *81*(2), 229–248. https://doi.org/10.1016/j.neuron.2013.12.034

Buss, A., Pech, K., Kakulas, B. A., Martin, D., Schoenen, J., Noth, J., & Brook, G. A. (2009). NG2 and phosphacan are present in the astroglial scar after human traumatic spinal cord injury. *BMC Neurology*, *9*, 32. https://doi.org/10.1186/1471-2377-9-32

Calcinotto, A., Kohli, J., Zagato, E., Pellegrini, L., Demaria, M., & Alimonti, A. (2019). Cellular Senescence: Aging, Cancer, and Injury. *Physiological Reviews*, *99*(2), 1047–1078. https://doi.org/10.1152/physrev.00020.2018

Campisi, J. (2005). Senescent Cells, Tumor Suppression, and Organismal Aging: Good Citizens, Bad Neighbors. *Cell*, *120*(4), 513–522. https://doi.org/10.1016/j.cell.2005.02.003

Campisi, J. (2013). Aging, Cellular Senescence, and Cancer. *Annual Review of Physiology*, *75*(1), 685–705. https://doi.org/10.1146/annurev-physiol-030212-183653

Cang, S., Iragavarapu, C., Savooji, J., Song, Y., & Liu, D. (2015). ABT-199 (venetoclax) and BCL-2 inhibitors in clinical development. *Journal of Hematology & Oncology*, *8*, 129. https://doi.org/10.1186/s13045-015-0224-3

Capogrosso, M., Milekovic, T., Borton, D., Wagner, F., Moraud, E. M., Mignardot, J.-B., Buse, N., Gandar, J., Barraud, Q., Xing, D., Rey, E., Duis, S., Jianzhong, Y., Ko, W. K. D., Li, Q., Detemple, P., Denison, T., Micera, S., Bezard, E., … Courtine, G. (2016). A brain–spine interface alleviating gait deficits after spinal cord injury in primates. *Nature*, *539*(7628), 284–288. https://doi.org/10.1038/nature20118

Caron, A., Xu, X., & Lin, X. (2012). Wnt/β-catenin signaling directly regulates Foxj1 expression and ciliogenesis in zebrafish Kupffer's vesicle. *Development (Cambridge, England)*, *139*(3), 514–524. https://doi.org/10.1242/dev.071746

Cazzalini, O., Scovassi, A. I., Savio, M., Stivala, L. A., & Prosperi, E. (2010). Multiple roles of the cell cycle inhibitor p21CDKN1A in the DNA damage response. *Mutation Research/Reviews in Mutation Research*, *704*(1), 12–20. https://doi.org/https://doi.org/10.1016/j.mrrev.2010.01.009

Cekanaviciute, E., & Buckwalter, M. S. (2016). Astrocytes: Integrative Regulators of Neuroinflammation in Stroke and Other Neurological Diseases. *Neurotherapeutics : The Journal of the American Society for Experimental NeuroTherapeutics*, *13*(4), 685–701. https://doi.org/10.1007/s13311-016-0477-8

Chandra, T., & Narita, M. (2013). High-order chromatin structure and the epigenome in SAHFs. *Nucleus (Austin, Tex.)*, *4*(1), 23–28. https://doi.org/10.4161/nucl.23189

Chang, J., Wang, Y., Shao, L., Laberge, R.-M., Demaria, M., Campisi, J., Janakiraman, K., Sharpless, N. E., Ding, S., Feng, W., Luo, Y., Wang, X., Aykin-Burns, N., Krager, K., Ponnappan, U., Hauer-Jensen, M., Meng, A., & Zhou, D. (2016). Clearance of senescent cells by ABT263 rejuvenates aged hematopoietic stem cells in mice. *Nature Medicine*, *22*(1), 78–83. https://doi.org/10.1038/nm.4010

Chapela, D., Sousa, S., Martins, I., Cristóvão, A. M., Pinto, P., Corte-Real, S., & Saúde, L. (2019). A zebrafish drug screening platform boosts the discovery of novel therapeutics for spinal cord injury in mammals. *Scientific Reports*, *9*(1), 10475. https://doi.org/10.1038/s41598-019-47006-w

Chen, Q., Fischer, A., Reagan, J. D., Yan, L.-J., & Ames, B. N. (1995). Oxidative DNA Damage and Senescence of Human Diploid Fibroblast Cells. *Proceedings of the National Academy of Sciences of the United States of America*, *92*(10), 4337–4341. http://www.jstor.org/stable/2367322

Chen, Z., Trotman, L. C., Shaffer, D., Lin, H.-K., Dotan, Z. A., Niki, M., Koutcher, J. A., Scher, H. I., Ludwig, T., Gerald, W., Cordon-Cardo, C., & Pandolfi, P. P. (2005). Crucial role of p53-dependent cellular senescence in suppression of Pten-deficient tumorigenesis. *Nature*, *436*(7051), 725–730. https://doi.org/10.1038/nature03918

Cheng, L.-Q., Zhang, Z.-Q., Chen, H.-Z., & Liu, D.-P. (2017). Epigenetic regulation in cell senescence. *Journal of Molecular Medicine*, *95*(12), 1257–1268. https://doi.org/10.1007/s00109-017-1581-x

Cheriyan, T., Ryan, D. J., Weinreb, J. H., Cheriyan, J., Paul, J. C., Lafage, V., Kirsch, T., & Errico, T. J. (2014). Spinal cord injury models: a review. *Spinal Cord*, *52*(8), 588–595. https://doi.org/10.1038/sc.2014.91

Chiche, A., Le Roux, I., von Joest, M., Sakai, H., Aguín, S. B., Cazin, C., Salam, R., Fiette, L., Alegria, O., Flamant, P., Tajbakhsh, S., & Li, H. (2017). Injury-Induced Senescence Enables In Vivo Reprogramming in Skeletal Muscle. *Cell Stem Cell*, *20*(3), 407-414.e4. https://doi.org/10.1016/j.stem.2016.11.020

Childs, B. G., Durik, M., Baker, D. J., & van Deursen, J. M. (2015). Cellular senescence in aging and age-related disease: from mechanisms to therapy. *Nature Medicine*, *21*(12), 1424–1435. https://doi.org/10.1038/nm.4000

Choo, A. M.-T., Liu, J., Liu, Z., Dvorak, M., Tetzlaff, W., & Oxland, T. R. (2009). Modeling spinal cord contusion, dislocation, and distraction: Characterization of vertebral clamps, injury severities, and node of Ranvier deformations. *Journal of Neuroscience Methods*, *181*(1), 6–17. https://doi.org/https://doi.org/10.1016/j.jneumeth.2009.04.007

Chuprin, A., Gal, H., Biron-Shental, T., Biran, A., Amiel, A., Rozenblatt, S., & Krizhanovsky, V. (2013). Cell fusion induced by ERVWE1 or measles virus causes cellular senescence. *Genes & Development*, *27*(21), 2356–2366. https://doi.org/10.1101/gad.227512.113

Cohen, J., & Torres, C. (2019). Astrocyte senescence: Evidence and significance. *Aging Cell*, *18*(3), e12937–e12937. https://doi.org/10.1111/acel.12937

Collado, M., Gil, J., Efeyan, A., Guerra, C., Schuhmacher, A. J., Barradas, M., Benguría, A., Zaballos, A., Flores, J. M., Barbacid, M., Beach, D., & Serrano, M. (2005). Senescence in premalignant tumours. *Nature*, *436*(7051), 642. https://doi.org/10.1038/436642a

Collado, M., & Serrano, M. (2010). Senescence in tumours: evidence from mice and humans. *Nature Reviews. Cancer*, *10*(1), 51–57. https://doi.org/10.1038/nrc2772

Coppé, J.-P., Desprez, P.-Y., Krtolica, A., & Campisi, J. (2010). The Senescence-Associated Secretory Phenotype: The Dark Side of Tumor Suppression. *Annual Review of Pathology:*

Mechanisms of Disease, *5*(1), 99–118. https://doi.org/10.1146/annurev-pathol-121808-102144

Coppé, J.-P., Kauser, K., Campisi, J., & Beauséjour, C. M. (2006). Secretion of Vascular Endothelial Growth Factor by Primary Human Fibroblasts at Senescence. *Journal of Biological Chemistry* , *281*(40), 29568–29574. http://www.jbc.org/content/281/40/29568.abstract

Coppé, J.-P., Patil, C. K., Rodier, F., Sun, Y., Muñoz, D. P., Goldstein, J., Nelson, P. S., Desprez, P.-Y., & Campisi, J. (2008). Senescence-Associated Secretory Phenotypes Reveal Cell-Nonautonomous Functions of Oncogenic RAS and the p53 Tumor Suppressor. *PLOS Biology*, *6*(12), e301.

Correia-Melo, C., Marques, F. D. M., Anderson, R., Hewitt, G., Hewitt, R., Cole, J., Carroll, B. M., Miwa, S., Birch, J., Merz, A., Rushton, M. D., Charles, M., Jurk, D., Tait, S. W. G., Czapiewski, R., Greaves, L., Nelson, G., Bohlooly-Y, M., Rodriguez-Cuenca, S., … Passos, J. F. (2016). Mitochondria are required for pro-ageing features of the senescent phenotype. *The EMBO Journal*, *35*(7), 724–742. https://doi.org/10.15252/embj.201592862

Cosgrove, B. D., Gilbert, P. M., Porpiglia, E., Mourkioti, F., Lee, S. P., Corbel, S. Y., Llewellyn, M. E., Delp, S. L., & Blau, H. M. (2014). Rejuvenation of the muscle stem cell population restores strength to injured aged muscles. *Nature Medicine*, *20*(3), 255–264. https://doi.org/10.1038/nm.3464

Côté, M.-P., Murray, M., & Lemay, M. A. (2017). Rehabilitation Strategies after Spinal Cord Injury: Inquiry into the Mechanisms of Success and Failure. *Journal of Neurotrauma*, *34*(10), 1841–1857. https://doi.org/10.1089/neu.2016.4577

Couillard-Despres, S., Bieler, L., & Vogl, M. (2017). *Pathophysiology of Traumatic Spinal Cord Injury BT - Neurological Aspects of Spinal Cord Injury* (N. Weidner, R. Rupp, & K. E. Tansey (eds.); pp. 503–528). Springer International Publishing. https://doi.org/10.1007/978-3-319-46293-6_19

Courtine, Grégoire, Gerasimenko, Y., van den Brand, R., Yew, A., Musienko, P., Zhong, H., Song, B., Ao, Y., Ichiyama, R. M., Lavrov, I., Roy, R. R., Sofroniew, M. V, & Edgerton, V. R. (2009). Transformation of nonfunctional spinal circuits into functional states after the loss of brain input. *Nature Neuroscience*, *12*(10), 1333–1342. https://doi.org/10.1038/nn.2401

Courtine, Grégoire, & Sofroniew, M. V. (2019). Spinal cord repair: advances in biology and technology. *Nature Medicine*, *25*(6), 898–908. https://doi.org/10.1038/s41591-019-0475-6

Courtine, Gregoire, Song, B., Roy, R. R., Zhong, H., Herrmann, J. E., Ao, Y., Qi, J., Edgerton, V. R., & Sofroniew, M. V. (2008). Recovery of supraspinal control of stepping via indirect propriospinal relay connections after spinal cord injury. *Nature Medicine*, *14*(1), 69–74. https://doi.org/10.1038/nm1682

Cregg, J. M., DePaul, M. A., Filous, A. R., Lang, B. T., Tran, A., & Silver, J. (2014). Functional regeneration beyond the glial scar. *Experimental Neurology*, *253*, 197–207. https://doi.org/10.1016/j.expneurol.2013.12.024

Cummings, B. J., Engesser-Cesar, C., Cadena, G., & Anderson, A. J. (2007). Adaptation of a ladder beam walking task to assess locomotor recovery in mice following spinal cord injury. *Behavioural Brain Research*, *177*(2), 232–241. https://doi.org/https://doi.org/10.1016/j.bbr.2006.11.042

d'Adda di Fagagna, F. (2008). Living on a break: cellular senescence as a DNA-damage response. *Nature Reviews Cancer*, *8*(7), 512–522. https://doi.org/10.1038/nrc2440

d'Adda di Fagagna, F., Reaper, P. M., Clay-Farrace, L., Fiegler, H., Carr, P., von Zglinicki, T., Saretzki, G., Carter, N. P., & Jackson, S. P. (2003). A DNA damage checkpoint response in telomere-initiated senescence. *Nature*, *426*(6963), 194–198. https://doi.org/10.1038/nature02118

Da Silva-Álvarez, S., Guerra-Varela, J., Sobrido-Cameán, D., Quelle, A., Barreiro-Iglesias, A., Sánchez, L., & Collado, M. (2019). Cell senescence contributes to tissue regeneration in zebrafish. *Aging Cell*, *n/a*(n/a), e13052. https://doi.org/10.1111/acel.13052

Dalamagkas, K., Tsintou, M., Seifalian, A., & Seifalian, A. M. (2018). Translational Regenerative Therapies for Chronic Spinal Cord Injury. *International Journal of Molecular Sciences*, *19*(6), 1776. https://doi.org/10.3390/ijms19061776

Dang, M., Henderson, R. E., Garraway, L. A., & Zon, L. I. (2016). Long-term drug administration in the adult zebrafish using oral gavage for cancer preclinical studies. *Disease Models & Mechanisms*, *9*(7), 811–820. https://doi.org/10.1242/dmm.024166

Davaapil, H., Brockes, J. P., & Yun, M. H. (2017). Conserved and novel functions of programmed cellular senescence during vertebrate development. *Development (Cambridge, England)*, *144*(1), 106–114. https://doi.org/10.1242/dev.138222

David, S, Greenhalgh, A. D., & Kroner, A. (2015). Macrophage and microglial plasticity in the injured spinal cord. *Neuroscience*, *307*, 311–318. https://doi.org/https://doi.org/10.1016/j.neuroscience.2015.08.064

David, Samuel, & Kroner, A. (2011). Repertoire of microglial and macrophage responses after spinal cord injury. *Nature Reviews Neuroscience*, *12*(7), 388–399. https://doi.org/10.1038/nrn3053

Demaria, M., Ohtani, N., Youssef, S. A., Rodier, F., Toussaint, W., Mitchell, J. R., Laberge, R.-M., Vijg, J., Van Steeg, H., Dollé, M. E. T., Hoeijmakers, J. H. J., de Bruin, A., Hara, E., & Campisi, J. (2014). An Essential Role for Senescent Cells in Optimal Wound Healing through Secretion of PDGF-AA. *Developmental Cell*, *31*(6), 722–733. https://doi.org/https://doi.org/10.1016/j.devcel.2014.11.012

Denoyelle, C., Abou-Rjaily, G., Bezrookove, V., Verhaegen, M., Johnson, T. M., Fullen, D. R., Pointer, J. N., Gruber, S. B., Su, L. D., Nikiforov, M. A., Kaufman, R. J., Bastian, B. C., & Soengas, M. S. (2006). Anti-oncogenic role of the endoplasmic reticulum differentially activated by mutations in the MAPK pathway. *Nature Cell Biology*, *8*(10), 1053–1063. https://doi.org/10.1038/ncb1471

Dey, A., Tergaonkar, V., & Lane, D. P. (2008). Double-edged swords as cancer therapeutics: simultaneously targeting p53 and NF-κB pathways. *Nature Reviews Drug Discovery*, *7*(12), 1031–1040. https://doi.org/10.1038/nrd2759

Di Micco, R., Sulli, G., Dobreva, M., Liontos, M., Botrugno, O. A., Gargiulo, G., dal Zuffo, R., Matti, V., d'Ario, G., Montani, E., Mercurio, C., Hahn, W. C., Gorgoulis, V., Minucci, S., & d'Adda di Fagagna, F. (2011). Interplay between oncogene-induced DNA damage response and heterochromatin in senescence and cancer. *Nature Cell Biology*, *13*(3), 292–302. https://doi.org/10.1038/ncb2170

Di Mitri, D., & Alimonti, A. (2016). Non-Cell-Autonomous Regulation of Cellular Senescence in Cancer. *Trends in Cell Biology*, *26*(3), 215–226. https://doi.org/10.1016/j.tcb.2015.10.005

Di Mitri, D., Toso, A., Chen, J. J., Sarti, M., Pinton, S., Jost, T. R., D'Antuono, R., Montani, E., Garcia-Escudero, R., Guccini, I., Da Silva-Alvarez, S., Collado, M., Eisenberger, M., Zhang, Z., Catapano, C., Grassi, F., & Alimonti, A. (2014). Tumour-infiltrating Gr-1+ myeloid cells antagonize senescence in cancer. *Nature*, *515*(7525), 134–137. https://doi.org/10.1038/nature13638

Dias, D. O., Kim, H., Holl, D., Werne Solnestam, B., Lundeberg, J., Carlén, M., Göritz, C., & Frisén, J. (2018). Reducing Pericyte-Derived Scarring Promotes Recovery after Spinal Cord Injury. *Cell*, *173*(1), 153-165.e22. https://doi.org/10.1016/j.cell.2018.02.004

Dias, T. B., Yang, Y.-J., Ogai, K., Becker, T., & Becker, C. G. (2012). Notch signaling controls

generation of motor neurons in the lesioned spinal cord of adult zebrafish. *The Journal of Neuroscience : The Official Journal of the Society for Neuroscience*, *32*(9), 3245–3252. https://doi.org/10.1523/JNEUROSCI.6398-11.2012

Dickendesher, T. L., Baldwin, K. T., Mironova, Y. A., Koriyama, Y., Raiker, S. J., Askew, K. L., Wood, A., Geoffroy, C. G., Zheng, B., Liepmann, C. D., Katagiri, Y., Benowitz, L. I., Geller, H. M., & Giger, R. J. (2012). NgR1 and NgR3 are receptors for chondroitin sulfate proteoglycans. *Nature Neuroscience*, *15*(5), 703–712. https://doi.org/10.1038/nn.3070

Dimri, G. P., Lee, X., Basile, G., Acosta, M., Scott, G., Roskelley, C., Medrano, E. E., Linskens, M., Rubelj, I., & Pereira-Smith, O. (1995). A biomarker that identifies senescent human cells in culture and in aging skin in vivo. *Proceedings of the National Academy of Sciences of the United States of America*, *92*(20), 9363–9367. https://doi.org/10.1073/pnas.92.20.9363

Ding, Z., Mathur, V., Ho, P. P., James, M. L., Lucin, K. M., Hoehne, A., Alabsi, H., Gambhir, S. S., Steinman, L., Luo, J., & Wyss-Coray, T. (2014). Antiviral drug ganciclovir is a potent inhibitor of microglial proliferation and neuroinflammation. *The Journal of Experimental Medicine*, *211*(2), 189–198. https://doi.org/10.1084/jem.20120696

Domínguez-Bajo, A., González-Mayorga, A., López-Dolado, E., & Serrano, M. C. (2017). Graphene-Derived Materials Interfacing the Spinal Cord: Outstanding in Vitro and in Vivo Findings. *Frontiers in Systems Neuroscience*, *11*, 71. https://doi.org/10.3389/fnsys.2017.00071

Donnelly, D. J., & Popovich, P. G. (2008). Inflammation and its role in neuroprotection, axonal regeneration and functional recovery after spinal cord injury. *Experimental Neurology*, *209*(2), 378–388. https://doi.org/10.1016/j.expneurol.2007.06.009

Dörr, J. R., Yu, Y., Milanovic, M., Beuster, G., Zasada, C., Däbritz, J. H. M., Lisec, J., Lenze, D., Gerhardt, A., Schleicher, K., Kratzat, S., Purfürst, B., Walenta, S., Mueller-Klieser, W., Gräler, M., Hummel, M., Keller, U., Buck, A. K., Dörken, B., … Schmitt, C. A. (2013). Synthetic lethal metabolic targeting of cellular senescence in cancer therapy. *Nature*, *501*(7467), 421–425. https://doi.org/10.1038/nature12437

Dumont, R. J., Okonkwo, D. O., Verma, S., Hurlbert, R. J., Boulos, P. T., Ellegala, D. B., & Dumont, A. S. (2001). Acute Spinal Cord Injury, Part I: Pathophysiologic Mechanisms. *Clinical Neuropharmacology*, *24*(5). https://journals.lww.com/clinicalneuropharm/Fulltext/2001/09000/Acute_Spinal_Cord_Injury,_Part_I__Pathophysiologic.2.aspx

Dyck, S., Kataria, H., Alizadeh, A., Santhosh, K. T., Lang, B., Silver, J., & Karimi-Abdolrezaee, S. (2018). Perturbing chondroitin sulfate proteoglycan signaling through LAR and PTPσ receptors promotes a beneficial inflammatory response following spinal cord injury. *Journal of Neuroinflammation*, *15*(1), 90. https://doi.org/10.1186/s12974-018-1128-2

Edgerton, V. R., Tillakaratne, N. J. K., Bigbee, A. J., de Leon, R. D., & Roy, R. R. (2004). PLASTICITY OF THE SPINAL NEURAL CIRCUITRY AFTER INJURY. *Annual Review of Neuroscience*, *27*(1), 145–167. https://doi.org/10.1146/annurev.neuro.27.070203.144308

Eisner, V., Picard, M., & Hajnóczky, G. (2018). Mitochondrial dynamics in adaptive and maladaptive cellular stress responses. *Nature Cell Biology*, *20*(7), 755–765. https://doi.org/10.1038/s41556-018-0133-0

Ekpenyong-Akiba, A. E., Canfarotta, F., Abd H., B., Poblocka, M., Casulleras, M., Castilla-Vallmanya, L., Kocsis-Fodor, G., Kelly, M. E., Janus, J., Althubiti, M., Piletska, E., Piletsky, S., & Macip, S. (2019). Detecting and targeting senescent cells using molecularly imprinted nanoparticles. *Nanoscale Horizons*, *4*(3), 757–768. https://doi.org/10.1039/C8NH00473K

Emery, E., Aldana, P., Bunge, M. B., Puckett, W., Srinivasan, A., Keane, R. W., Bethea, J., & Levi, A. D. O. (1998). Apoptosis after traumatic human spinal cord injury. *Journal of Neurosurgery*,

89(6), 911–920. https://doi.org/10.3171/jns.1998.89.6.0911

Ethier, C., Oby, E. R., Bauman, M. J., & Miller, L. E. (2012). Restoration of grasp following paralysis through brain-controlled stimulation of muscles. *Nature*, *485*(7398), 368–371. https://doi.org/10.1038/nature10987

Evangelou, K., Lougiakis, N., Rizou, S. V, Kotsinas, A., Kletsas, D., Muñoz-Espín, D., Kastrinakis, N. G., Pouli, N., Marakos, P., Townsend, P., Serrano, M., Bartek, J., & Gorgoulis, V. G. (2017). Robust, universal biomarker assay to detect senescent cells in biological specimens. *Aging Cell*, *16*(1), 192–197. https://doi.org/10.1111/acel.12545

Ewald, J. A., Desotelle, J. A., Wilding, G., & Jarrard, D. F. (2010). Therapy-induced senescence in cancer. *Journal of the National Cancer Institute*, *102*(20), 1536–1546. https://doi.org/10.1093/jnci/djq364

Faget, D. V, Ren, Q., & Stewart, S. A. (2019). Unmasking senescence: context-dependent effects of SASP in cancer. *Nature Reviews Cancer*, *19*(8), 439–453. https://doi.org/10.1038/s41568-019-0156-2

Fang, P., Lin, J.-F., Pan, H.-C., Shen, Y.-Q., & Schachner, M. (2012). A Surgery Protocol for Adult Zebrafish Spinal Cord Injury. *Journal of Genetics and Genomics*, *39*(9), 481–487. https://doi.org/https://doi.org/10.1016/j.jgg.2012.07.010

Fang, P., Pan, H.-C., Lin, S. L., Zhang, W.-Q., Rauvala, H., Schachner, M., & Shen, Y.-Q. (2014). HMGB1 Contributes to Regeneration After Spinal Cord Injury in Adult Zebrafish. *Molecular Neurobiology*, *49*(1), 472–483. https://doi.org/10.1007/s12035-013-8533-4

Fitch, M. T., & Silver, J. (1997). Activated Macrophages and the Blood–Brain Barrier: Inflammation after CNS Injury Leads to Increases in Putative Inhibitory Molecules. *Experimental Neurology*, *148*(2), 587–603. https://doi.org/https://doi.org/10.1006/exnr.1997.6701

Fleming, J. C., Norenberg, M. D., Ramsay, D. A., Dekaban, G. A., Marcillo, A. E., Saenz, A. D., Pasquale-Styles, M., Dietrich, W. D., & Weaver, L. C. (2006). The cellular inflammatory response in human spinal cords after injury. *Brain*, *129*(12), 3249–3269. https://doi.org/10.1093/brain/awl296

Flesher, S. N., Collinger, J. L., Foldes, S. T., Weiss, J. M., Downey, J. E., Tyler-Kabara, E. C., Bensmaia, S. J., Schwartz, A. B., Boninger, M. L., & Gaunt, R. A. (2016). Intracortical microstimulation of human somatosensory cortex. *Science Translational Medicine*, *8*(361), 361ra141 LP-361ra141. https://doi.org/10.1126/scitranslmed.aaf8083

Frescas, D., Roux, C. M., Aygun-Sunar, S., Gleiberman, A. S., Krasnov, P., Kurnasov, O. V, Strom, E., Virtuoso, L. P., Wrobel, M., Osterman, A. L., Antoch, M. P., Mett, V., Chernova, O. B., & Gudkov, A. V. (2017). Senescent cells expose and secrete an oxidized form of membrane-bound vimentin as revealed by a natural polyreactive antibody. *Proceedings of the National Academy of Sciences of the United States of America*, *114*(9), E1668–E1677. https://doi.org/10.1073/pnas.1614661114

Freund, A., Patil, C. K., & Campisi, J. (2011). p38MAPK is a novel DNA damage response-independent regulator of the senescence-associated secretory phenotype. *The EMBO Journal*, *30*(8), 1536–1548. https://doi.org/10.1038/emboj.2011.69

Fuhrmann-Stroissnigg, H., Ling, Y. Y., Zhao, J., McGowan, S. J., Zhu, Y., Brooks, R. W., Grassi, D., Gregg, S. Q., Stripay, J. L., Dorronsoro, A., Corbo, L., Tang, P., Bukata, C., Ring, N., Giacca, M., Li, X., Tchkonia, T., Kirkland, J. L., Niedernhofer, L. J., & Robbins, P. D. (2017). Identification of HSP90 inhibitors as a novel class of senolytics. *Nature Communications*, *8*(1), 422. https://doi.org/10.1038/s41467-017-00314-z

Fujita, K., Mondal, A. M., Horikawa, I., Nguyen, G. H., Kumamoto, K., Sohn, J. J., Bowman, E. D.,

Mathe, E. A., Schetter, A. J., Pine, S. R., Ji, H., Vojtesek, B., Bourdon, J.-C., Lane, D. P., & Harris, C. C. (2009). p53 isoforms Delta133p53 and p53beta are endogenous regulators of replicative cellular senescence. *Nature Cell Biology*, *11*(9), 1135–1142. https://doi.org/10.1038/ncb1928

Fukuda, S., Nakamura, T., Kishigami, Y., Endo, K., Azuma, T., Fujikawa, T., Tsutsumi, S., & Shimizu, Y. (2005). New canine spinal cord injury model free from laminectomy. *Brain Research Protocols*, *14*(3), 171–180. https://doi.org/https://doi.org/10.1016/j.brainresprot.2005.01.001

Gage, F. H. (2000). Mammalian Neural Stem Cells. *Science*, *287*(5457), 1433 LP – 1438. https://doi.org/10.1126/science.287.5457.1433

Gaudet, A. D., & Popovich, P. G. (2014). Extracellular matrix regulation of inflammation in the healthy and injured spinal cord. *Experimental Neurology*, *258*, 24–34. https://doi.org/10.1016/j.expneurol.2013.11.020

Genovese, T., Esposito, E., Mazzon, E., Di Paola, R., Caminiti, R., Bramanti, P., Cappelani, A., & Cuzzocrea, S. (2009). Absence of endogenous interleukin-10 enhances secondary inflammatory process after spinal cord compression injury in mice. *Journal of Neurochemistry*, *108*(6), 1360–1372. https://doi.org/10.1111/j.1471-4159.2009.05899.x

Genovese, T., Mazzon, E., Crisafulli, C., Di Paola, R., Muià, C., Esposito, E., Bramanti, P., & Cuzzocrea, S. (2008). TNF-alpha blockage in a mouse model of SCI: Evidence for improved outcome. *Shock (Augusta, Ga.)*, *29*, 32–41. https://doi.org/10.1097/shk.0b013e318059053a

Gensel, J. C., & Zhang, B. (2015). Macrophage activation and its role in repair and pathology after spinal cord injury. *Brain Research*, *1619*, 1–11. https://doi.org/https://doi.org/10.1016/j.brainres.2014.12.045

Georgilis, A., Klotz, S., Hanley, C. J., Herranz, N., Weirich, B., Morancho, B., Leote, A. C., D'Artista, L., Gallage, S., Seehawer, M., Carroll, T., Dharmalingam, G., Wee, K. B., Mellone, M., Pombo, J., Heide, D., Guccione, E., Arribas, J., Barbosa-Morais, N. L., … Gil, J. (2018). PTBP1-Mediated Alternative Splicing Regulates the Inflammatory Secretome and the Pro-tumorigenic Effects of Senescent Cells. *Cancer Cell*, *34*(1), 85-102.e9. https://doi.org/10.1016/j.ccell.2018.06.007

Ghosh, S., & Hui, S. P. (2018). Axonal regeneration in zebrafish spinal cord. *Regeneration (Oxford, England)*, *5*(1), 43–60. https://doi.org/10.1002/reg2.99

Gibaja, A., Aburto, M. R., Pulido, S., Collado, M., Hurle, J. M., Varela-Nieto, I., & Magariños, M. (2019). TGFβ2-induced senescence during early inner ear development. *Scientific Reports*, *9*(1), 5912. https://doi.org/10.1038/s41598-019-42040-0

Gil, J., Guerrero, A., & Harranz, N. (2018). *WO2018215795A2*. https://patents.google.com/patent/WO2018215795A2/en

Giulian, D., & Robertson, C. (1990). Inhibition of mononuclear phagocytes reduces ischemic injury in the spinal cord. *Annals of Neurology*, *27*(1), 33–42. https://doi.org/10.1002/ana.410270107

Godwin, J. W., Pinto, A. R., & Rosenthal, N. A. (2013). Macrophages are required for adult salamander limb regeneration. *Proceedings of the National Academy of Sciences of the United States of America*, *110*(23), 9415–9420. https://doi.org/10.1073/pnas.1300290110

Goldshmit, Y., Sztal, T. E., Jusuf, P. R., Hall, T. E., Nguyen-Chi, M., & Currie, P. D. (2012). Fgf-Dependent Glial Cell Bridges Facilitate Spinal Cord Regeneration in Zebrafish. *The Journal of Neuroscience*, *32*(22), 7477 LP – 7492. https://doi.org/10.1523/JNEUROSCI.0758-12.2012

Gorgey, A. S. (2018). Robotic exoskeletons: The current pros and cons. *World Journal of Orthopedics*, *9*(9), 112–119. https://doi.org/10.5312/wjo.v9.i9.112

Gorgoulis, V., Adams, P. D., Alimonti, A., Bennett, D. C., Bischof, O., Bishop, C., Campisi, J., Collado, M., Evangelou, K., Ferbeyre, G., Gil, J., Hara, E., Krizhanovsky, V., Jurk, D., Maier, A. B., Narita, M., Niedernhofer, L., Passos, J. F., Robbins, P. D., … Demaria, M. (2019). Cellular Senescence: Defining a Path Forward. *Cell*, *179*(4), 813–827. https://doi.org/https://doi.org/10.1016/j.cell.2019.10.005

Gorgoulis, V. G., Pefani, D.-E., Pateras, I. S., & Trougakos, I. P. (2018). Integrating the DNA damage and protein stress responses during cancer development and treatment. *The Journal of Pathology*, *246*(1), 12–40. https://doi.org/10.1002/path.5097

Göritz, C., Dias, D. O., Tomilin, N., Barbacid, M., Shupliakov, O., & Frisén, J. (2011). A Pericyte Origin of Spinal Cord Scar Tissue. *Science*, *333*(6039), 238 LP – 242. https://doi.org/10.1126/science.1203165

Grahn, P. J., Lavrov, I. A., Sayenko, D. G., Van Straaten, M. G., Gill, M. L., Strommen, J. A., Calvert, J. S., Drubach, D. I., Beck, L. A., Linde, M. B., Thoreson, A. R., Lopez, C., Mendez, A. A., Gad, P. N., Gerasimenko, Y. P., Edgerton, V. R., Zhao, K. D., & Lee, K. H. (2017). Enabling Task-Specific Volitional Motor Functions via Spinal Cord Neuromodulation in a Human With Paraplegia. *Mayo Clinic Proceedings*, *92*(4), 544–554. https://doi.org/10.1016/j.mayocp.2017.02.014

Greenhalgh, A. D., & David, S. (2014). Differences in the Phagocytic Response of Microglia and Peripheral Macrophages after Spinal Cord Injury and Its Effects on Cell Death. *The Journal of Neuroscience*, *34*(18), 6316 LP – 6322. https://doi.org/10.1523/JNEUROSCI.4912-13.2014

Grillner, S. (2006). Biological Pattern Generation: The Cellular and Computational Logic of Networks in Motion. *Neuron*, *52*(5), 751–766. https://doi.org/10.1016/j.neuron.2006.11.008

Guerrero, A., Herranz, N., Sun, B., Wagner, V., Gallage, S., Guiho, R., Wolter, K., Pombo, J., Irvine, E. E., Innes, A. J., Birch, J., Glegola, J., Manshaei, S., Heide, D., Dharmalingam, G., Harbig, J., Olona, A., Behmoaras, J., Dauch, D., … Gil, J. (2019). Cardiac glycosides are broad-spectrum senolytics. *Nature Metabolism*, *1*(11), 1074–1088. https://doi.org/10.1038/s42255-019-0122-z

Guerrero, A. R., Uchida, K., Nakajima, H., Watanabe, S., Nakamura, M., Johnson, W. E., & Baba, H. (2012). Blockade of interleukin-6 signaling inhibits the classic pathway and promotes an alternative pathway of macrophage activation after spinal cord injury in mice. *Journal of Neuroinflammation*, *9*, 40. https://doi.org/10.1186/1742-2094-9-40

Guha, A., Tator, C. H., & Rochon, J. (1989). Spinal cord blood flow and systemic blood pressure after experimental spinal cord injury in rats. *Stroke*, *20*(3), 372–377. https://doi.org/10.1161/01.STR.20.3.372

Gungor, B., Adiguzel, E., Gursel, I., Yilmaz, B., & Gursel, M. (2016). Intestinal Microbiota in Patients with Spinal Cord Injury. *PloS One*, *11*(1), e0145878–e0145878. https://doi.org/10.1371/journal.pone.0145878

Guo, Y., Kim, C., Ahmad, S., Zhang, J., & Mao, Y. (2012). CENP-E--dependent BubR1 autophosphorylation enhances chromosome alignment and the mitotic checkpoint. *The Journal of Cell Biology*, *198*(2), 205–217. https://doi.org/10.1083/jcb.201202152

Gynther, M., Kääriäinen, T. M., Hakkarainen, J. J., Jalkanen, A. J., Petsalo, A., Lehtonen, M., Peura, L., Kurkipuro, J., Samaranayake, H., Ylä-Herttuala, S., Rautio, J., & Forsberg, M. M. (2015). Brain Pharmacokinetics of Ganciclovir in Rats with Orthotopic BT4C Glioma. *Drug Metabolism and Disposition*, *43*(1), 140 LP – 146. https://doi.org/10.1124/dmd.114.059840

Hachmann, J. T., Grahn, P. J., Calvert, J. S., Drubach, D. I., Lee, K. H., & Lavrov, I. A. (2017). Electrical Neuromodulation of the Respiratory System After Spinal Cord Injury. *Mayo Clinic Proceedings*, *92*(9), 1401–1414. https://doi.org/10.1016/j.mayocp.2017.04.011

Halazonetis, T. D., Gorgoulis, V. G., & Bartek, J. (2008). An Oncogene-Induced DNA Damage Model for Cancer Development. *Science*, *319*(5868), 1352 LP – 1355. https://doi.org/10.1126/science.1140735

Hall, B. M., Balan, V., Gleiberman, A. S., Strom, E., Krasnov, P., Virtuoso, L. P., Rydkina, E., Vujcic, S., Balan, K., Gitlin, I. I., Leonova, K. I., Consiglio, C. R., Gollnick, S. O., Chernova, O. B., & Gudkov, A. V. (2017). p16(Ink4a) and senescence-associated β-galactosidase can be induced in macrophages as part of a reversible response to physiological stimuli. *Aging*, *9*(8), 1867–1884. https://doi.org/10.18632/aging.101268

Harley, C. B., Futcher, A. B., & Greider, C. W. (1990). Telomeres shorten during ageing of human fibroblasts. *Nature*, *345*(6274), 458–460. https://doi.org/10.1038/345458a0

Harrison, M., O'Brien, A., Adams, L., Cowin, G., Ruitenberg, M. J., Sengul, G., & Watson, C. (2013). Vertebral landmarks for the identification of spinal cord segments in the mouse. *NeuroImage*, *68*, 22–29. https://doi.org/https://doi.org/10.1016/j.neuroimage.2012.11.048

Hata, K., Fujitani, M., Yasuda, Y., Doya, H., Saito, T., Yamagishi, S., Mueller, B. K., & Yamashita, T. (2006). RGMa inhibition promotes axonal growth and recovery after spinal cord injury. *The Journal of Cell Biology*, *173*(1), 47–58. https://doi.org/10.1083/jcb.200508143

Hayes, K. C., Hull, T. C. L., Delaney, G. A., Potter, P. J., Sequeira, K. A. J., Campbell, K., & Popovich, P. G. (2002). Elevated Serum Titers of Proinflammatory Cytokines and CNS Autoantibodies in Patients with Chronic Spinal Cord Injury. *Journal of Neurotrauma*, *19*(6), 753–761. https://doi.org/10.1089/08977150260139129

Hayflick, L. (1965). The limited in vitro lifetime of human diploid cell strains. *Experimental Cell Research*, *37*(3), 614–636. https://doi.org/https://doi.org/10.1016/0014-4827(65)90211-9

Hayflick, L., & Moorhead, P. S. (1961). The serial cultivation of human diploid cell strains. *Experimental Cell Research*, *25*(3), 585–621. https://doi.org/https://doi.org/10.1016/0014-4827(61)90192-6

He, S., & Sharpless, N. E. (2017). Senescence in Health and Disease. *Cell*, *169*(6), 1000–1011. https://doi.org/10.1016/j.cell.2017.05.015

Hernandez-Segura, A., de Jong, T. V, Melov, S., Guryev, V., Campisi, J., & Demaria, M. (2017). Unmasking Transcriptional Heterogeneity in Senescent Cells. *Current Biology : CB*, *27*(17), 2652-2660.e4. https://doi.org/10.1016/j.cub.2017.07.033

Hernandez-Segura, A., Nehme, J., & Demaria, M. (2018). Hallmarks of Cellular Senescence. *Trends in Cell Biology*, *28*(6), 436–453. https://doi.org/10.1016/j.tcb.2018.02.001

Herranz, N., Gallage, S., Mellone, M., Wuestefeld, T., Klotz, S., Hanley, C. J., Raguz, S., Acosta, J. C., Innes, A. J., Banito, A., Georgilis, A., Montoya, A., Wolter, K., Dharmalingam, G., Faull, P., Carroll, T., Martínez-Barbera, J. P., Cutillas, P., Reisinger, F., … Gil, J. (2015). mTOR regulates MAPKAPK2 translation to control the senescence-associated secretory phenotype. *Nature Cell Biology*, *17*(9), 1205–1217. https://doi.org/10.1038/ncb3225

Herranz, N., & Gil, J. (2018). Mechanisms and functions of cellular senescence. *The Journal of Clinical Investigation*, *128*(4), 1238–1246. https://doi.org/10.1172/JCI95148

Herrmann, J. E., Imura, T., Song, B., Qi, J., Ao, Y., Nguyen, T. K., Korsak, R. A., Takeda, K., Akira, S., & Sofroniew, M. V. (2008). STAT3 is a critical regulator of astrogliosis and scar formation after spinal cord injury. *The Journal of Neuroscience : The Official Journal of the Society for Neuroscience*, *28*(28), 7231–7243. https://doi.org/10.1523/JNEUROSCI.1709-08.2008

Höhn, A., Weber, D., Jung, T., Ott, C., Hugo, M., Kochlik, B., Kehm, R., König, J., Grune, T., & Castro, J. P. (2017). Happily (n)ever after: Aging in the context of oxidative stress, proteostasis loss and cellular senescence. *Redox Biology*, *11*, 482–501.

https://doi.org/10.1016/j.redox.2016.12.001

Hong, H., Takahashi, K., Ichisaka, T., Aoi, T., Kanagawa, O., Nakagawa, M., Okita, K., & Yamanaka, S. (2009). Suppression of induced pluripotent stem cell generation by the p53-p21 pathway. *Nature*, *460*(7259), 1132–1135. https://doi.org/10.1038/nature08235

Hu, H. Z., Granger, N., Pai, S. B., Bellamkonda, R. V, & Jeffery, N. D. (2018). Therapeutic efficacy of microtube-embedded chondroitinase ABC in a canine clinical model of spinal cord injury. *Brain*, *141*(4), 1017–1027. https://doi.org/10.1093/brain/awy007

Huang, L., Wu, Z.-B., Zhuge, Q., Zheng, W., Shao, B., Wang, B., Sun, F., & Jin, K. (2014). Glial scar formation occurs in the human brain after ischemic stroke. *International Journal of Medical Sciences*, *11*(4), 344–348. https://doi.org/10.7150/ijms.8140

Huang, T., & Rivera-Pérez, J. A. (2014). Senescence-associated β-galactosidase activity marks the visceral endoderm of mouse embryos but is not indicative of senescence. *Genesis (New York, N.Y. : 2000)*, *52*(4), 300–308. https://doi.org/10.1002/dvg.22761

Huang, W., Vodovotz, Y., Kusturiss, M. B., Barclay, D., Greenwald, K., Boninger, M. L., Coen, P. M., Brienza, D., & Sowa, G. (2014). Identification of Distinct Monocyte Phenotypes and Correlation With Circulating Cytokine Profiles in Acute Response to Spinal Cord Injury: A Pilot Study. *PM&R*, *6*(4), 332–341. https://doi.org/https://doi.org/10.1016/j.pmrj.2013.10.006

Hubackova, S., Krejcikova, K., Bartek, J., & Hodny, Z. (2012). IL1- and TGFβ-Nox4 signaling, oxidative stress and DNA damage response are shared features of replicative, oncogene-induced, and drug-induced paracrine "bystander senescence." *Aging*, *4*(12), 932–951. https://doi.org/10.18632/aging.100520

Hui, S. P., Dutta, A., & Ghosh, S. (2010). Cellular response after crush injury in adult zebrafish spinal cord. *Developmental Dynamics*, *239*(11), 2962–2979. https://doi.org/10.1002/dvdy.22438

Itahana, K., Campisi, J., & Dimri, G. P. (2007). *Methods to Detect Biomarkers of Cellular Senescence BT - Biological Aging: Methods and Protocols* (T. O. Tollefsbol (ed.); pp. 21–31). Humana Press. https://doi.org/10.1007/978-1-59745-361-5_3

Ito, Y., Hoare, M., & Narita, M. (2017). Spatial and Temporal Control of Senescence. *Trends in Cell Biology*, *27*(11), 820–832. https://doi.org/10.1016/j.tcb.2017.07.004

Jahan, N., & Hannila, S. S. (2015). Transforming growth factor β-induced expression of chondroitin sulfate proteoglycans is mediated through non-Smad signaling pathways. *Experimental Neurology*, *263*, 372–384. https://doi.org/https://doi.org/10.1016/j.expneurol.2014.10.023

Janzen, V., Forkert, R., Fleming, H. E., Saito, Y., Waring, M. T., Dombkowski, D. M., Cheng, T., DePinho, R. A., Sharpless, N. E., & Scadden, D. T. (2006). Stem-cell ageing modified by the cyclin-dependent kinase inhibitor p16INK4a. *Nature*, *443*(7110), 421–426. https://doi.org/10.1038/nature05159

Jeon, O. H., Kim, C., Laberge, R.-M., Demaria, M., Rathod, S., Vasserot, A. P., Chung, J. W., Kim, D. H., Poon, Y., David, N., Baker, D. J., van Deursen, J. M., Campisi, J., & Elisseeff, J. H. (2017). Local clearance of senescent cells attenuates the development of post-traumatic osteoarthritis and creates a pro-regenerative environment. *Nature Medicine*, *23*(6), 775–781. https://doi.org/10.1038/nm.4324

Jeyapalan, J. C., Ferreira, M., Sedivy, J. M., & Herbig, U. (2007). Accumulation of senescent cells in mitotic tissue of aging primates. *Mechanisms of Ageing and Development*, *128*(1), 36–44. https://doi.org/10.1016/j.mad.2006.11.008

Jones, T. B. (2014). Lymphocytes and autoimmunity after spinal cord injury. *Experimental Neurology*, *258*, 78–90. https://doi.org/https://doi.org/10.1016/j.expneurol.2014.03.003

Jun, J.-I., & Lau, L. F. (2010). The matricellular protein CCN1 induces fibroblast senescence and restricts fibrosis in cutaneous wound healing. *Nature Cell Biology*, *12*(7), 676–685. https://doi.org/10.1038/ncb2070

Kang, C. (2019). Senolytics and Senostatics: A Two-Pronged Approach to Target Cellular Senescence for Delaying Aging and Age-Related Diseases. *Molecules and Cells*, *42*(12), 821–827. https://doi.org/10.14348/molcells.2019.0298

Kang, C., Xu, Q., Martin, T. D., Li, M. Z., Demaria, M., Aron, L., Lu, T., Yankner, B. A., Campisi, J., & Elledge, S. J. (2015). The DNA damage response induces inflammation and senescence by inhibiting autophagy of GATA4. *Science (New York, N.Y.)*, *349*(6255), aaa5612–aaa5612. https://doi.org/10.1126/science.aaa5612

Kang, H. T., Park, J. T., Choi, K., Kim, Y., Choi, H. J. C., Jung, C. W., Lee, Y.-S., & Park, S. C. (2017). Chemical screening identifies ATM as a target for alleviating senescence. *Nature Chemical Biology*, *13*(6), 616–623. https://doi.org/10.1038/nchembio.2342

Kaplon, J., Zheng, L., Meissl, K., Chaneton, B., Selivanov, V. A., Mackay, G., van der Burg, S. H., Verdegaal, E. M. E., Cascante, M., Shlomi, T., Gottlieb, E., & Peeper, D. S. (2013). A key role for mitochondrial gatekeeper pyruvate dehydrogenase in oncogene-induced senescence. *Nature*, *498*(7452), 109–112. https://doi.org/10.1038/nature12154

Karimi-Abdolrezaee, S., Eftekharpour, E., Wang, J., Schut, D., & Fehlings, M. G. (2010). Synergistic effects of transplanted adult neural stem/progenitor cells, chondroitinase, and growth factors promote functional repair and plasticity of the chronically injured spinal cord. *The Journal of Neuroscience : The Official Journal of the Society for Neuroscience*, *30*(5), 1657–1676. https://doi.org/10.1523/JNEUROSCI.3111-09.2010

Kaushik, S., & Cuervo, A. M. (2015). Proteostasis and aging. *Nature Medicine*, *21*(12), 1406–1415. https://doi.org/10.1038/nm.4001

Ke, S., Lai, Y., Zhou, T., Li, L., Wang, Y., Ren, L., & Ye, S. (2018). Molybdenum Disulfide Nanoparticles Resist Oxidative Stress-Mediated Impairment of Autophagic Flux and Mitigate Endothelial Cell Senescence and Angiogenic Dysfunctions. *ACS Biomaterials Science & Engineering*, *4*(2), 663–674. https://doi.org/10.1021/acsbiomaterials.7b00714

Kehr, P., & Kaech, D. L. (2014). Michael G. Fehlings, Alexander R. Vaccaro, Maxwell Boakye, Serge Rossignol, John F. Ditunno Jr, Anthony S. Burns: Essentials of spinal cord injury: basic research to clinical practice. *European Journal of Orthopaedic Surgery & Traumatology*, *24*(5), 837. https://doi.org/10.1007/s00590-014-1456-6

Kennedy, A. L., McBryan, T., Enders, G. H., Johnson, F. B., Zhang, R., & Adams, P. D. (2010). Senescent mouse cells fail to overtly regulate the HIRA histone chaperone and do not form robust Senescence Associated Heterochromatin Foci. *Cell Division*, *5*, 16. https://doi.org/10.1186/1747-1028-5-16

Kigerl, K. A., Gensel, J. C., Ankeny, D. P., Alexander, J. K., Donnelly, D. J., & Popovich, P. G. (2009). Identification of two distinct macrophage subsets with divergent effects causing either neurotoxicity or regeneration in the injured mouse spinal cord. *The Journal of Neuroscience : The Official Journal of the Society for Neuroscience*, *29*(43), 13435–13444. https://doi.org/10.1523/JNEUROSCI.3257-09.2009

Kigerl, K. A., Hall, J. C. E., Wang, L., Mo, X., Yu, Z., & Popovich, P. G. (2016). Gut dysbiosis impairs recovery after spinal cord injury. *The Journal of Experimental Medicine*, *213*(12), 2603–2620. https://doi.org/10.1084/jem.20151345

Kigerl, K. A., McGaughy, V. M., & Popovich, P. G. (2006). Comparative analysis of lesion development and intraspinal inflammation in four strains of mice following spinal contusion injury. *The Journal of Comparative Neurology*, *494*(4), 578–594.

https://doi.org/10.1002/cne.20827

Kim, K. M., Noh, J. H., Bodogai, M., Martindale, J. L., Yang, X., Indig, F. E., Basu, S. K., Ohnuma, K., Morimoto, C., Johnson, P. F., Biragyn, A., Abdelmohsen, K., & Gorospe, M. (2017). Identification of senescent cell surface targetable protein DPP4. *Genes & Development*, *31*(15), 1529–1534. https://doi.org/10.1101/gad.302570.117

Kim, W. Y., & Sharpless, N. E. (2006). The Regulation of INK4/ARF in Cancer and Aging. *Cell*, *127*(2), 265–275. https://doi.org/10.1016/j.cell.2006.10.003

Kjell, J., & Olson, L. (2016). Rat models of spinal cord injury: from pathology to potential therapies. *Disease Models & Mechanisms*, *9*(10), 1125–1137. https://doi.org/10.1242/dmm.025833

Kong, X., Feng, D., Wang, H., Hong, F., Bertola, A., Wang, F.-S., & Gao, B. (2012). Interleukin-22 induces hepatic stellate cell senescence and restricts liver fibrosis in mice. *Hepatology (Baltimore, Md.)*, *56*(3), 1150–1159. https://doi.org/10.1002/hep.25744

Korolchuk, V. I., Miwa, S., Carroll, B., & von Zglinicki, T. (2017). Mitochondria in Cell Senescence: Is Mitophagy the Weakest Link? *EBioMedicine*, *21*, 7–13. https://doi.org/10.1016/j.ebiom.2017.03.020

Krizhanovsky, V., & Lowe, S. W. (2009). The promises and perils of p53. *Nature*, *460*(7259), 1085–1086. https://doi.org/10.1038/4601085a

Krizhanovsky, V., Yon, M., Dickins, R. A., Hearn, S., Simon, J., Miething, C., Yee, H., Zender, L., & Lowe, S. W. (2008). Senescence of Activated Stellate Cells Limits Liver Fibrosis. *Cell*, *134*(4), 657–667. https://doi.org/https://doi.org/10.1016/j.cell.2008.06.049

Kroner, A., Greenhalgh, A. D., Zarruk, J. G., Passos dos Santos, R., Gaestel, M., & David, S. (2014). TNF and Increased Intracellular Iron Alter Macrophage Polarization to a Detrimental M1 Phenotype in the Injured Spinal Cord. *Neuron*, *83*(5), 1098–1116. https://doi.org/10.1016/j.neuron.2014.07.027

Kuilman, T., Michaloglou, C., Vredeveld, L. C. W., Douma, S., van Doorn, R., Desmet, C. J., Aarden, L. A., Mooi, W. J., & Peeper, D. S. (2008). Oncogene-Induced Senescence Relayed by an Interleukin-Dependent Inflammatory Network. *Cell*, *133*(6), 1019–1031. https://doi.org/10.1016/j.cell.2008.03.039

Kuilman, T., & Peeper, D. S. (2009). Senescence-messaging secretome: SMS-ing cellular stress. *Nature Reviews Cancer*, *9*(2), 81–94. https://doi.org/10.1038/nrc2560

Kwon, B. K., Streijger, F., Hill, C. E., Anderson, A. J., Bacon, M., Beattie, M. S., Blesch, A., Bradbury, E. J., Brown, A., Bresnahan, J. C., Case, C. C., Colburn, R. W., David, S., Fawcett, J. W., Ferguson, A. R., Fischer, I., Floyd, C. L., Gensel, J. C., Houle, J. D., … Tetzlaff, W. (2015). Large animal and primate models of spinal cord injury for the testing of novel therapies. *Experimental Neurology*, *269*, 154–168. https://doi.org/https://doi.org/10.1016/j.expneurol.2015.04.008

Kwon, Y., Kim, J. W., Jeoung, J. A., Kim, M.-S., & Kang, C. (2017). Autophagy Is Pro-Senescence When Seen in Close-Up, but Anti-Senescence in Long-Shot. *Molecules and Cells*, *40*(9), 607–612. https://doi.org/10.14348/molcells.2017.0151

Laberge, R-M, Adler, D., DeMaria, M., Mechtouf, N., Teachenor, R., Cardin, G. B., Desprez, P.-Y., Campisi, J., & Rodier, F. (2013). Mitochondrial DNA damage induces apoptosis in senescent cells. *Cell Death & Disease*, *4*(7), e727–e727. https://doi.org/10.1038/cddis.2013.199

Laberge, Remi-Martin, Sun, Y., Orjalo, A. V, Patil, C. K., Freund, A., Zhou, L., Curran, S. C., Davalos, A. R., Wilson-Edell, K. A., Liu, S., Limbad, C., Demaria, M., Li, P., Hubbard, G. B., Ikeno, Y., Javors, M., Desprez, P.-Y., Benz, C. C., Kapahi, P., … Campisi, J. (2015). MTOR regulates the pro-tumorigenic senescence-associated secretory phenotype by promoting IL1A

translation. *Nature Cell Biology*, *17*(8), 1049–1061. https://doi.org/10.1038/ncb3195

Laberge, Remi-Martin, Zhou, L., Sarantos, M. R., Rodier, F., Freund, A., de Keizer, P. L. J., Liu, S., Demaria, M., Cong, Y.-S., Kapahi, P., Desprez, P.-Y., Hughes, R. E., & Campisi, J. (2012). Glucocorticoids suppress selected components of the senescence-associated secretory phenotype. *Aging Cell*, *11*(4), 569–578. https://doi.org/10.1111/j.1474-9726.2012.00818.x

Lamming, D. W., Ye, L., Sabatini, D. M., & Baur, J. A. (2013). Rapalogs and mTOR inhibitors as anti-aging therapeutics. *The Journal of Clinical Investigation*, *123*(3), 980–989. https://doi.org/10.1172/JCI64099

Lang, B. T., Cregg, J. M., DePaul, M. A., Tran, A. P., Xu, K., Dyck, S. M., Madalena, K. M., Brown, B. P., Weng, Y.-L., Li, S., Karimi-Abdolrezaee, S., Busch, S. A., Shen, Y., & Silver, J. (2015). Modulation of the proteoglycan receptor PTPσ promotes recovery after spinal cord injury. *Nature*, *518*(7539), 404–408. https://doi.org/10.1038/nature13974

Le, O. N. L., Rodier, F., Fontaine, F., Coppe, J.-P., Campisi, J., DeGregori, J., Laverdière, C., Kokta, V., Haddad, E., & Beauséjour, C. M. (2010). Ionizing radiation-induced long-term expression of senescence markers in mice is independent of p53 and immune status. *Aging Cell*, *9*(3), 398–409. https://doi.org/10.1111/j.1474-9726.2010.00567.x

Le Roux, I., Konge, J., Le Cam, L., Flamant, P., & Tajbakhsh, S. (2015). Numb is required to prevent p53-dependent senescence following skeletal muscle injury. *Nature Communications*, *6*(1), 8528. https://doi.org/10.1038/ncomms9528

Lee, B. Y., Han, J. A., Im, J. S., Morrone, A., Johung, K., Goodwin, E. C., Kleijer, W. J., DiMaio, D., & Hwang, E. S. (2006). Senescence-associated β-galactosidase is lysosomal β-galactosidase. *Aging Cell*, *5*(2), 187–195. https://doi.org/10.1111/j.1474-9726.2006.00199.x

Lee, J.-S., Fang, S.-Y., Roan, J.-N., Jou, I.-M., & Lam, C.-F. (2016). Spinal cord injury enhances arterial expression and reactivity of α1-adrenergic receptors—mechanistic investigation into autonomic dysreflexia. *The Spine Journal*, *16*(1), 65–71. https://doi.org/10.1016/j.spinee.2015.09.030

Leontieva, O. V, Demidenko, Z. N., & Blagosklonny, M. V. (2015). Dual mTORC1/C2 inhibitors suppress cellular geroconversion (a senescence program). *Oncotarget*, *6*(27), 23238–23248. https://doi.org/10.18632/oncotarget.4836

Leverson, J. D., Phillips, D. C., Mitten, M. J., Boghaert, E. R., Diaz, D., Tahir, S. K., Belmont, L. D., Nimmer, P., Xiao, Y., Ma, X. M., Lowes, K. N., Kovar, P., Chen, J., Jin, S., Smith, M., Xue, J., Zhang, H., Oleksijew, A., Magoc, T. J., … Souers, A. J. (2015). Exploiting selective BCL-2 family inhibitors to dissect cell survival dependencies and define improved strategies for cancer therapy. *Science Translational Medicine*, *7*(279), 279ra40 LP-279ra40. https://doi.org/10.1126/scitranslmed.aaa4642

Li, H., Collado, M., Villasante, A., Strati, K., Ortega, S., Cañamero, M., Blasco, M. A., & Serrano, M. (2009). The Ink4/Arf locus is a barrier for iPS cell reprogramming. *Nature*, *460*(7259), 1136–1139. https://doi.org/10.1038/nature08290

Li, S., & Stys, P. K. (2000). Mechanisms of ionotropic glutamate receptor-mediated excitotoxicity in isolated spinal cord white matter. *The Journal of Neuroscience : The Official Journal of the Society for Neuroscience*, *20*(3), 1190–1198. https://doi.org/10.1523/JNEUROSCI.20-03-01190.2000

Li, S., & Stys, P. K. (2001). Na+–K+-ATPase inhibition and depolarization induce glutamate release via reverse Na+-dependent transport in spinal cord white matter. *Neuroscience*, *107*(4), 675–683. https://doi.org/https://doi.org/10.1016/S0306-4522(01)00385-2

Lim, H., Park, H., & Kim, H. P. (2015). Effects of flavonoids on senescence-associated secretory

phenotype formation from bleomycin-induced senescence in BJ fibroblasts. *Biochemical Pharmacology*, *96*(4), 337–348. https://doi.org/https://doi.org/10.1016/j.bcp.2015.06.013

Liu, J., Weaver, J., Jin, X., Zhang, Y., Xu, J., Liu, K. J., Li, W., & Liu, W. (2016). Nitric Oxide Interacts with Caveolin-1 to Facilitate Autophagy-Lysosome-Mediated Claudin-5 Degradation in Oxygen-Glucose Deprivation-Treated Endothelial Cells. *Molecular Neurobiology*, *53*(9), 5935–5947. https://doi.org/10.1007/s12035-015-9504-8

Liu, S., Li, Y., Choi, H. M. C., Sarkar, C., Koh, E. Y., Wu, J., & Lipinski, M. M. (2018). Lysosomal damage after spinal cord injury causes accumulation of RIPK1 and RIPK3 proteins and potentiation of necroptosis. *Cell Death & Disease*, *9*(5), 476. https://doi.org/10.1038/s41419-018-0469-1

Liu, Y., & Levine, B. (2015). Autosis and autophagic cell death: the dark side of autophagy. *Cell Death and Differentiation*, *22*(3), 367–376. https://doi.org/10.1038/cdd.2014.143

López-Dolado, E., González-Mayorga, A., Gutiérrez, M. C., & Serrano, M. C. (2016). Immunomodulatory and angiogenic responses induced by graphene oxide scaffolds in chronic spinal hemisected rats. *Biomaterials*, *99*, 72–81. https://doi.org/https://doi.org/10.1016/j.biomaterials.2016.05.012

Lozano-Torres, B., Galiana, I., Rovira, M., Garrido, E., Chaib, S., Bernardos, A., Muñoz-Espín, D., Serrano, M., Martínez-Máñez, R., & Sancenón, F. (2017). An OFF–ON Two-Photon Fluorescent Probe for Tracking Cell Senescence in Vivo. *Journal of the American Chemical Society*, *139*(26), 8808–8811. https://doi.org/10.1021/jacs.7b04985

Lucas, T., Waisman, A., Ranjan, R., Roes, J., Krieg, T., Müller, W., Roers, A., & Eming, S. A. (2010). Differential Roles of Macrophages in Diverse Phases of Skin Repair. *The Journal of Immunology*, *184*(7), 3964 LP – 3977. https://doi.org/10.4049/jimmunol.0903356

Mallick, S., & D'Mello, S. R. (2014). JAZ (Znf346), a SIRT1-interacting protein, protects neurons by stimulating p21 (WAF/CIP1) protein expression. *The Journal of Biological Chemistry*, *289*(51), 35409–35420. https://doi.org/10.1074/jbc.M114.597575

Marcotte, R., Lacelle, C., & Wang, E. (2004). Senescent fibroblasts resist apoptosis by downregulating caspase-3. *Mechanisms of Ageing and Development*, *125*(10), 777–783. https://doi.org/https://doi.org/10.1016/j.mad.2004.07.007

Marcoux, S., Le, O. N. L., Langlois-Pelletier, C., Laverdière, C., Hatami, A., Robaey, P., & Beauséjour, C. M. (2013). Expression of the senescence marker p16INK4a in skin biopsies of acute lymphoblastic leukemia survivors: a pilot study. *Radiation Oncology (London, England)*, *8*, 252. https://doi.org/10.1186/1748-717X-8-252

Martínez-Zamudio, R. I., Robinson, L., Roux, P.-F., & Bischof, O. (2017). SnapShot: Cellular Senescence Pathways. *Cell*, *170*(4), 816-816.e1. https://doi.org/10.1016/j.cell.2017.07.049

Martinez, F. O., Gordon, S., Locati, M., & Mantovani, A. (2006). Transcriptional Profiling of the Human Monocyte-to-Macrophage Differentiation and Polarization: New Molecules and Patterns of Gene Expression. *The Journal of Immunology*, *177*(10), 7303 LP – 7311. https://doi.org/10.4049/jimmunol.177.10.7303

McHugh, D., & Gil, J. (2018). Senescence and aging: Causes, consequences, and therapeutic avenues. *The Journal of Cell Biology*, *217*(1), 65–77. https://doi.org/10.1083/jcb.201708092

Meletis, K., Barnabé-Heider, F., Carlén, M., Evergren, E., Tomilin, N., Shupliakov, O., & Frisén, J. (2008). Spinal cord injury reveals multilineage differentiation of ependymal cells. *PLoS Biology*, *6*(7), e182–e182. https://doi.org/10.1371/journal.pbio.0060182

Metz, G. A. S., Curt, A., van de Meent, H., Klusman, I., Schwab, M. E., & Dietz, V. (2000). Validation of the Weight-Drop Contusion Model in Rats: A Comparative Study of Human

Spinal Cord Injury. *Journal of Neurotrauma*, *17*(1), 1–17. https://doi.org/10.1089/neu.2000.17.1

Meyer, K., Hodwin, B., Ramanujam, D., Engelhardt, S., & Sarikas, A. (2016). Essential Role for Premature Senescence of Myofibroblasts in Myocardial Fibrosis. *Journal of the American College of Cardiology*, *67*(17), 2018–2028. https://doi.org/https://doi.org/10.1016/j.jacc.2016.02.047

Middleton, J. W., Dayton, A., Walsh, J., Rutkowski, S. B., Leong, G., & Duong, S. (2012). Life expectancy after spinal cord injury: a 50-year study. *Spinal Cord*, *50*(11), 803–811. https://doi.org/10.1038/sc.2012.55

Milanovic, M., Fan, D. N. Y., Belenki, D., Däbritz, J. H. M., Zhao, Z., Yu, Y., Dörr, J. R., Dimitrova, L., Lenze, D., Monteiro Barbosa, I. A., Mendoza-Parra, M. A., Kanashova, T., Metzner, M., Pardon, K., Reimann, M., Trumpp, A., Dörken, B., Zuber, J., Gronemeyer, H., … Schmitt, C. A. (2018). Senescence-associated reprogramming promotes cancer stemness. *Nature*, *553*(7686), 96–100. https://doi.org/10.1038/nature25167

Moiseeva, O., Deschênes-Simard, X., St-Germain, E., Igelmann, S., Huot, G., Cadar, A. E., Bourdeau, V., Pollak, M. N., & Ferbeyre, G. (2013). Metformin inhibits the senescence-associated secretory phenotype by interfering with IKK/NF-κB activation. *Aging Cell*, *12*(3), 489–498. https://doi.org/10.1111/acel.12075

Mokalled, M. H., Patra, C., Dickson, A. L., Endo, T., Stainier, D. Y. R., & Poss, K. D. (2016). Injury-induced ctgfa directs glial bridging and spinal cord regeneration in zebrafish. *Science*, *354*(6312), 630 LP – 634. https://doi.org/10.1126/science.aaf2679

Morshead, C. M., Reynolds, B. A., Craig, C. G., McBurney, M. W., Staines, W. A., Morassutti, D., Weiss, S., & van der Kooy, D. (1994). Neural stem cells in the adult mammalian forebrain: A relatively quiescent subpopulation of subependymal cells. *Neuron*, *13*(5), 1071–1082. https://doi.org/10.1016/0896-6273(94)90046-9

Mosteiro, L., Pantoja, C., Alcazar, N., Marión, R. M., Chondronasiou, D., Rovira, M., Fernandez-Marcos, P. J., Muñoz-Martin, M., Blanco-Aparicio, C., Pastor, J., Gómez-López, G., De Martino, A., Blasco, M. A., Abad, M., & Serrano, M. (2016). Tissue damage and senescence provide critical signals for cellular reprogramming in vivo. *Science*, *354*(6315), aaf4445. https://doi.org/10.1126/science.aaf4445

Muir, E., Raza, M., Ellis, C., Burnside, E., Love, F., Heller, S., Elliot, M., Daniell, E., Dasgupta, D., Alves, N., Day, P., Fawcett, J., & Keynes, R. (2017). Trafficking and processing of bacterial proteins by mammalian cells: Insights from chondroitinase ABC. *PloS One*, *12*(11), e0186759–e0186759. https://doi.org/10.1371/journal.pone.0186759

Muñoz-Espín, D., Cañamero, M., Maraver, A., Gómez-López, G., Contreras, J., Murillo-Cuesta, S., Rodríguez-Baeza, A., Varela-Nieto, I., Ruberte, J., Collado, M., & Serrano, M. (2013). Programmed Cell Senescence during Mammalian Embryonic Development. *Cell*, *155*(5), 1104–1118. https://doi.org/10.1016/j.cell.2013.10.019

Muñoz-Espín, D., Rovira, M., Galiana, I., Giménez, C., Lozano-Torres, B., Paez-Ribes, M., Llanos, S., Chaib, S., Muñoz-Martín, M., Ucero, A. C., Garaulet, G., Mulero, F., Dann, S. G., VanArsdale, T., Shields, D. J., Bernardos, A., Murguía, J. R., Martínez-Máñez, R., & Serrano, M. (2018). A versatile drug delivery system targeting senescent cells. *EMBO Molecular Medicine*, *10*(9), e9355. https://doi.org/10.15252/emmm.201809355

Muñoz-Espín, D., & Serrano, M. (2014). Cellular senescence: from physiology to pathology. *Nature Reviews Molecular Cell Biology*, *15*(7), 482–496. https://doi.org/10.1038/nrm3823

Nacher, V., Carretero, A., Navarro, M., Armengol, C., Llombart, C., Rodríguez, A., Herrero-Fresneda, I., Ayuso, E., & Ruberte, J. (2006). The Quail Mesonephros: A New Model for Renal Senescence? *Journal of Vascular Research*, *43*(6), 581–586. https://doi.org/10.1159/000096076

Nakae, A., Nakai, K., Yano, K., Hosokawa, K., Shibata, M., & Mashimo, T. (2011). The animal model of spinal cord injury as an experimental pain model. *Journal of Biomedicine & Biotechnology*, *2011*, 939023. https://doi.org/10.1155/2011/939023

Nardone, R., Florea, C., Höller, Y., Brigo, F., Versace, V., Lochner, P., Golaszewski, S., & Trinka, E. (2017). Rodent, large animal and non-human primate models of spinal cord injury. *Zoology*, *123*, 101–114. https://doi.org/https://doi.org/10.1016/j.zool.2017.06.004

Narita, M., Nuñez, S., Heard, E., Narita, M., Lin, A. W., Hearn, S. A., Spector, D. L., Hannon, G. J., & Lowe, S. W. (2003). Rb-Mediated Heterochromatin Formation and Silencing of E2F Target Genes during Cellular Senescence. *Cell*, *113*(6), 703–716. https://doi.org/10.1016/S0092-8674(03)00401-X

Natale, F., Bizzarri, B., Cardi, V., Gaeta, A., Villani, P., Liuzzi, G., & De Curtis, M. (2015). Ganciclovir penetrates into the cerebrospinal fluid of an infant with congenital cytomegalovirus infection. *Italian Journal of Pediatrics*, *41*, 26. https://doi.org/10.1186/s13052-015-0132-8

Neirinckx, V., Coste, C., Franzen, R., Gothot, A., Rogister, B., & Wislet, S. (2014). Neutrophil contribution to spinal cord injury and repair. *Journal of Neuroinflammation*, *11*, 150. https://doi.org/10.1186/s12974-014-0150-2

Nesathurai, S., Graham, W. A., Mansfield, K., Magill, D., Sehgal, P., Westmoreland, S. V, Prusty, S., Rosene, D. L., & Sledge, J. B. (2006). Model of traumatic spinal cord injury in Macaca fascicularis: similarity of experimental lesions created by epidural catheter to human spinal cord injury. *Journal of Medical Primatology*, *35*(6), 401–404. https://doi.org/10.1111/j.1600-0684.2006.00162.x

Nesic, O., Xu, G.-Y., McAdoo, D., Westlund High, K., Hulsebosch, C., & Perez-Polo, R. (2001). IL-1 Receptor Antagonist Prevents Apoptosis and Caspase-3 Activation after Spinal Cord Injury. *Journal of Neurotrauma*, *18*(9), 947–956. https://doi.org/10.1089/089771501750451857

Ness, K. K., Armstrong, G. T., Kundu, M., Wilson, C. L., Tchkonia, T., & Kirkland, J. L. (2015). Frailty in childhood cancer survivors. *Cancer*, *121*(10), 1540–1547. https://doi.org/10.1002/cncr.29211

Noble, B. T., Brennan, F. H., & Popovich, P. G. (2018). The spleen as a neuroimmune interface after spinal cord injury. *Journal of Neuroimmunology*, *321*, 1–11. https://doi.org/https://doi.org/10.1016/j.jneuroim.2018.05.007

Nout, Y. S., Rosenzweig, E. S., Brock, J. H., Strand, S. C., Moseanko, R., Hawbecker, S., Zdunowski, S., Nielson, J. L., Roy, R. R., Courtine, G., Ferguson, A. R., Edgerton, V. R., Beattie, M. S., Bresnahan, J. C., & Tuszynski, M. H. (2012). Animal models of neurologic disorders: a nonhuman primate model of spinal cord injury. *Neurotherapeutics : The Journal of the American Society for Experimental NeuroTherapeutics*, *9*(2), 380–392. https://doi.org/10.1007/s13311-012-0114-0

Nyström, T. (2005). Role of oxidative carbonylation in protein quality control and senescence. *The EMBO Journal*, *24*(7), 1311–1317. https://doi.org/10.1038/sj.emboj.7600599

O'Shea, T. M., Burda, J. E., & Sofroniew, M. V. (2017). Cell biology of spinal cord injury and repair. *The Journal of Clinical Investigation*, *127*(9), 3259–3270. https://doi.org/10.1172/JCI90608

O'Shea, T. M., Wollenberg, A. L., Bernstein, A. M., Sarte, D. B., Deming, T. J., & Sofroniew, M. V. (2017). CHAPTER 19 Smart Materials for Central Nervous System Cell Delivery and Tissue Engineering. In *Smart Materials for Tissue Engineering: Applications* (pp. 529–557). The Royal Society of Chemistry. https://doi.org/10.1039/9781788010542-00529

Ogai, K., Hisano, S., Mawatari, K., Sugitani, K., Koriyama, Y., Nakashima, H., & Kato, S. (2012). Upregulation of anti-apoptotic factors in upper motor neurons after spinal cord injury in adult

zebrafish. *Neurochemistry International*, *61*(7), 1202–1211. https://doi.org/https://doi.org/10.1016/j.neuint.2012.08.015

Ogrodnik, M., Miwa, S., Tchkonia, T., Tiniakos, D., Wilson, C. L., Lahat, A., Day, C. P., Burt, A., Palmer, A., Anstee, Q. M., Grellscheid, S. N., Hoeijmakers, J. H. J., Barnhoorn, S., Mann, D. A., Bird, T. G., Vermeij, W. P., Kirkland, J. L., Passos, J. F., von Zglinicki, T., & Jurk, D. (2017). Cellular senescence drives age-dependent hepatic steatosis. *Nature Communications*, *8*(1), 15691. https://doi.org/10.1038/ncomms15691

Ohtake, Y., & Li, S. (2015). Molecular mechanisms of scar-sourced axon growth inhibitors. *Brain Research*, *1619*, 22–35. https://doi.org/10.1016/j.brainres.2014.08.064

Ohtani, N., Imamura, Y., Yamakoshi, K., Hirota, F., Nakayama, R., Kubo, Y., Ishimaru, N., Takahashi, A., Hirao, A., Shimizu, T., Mann, D. J., Saya, H., Hayashi, Y., Arase, S., Matsumoto, M., Kazuki, N., & Hara, E. (2007). Visualizing the dynamics of p21(Waf1/Cip1) cyclin-dependent kinase inhibitor expression in living animals. *Proceedings of the National Academy of Sciences of the United States of America*, *104*(38), 15034–15039. https://doi.org/10.1073/pnas.0706949104

Ohtani, N., Zebedee, Z., Huot, T. J. G., Stinson, J. A., Sugimoto, M., Ohashi, Y., Sharrocks, A. D., Peters, G., & Hara, E. (2001). Opposing effects of Ets and Id proteins on p16INK4a expression during cellular senescence. *Nature*, *409*(6823), 1067–1070. https://doi.org/10.1038/35059131

Okada, M., Miyamoto, O., Shibuya, S., Zhang, X., Yamamoto, T., & Itano, T. (2007). Expression and role of type I collagen in a rat spinal cord contusion injury model. *Neuroscience Research*, *58*(4), 371–377. https://doi.org/https://doi.org/10.1016/j.neures.2007.04.009

Okada, S., Nakamura, M., Katoh, H., Miyao, T., Shimazaki, T., Ishii, K., Yamane, J., Yoshimura, A., Iwamoto, Y., Toyama, Y., & Okano, H. (2006). Conditional ablation of Stat3 or Socs3 discloses a dual role for reactive astrocytes after spinal cord injury. *Nature Medicine*, *12*(7), 829–834. https://doi.org/10.1038/nm1425

Oyinbo, C. (2011). Secondary injury mechanisms in traumatic spinal cord injury: A nugget of this multiply cascade. *Acta Neurobiologiae Experimentalis*, *71*, 281–299.

Paez-Ribes, M., González-Gualda, E., Doherty, G. J., & Muñoz-Espín, D. (2019). Targeting senescent cells in translational medicine. *EMBO Molecular Medicine*, *11*(12), e10234. https://doi.org/10.15252/emmm.201810234

Pan, H.-C., Lin, J.-F., Ma, L.-P., Shen, Y.-Q., & Schachner, M. (2013). Major vault protein promotes locomotor recovery and regeneration after spinal cord injury in adult zebrafish. *European Journal of Neuroscience*, *37*(2), 203–211. https://doi.org/10.1111/ejn.12038

Park, J. T., Lee, Y.-S., Cho, K. A., & Park, S. C. (2018). Adjustment of the lysosomal-mitochondrial axis for control of cellular senescence. *Ageing Research Reviews*, *47*, 176–182. https://doi.org/https://doi.org/10.1016/j.arr.2018.08.003

Passos, J. F., Nelson, G., Wang, C., Richter, T., Simillion, C., Proctor, C. J., Miwa, S., Olijslagers, S., Hallinan, J., Wipat, A., Saretzki, G., Rudolph, K. L., Kirkwood, T. B. L., & von Zglinicki, T. (2010). Feedback between p21 and reactive oxygen production is necessary for cell senescence. *Molecular Systems Biology*, *6*, 347. https://doi.org/10.1038/msb.2010.5

Passos, J. F., Saretzki, G., Ahmed, S., Nelson, G., Richter, T., Peters, H., Wappler, I., Birket, M. J., Harold, G., Schaeuble, K., Birch-Machin, M. A., Kirkwood, T. B. L., & von Zglinicki, T. (2007). Mitochondrial dysfunction accounts for the stochastic heterogeneity in telomere-dependent senescence. *PLoS Biology*, *5*(5), e110–e110. https://doi.org/10.1371/journal.pbio.0050110

Pasterkamp, R. J., Giger, R. J., Ruitenberg, M.-J., Holtmaat, A. J. G. D., De Wit, J., De Winter, F., &

Verhaagen, J. (1999). Expression of the Gene Encoding the Chemorepellent Semaphorin III Is Induced in the Fibroblast Component of Neural Scar Tissue Formed Following Injuries of Adult But Not Neonatal CNS. *Molecular and Cellular Neuroscience*, *13*(2), 143–166. https://doi.org/https://doi.org/10.1006/mcne.1999.0738

Patel, P. L., Suram, A., Mirani, N., Bischof, O., & Herbig, U. (2016). Derepression of hTERT gene expression promotes escape from oncogene-induced cellular senescence. *Proceedings of the National Academy of Sciences of the United States of America*, *113*(34), E5024–E5033. https://doi.org/10.1073/pnas.1602379113

Pechnick, R., Zonis, S., Wawrowsky, K., Pourmorady, J., & Chesnokova, V. (2008). p21Cip1 restricts neuronal proliferation in the subgranular zone of the dentate gyrus of the hippocampus. *Proceedings of the National Academy of Sciences of the United States of America*, *105*, 1358–1363. https://doi.org/10.1073/pnas.0711030105

Perrott, K. M., Wiley, C. D., Desprez, P.-Y., & Campisi, J. (2017). Apigenin suppresses the senescence-associated secretory phenotype and paracrine effects on breast cancer cells. *GeroScience*, *39*(2), 161–173. https://doi.org/10.1007/s11357-017-9970-1

Perry, V. H., & Teeling, J. (2013). Microglia and macrophages of the central nervous system: the contribution of microglia priming and systemic inflammation to chronic neurodegeneration. *Seminars in Immunopathology*, *35*(5), 601–612. https://doi.org/10.1007/s00281-013-0382-8

Petteys, R., Spitz, S., Syed, H., Rice, R., Sarabia-Estrada, R., Goodwin, C., Sciubba, D., & Freedman, B. (2017). Design and testing of a controlled electromagnetic spinal cord impactor for use in large animal models of acute traumatic spinal cord injury. *Journal of Clinical Neuroscience*, *43*. https://doi.org/10.1016/j.jocn.2017.04.031

Phillips, A. A., Squair, J. W., Sayenko, D. G., Edgerton, V. R., Gerasimenko, Y., & Krassioukov, A. V. (2018). An Autonomic Neuroprosthesis: Noninvasive Electrical Spinal Cord Stimulation Restores Autonomic Cardiovascular Function in Individuals with Spinal Cord Injury. *Journal of Neurotrauma*, *35*(3), 446–451. https://doi.org/10.1089/neu.2017.5082

Pineau, I., Sun, L., Bastien, D., & Lacroix, S. (2010). Astrocytes initiate inflammation in the injured mouse spinal cord by promoting the entry of neutrophils and inflammatory monocytes in an IL-1 receptor/MyD88-dependent fashion. *Brain, Behavior, and Immunity*, *24*(4), 540–553. https://doi.org/https://doi.org/10.1016/j.bbi.2009.11.007

Pitozzi, V., Mocali, A., Laurenzana, A., Giannoni, E., Cifola, I., Battaglia, C., Chiarugi, P., Dolara, P., & Giovannelli, L. (2012). Chronic Resveratrol Treatment Ameliorates Cell Adhesion and Mitigates the Inflammatory Phenotype in Senescent Human Fibroblasts. *The Journals of Gerontology: Series A*, *68*(4), 371–381. https://doi.org/10.1093/gerona/gls183

Pivovarova, N. B., & Andrews, S. B. (2010). Calcium-dependent mitochondrial function and dysfunction in neurons. *The FEBS Journal*, *277*(18), 3622–3636. https://doi.org/10.1111/j.1742-4658.2010.07754.x

Poon, P., Gupta, D., Shoichet, M., & Tator, C. (2007). Clip compression model is useful for thoracic spinal cord injuries - Histologic and functional correlates. *Spine*, *32*, 2853–2859. https://doi.org/10.1097/BRS.0b013e31815b7e6b

Popa, C., Popa, F., Grigorean, V. T., Onose, G., Sandu, A. M., Popescu, M., Burnei, G., Strambu, V., & Sinescu, C. (2010). Vascular dysfunctions following spinal cord injury. *Journal of Medicine and Life*, *3*(3), 275–285. https://www.ncbi.nlm.nih.gov/pubmed/20945818

Popovich, P. G., Guan, Z., Wei, P., Huitinga, I., van Rooijen, N., & Stokes, B. T. (1999). Depletion of Hematogenous Macrophages Promotes Partial Hindlimb Recovery and Neuroanatomical Repair after Experimental Spinal Cord Injury. *Experimental Neurology*, *158*(2), 351–365. https://doi.org/https://doi.org/10.1006/exnr.1999.7118

Popovich, P. G., Wei, P., & Stokes, B. T. (1997). Cellular inflammatory response after spinal cord injury in sprague-dawley and lewis rats. *Journal of Comparative Neurology*, *377*(3), 443–464. https://doi.org/10.1002/(SICI)1096-9861(19970120)377:3<443::AID-CNE10>3.0.CO;2-S

Quadri, S. A., Farooqui, M., Ikram, A., Zafar, A., Khan, M. A., Suriya, S. S., Claus, C. F., Fiani, B., Rahman, M., Ramachandran, A., Armstrong, I. I. T., Taqi, M. A., & Mortazavi, M. M. (2018). Recent update on basic mechanisms of spinal cord injury. *Neurosurgical Review*. https://doi.org/10.1007/s10143-018-1008-3

Quijano, C., Cao, L., Fergusson, M. M., Romero, H., Liu, J., Gutkind, S., Rovira, I. I., Mohney, R. P., Karoly, E. D., & Finkel, T. (2012). Oncogene-induced senescence results in marked metabolic and bioenergetic alterations. *Cell Cycle (Georgetown, Tex.)*, *11*(7), 1383–1392. https://doi.org/10.4161/cc.19800

R., F. A., Sandra, F.-R., Gloria, V., & Carlos, L.-O. (2018). Mouse Models to Disentangle the Hallmarks of Human Aging. *Circulation Research*, *123*(7), 905–924. https://doi.org/10.1161/CIRCRESAHA.118.312204

Radaeva, S., Sun, R., Jaruga, B., Nguyen, V. T., Tian, Z., & Gao, B. (2006). Natural Killer Cells Ameliorate Liver Fibrosis by Killing Activated Stellate Cells in NKG2D-Dependent and Tumor Necrosis Factor–Related Apoptosis-Inducing Ligand–Dependent Manners. *Gastroenterology*, *130*(2), 435–452. https://doi.org/10.1053/j.gastro.2005.10.055

Rai, T. S., & Adams, P. D. (2012). Lessons from senescence: Chromatin maintenance in non-proliferating cells. *Biochimica et Biophysica Acta*, *1819*(3–4), 322–331. https://doi.org/10.1016/j.bbagrm.2011.07.014

Rajagopalan, S., & Long, E. O. (2012). Cellular senescence induced by CD158d reprograms natural killer cells to promote vascular remodeling. *Proceedings of the National Academy of Sciences of the United States of America*, *109*(50), 20596–20601. https://doi.org/10.1073/pnas.1208248109

Ran, C., Hoon, M. A., & Chen, X. (2016). The coding of cutaneous temperature in the spinal cord. *Nature Neuroscience*, *19*(9), 1201–1209. https://doi.org/10.1038/nn.4350

Ray, P., De, A., Min, J.-J., Tsien, R. Y., & Gambhir, S. S. (2004). Imaging tri-fusion multimodality reporter gene expression in living subjects. *Cancer Research*, *64*(4), 1323–1330. https://doi.org/10.1158/0008-5472.can-03-1816

Reimann, M., Lee, S., Loddenkemper, C., Dörr, J. R., Tabor, V., Aichele, P., Stein, H., Dörken, B., Jenuwein, T., & Schmitt, C. A. (2010). Tumor Stroma-Derived TGF-β Limits Myc-Driven Lymphomagenesis via Suv39h1-Dependent Senescence. *Cancer Cell*, *17*(3), 262–272. https://doi.org/10.1016/j.ccr.2009.12.043

Reimer, M. M., Kuscha, V., Wyatt, C., Sörensen, I., Frank, R. E., Knüwer, M., Becker, T., & Becker, C. G. (2009). Sonic hedgehog is a polarized signal for motor neuron regeneration in adult zebrafish. *The Journal of Neuroscience : The Official Journal of the Society for Neuroscience*, *29*(48), 15073–15082. https://doi.org/10.1523/JNEUROSCI.4748-09.2009

Reimer, M. M., Sörensen, I., Kuscha, V., Frank, R. E., Liu, C., Becker, C. G., & Becker, T. (2008). Motor neuron regeneration in adult zebrafish. *The Journal of Neuroscience : The Official Journal of the Society for Neuroscience*, *28*(34), 8510–8516. https://doi.org/10.1523/JNEUROSCI.1189-08.2008

Ren, Y., & Young, W. (2013). Managing inflammation after spinal cord injury through manipulation of macrophage function. *Neural Plasticity*, *2013*, 945034. https://doi.org/10.1155/2013/945034

Rhinn, M., Ritschka, B., & Keyes, W. M. (2019). Cellular senescence in development, regeneration and disease. *Development*, *146*(20), dev151837. https://doi.org/10.1242/dev.151837

Ribeiro, A., Monteiro, J. F., Certal, A. C., Cristovão, A. M., & Saúde, L. (2017). Foxj1a is expressed

in ependymal precursors, controls central canal position and is activated in new ependymal cells during regeneration in zebrafish. *Open Biology*, *7*(11), 170139. https://doi.org/10.1098/rsob.170139

Richter, T., & Zglinicki, T. von. (2007). A continuous correlation between oxidative stress and telomere shortening in fibroblasts. *Experimental Gerontology*, *42*(11), 1039–1042. https://doi.org/https://doi.org/10.1016/j.exger.2007.08.005

Ridker, P. M., MacFadyen, J. G., Thuren, T., Everett, B. M., Libby, P., Glynn, R. J., Ridker, P., Lorenzatti, A., Krum, H., Varigos, J., Siostrzonek, P., Sinnaeve, P., Fonseca, F., Nicolau, J., Gotcheva, N., Genest, J., Yong, H., Urina-Triana, M., Milicic, D., … Glynn, R. J. (2017). Effect of interleukin-1β inhibition with canakinumab on incident lung cancer in patients with atherosclerosis: exploratory results from a randomised, double-blind, placebo-controlled trial. *The Lancet*, *390*(10105), 1833–1842. https://doi.org/10.1016/S0140-6736(17)32247-X

Ritschka, B., Storer, M., Mas, A., Heinzmann, F., Ortells, M. C., Morton, J. P., Sansom, O. J., Zender, L., & Keyes, W. M. (2017). The senescence-associated secretory phenotype induces cellular plasticity and tissue regeneration. *Genes & Development*, *31*(2), 172–183. https://doi.org/10.1101/gad.290635.116

Robinson, A. R., Yousefzadeh, M. J., Rozgaja, T. A., Wang, J., Li, X., Tilstra, J. S., Feldman, C. H., Gregg, S. Q., Johnson, C. H., Skoda, E. M., Frantz, M.-C., Bell-Temin, H., Pope-Varsalona, H., Gurkar, A. U., Nasto, L. A., Robinson, R. A. S., Fuhrmann-Stroissnigg, H., Czerwinska, J., McGowan, S. J., … Niedernhofer, L. J. (2018). Spontaneous DNA damage to the nuclear genome promotes senescence, redox imbalance and aging. *Redox Biology*, *17*, 259–273. https://doi.org/10.1016/j.redox.2018.04.007

Robles, S. J., & Adami, G. R. (1998). Agents that cause DNA double strand breaks lead to p16INK4a enrichment and the premature senescence of normal fibroblasts. *Oncogene*, *16*(9), 1113–1123. https://doi.org/10.1038/sj.onc.1201862

Rodier, F., & Campisi, J. (2011). Four faces of cellular senescence. *The Journal of Cell Biology*, *192*(4), 547–556. https://doi.org/10.1083/jcb.201009094

Rodier, F., Muñoz, D. P., Teachenor, R., Chu, V., Le, O., Bhaumik, D., Coppé, J.-P., Campeau, E., Beauséjour, C. M., Kim, S.-H., Davalos, A. R., & Campisi, J. (2011). DNA-SCARS: distinct nuclear structures that sustain damage-induced senescence growth arrest and inflammatory cytokine secretion. *Journal of Cell Science*, *124*(Pt 1), 68–81. https://doi.org/10.1242/jcs.071340

Roos, C. M., Zhang, B., Palmer, A. K., Ogrodnik, M. B., Pirtskhalava, T., Thalji, N. M., Hagler, M., Jurk, D., Smith, L. A., Casaclang-Verzosa, G., Zhu, Y., Schafer, M. J., Tchkonia, T., Kirkland, J. L., & Miller, J. D. (2016). Chronic senolytic treatment alleviates established vasomotor dysfunction in aged or atherosclerotic mice. *Aging Cell*, *15*(5), 973–977. https://doi.org/10.1111/acel.12458

Rosenzweig, E. S., Courtine, G., Jindrich, D. L., Brock, J. H., Ferguson, A. R., Strand, S. C., Nout, Y. S., Roy, R. R., Miller, D. M., Beattie, M. S., Havton, L. A., Bresnahan, J. C., Edgerton, V. R., & Tuszynski, M. H. (2010). Extensive spontaneous plasticity of corticospinal projections after primate spinal cord injury. *Nature Neuroscience*, *13*(12), 1505–1510. https://doi.org/10.1038/nn.2691

Rosenzweig, E. S., Salegio, E. A., Liang, J. J., Weber, J. L., Weinholtz, C. A., Brock, J. H., Moseanko, R., Hawbecker, S., Pender, R., Cruzen, C. L., Iaci, J. F., Caggiano, A. O., Blight, A. R., Haenzi, B., Huie, J. R., Havton, L. A., Nout-Lomas, Y. S., Fawcett, J. W., Ferguson, A. R., … Tuszynski, M. H. (2019). Chondroitinase improves anatomical and functional outcomes after primate spinal cord injury. *Nature Neuroscience*, *22*(8), 1269–1275. https://doi.org/10.1038/s41593-019-0424-1

Rudin, C. M., Hann, C. L., Garon, E. B., Ribeiro de Oliveira, M., Bonomi, P. D., Camidge, D. R.,

Chu, Q., Giaccone, G., Khaira, D., Ramalingam, S. S., Ranson, M. R., Dive, C., McKeegan, E. M., Chyla, B. J., Dowell, B. L., Chakravartty, A., Nolan, C. E., Rudersdorf, N., Busman, T. A., … Gandhi, L. (2012). Phase II study of single-agent navitoclax (ABT-263) and biomarker correlates in patients with relapsed small cell lung cancer. *Clinical Cancer Research : An Official Journal of the American Association for Cancer Research*, *18*(11), 3163–3169. https://doi.org/10.1158/1078-0432.CCR-11-3090

Sagiv, A., Biran, A., Yon, M., Simon, J., Lowe, S. W., & Krizhanovsky, V. (2013). Granule exocytosis mediates immune surveillance of senescent cells. *Oncogene*, *32*(15), 1971–1977. https://doi.org/10.1038/onc.2012.206

Saha, R. N., Jana, M., & Pahan, K. (2007). MAPK p38 regulates transcriptional activity of NF-kappaB in primary human astrocytes via acetylation of p65. *Journal of Immunology (Baltimore, Md. : 1950)*, *179*(10), 7101–7109. https://doi.org/10.4049/jimmunol.179.10.7101

Salama, R., Sadaie, M., Hoare, M., & Narita, M. (2014). Cellular senescence and its effector programs. *Genes & Development*, *28*(2), 99–114. https://doi.org/10.1101/gad.235184.113

Saleh, T., Tyutyunyk-Massey, L., & Gewirtz, D. A. (2019). Tumor Cell Escape from Therapy-Induced Senescence as a Model of Disease Recurrence after Dormancy. *Cancer Research*, *79*(6), 1044 LP – 1046. https://doi.org/10.1158/0008-5472.CAN-18-3437

Samaraweera, L., Adomako, A., Rodriguez-Gabin, A., & McDaid, H. M. (2017). A Novel Indication for Panobinostat as a Senolytic Drug in NSCLC and HNSCC. *Scientific Reports*, *7*(1), 1900. https://doi.org/10.1038/s41598-017-01964-1

Sarig, R., Rimmer, R., Bassat, E., Zhang, L., Kfir, U. B., Lendengolts, D., Perlmoter, G., Yaniv, K., & Tzahor, E. (2019). Transient p53-Mediated Regenerative Senescence in the Injured Heart. *Circulation*, *139*(21), 2491–2494. https://doi.org/10.1161/CIRCULATIONAHA.119.040125

Sauerbeck, A. D., Laws, J. L., Bandaru, V. V. R., Popovich, P. G., Haughey, N. J., & McTigue, D. M. (2015). Spinal cord injury causes chronic liver pathology in rats. *Journal of Neurotrauma*, *32*(3), 159–169. https://doi.org/10.1089/neu.2014.3497

Schachtrup, C., Ryu, J. K., Helmrick, M. J., Vagena, E., Galanakis, D. K., Degen, J. L., Margolis, R. U., & Akassoglou, K. (2010). Fibrinogen triggers astrocyte scar formation by promoting the availability of active TGF-beta after vascular damage. *The Journal of Neuroscience : The Official Journal of the Society for Neuroscience*, *30*(17), 5843–5854. https://doi.org/10.1523/JNEUROSCI.0137-10.2010

Schafer, M. J., White, T. A., Iijima, K., Haak, A. J., Ligresti, G., Atkinson, E. J., Oberg, A. L., Birch, J., Salmonowicz, H., Zhu, Y., Mazula, D. L., Brooks, R. W., Fuhrmann-Stroissnigg, H., Pirtskhalava, T., Prakash, Y. S., Tchkonia, T., Robbins, P. D., Aubry, M. C., Passos, J. F., … LeBrasseur, N. K. (2017). Cellular senescence mediates fibrotic pulmonary disease. *Nature Communications*, *8*(1), 14532. https://doi.org/10.1038/ncomms14532

Scheff, S. W., Rabchevsky, A. G., Fugaccia, I., Main, J. A., & Lumpp, J. E. (2003). Experimental Modeling of Spinal Cord Injury: Characterization of a Force-Defined Injury Device. *Journal of Neurotrauma*, *20*(2), 179–193. https://doi.org/10.1089/08977150360547099

Schindelin, J., Arganda-Carreras, I., Frise, E., Kaynig, V., Longair, M., Pietzsch, T., Preibisch, S., Rueden, C., Saalfeld, S., Schmid, B., Tinevez, J.-Y., White, D. J., Hartenstein, V., Eliceiri, K., Tomancak, P., & Cardona, A. (2012). Fiji: an open-source platform for biological-image analysis. *Nature Methods*, *9*(7), 676–682. https://doi.org/10.1038/nmeth.2019

Schmitt, C. A., Fridman, J. S., Yang, M., Lee, S., Baranov, E., Hoffman, R. M., & Lowe, S. W. (2002). A Senescence Program Controlled by p53 and $p16^{INK4a}$ Contributes to the Outcome of Cancer Therapy. *Cell*, *109*(3), 335–346. https://doi.org/10.1016/S0092-8674(02)00734-1

Schwab, J. M., Conrad, S., Monnier, P. P., Julien, S., Mueller, B. K., & Schluesener, H. J. (2005). Spinal cord injury-induced lesional expression of the repulsive guidance molecule (RGM). *European Journal of Neuroscience*, *21*(6), 1569–1576. https://doi.org/10.1111/j.1460-9568.2005.03962.x

Schwab, M. E., & Strittmatter, S. M. (2014). Nogo limits neural plasticity and recovery from injury. *Current Opinion in Neurobiology*, *27*, 53–60. https://doi.org/10.1016/j.conb.2014.02.011

Schweitzer, J., Gimnopoulos, D., Lieberoth, B. C., Pogoda, H.-M., Feldner, J., Ebert, A., Schachner, M., Becker, T., & Becker, C. G. (2007). Contactin1a expression is associated with oligodendrocyte differentiation and axonal regeneration in the central nervous system of zebrafish. *Molecular and Cellular Neuroscience*, *35*(2), 194–207. https://doi.org/https://doi.org/10.1016/j.mcn.2007.02.018

Serrano, M., Lin, A. W., McCurrach, M. E., Beach, D., & Lowe, S. W. (1997). Oncogenic ras Provokes Premature Cell Senescence Associated with Accumulation of p53 and $p16^{INK4a}$. *Cell*, *88*(5), 593–602. https://doi.org/10.1016/S0092-8674(00)81902-9

Shah, P. P., Donahue, G., Otte, G. L., Capell, B. C., Nelson, D. M., Cao, K., Aggarwala, V., Cruickshanks, H. A., Rai, T. S., McBryan, T., Gregory, B. D., Adams, P. D., & Berger, S. L. (2013). Lamin B1 depletion in senescent cells triggers large-scale changes in gene expression and the chromatin landscape. *Genes & Development*, *27*(16), 1787–1799. https://doi.org/10.1101/gad.223834.113

Shah, P. T., Stratton, J. A., Stykel, M. G., Abbasi, S., Sharma, S., Mayr, K. A., Koblinger, K., Whelan, P. J., & Biernaskie, J. (2018). Single-Cell Transcriptomics and Fate Mapping of Ependymal Cells Reveals an Absence of Neural Stem Cell Function. *Cell*, *173*(4), 1045-1057.e9. https://doi.org/10.1016/j.cell.2018.03.063

Sharpless, N. E. (2005). INK4a/ARF: a multifunctional tumor suppressor locus. *Mutation Research*, *576*(1–2), 22–38. https://doi.org/10.1016/j.mrfmmm.2004.08.021

Sharpless, N. E., & Sherr, C. J. (2015). Forging a signature of in vivo senescence. *Nature Reviews Cancer*, *15*(7), 397–408. https://doi.org/10.1038/nrc3960

Shim, J., Choi, J.-H., Park, M.-H., Kim, H., Kim, J. H., Kim, S.-Y., Hong, D., Kim, S., Lee, J. E., Kim, C.-H., Lee, J.-S., & Bae, Y.-K. (2017). Development of zebrafish medulloblastoma-like PNET model by TALEN-mediated somatic gene inactivation. *Oncotarget*, *8*(33), 55280–55297. https://doi.org/10.18632/oncotarget.19424

Shimi, T., Butin-Israeli, V., Adam, S. A., Hamanaka, R. B., Goldman, A. E., Lucas, C. A., Shumaker, D. K., Kosak, S. T., Chandel, N. S., & Goldman, R. D. (2011). The role of nuclear lamin B1 in cell proliferation and senescence. *Genes & Development*, *25*(24), 2579–2593. https://doi.org/10.1101/gad.179515.111

Shtutman, M., Chang, B.-D., Schools, G. P., & Broude, E. V. (2017). Cellular Model of p21-Induced Senescence. *Methods in Molecular Biology (Clifton, N.J.)*, *1534*, 31–39. https://doi.org/10.1007/978-1-4939-6670-7_3

Siddiqui, A. M., Khazaei, M., & Fehlings, M. G. (2015). Chapter 2 - Translating mechanisms of neuroprotection, regeneration, and repair to treatment of spinal cord injury. In N. Dancause, S. Nadeau, & S. B. T.-P. in B. R. Rossignol (Eds.), *Sensorimotor Rehabilitation* (Vol. 218, pp. 15–54). Elsevier. https://doi.org/https://doi.org/10.1016/bs.pbr.2014.12.007

Sinnett-Smith, J., Kisfalvi, K., Kui, R., & Rozengurt, E. (2013). Metformin inhibition of mTORC1 activation, DNA synthesis and proliferation in pancreatic cancer cells: dependence on glucose concentration and role of AMPK. *Biochemical and Biophysical Research Communications*, *430*(1), 352–357. https://doi.org/10.1016/j.bbrc.2012.11.010

Soderblom, C., Luo, X., Blumenthal, E., Bray, E., Lyapichev, K., Ramos, J., Krishnan, V., Lai-Hsu, C., Park, K. K., Tsoulfas, P., & Lee, J. K. (2013). Perivascular Fibroblasts Form the Fibrotic Scar after Contusive Spinal Cord Injury. *The Journal of Neuroscience*, *33*(34), 13882 LP – 13887. https://doi.org/10.1523/JNEUROSCI.2524-13.2013

Sofroniew, M. V. (2014). Astrogliosis. *Cold Spring Harbor Perspectives in Biology*, *7*(2), a020420–a020420. https://doi.org/10.1101/cshperspect.a020420

Sofroniew, M. V. (2015). Astrocyte barriers to neurotoxic inflammation. *Nature Reviews. Neuroscience*, *16*(5), 249–263. https://doi.org/10.1038/nrn3898

Sousa-Victor, P., Gutarra, S., García-Prat, L., Rodriguez-Ubreva, J., Ortet, L., Ruiz-Bonilla, V., Jardí, M., Ballestar, E., González, S., Serrano, A. L., Perdiguero, E., & Muñoz-Cánoves, P. (2014). Geriatric muscle stem cells switch reversible quiescence into senescence. *Nature*, *506*(7488), 316–321. https://doi.org/10.1038/nature13013

Sroga, J. M., Jones, T. B., Kigerl, K. A., McGaughy, V. M., & Popovich, P. G. (2003). Rats and mice exhibit distinct inflammatory reactions after spinal cord injury. *Journal of Comparative Neurology*, *462*(2), 223–240. https://doi.org/10.1002/cne.10736

Starkov, A. A., Chinopoulos, C., & Fiskum, G. (2004). Mitochondrial calcium and oxidative stress as mediators of ischemic brain injury. *Cell Calcium*, *36*(3), 257–264. https://doi.org/https://doi.org/10.1016/j.ceca.2004.02.012

Stein, G. H., Drullinger, L. F., Soulard, A., & Dulić, V. (1999). Differential roles for cyclin-dependent kinase inhibitors p21 and p16 in the mechanisms of senescence and differentiation in human fibroblasts. *Molecular and Cellular Biology*, *19*(3), 2109–2117. https://doi.org/10.1128/mcb.19.3.2109

Stirling, D. P., Liu, S., Kubes, P., & Yong, V. W. (2009). Depletion of Ly6G/Gr-1 leukocytes after spinal cord injury in mice alters wound healing and worsens neurological outcome. *The Journal of Neuroscience : The Official Journal of the Society for Neuroscience*, *29*(3), 753–764. https://doi.org/10.1523/JNEUROSCI.4918-08.2009

Storer, M., Mas, A., Robert-Moreno, A., Pecoraro, M., Ortells, M. C., Di Giacomo, V., Yosef, R., Pilpel, N., Krizhanovsky, V., Sharpe, J., & Keyes, W. M. (2013). Senescence Is a Developmental Mechanism that Contributes to Embryonic Growth and Patterning. *Cell*, *155*(5), 1119–1130. https://doi.org/10.1016/j.cell.2013.10.041

Strand, N., Hoi, K., Phan, T., Ray, C., Berndt, J., & Moon, R. (2016). Wnt/β-catenin signaling promotes regeneration after adult zebrafish Spinal Cord injury. *Biochemical and Biophysical Research Communications*, *477*. https://doi.org/10.1016/j.bbrc.2016.07.006

Streeter, K. A., Sunshine, M. D., Brant, J. O., Sandoval, M. A. G. W., Maden, M., & Fuller, D. D. (2019). Molecular and histologic outcomes following spinal cord injury in spiny mice, Acomys cahirinus *BioRxiv*, 793133. https://doi.org/10.1101/793133

Stys, P. K., Waxman, S. G., & Ransom, B. R. (1992). Ionic mechanisms of anoxic injury in mammalian CNS white matter: role of Na+ channels and Na(+)-Ca2+ exchanger. *The Journal of Neuroscience : The Official Journal of the Society for Neuroscience*, *12*(2), 430–439. https://doi.org/10.1523/JNEUROSCI.12-02-00430.1992

Sun, N., Grzybicki, D., Castro, R. F., Murphy, S., & Perlman, S. (1995). Activation of Astrocytes in the Spinal Cord of Mice Chronically Infected with a Neurotropic Coronavirus. *Virology*, *213*(2), 482–493. https://doi.org/https://doi.org/10.1006/viro.1995.0021

Suwanwela, C., Alexander, E., & Davis, C. H. (1962). Prognosis in Spinal Cord Injury, with Special Reference to Patients with Motor Paralysis and Sensory Preservation. *Journal of Neurosurgery*, *19*(3), 220–227. https://doi.org/10.3171/jns.1962.19.3.0220

Takahashi, A., Ohtani, N., Yamakoshi, K., Iida, S., Tahara, H., Nakayama, K., Nakayama, K. I., Ide, T., Saya, H., & Hara, E. (2006). Mitogenic signalling and the p16INK4a–Rb pathway cooperate to enforce irreversible cellular senescence. *Nature Cell Biology*, *8*(11), 1291–1297. https://doi.org/10.1038/ncb1491

Takahashi, K., Tanabe, K., Ohnuki, M., Narita, M., Ichisaka, T., Tomoda, K., & Yamanaka, S. (2007). Induction of Pluripotent Stem Cells from Adult Human Fibroblasts by Defined Factors. *Cell*, *131*(5), 861–872. https://doi.org/10.1016/j.cell.2007.11.019

Takahashi, K., & Yamanaka, S. (2006). Induction of Pluripotent Stem Cells from Mouse Embryonic and Adult Fibroblast Cultures by Defined Factors. *Cell*, *126*(4), 663–676. https://doi.org/10.1016/j.cell.2006.07.024

Tanaka, H. V., Ng, N. C. Y., Yang Yu, Z., Casco-Robles, M. M., Maruo, F., Tsonis, P. A., & Chiba, C. (2016). A developmentally regulated switch from stem cells to dedifferentiation for limb muscle regeneration in newts. *Nature Communications*, *7*(1), 11069. https://doi.org/10.1038/ncomms11069

Taoka, Y., Okajima, K., Uchiba, M., Murakami, K., Kushimoto, S., Johno, M., Naruo, M., Okabe, H., & Takatsuki, K. (1997). Role of neutrophils in spinal cord injury in the rat. *Neuroscience*, *79*(4), 1177–1182. https://doi.org/https://doi.org/10.1016/S0306-4522(97)00011-0

Tator, C. H., & Fehlings, M. G. (1991). Review of the secondary injury theory of acute spinal cord trauma with emphasis on vascular mechanisms. *Journal of Neurosurgery*, *75*(1), 15–26. https://doi.org/10.3171/jns.1991.75.1.0015

Tazaki, A., Tanaka, E. M., & Fei, J.-F. (2017). Salamander spinal cord regeneration: The ultimate positive control in vertebrate spinal cord regeneration. *Developmental Biology*, *432*(1), 63–71. https://doi.org/https://doi.org/10.1016/j.ydbio.2017.09.034

Thapa, R. K., Nguyen, H. T., Jeong, J.-H., Kim, J. R., Choi, H.-G., Yong, C. S., & Kim, J. O. (2017). Progressive slowdown/prevention of cellular senescence by CD9-targeted delivery of rapamycin using lactose-wrapped calcium carbonate nanoparticles. *Scientific Reports*, *7*, 43299. https://doi.org/10.1038/srep43299

Toso, A., Revandkar, A., Di Mitri, D., Guccini, I., Proietti, M., Sarti, M., Pinton, S., Zhang, J., Kalathur, M., Civenni, G., Jarrossay, D., Montani, E., Marini, C., Garcia-Escudero, R., Scanziani, E., Grassi, F., Pandolfi, P. P., Catapano, C. V., & Alimonti, A. (2014). Enhancing Chemotherapy Efficacy in Pten-Deficient Prostate Tumors by Activating the Senescence-Associated Antitumor Immunity. *Cell Reports*, *9*(1), 75–89. https://doi.org/10.1016/j.celrep.2014.08.044

Totoiu, M. O., & Keirstead, H. S. (2005). Spinal cord injury is accompanied by chronic progressive demyelination. *Journal of Comparative Neurology*, *486*(4), 373–383. https://doi.org/10.1002/cne.20517

Tran, A. P., Sundar, S., Yu, M., Lang, B. T., & Silver, J. (2018). Modulation of Receptor Protein Tyrosine Phosphatase Sigma Increases Chondroitin Sulfate Proteoglycan Degradation through Cathepsin B Secretion to Enhance Axon Outgrowth. *The Journal of Neuroscience : The Official Journal of the Society for Neuroscience*, *38*(23), 5399–5414. https://doi.org/10.1523/JNEUROSCI.3214-17.2018

Triana-Martínez, F., Picallos-Rabina, P., Da Silva-Álvarez, S., Pietrocola, F., Llanos, S., Rodilla, V., Soprano, E., Pedrosa, P., Ferreirós, A., Barradas, M., Hernández-González, F., Lalinde, M., Prats, N., Bernadó, C., González, P., Gómez, M., Ikonomopoulou, M. P., Fernández-Marcos, P. J., García-Caballero, T., … Collado, M. (2019). Identification and characterization of Cardiac Glycosides as senolytic compounds. *Nature Communications*, *10*(1), 4731. https://doi.org/10.1038/s41467-019-12888-x

Tsarouchas, T. M., Wehner, D., Cavone, L., Munir, T., Keatinge, M., Lambertus, M., Underhill, A., Barrett, T., Kassapis, E., Ogryzko, N., Feng, Y., van Ham, T. J., Becker, T., & Becker, C. G. (2018). Dynamic control of proinflammatory cytokines Il-1β and Tnf-α by macrophages in zebrafish spinal cord regeneration. *Nature Communications*, *9*(1), 4670. https://doi.org/10.1038/s41467-018-07036-w

Vajn, K., Plunkett, J. A., Tapanes-Castillo, A., & Oudega, M. (2013). Axonal regeneration after spinal cord injury in zebrafish and mammals: differences, similarities, translation. *Neuroscience Bulletin*, *29*(4), 402–410. https://doi.org/10.1007/s12264-013-1361-8

van Deursen, J. M. (2014). The role of senescent cells in ageing. *Nature*, *509*(7501), 439–446. https://doi.org/10.1038/nature13193

Vicente, R., Mausset-Bonnefont, A.-L., Jorgensen, C., Louis-Plence, P., & Brondello, J.-M. (2016). Cellular senescence impact on immune cell fate and function. *Aging Cell*, *15*(3), 400–406. https://doi.org/10.1111/acel.12455

Villiard, É., Denis, J.-F., Hashemi, F. S., Igelmann, S., Ferbeyre, G., & Roy, S. (2017). Senescence gives insights into the morphogenetic evolution of anamniotes. *Biology Open*, *6*(6), 891 LP – 896. https://doi.org/10.1242/bio.025809

Vogler, M., Dickens, D., Dyer, M. J. S., Owen, A., Pirmohamed, M., & Cohen, G. M. (2011). The B-cell lymphoma 2 (BCL2)-inhibitors, ABT-737 and ABT-263, are substrates for P-glycoprotein. *Biochemical and Biophysical Research Communications*, *408*(2), 344–349. https://doi.org/https://doi.org/10.1016/j.bbrc.2011.04.043

Wada, S., Yone, K., Ishidou, Y., Nagamine, T., Nakahara, S., Niiyama, T., & Sakou, T. (1999). Apoptosis following spinal cord injury in rats and preventative effect of N-methyl-d-aspartate receptor antagonist. *Journal of Neurosurgery: Spine*, *91*(1), 98–104. https://doi.org/10.3171/spi.1999.91.1.0098

Wajapeyee, N., Serra, R. W., Zhu, X., Mahalingam, M., & Green, M. R. (2008). Oncogenic BRAF induces senescence and apoptosis through pathways mediated by the secreted protein IGFBP7. *Cell*, *132*(3), 363–374. https://doi.org/10.1016/j.cell.2007.12.032

Wang, C., Jurk, D., Maddick, M., Nelson, G., Martin-Ruiz, C., & Von Zglinicki, T. (2009). DNA damage response and cellular senescence in tissues of aging mice. *Aging Cell*, *8*(3), 311–323. https://doi.org/10.1111/j.1474-9726.2009.00481.x

Wang, E. (1995). Senescent Human Fibroblasts Resist Programmed Cell Death, and Failure to Suppress bcl2 Is Involved. *Cancer Research*, *55*(11), 2284 LP – 2292. http://cancerres.aacrjournals.org/content/55/11/2284.abstract

Wang, R., Yu, Z., Sunchu, B., Shoaf, J., Dang, I., Zhao, S., Caples, K., Bradley, L., Beaver, L. M., Ho, E., Löhr, C. V, & Perez, V. I. (2017). Rapamycin inhibits the secretory phenotype of senescent cells by a Nrf2-independent mechanism. *Aging Cell*, *16*(3), 564–574. https://doi.org/10.1111/acel.12587

Wang, Ying, Liu, J., Ma, X., Cui, C., Deenik, P. R., Henderson, P. K. P., Sigler, A. L., & Cui, L. (2019). Real-time imaging of senescence in tumors with DNA damage. *Scientific Reports*, *9*(1), 2102. https://doi.org/10.1038/s41598-019-38511-z

Wang, Yingying, Chang, J., Liu, X., Zhang, X., Zhang, S., Zhang, X., Zhou, D., & Zheng, G. (2016). Discovery of piperlongumine as a potential novel lead for the development of senolytic agents. *Aging*, *8*(11), 2915–2926. https://doi.org/10.18632/aging.101100

Wanner, I. B., Anderson, M. A., Song, B., Levine, J., Fernandez, A., Gray-Thompson, Z., Ao, Y., & Sofroniew, M. V. (2013). Glial scar borders are formed by newly proliferated, elongated astrocytes that interact to corral inflammatory and fibrotic cells via STAT3-dependent

mechanisms after spinal cord injury. *The Journal of Neuroscience : The Official Journal of the Society for Neuroscience*, *33*(31), 12870–12886. https://doi.org/10.1523/JNEUROSCI.2121-13.2013

Watson, J. L., Hala, T. J., Putatunda, R., Sannie, D., & Lepore, A. C. (2014). Persistent At-Level Thermal Hyperalgesia and Tactile Allodynia Accompany Chronic Neuronal and Astrocyte Activation in Superficial Dorsal Horn following Mouse Cervical Contusion Spinal Cord Injury. *PLOS ONE*, *9*(9), e109099.

Whetstone, W. D., Hsu, J.-Y. C., Eisenberg, M., Werb, Z., & Noble-Haeusslein, L. J. (2003). Blood-spinal cord barrier after spinal cord injury: Relation to revascularization and wound healing. *Journal of Neuroscience Research*, *74*(2), 227–239. https://doi.org/10.1002/jnr.10759

Wiese, S., Karus, M., & Faissner, A. (2012). Astrocytes as a source for extracellular matrix molecules and cytokines. *Frontiers in Pharmacology*, *3*, 120. https://doi.org/10.3389/fphar.2012.00120

Wiley, C. D., Schaum, N., Alimirah, F., Lopez-Dominguez, J. A., Orjalo, A. V, Scott, G., Desprez, P.-Y., Benz, C., Davalos, A. R., & Campisi, J. (2018). Small-molecule MDM2 antagonists attenuate the senescence-associated secretory phenotype. *Scientific Reports*, *8*(1), 2410. https://doi.org/10.1038/s41598-018-20000-4

Wiley, C. D., Velarde, M. C., Lecot, P., Liu, S., Sarnoski, E. A., Freund, A., Shirakawa, K., Lim, H. W., Davis, S. S., Ramanathan, A., Gerencser, A. A., Verdin, E., & Campisi, J. (2016). Mitochondrial Dysfunction Induces Senescence with a Distinct Secretory Phenotype. *Cell Metabolism*, *23*(2), 303–314. https://doi.org/10.1016/j.cmet.2015.11.011

Wilson, J. R., Cadotte, D. W., & Fehlings, M. G. (2012). Clinical predictors of neurological outcome, functional status, and survival after traumatic spinal cord injury: a systematic review. *Journal of Neurosurgery: Spine SPI*, *17*(Suppl1), 11–26. https://doi.org/10.3171/2012.4.AOSPINE1245

Wilson, J. R., Hashimoto, R. E., Dettori, J. R., & Fehlings, M. G. (2011). Spinal cord injury and quality of life: a systematic review of outcome measures. *Evidence-Based Spine-Care Journal*, *2*(1), 37–44. https://doi.org/10.1055/s-0030-1267085

Wolman, L. (1965). The disturbance of circulation in traumatic paraplegia in acute and late stages: A pathological study. *Spinal Cord*, *2*(4), 213–226. https://doi.org/10.1038/sc.1964.39

Wu, J.-C., Huang, W.-C., Chen, Y.-C., Tu, T.-H., Tsai, Y.-A., Huang, S.-F., Huang, H.-C., & Cheng, H. (2011). Acidic fibroblast growth factor for repair of human spinal cord injury: a clinical trial. *Journal of Neurosurgery: Spine SPI*, *15*(3), 216–227. https://doi.org/10.3171/2011.4.SPINE10404

Xu, G.-Y., Liu, S., Hughes, M. G., & McAdoo, D. J. (2008). Glutamate-induced losses of oligodendrocytes and neurons and activation of caspase-3 in the rat spinal cord. *Neuroscience*, *153*(4), 1034–1047. https://doi.org/10.1016/j.neuroscience.2008.02.065

Xu, M., Tchkonia, T., Ding, H., Ogrodnik, M., Lubbers, E. R., Pirtskhalava, T., White, T. A., Johnson, K. O., Stout, M. B., Mezera, V., Giorgadze, N., Jensen, M. D., LeBrasseur, N. K., & Kirkland, J. L. (2015). JAK inhibition alleviates the cellular senescence-associated secretory phenotype and frailty in old age. *Proceedings of the National Academy of Sciences of the United States of America*, *112*(46), E6301–E6310. https://doi.org/10.1073/pnas.1515386112

Xu, M., Tchkonia, T., & Kirkland, J. L. (2016). Perspective: Targeting the JAK/STAT pathway to fight age-related dysfunction. *Pharmacological Research*, *111*, 152–154. https://doi.org/10.1016/j.phrs.2016.05.015

Xu, S., Wu, W., Huang, H., Huang, R., Xie, L., Su, A., Liu, S., Zheng, R., Yuan, Y., Zheng, H.-L., Sun, X., Xiong, X.-D., & Liu, X. (2019). The p53/miRNAs/Ccna2 pathway serves as a novel regulator of cellular senescence: Complement of the canonical p53/p21 pathway. *Aging Cell*,

18(3), e12918–e12918. https://doi.org/10.1111/acel.12918

Yalcin, I., Charlet, A., Freund-Mercier, M.-J., Barrot, M., & Poisbeau, P. (2009). Differentiating Thermal Allodynia and Hyperalgesia Using Dynamic Hot and Cold Plate in Rodents. *The Journal of Pain*, *10*(7), 767–773. https://doi.org/https://doi.org/10.1016/j.jpain.2009.01.325

Yamaguchi, R., & Perkins, G. (2012). Finding a Panacea among combination cancer therapies. *Cancer Research*, *72*(1), 18–23. https://doi.org/10.1158/0008-5472.CAN-11-3091

Yang, H., & Fogo, A. B. (2010). Cell Senescence in the Aging Kidney. *Journal of the American Society of Nephrology*, *21*(9), 1436 LP – 1439. https://doi.org/10.1681/ASN.2010020205

Yokota, K., Kobayakawa, K., Saito, T., Hara, M., Kijima, K., Ohkawa, Y., Harada, A., Okazaki, K., Ishihara, K., Yoshida, S., Kudo, A., Iwamoto, Y., & Okada, S. (2017). Periostin Promotes Scar Formation through the Interaction between Pericytes and Infiltrating Monocytes/Macrophages after Spinal Cord Injury. *The American Journal of Pathology*, *187*(3), 639–653. https://doi.org/10.1016/j.ajpath.2016.11.010

Yosef, R., Pilpel, N., Tokarsky-Amiel, R., Biran, A., Ovadya, Y., Cohen, S., Vadai, E., Dassa, L., Shahar, E., Condiotti, R., Ben-Porath, I., & Krizhanovsky, V. (2016). Directed elimination of senescent cells by inhibition of BCL-W and BCL-XL. *Nature Communications*, *7*, 11190. https://doi.org/10.1038/ncomms11190

Yoshimura, N. (1999). Bladder afferent pathway and spinal cord injury: possible mechanisms inducing hyperreflexia of the urinary bladder. *Progress in Neurobiology*, *57*(6), 583–606. https://doi.org/https://doi.org/10.1016/S0301-0082(98)00070-7

Young, A. R. J., Narita, M., Ferreira, M., Kirschner, K., Sadaie, M., Darot, J. F. J., Tavaré, S., Arakawa, S., Shimizu, S., Watt, F. M., & Narita, M. (2009). Autophagy mediates the mitotic senescence transition. *Genes & Development*, *23*(7), 798–803. https://doi.org/10.1101/gad.519709

Yousefzadeh, M. J., Zhu, Y., McGowan, S. J., Angelini, L., Fuhrmann-Stroissnigg, H., Xu, M., Ling, Y. Y., Melos, K. I., Pirtskhalava, T., Inman, C. L., McGuckian, C., Wade, E. A., Kato, J. I., Grassi, D., Wentworth, M., Burd, C. E., Arriaga, E. A., Ladiges, W. L., Tchkonia, T., … Niedernhofer, L. J. (2018). Fisetin is a senotherapeutic that extends health and lifespan. *EBioMedicine*, *36*, 18–28. https://doi.org/10.1016/j.ebiom.2018.09.015

Yu, W. R., & Fehlings, M. G. (2011). Fas/FasL-mediated apoptosis and inflammation are key features of acute human spinal cord injury: implications for translational, clinical application. *Acta Neuropathologica*, *122*(6), 747–761. https://doi.org/10.1007/s00401-011-0882-3

Yu, Y., & Schachner, M. (2013). Syntenin-a promotes spinal cord regeneration following injury in adult zebrafish. *European Journal of Neuroscience*, *38*(2), 2280–2289. https://doi.org/10.1111/ejn.12222

Yun, M. (2018). Cellular senescence in tissue repair: Every cloud has a silver lining. *The International Journal of Developmental Biology*, *62*, 591–604. https://doi.org/10.1387/ijdb.180081my

Yun, M. H., Davaapil, H., & Brockes, J. P. (2015). Recurrent turnover of senescent cells during regeneration of a complex structure. *ELife*, *4*, e05505. https://doi.org/10.7554/eLife.05505

Zhang, N., Yin, Y., Xu, S.-J., Wu, Y.-P., & Chen, W.-S. (2012). Inflammation & apoptosis in spinal cord injury. *The Indian Journal of Medical Research*, *135*(3), 287–296. https://www.ncbi.nlm.nih.gov/pubmed/22561613

Zhang, Y., Guan, Z., Reader, B., Shawler, T., Mandrekar-Colucci, S., Huang, K., Weil, Z., Bratasz, A., Wells, J., Powell, N. D., Sheridan, J. F., Whitacre, C. C., Rabchevsky, A. G., Nash, M. S., & Popovich, P. G. (2013). Autonomic dysreflexia causes chronic immune suppression after spinal

cord injury. *The Journal of Neuroscience : The Official Journal of the Society for Neuroscience*, *33*(32), 12970–12981. https://doi.org/10.1523/JNEUROSCI.1974-13.2013

Zhao, Y., Tyshkovskiy, A., Muñoz-Espín, D., Tian, X., Serrano, M., de Magalhaes, J. P., Nevo, E., Gladyshev, V. N., Seluanov, A., & Gorbunova, V. (2018). Naked mole rats can undergo developmental, oncogene-induced and DNA damage-induced cellular senescence. *Proceedings of the National Academy of Sciences of the United States of America*, *115*(8), 1801–1806. https://doi.org/10.1073/pnas.1721160115

Zhu, F., Li, Y., Zhang, J., Piao, C., Liu, T., Li, H.-H., & Du, J. (2013). Senescent cardiac fibroblast is critical for cardiac fibrosis after myocardial infarction. *PloS One*, *8*(9), e74535–e74535. https://doi.org/10.1371/journal.pone.0074535

Zhu, Y., Doornebal, E. J., Pirtskhalava, T., Giorgadze, N., Wentworth, M., Fuhrmann-Stroissnigg, H., Niedernhofer, L. J., Robbins, P. D., Tchkonia, T., & Kirkland, J. L. (2017). New agents that target senescent cells: the flavone, fisetin, and the BCL-X(L) inhibitors, A1331852 and A1155463. *Aging*, *9*(3), 955–963. https://doi.org/10.18632/aging.101202

Zhu, Y., Tchkonia, T., Fuhrmann-Stroissnigg, H., Dai, H. M., Ling, Y. Y., Stout, M. B., Pirtskhalava, T., Giorgadze, N., Johnson, K. O., Giles, C. B., Wren, J. D., Niedernhofer, L. J., Robbins, P. D., & Kirkland, J. L. (2016). Identification of a novel senolytic agent, navitoclax, targeting the Bcl-2 family of anti-apoptotic factors. *Aging Cell*, *15*(3), 428–435. https://doi.org/10.1111/acel.12445

Zhu, Y., Tchkonia, T., Pirtskhalava, T., Gower, A. C., Ding, H., Giorgadze, N., Palmer, A. K., Ikeno, Y., Hubbard, G. B., Lenburg, M., O'Hara, S. P., LaRusso, N. F., Miller, J. D., Roos, C. M., Verzosa, G. C., LeBrasseur, N. K., Wren, J. D., Farr, J. N., Khosla, S., … Kirkland, J. L. (2015). The Achilles' heel of senescent cells: from transcriptome to senolytic drugs. *Aging Cell*, *14*(4), 644–658. https://doi.org/10.1111/acel.12344

ANNEXING INFORMATION